EPRI | ELECTRIC POWER RESEARCH INSTITUTE

Stress Corrosion Cracking Testing Guidelines

With Emphasis on High Temperature Water

2020 TECHNICAL REPORT

PORTIONS TRANSLATED

Stress Corrosion Cracking Testing Guidelines

With Emphasis on High Temperature Water

3002018265

Final Report, August 2020

EPRI Project Manager
G. Stevens

All or a portion of the requirements of the EPRI Nuclear Quality Assurance Program apply to this product.

YES NO

ELECTRIC POWER RESEARCH INSTITUTE
3420 Hillview Avenue, Palo Alto, California 94304-1338 ▪ PO Box 10412, Palo Alto, California 94303-0813 ▪ USA
800.313.3774 ▪ 650.855.2121 ▪ askepri@epri.com ▪ www.epri.com

DISCLAIMER OF WARRANTIES AND LIMITATION OF LIABILITIES

THE FOLLOWING ORGANIZATION, UNDER CONTRACT TO EPRI, PREPARED THIS REPORT:

JLN Consulting

NOTE

For further information about EPRI, call the EPRI Customer Assistance Center at 800.313.3774 or e-mail askepri@epri.com.

ACKNOWLEDGMENTS

The following organization, under contract to the Electric Power Research Institute (EPRI), prepared this report:

JLN Consulting
56 Bradford Farm Road
Mills River, NC 28759

Principal Investigator
P. Andresen

This report describes research sponsored by EPRI.

Hans-Peter Seifert of the Paul Scherrer Institut (PSI) provided an invaluable technical review of the report.

Valuable contributions were also provided by Katsuhiko Kumagai (Tokyo Electric Power Company), Mikiro Itow (Toshiba), Hans-Peter Seifert and Stefan Ritter (PSI), Mychailo Toloczko (Pacific Northwest Nuclear Laboratory), Armin Roth (Framatome), Larry Nelson (JLN Consulting), and Kai Chen and Donghai Du (Shanghai Jiao Tong University, China).

This publication is a corporate document that should be cited in the literature in the following manner:

Stress Corrosion Cracking Testing Guidelines: With Emphasis on High Temperature Water. EPRI, Palo Alto, CA: 2020. 3002018265.

ABSTRACT

This report is designed to provide essential information, reference data, and guidance for conducting stress corrosion cracking (SCC) and corrosion fatigue (CF) tests in high temperature water. Crack growth rate testing is a major emphasis, and a section is included on SCC initiation testing. Much of the report is also applicable to SCC and CF tests in other environments. The report is focused on experimental issues and not on SCC understanding and dependencies, although these are complementary in that one guides the other.

The report is specifically titled a “guideline” because a “standard” implies that, if followed, obtaining high quality data is a certainty. This is rarely the case for environmentally assisted cracking (EAC), where there are many complex interdependencies and seemingly subtle testing variations that can have a large impact on the data. The report seeks to highlight key issues rather than addressing all testing subtleties or nuances; it is not a compendium of everything known about optimal testing techniques for all possible materials, environments, and EAC phenomena. The report strives to identify many important issues and best practices and to provide basic reference data, with the underlying intent being to alert the experimentalist to observe carefully, question techniques and observations, repeat experiments, interact with international colleagues, and learn to manage testing.

Keywords
Corrosion fatigue
Crack growth rate
Environmentally assisted cracking
Environmentally assisted fatigue
Stress corrosion cracking
Testing

Deliverable Number: 3002018265

Product Type: Technical Report

Product Title: Stress Corrosion Cracking Testing Guidelines: With Emphasis on High Temperature Water

PRIMARY AUDIENCE: Researchers focused on environmental crack growth rate testing

SECONDARY AUDIENCE: Program engineers interested in environmental crack growth rate testing and related studies

KEY RESEARCH QUESTION

What guidance is available for conducting stress corrosion cracking (SCC) testing in high temperature water?

RESEARCH OVERVIEW

The objectives of this report are the following:

- To provide critical information, reference data, and guidance for conducting SCC and corrosion fatigue (CF) tests in high temperature water.
- To highlight key issues based on the current state of knowledge about optimal SCC and CF testing techniques.
- To serve as a knowledge transfer document for SCC and CF testing best practices.
- To provide guidance specific to water chemistry, temperature control, direct current potential drop techniques and optimization, specimen types, SCC growth rate and initiation testing, machine control (software requirements), corrosion potential theory and measurements, and test techniques.

The focus of the report is placed on SCC (crack growth) and mostly intergranular stress corrosion cracking (IGSCC) in stainless steels and nickel-alloys and is also pertinent for SCC testing of carbon steel and low alloy steel, and CF testing. Much of the report is also applicable to SCC and CF testing in environments other than high temperature water. The report is not focused on SCC understanding and dependencies, but rather on experimental issues, although these are complementary elements in any SCC study. As a result, the report is not intended for novices, and some amount of reader background knowledge is assumed.

KEY FINDINGS

- The evaluation of environmentally assisted cracking (EAC) response is complex in any environment but is especially challenging in high temperature water. The incentive to quantify the kinetics and dependencies of EAC in high temperature water is high given the need for reliable, long-lifetime, and safe light water reactor operation.
- The guideline is designed to provide essential information, reference data, and guidance for conducting SCC and CF tests in high temperature water. Crack growth rate testing is a major emphasis, and a section is included on SCC initiation testing. While focused on high temperature water, much of the report is also applicable to EAC testing in other environments.

- EAC is very different than ordinary mechanical or fatigue testing because there are many complex interdependencies and large effects of subtle testing differences. Addressing all testing subtleties and nuances is beyond the scope of the report; rather, it strives to identify important issues and best practices and provide basic reference data with an underlying intent to alert the experimentalist to observe carefully, question and steadily improve techniques and observations, repeat experiments, interact with international colleagues, and optimize test management.

WHY THIS MATTERS

There have been over five decades of SCC and CF data generated for use in the nuclear industry, and large scatter and limited reproducibility point to significant shortcomings in some of the experimental techniques. The shortcomings cannot be resolved by posttest expert evaluation of the data; rather, they need to be addressed prior to and during testing. With hundreds of system-years of experience in studying and testing for SCC and CF, and significant interaction among most international laboratories, substantial background material has been collected that can be used to develop a comprehensive guideline for future SCC and CF testing in high temperature water. The report summarizes such key information, with the intent of providing guidance for researchers to consider in future testing efforts to minimize the shortcomings of the testing results.

HOW TO APPLY RESULTS

The report can be used by experimentalists as a reference to assist them in their testing activities. The report identifies key issues and best practices, provides basic reference data, and highlights issues that the experimentalist should carefully observe and manage. The report encourages readers to question their techniques and observations, reproduce experimental results, interact with international colleagues, and learn to manage their testing activities. It is a useful compendium for researchers who perform or plan to perform SCC tests in high temperature water and strive for high quality data.

LEARNING AND ENGAGEMENT OPPORTUNITIES

- International research technical conferences, for example, International Cooperative Group on Environmentally Assisted Cracking (ICG-EAC)
- Conference on Environmental Degradation of Materials in Nuclear Power Systems-Water Reactors
- Materials Reliability Program and BWR Vessels and Internals Project meetings

EPRI CONTACT: Gary L. Stevens, Technical Executive, gstevens@epri.com

PROGRAMS: Nuclear Power, P41; Boiling Water Reactor Vessels and Internals (BWRVIP), P41.01.03; Pressurized Water Reactor Materials Reliability (MRP), P41.01.04

IMPLEMENTATION CATEGORY: Reference

Electric Power Research Institute
3420 Hillview Avenue, Palo Alto, California 94304-1338 • PO Box 10412, Palo Alto, California 94303-0813 USA
800.313.3774 • 650.855.2121 • askepri@epri.com • www.epri.com

ACRONYMS AND ABBREVIATIONS

AC	alternating current
ASME	American Society of Mechanical Engineers
bcc	body-centered cubic
CDCB	contoured double cantilever beam
CF	corrosion fatigue
CMRR	common mode rejection ratio
CS	carbon steel
CT	compact tension
DC	direct current
DCB	double cantilever beam
DCPD	direct current potential drop
dpa	displacements per atom
DVM	digital voltmeter
EAC	environmentally assisted cracking
EAF	environmentally assisted fatigue
ECP	electrochemical corrosion potential *or* electrochemical potential
EDM	electrical discharge machined
EF	environmental fracture
EPFM	elastic plastic fracture mechanics
EPRI	Electric Power Research Institute
FEM	finite element model
GE	General Electric Company

HAZ	heat affected zone
Hz	hertz, cycles per second
IG	intergranular
K	stress intensity factor
K_w	thermodynamic equilibrium constant for the dissociation of water = $[H^+][OH^-]/[H_2O]$. At 25°C, $K_w = 1x10^{-14}$
LAS	low alloy steel
LEFM	linear elastic fracture mechanics
LVDT	linear variable differential transformer
LWR	light water reactor
MeV	million electron volts
PEEK	polyether ether ketone
pH	-log $[H^+]$. For pure water at 25°C, $[H^+] = [OH^-]$, so the concentration of each is $1x10^{-7}$ and the pH is 7
PID	proportional integral derivative used in temperature and other process controllers
pK_w	-log(K_w)
PLC	power line cycle
ppb	parts per billion
ppm	part per million
PPU	periodic partial unloading
PSZ	partially stabilized zirconia
PWHT	post-weld heat treatment (to temper the low alloy steel after welding)
PWR	pressurized water reactor
R	load ratio, minimum load divided by maximum load
RCT	round CT
σ_f	flow stress (generally the average of the yield and ultimate tensile strength)
σ_{ys}	yield strength

σ_u	ultimate tensile strength
SCC	stress corrosion cracking
SHE	standard hydrogen electrode, used in electrochemistry
SS	stainless steel
SSR	solid state relay
SSRT	slow strain rate test
SSY	small scale yielding
STP	standard temperature and pressure
TG	transgranular

CONTENTS

LIST OF FIGURES

LIST OF TABLES

1
INTRODUCTION

There has been over five decades of stress corrosion cracking (SCC) and corrosion fatigue (CF) data generated for use in the nuclear industry, and large scatter and limited reproducibility point to significant shortcomings in some of the experimental techniques. The shortcomings cannot be resolved by post-test expert evaluation of the data; rather, they need to be addressed prior to and during testing. With hundreds of system-years of experience in studying and testing for SCC and CF, and significant interaction among most international laboratories, substantial background material has been collected that can be used to develop a comprehensive guideline for future SCC and CF testing in high temperature water.

This SCC guideline document is designed to provide critical information, reference data and guidance for conducting SCC and CF tests in high temperature water. Much of this report is also applicable to SCC and CF testing in other environments. The report is not focused on SCC understanding and dependencies, but rather on experimental issues, although these are complementary elements in any SCC study. As a result, it is not intended for novices, and some amount of background knowledge is assumed.

This SCC guideline document is designed to be used as a knowledge transfer document and a "guideline" and does not serve as a testing standard that, when nominally followed, will ensure that high quality data will be obtained. In SCC and CF testing, there are many complex inter-dependencies, and subtle testing variations and practices between testing laboratories can have a large impact on the quality of the resulting data. Therefore, this document highlights key issues based on the current state of knowledge about optimal testing techniques. This report is by no means exhaustive for all possible materials, environments and environmentally assisted cracking (EAC) phenomena, nor does it represent a comprehensive manual for SCC testing. Rather, it identifies key issues and best practices, provides basic reference data, and highlights issues that the experimentalist should carefully observe and manage. The report encourages readers to question their techniques and observations, reproduce experimental results, interact with international colleagues, and learn to manage their testing activities. It is a useful compendium for researchers who perform, or plan to perform, SCC tests in high-temperature water and strive for high data quality.

This SCC guideline document addresses water chemistry, temperature control, direct current potential drop (DCPD) techniques and optimization, specimen types, SCC growth rate and initiation testing, machine control (software requirements), corrosion potential theory and measurements, and test techniques (fatigue pre-cracking, intergranular transitioning, test management, data interpretation, "on-the-fly" testing, resolving sluggish chemistry transitions, and so on). The focus of the report is placed to SCC (crack growth) and mostly intergranular stress corrosion cracking (IGSCC) in stainless steel (SS) and nickel (Ni)-alloys and is also pertinent for SCC testing of carbon steel (CS) and low alloy steel (LAS), and CF testing.

1.1 Related Documents

There are many documents that parallel and complement this guideline. ASTM documents E399 [1] (fracture), E647 [2] (fatigue) and others [3, 4] are examples, but they do not address hundreds of key details when environments are involved, nor do they speak to a myriad of other key testing issues. Other guidelines have also been written [5, 6, 7, 8, 9] but they are not as comprehensive as this report. It must be recognized that evaluating environmental effects on cracking (SCC, CF and environmental fracture [EF]) adds complexity in many cases, and individuals require a diverse multi-disciplinary background to properly manage the simultaneous requirements. The primary testing issues that must be carefully considered are related to controlling metallurgy, cold work, fracture mechanics, water chemistry, electrochemistry, radiation effects, and instrumentation. In addition, experimental details must address low electromagnetic noise, high stability loading and temperatures, accurate electrochemical measurements, achieving low contaminant environments, data acquisition and analysis.

1.2 Terminology

Some of the most important terms used throughout this report are defined in this section.

Average crack advance is generally taken to be the average of the cracked area over the specimen thickness (SCC area/specimen thickness), which can be approximated using many equal-spaced measurements of crack length. In the event of incomplete engagement, the average of the engaged areas is often used. If there is less than 50–70% engagement from the fatigue pre-crack, the data are considered to be of questionable value. Other methods are also used to determine the relevant average crack advance.

Compliance crack monitoring is a nondestructive, crack perturbing method that relies on the relationship between changes in load and crack mouth opening displacement as the crack grows, which requires a substantial load cycle. A less quantitative variation of this technique monitors crack mouth opening (or load-line) displacement at constant load, but the contribution of all sources of motion, including creep, undermine its accuracy.

Crack engagement can refer to fatigue pre-cracking (from the machined notch) or to SCC transitioning and growth (from the fatigue pre-crack). In both cases, 100% engagement and relatively uniform growth is the objective. The use of low ΔK during either situation can lead to incomplete engagement and inherently non-uniform crack fronts, with wide-reaching repercussions. There is no way to be certain that the fatigue pre-crack has created a uniform crack, but comparison with the expected air fatigue crack growth rates and ensuring that the growth rate does not decay vs. time are strong indicators.

Crack growth rate is generally reported as a time-based quantity as the change in crack depth over time, da/dt, for SCC, and a cycle-based quantity as the change in crack depth over the applied number of load cycles, da/dN, for fatigue and CF. When environmental effects are observed, there is inevitably a time-based component and thus the growth rate per cycle generally increases as frequency decreases or hold time at K_{max} increases. Numerous subtle factors can affect the measured and/or post-test corrected crack growth rate. Therefore, the investigator must evaluate and report these factors, ideally reproduce the growth rate several

times, demonstrate that high quality test conditions were maintained, and demonstrate that the crack front was fully engaged and relatively uniform. *K*/size criteria are also important, but there is rarely a sudden point at which validity is compromised or a specific value that applies to all materials and heats.

Crack growth reactivation is used as part of test management to reestablish sustained crack growth using slow cycling, often with a multi-hour hold time at K_{max}. SCC is not always reproducible, and a decay in the crack growth rate is sometimes observed. It may be necessary to reactivate the crack several times before a sustained, non-decaying crack growth rate is observed.

Crack length, *a*, is the distance from the load line to the crack tip.

Crack tip strain rate, $\dot{\varepsilon}_{ct}$. Crack tip strain rate is important because it controls the EAC behavior for a given material and water chemistry by producing shear strain (dislocation avalanches) that disrupt passivity and, along with the crack crevice chemistry and local material chemistry, it controls the EAC growth rate. Neither *K* (which is a pure mechanical parameter that characterizes the stress singularity at the crack-tip for a stationary crack under linear elastic fracture mechanics (LEFM) and small scale yielding (SSY) conditions) or bulk environment directly control EAC growth rates. Many factors affect EAC growth rates and are usually categorized in terms of the effects of material (yield strength, Cr content, MnS inclusions, dynamic strain aging, and so on), loading (*K*, *dK*/*da*, *dK*/*dt*, stress state/constraints, and so on) and environment (corrosion potential, impurities, temperature, and so on) The crack-tip strain rate and, at least for LAS, the crack chemistry can depend on the crack-growth rate itself. There is not always a unique relationship between da/dt and *K*, although appropriate *da*/*dt* vs. *K* curves can be defined for specific situations for use in flaw tolerance evaluations.

Fatigue pre-cracking is used in crack growth rate tests to produce a sharp crack from a machined notch. Such cracks are generally created at loading frequencies above 0.5 hertz (Hz), and thus are inevitably transgranular (TG), even for testing performed in the environment. A high stress intensity factor range, ΔK (for example, > 20 MPa$\sqrt{\text{m}}$), helps ensure a uniform crack front – if a lower maximum load, K_{max}, or ΔK is needed, it is often best to start at higher ΔK and decrease K_{max} and/or ΔK after well behaved growth rate response is obtained. Subsequent SCC transitioning is very strongly encouraged.

Final crack length, a_f, is distance from the load line to the final crack tip as determined from post-test measurements, generally by examining the fracture surface, and is sometimes based on measurements from multiple cross-sections of the specimen.

Flow stress, σ_f, is considered to be the average of the yield strength, σ_{ys}, and ultimate tensile strength, σ_u, at the test temperature and can be used in place of σ_{ys} for *K*/size formulations if the material exhibits substantial work hardening.

Initial crack length, a_0, is the initial distance from the load line to the crack tip, ideally determined by physical measurement.

Minimum and maximum crack advance are generally measured separately for the fatigue pre-crack and for the subsequent SCC crack. All crack monitoring techniques are non-linearly affected by an uneven crack front, so the magnitude of the variation from the average crack depth is important to quantify.

Normalized crack length, *a*/*W*, is used to normalize crack measurements for specimens of different sizes and designs, where *a* is the crack length the distance from the load line to the crack tip), and *W* is the specimen width (in the direction of crack advance). For the most common crack growth specimen – the compact (or compact tension or CT) specimen – there are well established relationships between stress intensity factor (*K*), *a*/*W*, effective thickness (B_{eff}) and loading.

Periodic partial unloading (PPU) is alternative wording for long hold time testing. PPU is used to transition from fatigue cracking to SCC evaluation, generally performed at low frequency with a hold at K_{max}, and to reactivate the crack (from no growth, a decaying growth rate vs. time, or to evaluate reproducibility of the constant *K* response). Under some situations, typically high growth rates, PPU can be used as a surrogate for constant load/*K* evaluation, but it must be recognized that the cyclic contribution depends strongly on the constant load/*K* SCC growth rate. Cyclic loading will always bias low growth rate data more than higher growth rate data and is never preferable to constant *K* data (when the behavior at static load is of interest).

Potential drop (PD) crack monitoring is a nondestructive method for measuring a crack length from the change in the potential field of a specimen as a crack propagates. In modern implementations and in light water reactor (LWR) water, PD rarely, if ever, perturbs the cracking response, unlike unloading compliance where load cycling is essential. It is most often implemented as reversing direct current potential drop (DCPD) using a constant current in which the direction is repeatedly reversed after measuring the voltage that develops in the specimen. The current reversal is a very effective means to eliminate dissimilar metal electrical potentials that are present along the voltage measurement path. In concept, it would be possible to apply a voltage and measure the current, but this is rarely done because controlling a constant voltage on a specimen in an autoclave is difficult. Instead, constant current can be achieved to high precision, and is much more likely to result in a constant current flowing through the specimen. Additionally, very low voltage measurements are more accurate. Alternating current (AC) potential drop has been used, but it is more complex and expensive to implement (including lock-in amplifiers), it requires more knowledge and finesse to design and operate, and it is much more sensitive to lead placement and motion, presence of people or other equipment, and so on. The advantage of the ‘skin effect’ with high frequency AC (whereby most of the current flows near the surface of a metal conductor) is more than offset by the superior noise rejection of direct current (DC) measurements.

Remaining ligament is the distance from the tip of the crack to the back of a specimen, or $W - a$, where *W* is the specimen width (in the direction of crack advance) and *a* is the crack length.

SCC transitioning is used following fatigue crack advance (initially or later in the test) and is designed to produce sustained growth along the entire crack front and transition it so it behaves as if it had always been an SCC (or CF) crack. This is sometimes viewed as transitioning to an intergranular (IG) morphology (for austenitic structural materials, SCC is predominantly IG in high temperature water), but there are many other elements of transitioning, including transforming the fatigue hardened plastic zone.

Slow strain rate test (SSRT) is a test method where there is continuous straining of the specimen during the test. It is also called a constant extension rate test (CERT), which is somewhat more accurate because almost all testing is done by controlling the motion of the loading actuator, which is not the same as the strain rate on the specimen. Fluctuations in room

or test temperature can produce a cyclic variation in the nominally rising stress. SSRT is an accelerated test method that always produces failure, sometimes before any EAC can develop. It can produce conservative estimates of EAC susceptibility (due to the higher strain rate), or non-conservative estimates (due to the relatively short time of the test). Because essentially no plant components undergo continuous straining (none at the strain rates used in SSRT) it is, at best, a simplistic screening test and, at worst, very misleading. The imposed strain rate masks the interaction between crack growth and sustained strain rate in an SCC crack.

Specimen thickness, *B*, is the distance from side-to-side of the specimen. If side grooves are used, the effective thickness B_{eff} is calculated as the root-mean-square of the nominal thickness (B_{nom}) and the thickness at the base of the side grooves (BSG), that is, $B_{eff} = \sqrt{B_{Nom}B_{SG}}$. Alternative formulas exist, for example, in ASTM E1820 [4], $B_{eff} = B_{Nom} - \frac{(B_{Nom}-B_{SG})^2}{B}$.

Stress intensity factor, *K*, is a measure of the crack driving force and is proportional to the stress times the square root of the crack length, a. K represents a normalizing factor that provides similitude across a spectrum of crack depths, crack geometries and specimen sizes. It is particularly meaningful in fatigue, where the Paris Law regime describes the crack growth rate vs. stress intensity factor range, ΔK, for cyclic loading amplitude as ΔK^m, where m is the Paris law exponent It is generally not considered to be a fundamental parameter when assessing the effects of environment since the dependency of crack growth on K and ΔK often varies with the environment.

1.3 Contents of This Report

The contents of this report are summarized as follows:

- Section 2 introduces EAC, describes test system design, and provides testing recommendations.
- Section 3 provides recommendations and guidance on the control and monitoring of the testing environment.
- Section 4 provides recommendations and guidance for crack monitoring during testing.
- Section 5 provides recommendations and guidance for crack initiation testing.
- Section 6 provides a short summary of this report and conclusions for SCC testing.
- Section 7 provides the references cited throughout this report.

2
INTRODUCTION TO ENVIRONMENTALLY ASSISTED CRACKING, SYSTEM DESIGN AND TESTING RECOMMENDATIONS

2.1 Introduction to Environmentally Assisted Cracking and Test Objectives

EAC is a general term for all types of cracking driven or accelerated by an environment. Environmentally assisted fatigue (EAF) or CF describes fatigue cracking in an (accelerating) environment. Stress corrosion cracking (SCC) describes EAC under constant load or K (or nearly so), although it is also used for monotonically increasing load or strain, such as experienced during SSRTs (often referred to as strain-induced corrosion cracking (SICC) for CS and LAS materials). There are three broad categories that characterize SCC: the material, stress and environment. However, many investigators highlight about eight key factors, each with many sub-factors:

- Environment:
  - Corrosion potential (especially oxidants)
  - Water purity – especially Cl^-, SO_4^{2-} and pH
  - Temperature
- Stress and stress intensity factor, cycling, vibration, *dK*/*da*
- Material
  - Yield strength/cold work in bulk, surface or weld HAZ
  - Composition (although minor variations are often not important)
  - Sensitization (grain boundary chromium, Cr, depletion)
  - Manganese sulfide, MnS, inclusion content and morphology, especially for CS and LAS
  - Grain boundary carbides; low energy boundaries

While SCC initiation may occur by different mechanisms (pitting, grain boundary oxidation/attack, grain boundary sliding, and so on), for SCC growth most investigators ascribe fundamental importance to dynamic strain at the crack tip, which produces shear strains and disrupts the protective (passive) film. Iron (Fe) and nickel (Ni) alloys are thermodynamically unstable in water and, without the passive film, they undergo very high reaction rates in high temperature water. Crack tip strain rate can be quantified with reasonable accuracy for cyclic loading and continuous straining, but at constant load (or constant *K*), both the measurement and calculation of crack tip strain rate is very challenging. Stress and *K* are much more easily determined and therefore more convenient to use. But in both CF and SCC, there is compelling

evidence that plastic strain rate controls the behavior. When growth rate is plotted vs. crack tip strain rate (Figure 2-1), the response is well behaved over a spectrum of fatigue loading, continuous strain rate, and constant *K* loading for a given material and water chemistry. This implies that the data at lower frequencies and long hold times are asymptotic for constant *K* growth rates, but there is no guarantee with highly resistant materials that crack tip strain rates will be sustained without cycling. In cases where the general corrosion rate is moderately high, such as in CS and LAS, crack tip blunting can produce crack arrest.

SCC growth rates (da/dt) are most often modeled as a function of the applied stress intensity factor, K_I, where the subscript "*I*" refers to Mode I loading (that is, the primary crack driving force is perpendicular to the crack face). After transitioning to constant load (or constant *K*), the crack depth is usually continuously monitored using DCPD, and the crack growth rate is measured. Unmonitored, single-condition tests have some advantages and many disadvantages (including identification of when the cracking started); when cracks grow relatively uniformly in depth, they are a valuable complement to monitored and transitioned tests.

Failures of steam boilers became epidemic in the middle 1800s, but it was not until 1914 that the first design codes were issued (for example, the American Society of Mechanical Engineers [ASME] Boiler and Pressure Vessel Code). However, these are fundamentally engineering mechanics codes that address fatigue and fracture while the effects of environment are simplistically addressed as offsets to the air fatigue curves. The effects of environment introduce a time dependence to the cracking process which is not addressed by most codes – indeed, most codes primarily address SCC by assigning the responsibility of ensuring it does not occur to the designer.

It must be recognized that plant components often represent millions of microstructural opportunities for cracking and hundreds of thousands of hours in which to crack. A single laboratory test is unlikely to assess this cracking susceptibility. Evaluation of growth rates must focus on steady state, reproducible crack growth rates, not on ambiguous, decaying growth rates. Additionally, a major objective of laboratory studies is to identify dependencies on corrosion potential, temperature, cold work, impurities, *K*, and so on, which often represent a factor of 2 to 20 change in growth rate. These dependencies will not be quantified with any statistical confidence when the data are scattered by a factor of 100 to 1,000, which is not unusual.

This guideline focuses on determining SCC growth rates using fracture mechanics specimens in high temperature LWR environments, but it also addresses many aspects of SCC initiation and CF testing that share many things in common with SCC testing. Crack initiation is not well defined. It is considered by some to be the earliest geometric indication of cracking on a micrometer or nanometer scale, whereas others define it based on an in-situ crack monitoring technique, an ultrasonic indication in a plant component, leakage or complete failure. In any event, crack growth is necessary to produce through-wall cracking or compromise the structural integrity of components; it can be quantified much better than crack initiation and be much more representative of plant components, as discussed in Section 5.

This guideline addresses many facets of test system design, test and specimen preparation, test performance, test management and data interpretation. However, although comprehensive, this guideline does not address all possible testing details. Investigators are encouraged to fully digest this guideline and related documents before commencing with testing, ideally before the design

and construction of the system, and should be particularly aware of the need to manage tests and reproduce data. Over five decades of environmental cracking studies in high temperature water have unambiguously demonstrated that there are many ways to obtain misleading and erroneous data.

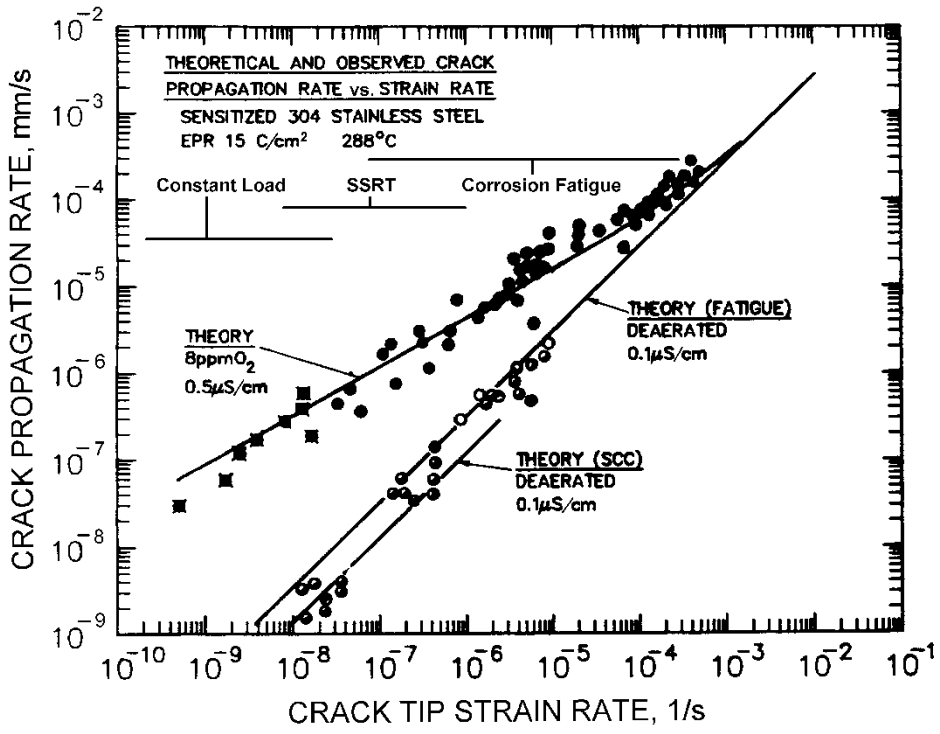

Note: Environmental cracking is time dependent, and damage to the passive film is a fundamental factor, and thus the behavior for a given material and water chemistry is controlled by crack tip strain rate, which produces shear strain (dislocation avalanches) that disrupt passivity.

Figure 2-1
Time-Dependent Behavior of Environmental Cracking in Hot Water

2.2 System Design

Overall, SCC/CF testing system design varies with the purpose and the flexibility needed, as well as with individual experience and available equipment. The autoclave material must be corrosion resistant in the test environment – common concerns are high halide content with dissolved oxygen present, and low or high pH values. The internal pressure must not exceed the rating of the autoclave at the test temperature.

The autoclave is sized to accommodate the specimen(s) under test. The best water chemistry (especially for pure water) is achieved with a small volume and a high flow rate. Stainless steel (SS), titanium and Teflon 'cylinders' have been used to occupy unused space in the autoclave when necessary – but a smaller autoclave is generally simpler and better, provided it meets the current and foreseeable testing needs (specimen sizes). Generally, 4-liter, 5-inch (127 mm) inside diameter autoclaves are adequate in size for standard testing, but much smaller or much larger autoclaves may also be used.

It is almost always best to use the autoclave in an inverted configuration, where the head and seals are at the bottom and will remain at cooler temperatures (Figure 2-2), because polytetrafluoroethylene (PTFE) Teflon is the preferred (and ideal) material for both electrical insulation and sliding (low friction) seals. Teflon has practical temperature limits for breakdown and creep/extrusion, and the inverted configuration allows Teflon seals to be used for autoclave temperatures even above 500°C (for example, for steam and supercritical water). For non-inverted configurations, water-cooled extensions can help keep the seals cool, but water cooling is not nearly as effective as an inverted configuration. Alternatively, for wire seals, a feed-through pipe can be bent at greater than a 90-degree angle so that the polymer seal part is not heated by convection.

The most important seals are multi-wire feedthroughs for DCPD and the pull-rod (ideally a very low friction seal). Various companies sell multi-wire feedthroughs – Conax 2-, 4- and 8-wire feedthroughs (EG style) with 1/4" NPT threads are commonly used in the U.S. The 4-wire feedthroughs can accommodate 0.75 mm diameter wires, and the 8-wire feedthroughs readily accommodate 0.5 mm diameter wires. Ideally, the wires are insulated with Teflon tubing that extends from outside the autoclave all the way to the specimen. This is not possible when operating above ~300°C, but Teflon can extend through the seal by ~10 mm so that small bore zirconia tube insulation can overlap the Teflon. One example is to use ~2 mm outside diameter, 1.2 mm inside diameter zirconia tubing made from TTZ/DURA-Z by Coorstek. The Conax seal ceramic support piece may need to be drilled out to accommodate the Teflon insulation.

Standard Teflon tubing can be used if the inside diameter is a close fit for the platinum (Pt) wires that are used for potential drop and other electrical connections to specimens and coupons. However, often heat-shrink Teflon is needed. Heat shrinking using a heat gun can easily overheat the Teflon and make it much more prone to developing cracks. A small tube furnace set for the specified temperature (typically 310–340°C) provides a much more uniform, high quality heat shrink.

For the pull rod, a pure Teflon Bal lip seal is ideal (for example, Furon Corporation) because it forms a line contact around the pull rod. The static friction is almost zero, although there is some dynamic friction (its magnitude can be ascertained by plotting the hysteresis in the actuator load and position signals using an X-Y oscilloscope and looking at the load offset). The Bal seal requires polished metal surfaces and works best if it is housed in a short extension to the autoclave head to keep it cooler – water cooling is also an option but is rarely necessary in the inverted configuration. The seal also needs to be supported to prevent extrusion of the Teflon; a graphite and Teflon filled polyimide sold by DuPont, called Vespel SP-211, is one way to accomplish this. Despite the carbon fill, the polyimide has very high electrical resistivity, but it needs to be sized carefully to avoid binding/grabbing the pull rod at temperature.

There are other approaches for pull rod seals, including metallic bellows, but such designs have disadvantages because the loading from internal pressure is higher and less defined because of the stiffness of the bellows. There are also pressure balanced seals, but they are more complex, can alter the load amplitude at higher frequencies, create a dead volume of liquid that can significantly prolong the time to change water chemistry, and so on. Pressure balanced seals are generally unnecessary because the load from the internal autoclave pressure can easily be

accounted for and is stable if the pressure is maintained constant using a high quality back pressure regulator (Tescom is one example) preceded by a ~90 μm sintered metal filter to remove particulates that build up and affect the regulator stability. Adaptors can be made to reduce the pull rod diameter if very small specimens or very high pressures are used.

Autoclave pressure stability is very important, even with a pressure balanced seal (which might not track sudden changes in pressure very well). Almost all high-pressure pumps are piston pumps that have a sinusoidal half-wave inlet and half-wave output flow, giving a peak flow rate of ~3.1 times higher than the average flow. Dual piston pumps provide some positive flow most of the time, but the response is still sinusoidal, and the peak-to-average flow rate is a factor of ~1.55. The flow variation (typically at 1–2 Hz) produces a pressure fluctuation and careful measurements at the autoclave can show more than a 300 psi (20.7 bar) variation in some cases. In most cases, this translates directly to ~1 Hz cyclic loading on the specimen and if the load from the internal pressure is a large fraction of the total load, the cyclic contribution can also be high. For this reason, and to help the high pressure pump operate more reliably, a pulse dampener (accumulator) should be positioned as close to the pump as possible – this can be right at the outlet of the pump, with the flow from the pump flowing directly into the accumulator so that it is not a 'dead' (stagnant) volume. For accumulators to operate effectively, they need to be properly sized, filled on the gas side of the bladder to the recommended pressure (often 50–70% of the operating pressure), and be directly in the flow path. Accumulators that are placed a long distance down a stagnant line from the main flow line are very ineffective. It is also recommended that larger diameter tubing be used along with providing a positive pressure to the inlet of the high-pressure pump, and/or using a low-pressure accumulator at the inlet. The pump inlet should never be 'starved' for water, nor should the outlet be restricted.

The ability to apply cyclic loading is valuable, if not critical, because transitioning from aggressive fatigue pre-cracking to static loading should be accomplished using progressively slower loading frequency, then a progressively longer hold time at the maximum load or K. For static load testing, servo-electric actuators with ball screws (lower friction and higher precision) are generally more suitable because they provide a more stable load over time and are not subject to "silting" (the collection of fine particulates at the hydraulic servo-valve). Single stage servo-valves are less prone to "silting" at static load, but it can still develop. The advantage of servo-hydraulic systems is their generally higher frequency and loading capability.

Internal loading posts and an upper plate are often used to carry the load applied to the specimen (Figure 2-3) and, when necessary, zirconia washer and sleeve insulators can be used to electrically isolate the clevis from the upper plate. The Bal seal electrically isolates the pull rod from the autoclave head. Outside the autoclave, it is also wise to electrically isolate the pull rod from the loading system, and Figure 2-2 shows an example of a design that uses a 'loading box' with a Teflon sheet around the pull rod and a Bakelite compression washer for insulation. There are two primary issues with electrical insulation. First, crack monitoring by potential drop requires that a single, controlled current path through a specimen is needed, and thus insulation must exist somewhere in the conductive path from the upper loading pin to the lower loading pin. The second issue can occur when the corrosion potential of a CT specimen is measured (all surfaces electrically connected to the CT specimen contribute to the measured potential).

To maximize frequency response and minimize thermal expansion effects (discussed next), load should be transferred as directly as possible by minimizing the load path. With an inverted autoclave and the actuator below, it is best to use columns between the actuator and the autoclave. Often more actuator motion is needed because of system compliance rather than specimen compliance. This limits the frequency response, adds stored (elastic) energy to the system, and makes the system more sensitive to changes in room temperature because of thermal expansion of the load path. These factors are crucial in differentiating constant displacement loading in plant components (such as weld residual or bolting stresses) with constant displacement loading in the laboratory – they are generally very different. Weld residual stresses in particular are poorly represented by constant load or constant displacement tests because the variation in K as the crack grows is complex (Figure 2-4) and is best studied using active control of dK/da [10] in the laboratory.

These factors are also important in understanding the response during SSRT testing because, while the actuator might move at a fixed rate, the load and strain on the specimen will vary cyclically with changes in room temperature – generally very significantly. Because essentially no plant components undergo continuous straining, there are many concerns for the relevance of SSRT tests, which impose strain rate and thereby mask the inherent mechanical response of the material to loading and crack advance. SSRT testing was developed to reveal materials and environments that produce high SCC susceptibility, but the results have been mixed - overly conservative in some cases and non-conservative in other cases. It is particularly troublesome and inappropriate when only TG cracking is observed in austenitic materials, which in practice predominantly exhibit IG cracking.

Multiple specimens can be tested under series loading, but the control of load and K can only be maintained on one specimen. If series loaded CT specimens are tested, it is necessary to electrically isolate at least some (and it is best to isolate all) of the loading pins so that the DCPD current enters the specimen at the desired spot-weld location. Partially stabilized (3% MgO) zirconia (PSZ) sleeves in oversized holes in the specimen can be used, along with thin pieces of Teflon (below 300°C) or PSZ to prevent contact of the specimen sides with the clevises.

Immersion metal-sheathed thermocouples have excellent thermal response but can crack over time. It is often simpler and better to use a “thermowell” comprised of small diameter (for example, 0.25 in., 6.35 mm) SS or titanium tubing that has been seal-welded closed on one end which is inserted into the autoclave. Simple fiberglass insulated thermocouples can be inserted into the thermowell and can also be moved vertically to evaluate the temperature distribution in the autoclave. Double-high (8-liter) autoclave bodies can be used that are interchangeable with the 4-liter bodies (as well as larger, 65-liter autoclaves), but their greater aspect ratio (length-to-diameter) requires that a three-zone temperature control scheme be used. This is comprised of three thermocouples at different heights, three independent heaters, and three temperature controllers. Contact heaters (heating mantles or heating bands) are recommended over radiant heating because radiant heaters have a longer lag time which makes it harder for the temperature controller to maintain stable temperature.

The temperature controller should be designed and tuned to avoid overshooting the setpoint, especially at higher temperatures where the change in the vapor pressure and volume expansion of water vs. temperature is large. Cascade control can help prevent overshoot, but it is generally possible to heat to a somewhat lower temperature (such as 20°C below the target temperature),

and once that temperature is achieved, the setpoint can be increased. The proportional integral derivative (PID) settings on the controller, coupled with the heating power relative to the steady state requirement, strongly affect both temperature overshoot and the temperature stability at the setpoint. While 1–2°C is often not critical to the experiment, it can have a large effect on the potential drop (and other) measurements. A desired target is to achieve less than ±0.1°C temperature fluctuation. The temperature controller must be configured to shut off power to the heaters in the event of a failed or disconnected thermocouple (or other temperature sensor) and some use a separate over-temperature monitoring device to interrupt power.

The temperature uniformity within the autoclave is important to quantify and maintain. Heat rises, so the top of the autoclave tends to be hotter, and the bottom cooler. Heat loss can be minimized using metal washers between the autoclave and loading linkage to limit the surface area of the contact. Even for autoclaves whose internal height-to-diameter is less than 3:1, greater temperature uniformity is achieved if heat is applied to the lower 50–70% of the autoclave. When properly designed, a 12.5-inch (318 mm) height × 5-inch (127 mm) diameter autoclave will have about 8-inches (203 mm) in the center of the height where the temperature is within a few °C.

From the water supply system, the inlet water is heat exchanged with the outlet water (coaxial, tube-in-tube heat exchangers can be used), then flows to the autoclave in coaxial tubing and is generally preheated before flowing into the autoclave. This latter step is especially important if the water will be directed toward the specimen. In such cases, the preheater can be controlled by a thermocouple immersed in the water as it flows toward the specimen. It is recommended that the inlet water flow be introduced near the top of the autoclave to reduce the tendency for higher temperatures near the top of the autoclave and ensure the inlet water is fully heated.

Provision should be made to purge the gas space of the autoclave with an inert gas before filling with water and to release the gas as the autoclave is filled. Air trapped in the autoclave and pressurized to 100 atmospheres (1 atmosphere = 14.7 psia = 101.3 kPa) will produce an initial dissolved oxygen content of ~900 parts per million (ppm) which will drop over time due to oxygen consumption by corrosion. For tests in deaerated water, the dissolved oxygen should be less than 1 part per billion (ppb). Achieving this factor of about a million reduction takes a while, and these high levels of oxygen can be recirculated back to the reservoir and where they may not be fully stripped (carbon dioxide, CO_2, in air will also produce an elevated outlet conductivity). Also, while the trapped gases will dissolve in the water, they will also be released downstream of the back-pressure regulator, resulting in the gas bubbles creating challenges for flow meters, conductivity cells, demineralizers and sub-micron filters. Similarly, provision should be made for draining the autoclave, especially when an inverted configuration is used. The inlet flow, outlet flow, gas purge and water drain can be accomplished with one penetration containing coaxial tubes, although some testing labs use four tubes in two coaxial penetrations. The outlet water flows counter to the inlet water in the coaxial tubing and heat exchangers, and then passes through a cooler (coaxial cooling coil) to ensure the water temperature is near room temperature. Under some scenarios, the autoclave outlet flow can be higher than the inlet flow, and sometimes the inlet flow might cease if the high pressure pump has problems) – it's important not to let ~300°C water damage the back pressure regulator, flow meter, conductivity cell, oxygen and hydrogen meters, demineralizers, and so on.

For safety reasons, no autoclave should be used without a rupture disc or pressure relief valve that is directly connected to the autoclave; that is, there should never be a valve or other obstruction to the flow. In turn, the outlet of the rupture disc or pressure relief valve should be directed where it will not cause problems, and the outlet tubing must be well anchored to ensure it does not whip around. If vented outside (generally not necessary), caution must be taken that the outlet does not become plugged by ice in freezing climates. Some laboratories have used quench tanks filled with 100 or more liters of water, and it is crucial to ensure that the outlet vent from such a tank be much larger in diameter than the high-pressure inlet to prevent over-pressurization and explosion. There is also a risk of ejecting water throughout the lab as the high-pressure autoclave vents into the tank.

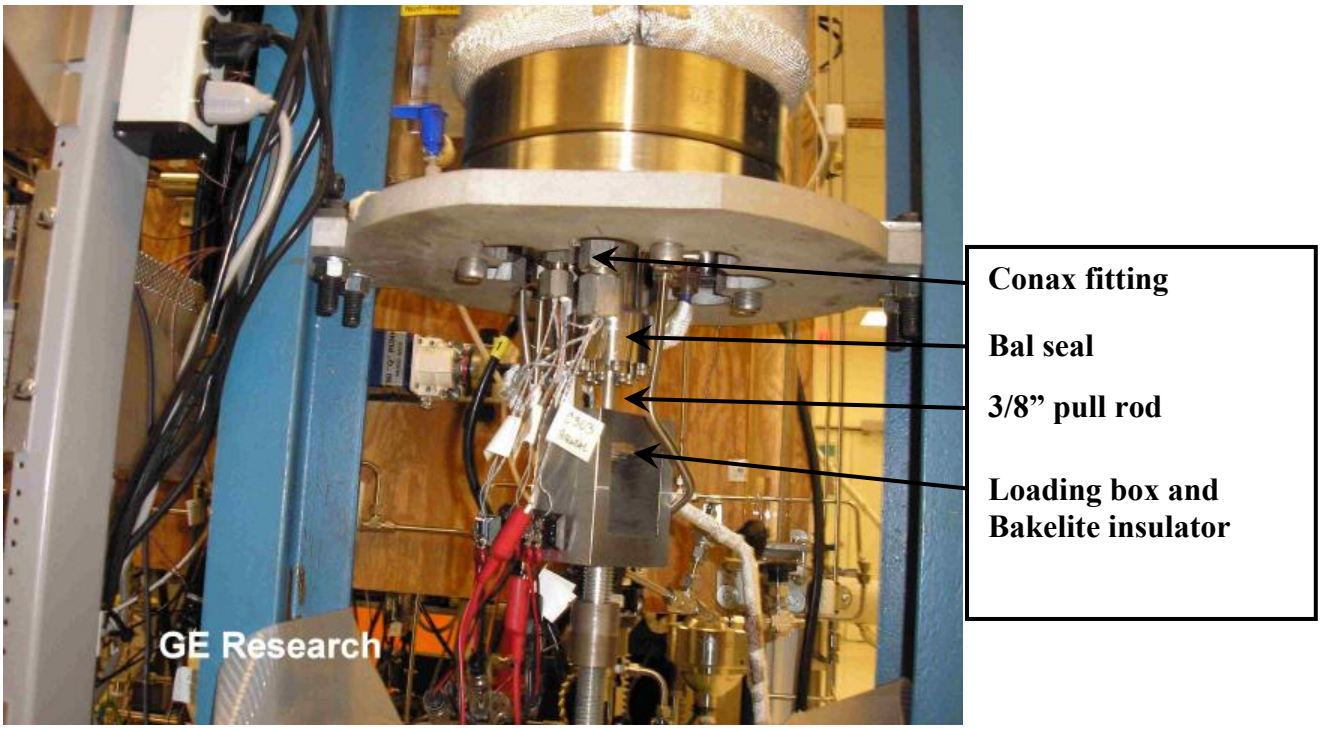

Figure 2-2
The 'Loading Box' with a Teflon Sheet Around the Pull Rod and a Bakelite Compression Washer for Electrical Insulation

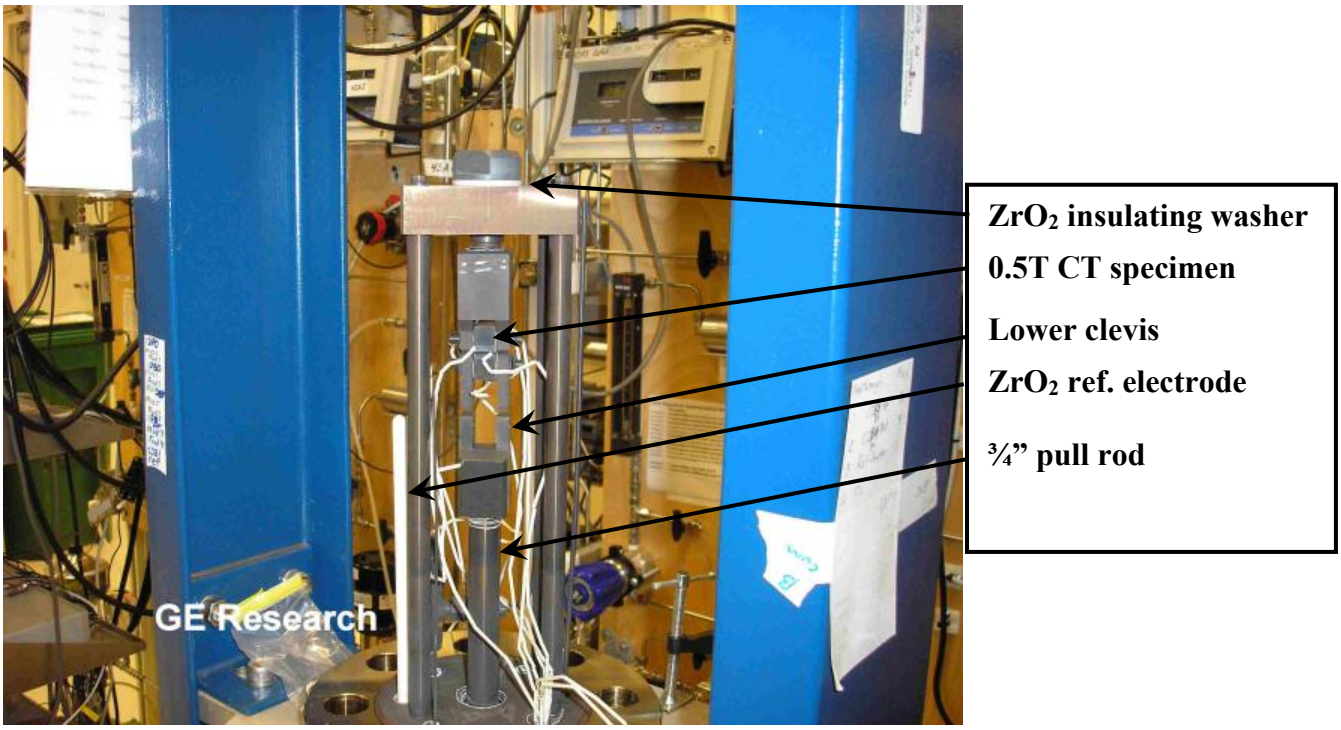

Figure 2-3
Internal Loading Posts and an Upper Plate Used to Carry the Load Applied to the Specimen and Zirconia Compression Washer and Sleeve Insulators (not visible) to Electrically Isolate the Upper Pull Rod from the Upper Plate

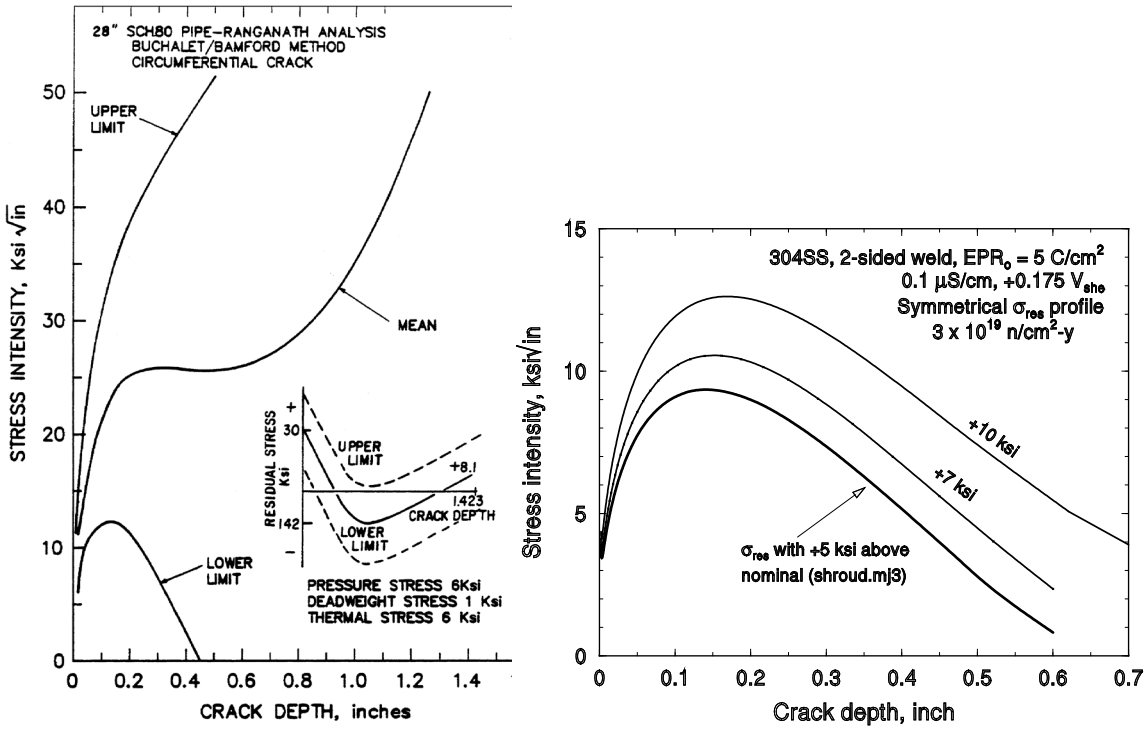

Note: The weld residual stress profile is shown as an inset. Constant load and constant *K* conditions are not as relevant to plant components as *dK/da* because crack depth itself is a primary determinant of *K*.

Figure 2-4
Examples of Stress Intensity Factor vs. Crack Depth in Components with the Crack Growing in the HAZ

2.3 Water Chemistry System Design

The design, control and measurement of the water environment is critical to EAC testing and is addressed in detail in Section 3. A closed-loop design achieves higher purity water (especially organic content), avoids wasting chemicals (for example, for pressurized water reactor [PWR] primary water environments with boron [B] and lithium [Li]), and is representative of plant operation. The water flow rate requirements vary enormously with the target chemistry. For buffered solutions with dissolved hydrogen (such as B/Li solutions), 0.5–1 autoclave volume exchanges per hour is often more than adequate. By contrast, tests in high purity water at low but finite levels of dissolved oxygen (for example, 20 ppb) might require more than 10–20 volume exchanges per hour and the use of titanium structural materials and tubing in the hot section to maintain high purity and the dissolved oxygen at the autoclave outlet. Inlet and outlet solution conductivity is a very reliable and sensitive measurement and should always be used. In-line pH sensors are less reliable, and for pure water, the solution conductivity narrowly defines the possible range in pH.

Dissolved oxygen and hydrogen are key factors, and the inlet water concentrations are accurately defined by bubbling a known composition of gas at a known over-pressure in the water. This is ideally accomplished using a fritted bubbler (to create fine bubbles) and a relatively tall, narrow column of water of limited volume, for efficient equilibration. Various dissolved gas concentrations can be achieved using gas cylinders of custom mixed gases or mass flow

controllers to mix two or more gases. The dissolved gas concentration at the autoclave outlet must be verified. In water containing only dissolved hydrogen, there is rarely a concern for the autoclave outlet concentration because hydrogen is rarely consumed and diffuses through system materials very slowly compared to the water flow rate. In water containing only dissolved oxygen, there are large concerns for the autoclave outlet level, especially for levels below ~100–200 ppb which is highly dependent on system design, materials, flow rate, temperature, and so on. The corrosion potential can vary by more than 0.5 volt (V) over the range of ~3–20 ppb in dissolved oxygen (in the autoclave), so there are major concerns for tests where the inlet water has 50 ppb oxygen and the outlet has ~0 ppb oxygen. Ideally, the dissolved oxygen level at the outlet should be above ~90% of the inlet dissolved oxygen level.

Controlled levels of impurities can be added by closed-loop control of solution conductivity but, below about 5–10 ppb where the change in conductivity is low, it is wiser to use a flow-dilution method (for example, involving a 1% injection of 100 times more concentrated solution into the main flow path). In all cases, the use of solution conductivity to control impurity concentrations requires that the baseline (no injection) conductivity is excellent (for example, 0.055 μS/cm).

2.4 Specimen Design and Loading

Many crack growth specimens have been used, and two key requirements are the relationships between DCPD response, normalized crack length (a/W), and a/W vs. K. The most commonly used crack growth specimen is a CT specimen (Figure 2-5). The specimen size can be changed by scaling all dimensions, with the most common sizes in the range of 0.5T–1T, where T is thickness, and less common in the range of 0.25T–2T. However, any size can be used if it satisfies other testing criteria, such as K/size validity. In some cases, only the thickness is reduced to accommodate the available material. In all cases, the K/size criteria should be applied to both the effective thickness and the remaining ligament.

A side groove on both sides of the CT specimen is recommended to help maintain a single, in-plane crack; in a CT specimen, the stress intensity factor for out-of-plane growth is not that different than the in-plane value. In CT specimens, there is a high Mode I K value even at a high deviation angle. Out-of-mid-plane cracking produces mixed Mode I and II loading. This results in crack flank interference (in particular, in the case of rough fracture surfaces) even under static load with drastically reduced accuracy of DCPD (significant underestimation of SCC crack growth). The side grooves produce a similar stress state as in the center of the specimen (plane strain instead of plane stress). If there is a strong tendency for branching or if there is a preferential microstructural crack path, the 5% side grooving on each side may not be sufficient to keep the crack in the mid-plane.

The most common geometry for CT specimen side grooves is hemispherical, but “V” shaped side grooves have also been used. Cold worked materials are often prone to out of plane growth and any material (such as weld metal) may have a preferred growth direction that will cause the crack to grow out-of-plane if alignment is not along the favored orientation. Orientation is defined in Figure 2-6 and should be separately documented relative to “product form” or “weld dendrite length”, and to “plane of cold work”. Often the orientation vs. cold work is more important than orientation vs. product form. Also, it should be recognized that cold work from weld residual strains should be considered in SCC evaluations [11-16]. Side grooves also reduce the tendency for the crack front to lag at the sides of the specimen. The lag in the growth of the

crack front at the sides of a specimen is caused by reduced constraint which allows for plasticity and a reduced *K* that slows the SCC growth. To counter this lag in crack growth and help straighten the crack front, it is recommended that side grooves be machined on both sides of the specimen with a combined depth of about 10% of the specimen thickness (*B*).

Alternative specimen designs include round CT (RCT), double cantilever beam (DCB), contoured double cantilever beam (CDCB) specimens (to maintain a constant *K* as the crack grows), surface crack, 3- and 4-point bent beam, and others. Some are much more complex to machine and/or pre-crack. All specimens require that the *a*/*W* vs. DCPD and *K* vs. *a*/*W* relationships be known or determined to provide continuous crack monitoring and constant *K* conditions.

The relationship between *K* and *a*/*W* is well defined for CT specimens [1], and the following equation applies for LEFM conditions (that is, small scale yielding conditions: size of plastic zone is much less than *B*, *W* - *a*, and *a*) over the range of *a*/*W* of ~0.20 to ~0.99 with an accuracy of ±0.5% (for straight cracks):

$$K = \frac{P}{B\sqrt{W}}\left[\frac{2+\frac{a}{W}}{\left(1-\frac{a}{W}\right)^{3/2}}\right]\left(0.886 + 4.64\frac{a}{W} - 13.32\left(\frac{a}{W}\right)^2 + 14.72\left(\frac{a}{W}\right)^3 - 5.6\left(\frac{a}{W}\right)^4\right) \qquad \textbf{Eq. 2-1}$$

where *P* is the applied load, *B* is the effective thickness (B_{eff}), *W* is the specimen width (2 inches (50.8 mm) for a 1T CT), and *a* is the crack depth from the load line. In case of uneven crack fronts or large un-cracked ligaments, there is a *K* distribution along the crack front and *K* values can strongly deviate from the values in Eqn. 2-1. The un-cracked ligament carries more load and *K* can be significantly higher than at the deepest point of the crack. In the case of finger-like crack growth in Alloy 182 material, the local *K* from the external load can be very low. Thus, constant *K* tests evidently require a relatively straight crack front for *K* to be very meaningful, as well as for DCPD accuracy. Crack branching usually results in a lower *K* and out-of-mid-plane cracking produces mixed Mode I/II loading and different *K* values.

While elastic-plastic fracture mechanics (EPFM) dominates at the crack tip for most materials of relevance, *K* determined from *J*-integral calculations generally matches up well with *K* from LEFM, if SSY conditions prevail. Provisions to maintain constant *K* are desirable, although for *a*/*W* below ~0.5, the increase in *K* with crack advance for a constant applied load is not that significant and load corrections to maintain constant *K* conditions can often be done manually when the growth rate is below about 10^{-7} mm/s. Note that neither constant load nor constant *K* conditions are highly representative of plant components, where crack depth itself is a primary determinant of *K*; that is, the crack grows in a *dK*/*da* mode (Figure 2-4) [10]. Constant load can be reasonably representative of some structural components where *dK*/*da* is neither significantly negative nor positive (for example, changing by less than 10 MPa$\sqrt{\text{m}}$ per mm of growth), and provided the crack length is limited to *a*/*W* values below about 0.5 or 0.6, where the change in *K* is not that high as the crack advances. In components, +*dK*/*da* is generally only high for short and very deep cracks; otherwise, it falls in a moderate range (not unlike CT specimens) for typical flaws that are detected during in-service inspections. Such moderate values of +*dK*/*da* or -*dK*/*da* usually have little effect on steady-state SCC growth rates.

In general, the surface finish of crack growth specimens is much less important than for crack initiation specimens, but effort should be made to remove cold worked layers and non-representative surfaces, such as electrical discharge machined (EDM) surfaces, which can have a different electrochemical response or contain undesirable elements. In both cases (cold work effects and electrochemical response), the key region of interest is within a few millimeters of the crack plane. Typical corrosion potential measurements will reflect the averaged response over the overall specimen, but the effect on SCC is primarily controlled by the material adjacent to and just inside the crack mouth, where the corrosion potential may be different.

The *K*/size criteria are much more uncertain than most documents suggest in that the deviation in growth rate vs. *K* varies from material to material and heat to heat. The intent of these criteria is to preserve the *K* vs. crack growth rate response as *K* rises or the specimen size decreases. The investigator should not rely solely on a single formulation but always be evaluating the data in the light of the underlying intent. The most definitive study on *K*/size effects in SCC for unirradiated materials (Figure 2-7) [17] indicates that, for materials that work harden extensively (that is, not cold worked above 15–25% reduction in thickness), the ASTM E399 K/size criteria [1] are very conservative for SCC growth rates. For higher levels of cold work or irradiated materials [18,19], the E399 criteria can be very non-conservative. While guidelines are provided, the key factor is that the investigator must be alert to the issue and verify that the *K* dependency obtained at relatively high *K* values (in the vicinity of the *K*/size criteria) is not affected by atypical cracking behavior due to improper specimen size. Key issues include:

1. The effective thickness and remaining ligament should be considered symmetrically, with the limiting factor being the smaller of the two values. For high work hardening (low cold work/yield strength) materials, a conservative estimate is to ensure that both dimensions exceed $(4/\pi)K^2/\sigma_{ys}^2$, where σ_{ys} is the yield strength at temperature. One approach to reducing conservatism is to use the flow stress, σ_f, (average of yield and tensile strengths) in place of σ_{ys}. However, all approaches must be viewed as approximations to the underlying desire for specimen size to have a limited effect on the measured growth rates.
2. For high work hardening materials such as non-cold-worked SS or nickel alloys, the E399 criterion should be assumed as conservative by about a factor of 2 on *K*.
3. For very low work hardening materials (irradiated to greater than 1 displacement per atom [dpa] or greater than 20% - 30% cold work), the E399 criterion can be non-conservative by about a factor of 2 on *K*. This has been addressed in terms of the appropriate "effective yield strength" to use, and for irradiated materials, this value is determined by discounting the irradiated increase in yield strength by 2 to 3 times [18,19]. Thus, the effective yield strength is the unirradiated yield strength plus about half of the increase in yield strength after irradiation. The 'discount' is larger for irradiated materials because they often undergo work softening – that is, the first few dislocations clear the obstacles (vacancy and interstitial loops), so that subsequent deformation occurs in these 'channels'.
4. For ferritic materials, there is evidence that *K*/size plays a more important role, with the upper range of allowed *K* values being more likely to promote sustained crack growth. This may be related to the transient creep response as the crack advances and the stress/strain profiles at the crack tip are redistributed. At lower *K* values and in purer water, there is a pronounced tendency for crack arrest [20].

5. As with many aspects of EAC testing, simple formulas and recipes mask the actual complexity of obtaining good data. A detailed knowledge of the literature and past experience, as well as ongoing evaluation of specimen response are needed to produce high quality, relevant tests.

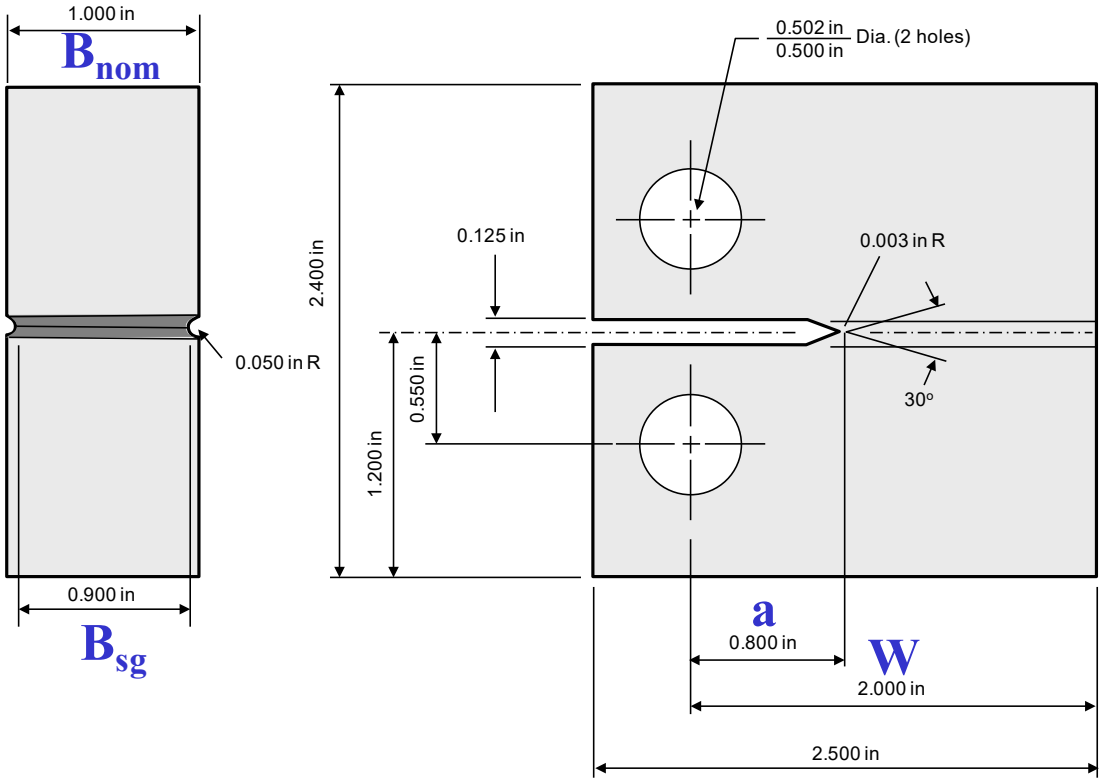

Figure 2-5
Schematic of a 1T CT Specimen

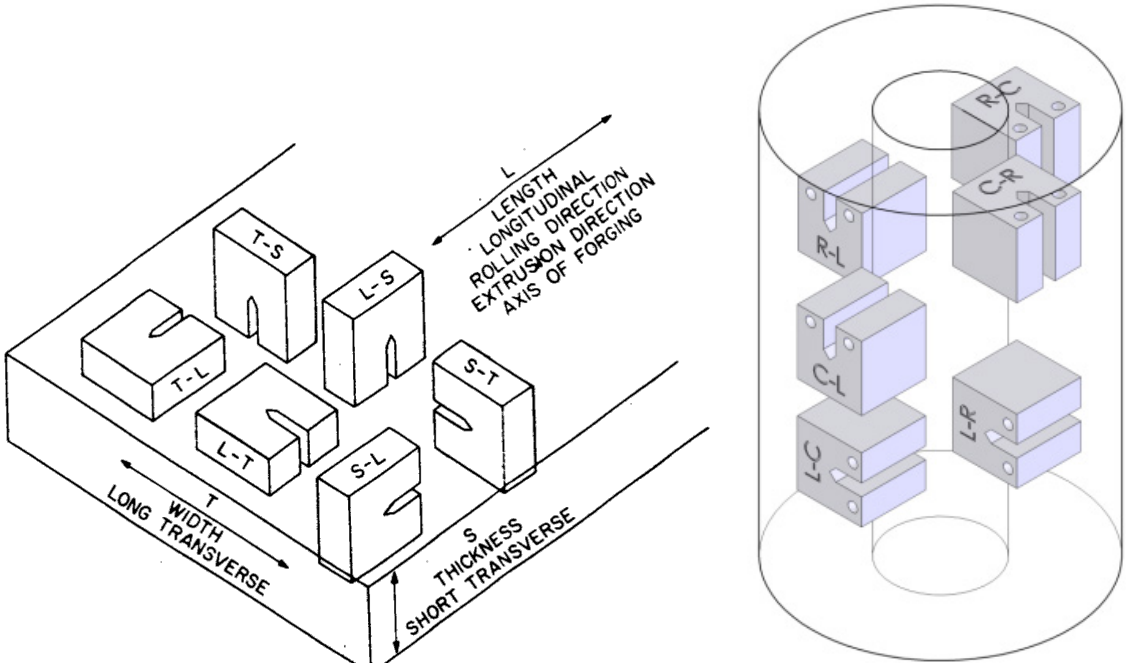

Note: It is also important to specify orientation vs. cold work added before testing, which typically is done by forging or rolling, and thus the plate designations are used.

Figure 2-6
Designations of Specimen Orientation for Plate and Cylindrical Product Forms

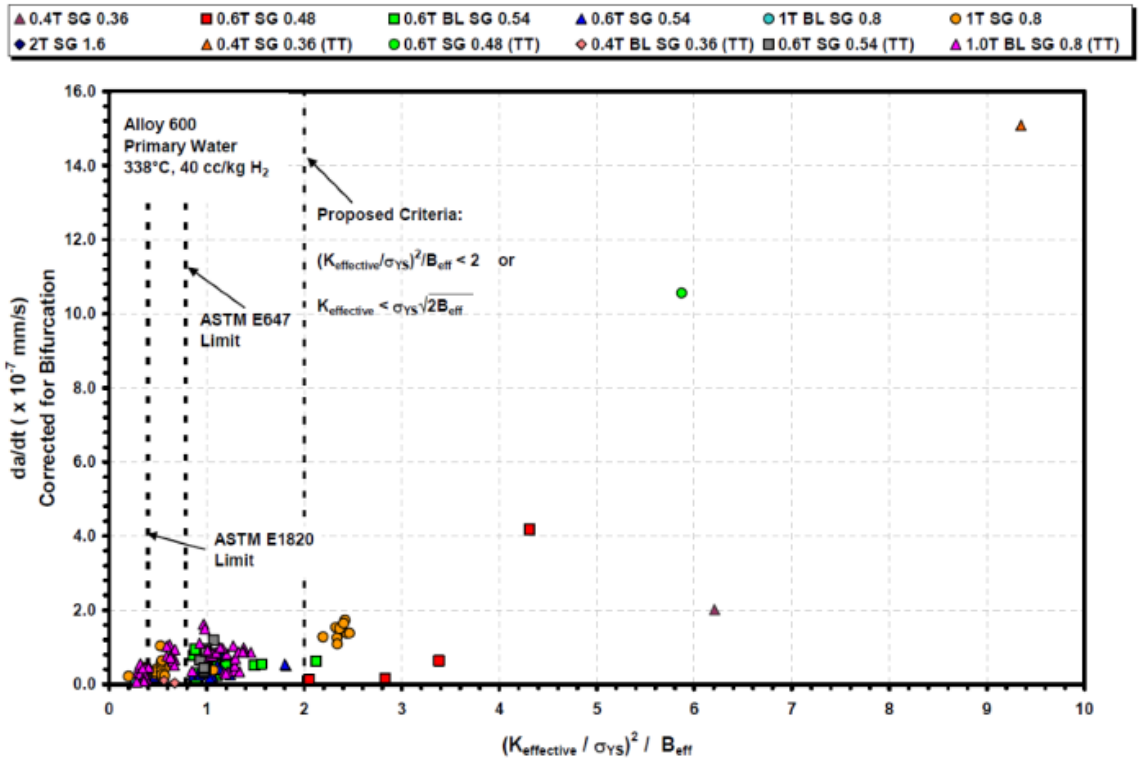

Note: The figure shows that, for materials that work harden extensively (that is, are not cold worked above 15–25% reduction in thickness), the E399 *K*/size criteria [1] are very conservative.

Figure 2-7
The Effect of *K*/Size on SCC Growth Rate for Unirradiated Materials
Republished with permission of NACE International from [17]; permission conveyed through Copyright Clearance Center, Inc.

2.5 Testing Protocols

Fatigue Pre-cracking can be performed in air or in-situ, although each specimen in a multi-specimen test must be individually fatigue pre-cracked. A sharp machined notch (less than 0.1 mm notch radius) and at least moderate ΔK (ideally greater than 20 MPa$\sqrt{m}$) should be used, if possible. Lower ΔK values and larger notch radii may work, but they are prone to producing incomplete growth along the notch (cracks can initiate only from the corners and may not grow together in the center) or a very uneven crack front. Visual examination of the specimen sides provides no insight into the interior. The objective is to develop a crack of uniform depth, which is accurately registered by DCPD and creates a well-defined, uniform K along the crack front. Thus, a low load ratio ($R = K_{min}/K_{max} < 0.3$) is recommended. Frequency is not important apart from the additional time used to develop the fatigue pre-crack. Most laboratories use 0.5–5 Hz sine wave loading. It is wise to compare the observed growth rates with the equations for air growth rates for the same materials to determine if there are any issues during the pre-cracking.

In general, the final K_{max} should be identical or slightly less than the K evaluated under static load conditions. Large sudden changes upward or downward in K after pre-cracking (or any time during the test) can lead to cessation of crack growth along part or all of the crack front. If there is interest in evaluating SCC behavior at lower K values, it is generally best to begin the fatigue pre-crack at

higher ΔK and K_{max}; then after uniform cracking has developed (generally 0.5 mm or so), the ΔK and K_{max} values can be reduced. Some testers insist on moderately large fatigue pre-cracking increments, but other experience shows this is generally unnecessary – crack initiation from blunt notch CT specimen shows that even at 50–100 μm of growth, long crack behavior is observed, and is unchanged out to many millimeters of crack advance. The key concern is not the increment in fatigue crack advance itself, but the uniformity of crack development. However, for LAS, the pre-crack length can play a role under some conditions due to the MnS inclusions that are exposed during pre-cracking, and their role in forming an aggressive crevice chemistry.

Because SCC is usually studied using (and is most relevant to) static loading, fatigue pre-cracking is often done in two or three stages of increasing load ratio, R. An initial load ratio of 0.05 or 0.1 is ideal. After enough growth has occurred (usually ~0.5 mm) to ensure a uniform crack front, shorter increments at R values of 0.3 and/or 0.5 are often used prior to transitioning. When testing in a pressurized autoclave, external compressive loading (to overcome the internal pressure loading) should be avoided unless the loading linkage is rigid (no play) and there is no concern for buckling or sideways motion of the pull rod that might affect the pressure seal.

SCC Transitioning is used to alter the crack path (morphology) and the (fatigue hardened) plastic zone at the crack tip so that the crack behaves as if it had always been an SCC or CF crack. This is less important when the growth rates are very high but still is recommended. As the SCC growth rate drops below about 10^{-7} mm/s, it becomes increasingly important. It has long been shown that in such cases, a fatigue pre-cracked and fixed loaded specimen will rarely exhibit any growth, and this has been widely misinterpreted as immunity to SCC. However, transitioning has consistently shown that austenitic materials will exhibit sustained growth at moderate, low and very low growth rates (below 10^{-9} mm/s), and this has altered the understanding of SCC.

There are no rules that guarantee successful transitioning, but there are guidelines, and the intent is always the same – to sustain crack growth while reducing the cyclic contribution by decreasing the frequency and increasing the hold time at K_{max}. Using a high load ratio (for example, 0.8 or greater, depending on K_{max}) is unwise because often sufficient oxide forms in the crack to eliminate the cyclic contribution at the crack tip, and the growth rate decays to zero (Figure 2-8). Indeed, in water environments very high ΔK thresholds have been observed (Figure 2-9) [21], and thus even for moderate ΔK values (for example, 15–25 MPa$\sqrt{\text{m}}$), crack monitoring should be used to verify stable and linear crack growth at each stage. Even good transitioning does not guarantee well behaved SCC growth rates. The continuously decaying growth rates shown in Figure 2-10 pose major challenges in terms of different rates reported for different test times and/or by different investigators. It also represents a major contribution to the scatter in growth rate data that usually makes it impossible to identify dependencies with statistical confidence (Figure 2-11). Examples of fracture surfaces that reflect incomplete engagement from the fatigue pre-crack are shown in Figure 2-12.

Ideally, transitioning should be designed to produce crack growth along the entire fatigue pre-crack front then continue at lower frequencies. Figure 2-13 is an example of very successful transitioning in a moderately susceptible situation. While there is some transient behavior after each change in loading conditions, there are no major disruptions and an excellent long-term, linear response at each step. The net result of excellent transitioning and test techniques is that

very compelling, reproducible behavior can be observed (Figure 2-14). In turn, widespread opinions regarding conditions of immunity to SCC have been shown to be incorrect (Figure 2-15), such as the immunity of annealed SS and thresholds (conditions where immunity is observed) in corrosion potential and water purity.

With experience, an estimate can be made regarding when the crack will shift from TG to IG (for example, in austenitic materials) – a shift that depends on the material susceptibility (for example, sensitized SS) and aggressiveness of the environment. In highly susceptible situations, IG morphology is sustained at a ΔK of 20 MPa$\sqrt{\text{m}}$ and 0.1 Hz. In highly resistant materials (such as Alloy 690 without sensitization or cold work), the preference for IG over TG cracking might be very subtle and even cycling at 0.0001 Hz with one day hold time might produce predominantly TG cracking.

Ideally, the growth increment from this point onward (to lower frequencies and longer hold time) should be a half to a whole grain size or more (although this may be difficult for some weld metals). Given that the TG fatigue pre-crack can be anywhere within a grain, the goal is to allow the crack to reach a grain boundary and then grow along the encountered boundary (IG). There is a balance between driving the crack forward to encounter grain boundaries while having a cyclic loading condition that is gentle enough for the crack to stay on the boundary rather than be driven forward in fatigue. For materials highly susceptible to IGSCC, the transition to IGSCC can happen at relatively aggressive cyclic loading conditions, while in more resistant materials, the transition may happen at gentle cyclic loading conditions. It takes much longer to successfully transition more resistant materials because the gentler cyclic loading conditions drive the crack forward more slowly. Nickel alloy weld metals are challenging because the most relevant orientation is growth along the length of the dendrite where the grain size can be very large (in the mm range).

A typical transitioning protocol is shown in Table 2-1. It is best to use an asymmetric waveform that utilizes a fast unload and slow reload (90–95% of the overall cycle) because SCC is stimulated by the rising load portion of the waveform. At each stage, no large change in growth rate should occur and a decaying growth rate vs. time is a sign that parts of the crack front are no longer growing. In general, a lower load ratio, R, is needed for a low K_{max} (for example, $R < 0.3$ for $K < 20$ MPa$\sqrt{\text{m}}$) and a higher R at higher K_{max} (for example, $R > 0.7$ for $K > 60$ MPa$\sqrt{\text{m}}$). Judgment, experience and observation are essential.

As the cyclic loading conditions become less aggressive, whether by decreasing ΔK or frequency, or increasing the load ratio, R, an estimate of the expected crack growth rate can be made by one of various formulations. Ford and Andresen [22] formulated the growth rate under cyclic conditions as shown below and used in Figure 2-1. The value of n depends on the material and environmental conditions, but values between 0.5 (high susceptibility) and 0.9 (low susceptibility) are reasonable estimates. Frequency assumes a symmetrical waveform and non-symmetric waveforms should consider the frequency to be determined by the rise time $1/(2t_r)$, then adjusted to account for the (usually shorter) fall time. The adjustment is small if the rise time is only 5% or 10% of the loading cycle. Hold time is more complex to address, as SCC can occur. Many deviations from the expected response can be observed, including crack closure effects that can give rise to surprisingly high ΔK thresholds (for example, Figure 2-9) [21].

For austenitic materials:

$$V = 0.0034n^{3.6}(\dot{\varepsilon}_{ct})^{n} \quad \textbf{Eq. 2-2}$$

where:

V	=	crack growth rate (mm/s)
	=	$34\dot{\upsilon}A_R\Delta K^4$
ΔK	=	stress intensity factor range (MPa$\sqrt{\text{m}}$)
$\dot{\upsilon}$	=	cyclic loading frequency (Hz)
A_R	=	2.44×10^{-11} (for $R \leq 0.42$)
	=	$-2.79\times10^{-11} + 1.115\times10^{-10}\,R + 5.55\times10^{-11}\,R^2$ (for $R > 0.42$)

For LAS the crack tip strain rates in fatigue loading is ~8X higher.

The transitioning procedure may need to be adjusted for CS and LAS. PPU may not sustain SCC in LAS, there crack growth occurs more selectively during the raising load phase by SICC, especially in high-purity water and at K levels below 50 MPa$\sqrt{\text{m}}$. Fast falling load followed by a slow rising load increases the time spent in the rising load phase. Hold times of 9,000 s or 30,000 s can produce growth rates that are 1 to 3 orders of magnitudes higher than the growth rates without cycling. On the other hand, there can be situations where the partial unloading in PPU results in SCC pinning/cessation due to roughness- or oxide-induced crack closure, without re-initiation in the subsequent re-loading. Particular attention has to be paid to constant K tests in LAS, where very small load reductions can result in cessation of SCC in low susceptibility, slow growth rates situations.

SCC Evaluation should recognize the following desirable elements:

1. Transition from fatigue to constant load/K conditions with full engagement at all steps. While full engagement cannot be guaranteed, it should be very aggressively targeted, with linear, steady-state response.
2. No test interruptions or perturbations during the SCC evaluation. An uninterruptible power supply for the systems is recommended, although it is more challenging for the heaters and high-pressure pump. If power is lost and the actuator remains in a fixed position while the temperature drops, there is a risk of overloading the specimen.
3. Stable autoclave and room temperatures, pressure, loading, and chemistry.
4. Evaluation using on-the-fly testing when possible (water chemistry, temperature, and so on) using rapid changes and a return to the prior condition.
5. Repeat the data to evaluate reproducibility, preferably including advancing the crack by cycling to straighten the crack and evaluate different microstructures.
6. Achieve high crack length resolution and accuracy (see Section 4 on DCPD).
7. Give low credence to “no-growth” and low-growth data unless carefully reproduced and the transitioning response was good. Alloy 690/52/152 materials where the transitioning was done well, and the crack growth rate is low are normally considered to be very good data.

8. Use sufficient crack increment (ideally greater than 10X the resolution) and test time (typically more than 100 hours at higher crack growth rates, and much longer at low crack growth rates, where more averaging can be used to increase the resolution).
9. Consider *K*/size validity and small-scale yielding.
10. Avoid sudden changes in K_{max} including between fatigue pre-cracking, transitioning and testing.
11. Report/plot specifics of test conditions and crack length response on a scale that reveals important details.
12. Provide a macro photograph ("fractograph") of the fracture surface showing crack front straightness and post-test correction factor (often a function of the minimum vs. average crack growth). Documentation of the cracking morphology should be provided.
13. Avoid decaying crack growth rate behavior, especially during transitioning. Whenever it is observed, consider reactivating the crack, or, if cycling, shifting to a lower *R*.

Post-Test Crack Length Correction is addressed in Section 4 on DCPD.

Table 2-1
Example SCC Transitioning Protocol for K_{max} of About 30 MPa$\sqrt{m}$ and Medium SCC Susceptibility

Load Ratio, *R*[1]	Frequency (Hz)[2]	Hold Time at K_{max} (s)
0.5	0.01	0
0.5	0.001	0
0.5	0.001	3,000
0.5	0.001	9,000
0.5	0.001	85,000

Notes:
1. At lower K_{max}, a lower *R* ratio is recommended, and at high K_{max}, a higher *R* is recommended.
2. A 5–10% fall time and 90–95% rise time is preferable to a symmetrical waveform. Successful transitioning requires that a stable growth rate be observed. Decaying growth rate during transitioning is unacceptable.

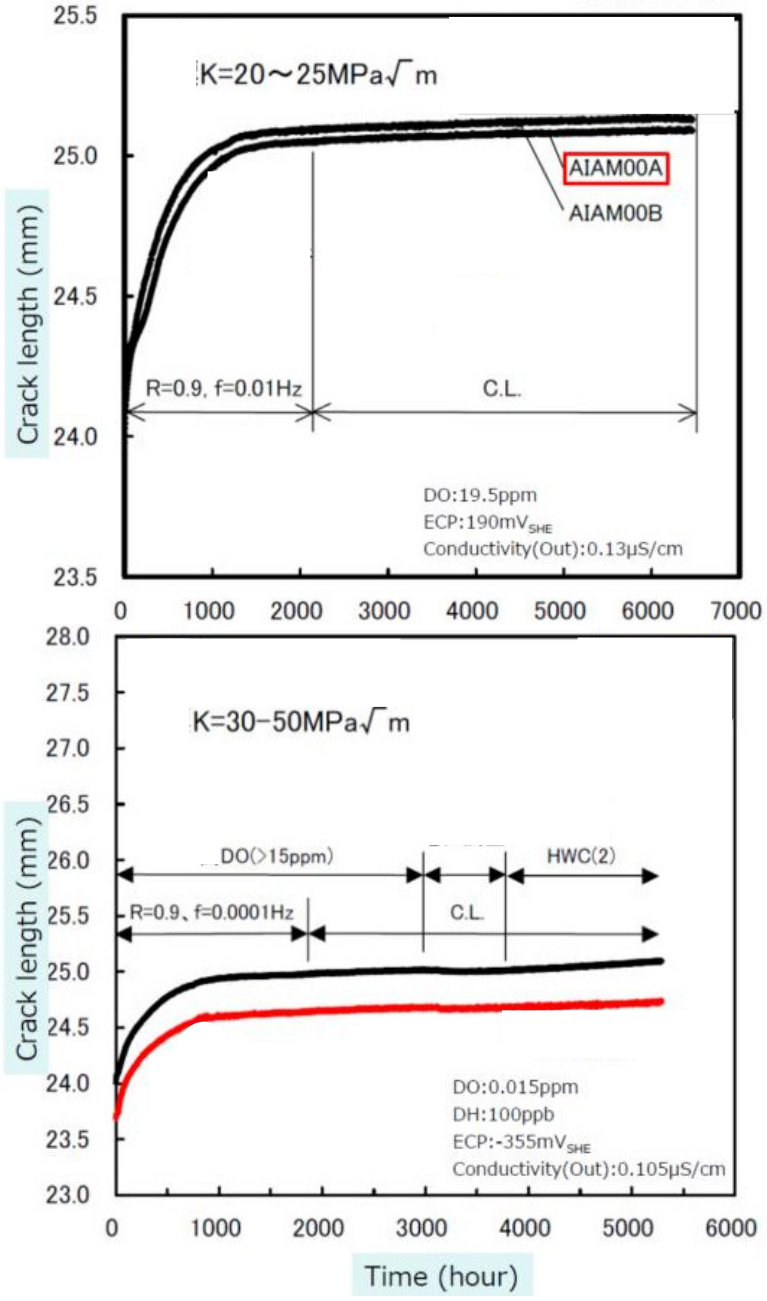

Note: These examples shown decay to about zero during fixed cycling conditions at high load ratio, *R*. This must always be managed by choosing a lower *R*.

Figure 2-8
Two Examples of the Growth Rate Decay

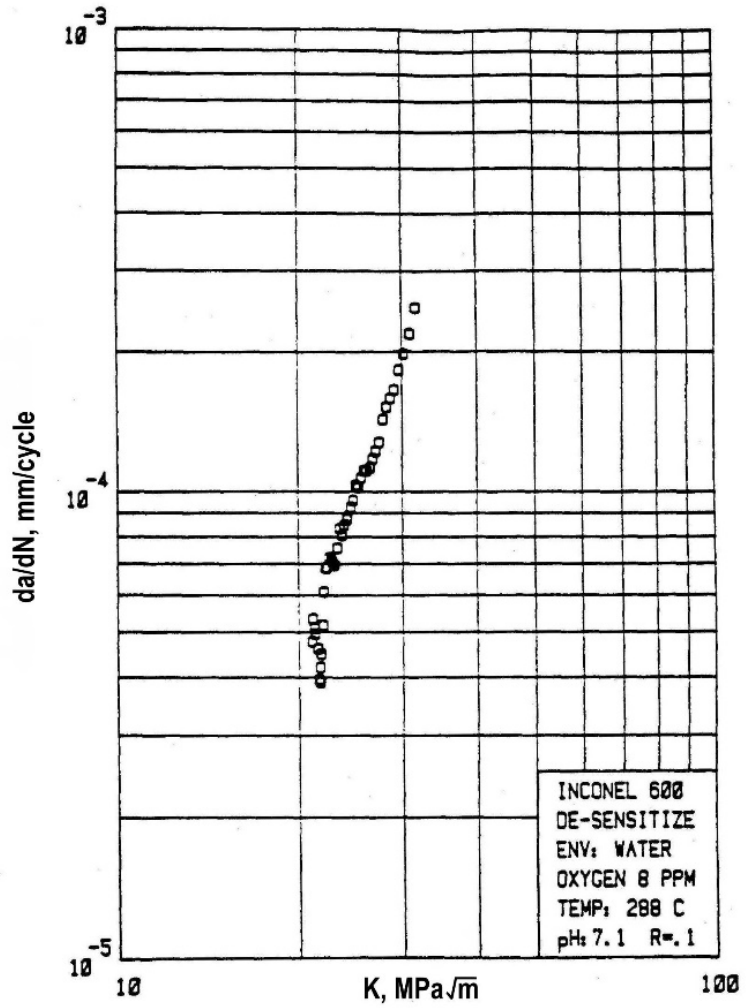

Note: Crack monitoring and transitioning management must be used to avoid decaying growth rate.

Figure 2-9
Corrosion Fatigue Tests in a Pure Water Environment that Show a Very High ΔK Threshold (ΔK_{th}) [21]

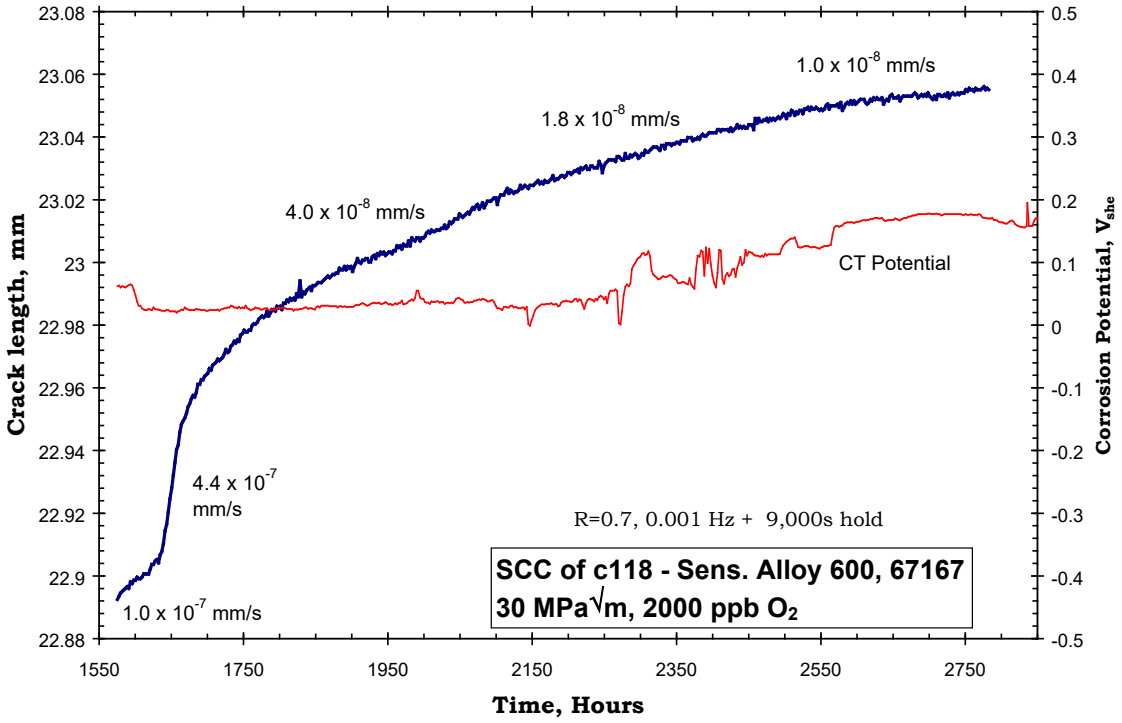

Note: If the test is run for 100 vs. 500 vs. 1,000 hours, a different result is obtained, giving rise to unacceptable scatter.

Figure 2-10
Crack Depth vs. Time of Alloy 600 in 288°C Water with 2 ppm Oxygen Showing a Continuously Decaying Growth Rate

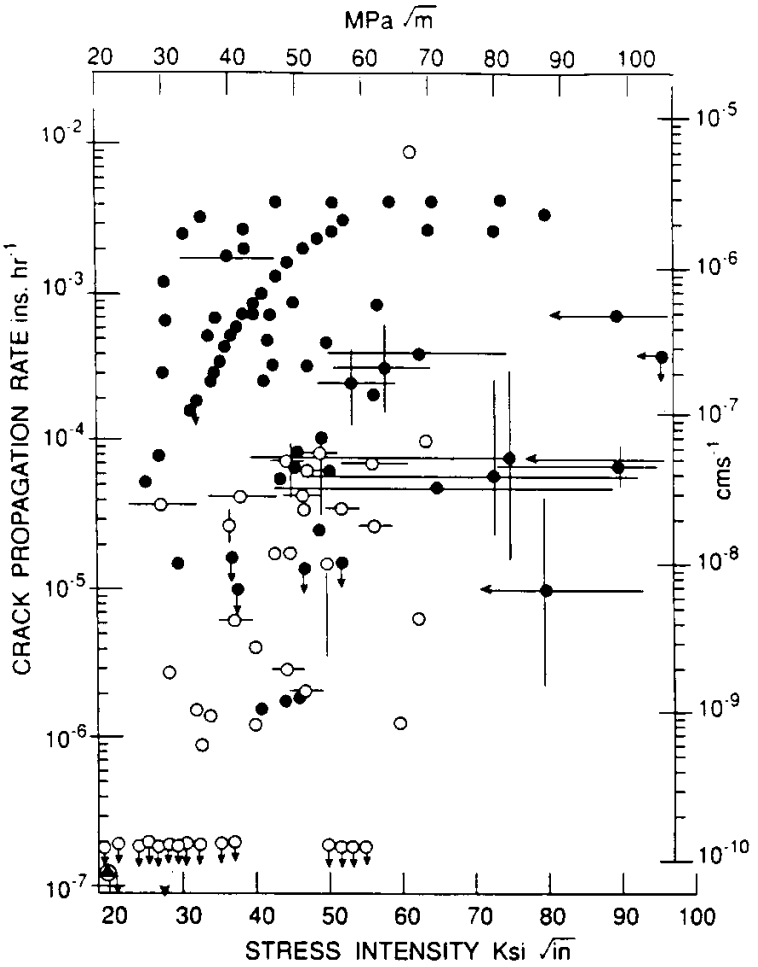

Note: Examples of poor experimental techniques include poor loading, transitioning and water chemistry.

Figure 2-11
Large Scatter in the Crack Growth Rate Data from Many Investigators on LAS Resulting from Poor Experimental Techniques

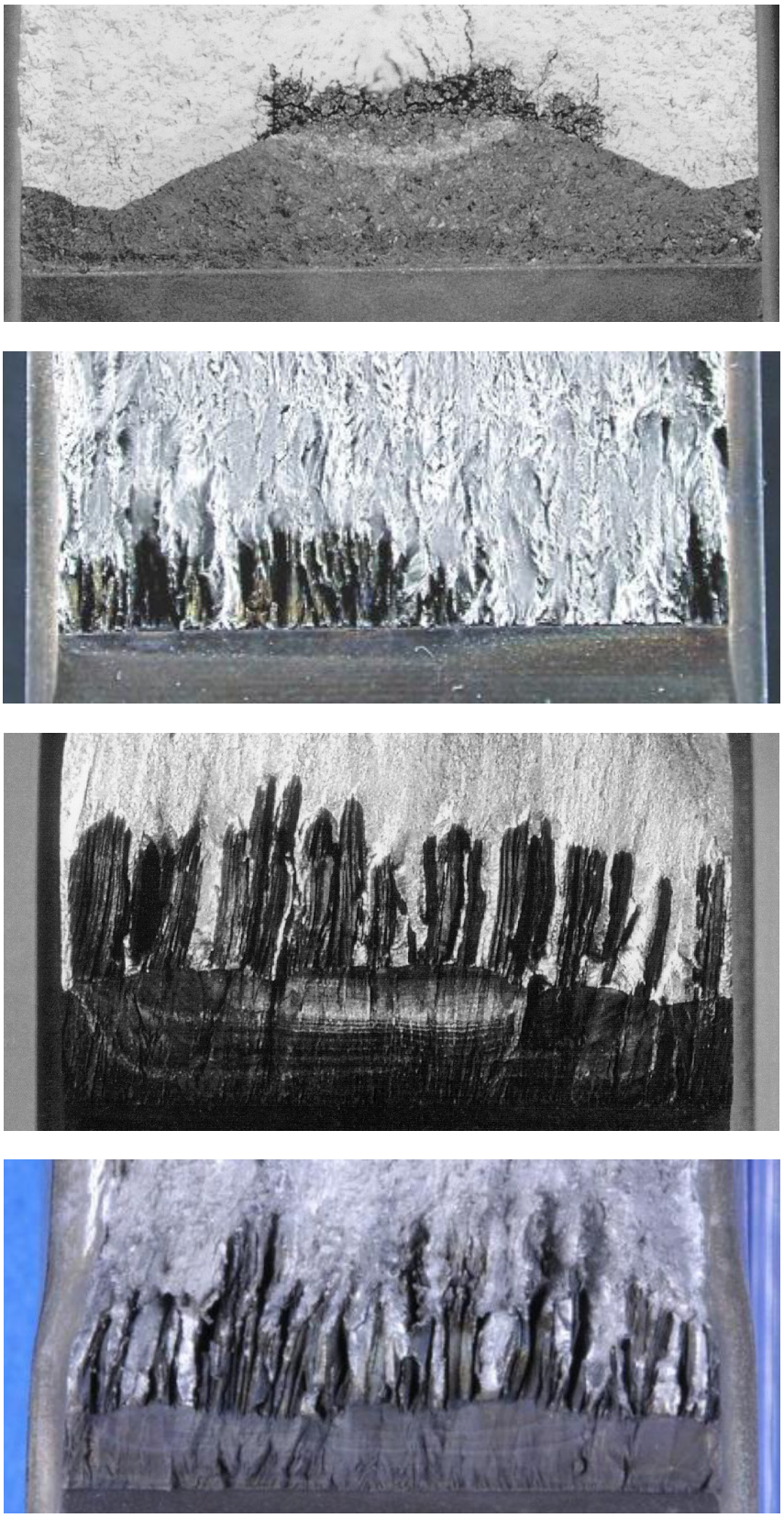

Figure 2-12
Examples of Partially Engaged, Very Uneven Crack Fronts Resulting from Poor Transitioning

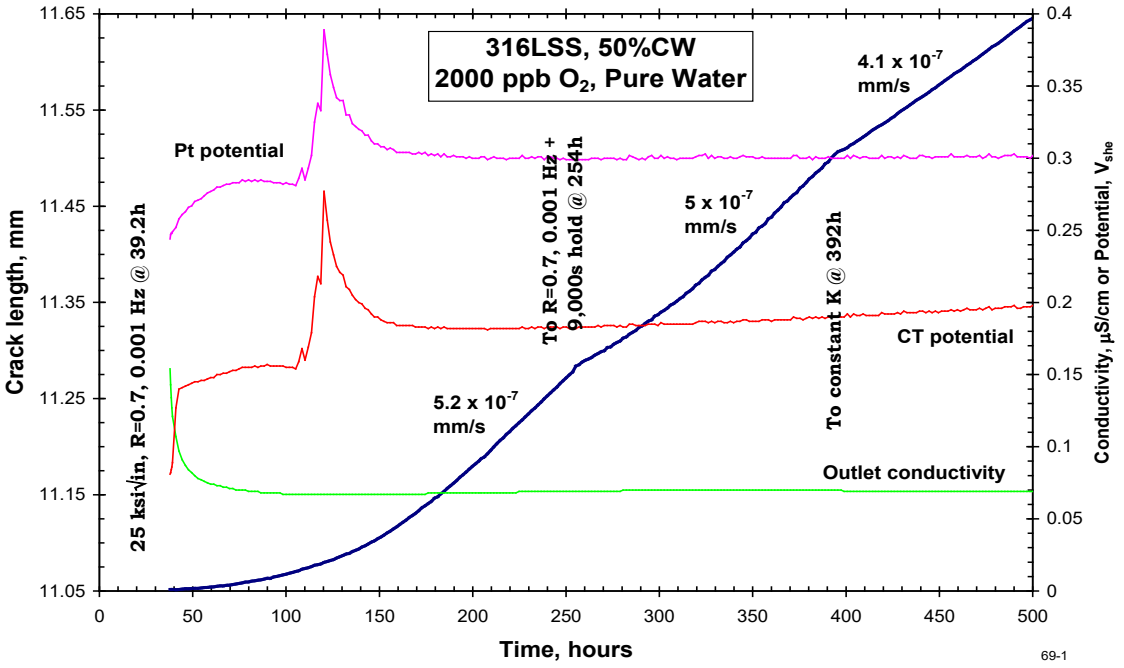

Note: Some transient behavior is observed after changing loading conditions, but there is no major disruption in the crack length and there is excellent linear response at each step.

Figure 2-13
Crack Length vs. Time Showing Ideal Transitioning Response

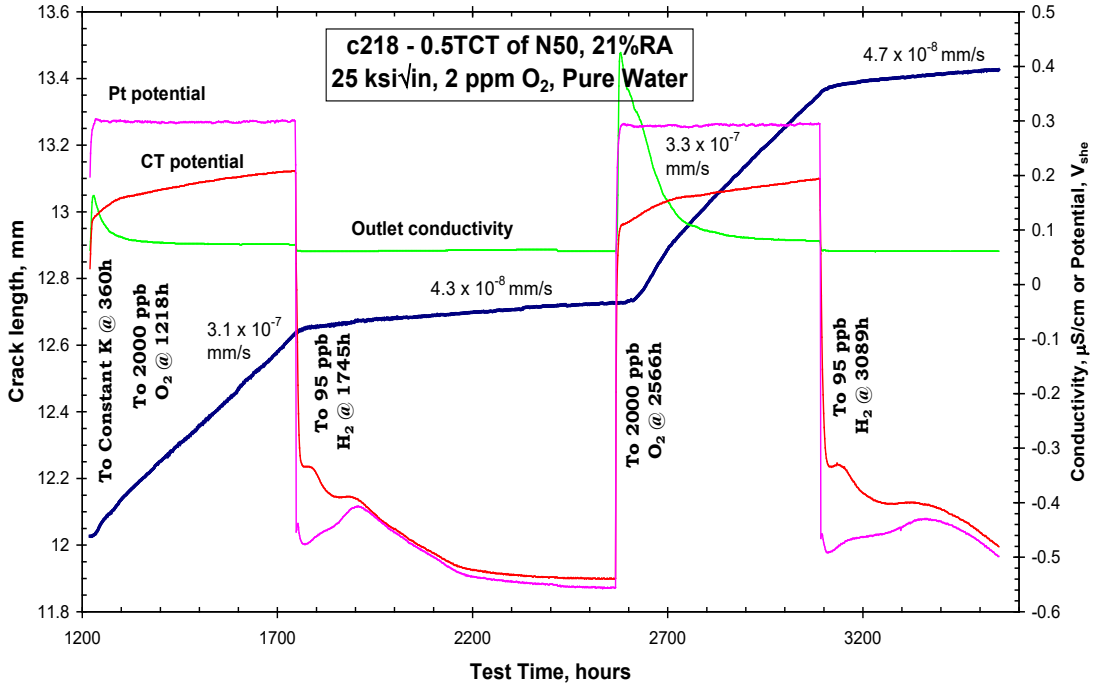

Figure 2-14
Crack Length vs. Time Showing the Crack Length Resolution, the Effects of "On-the-Fly" Changes in Water Chemistry, and Growth Rate Repeatability

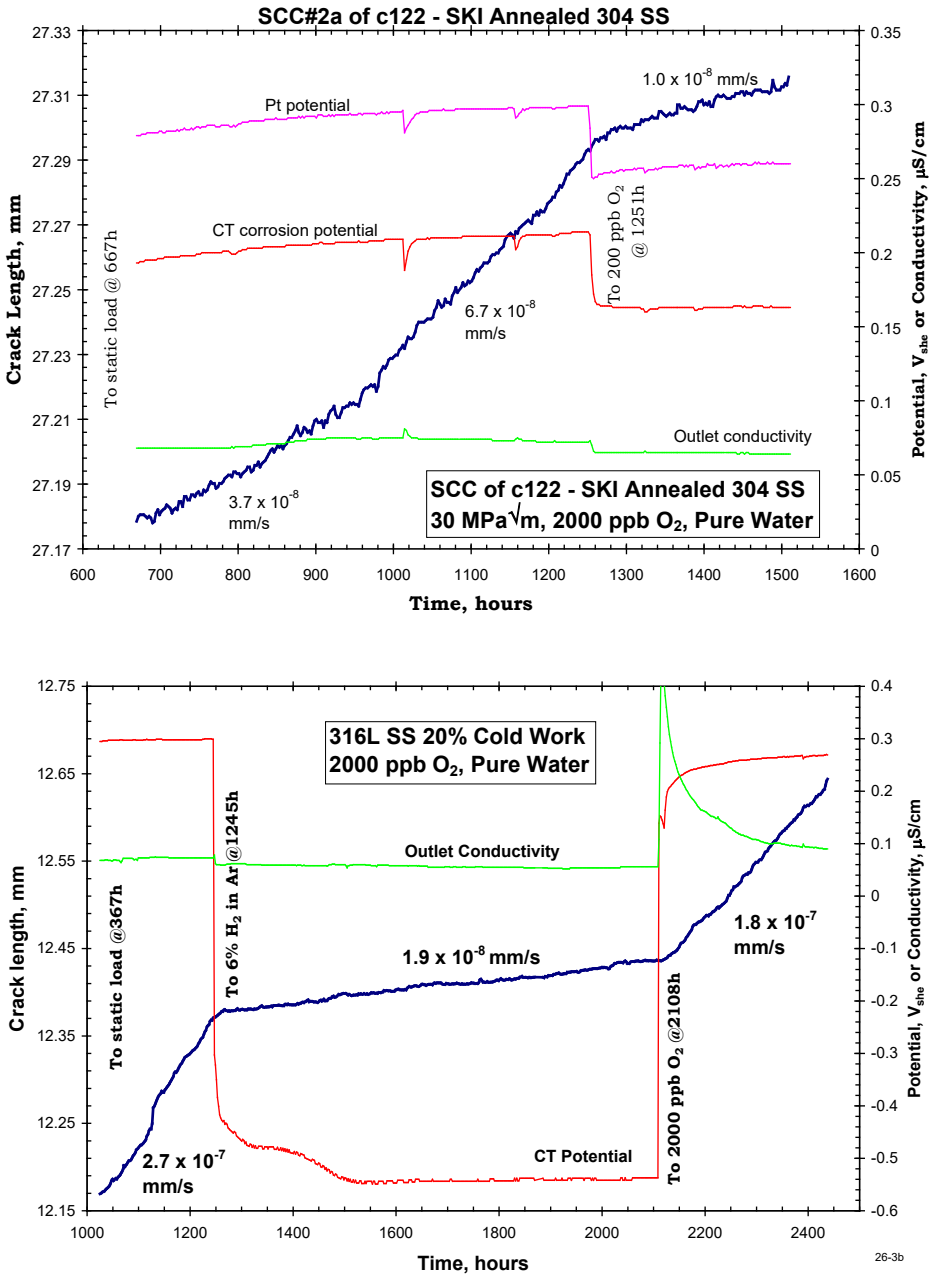

Note: Long-held opinions about SCC immunity of annealed SS, SCC at low potentials, and SCC in high purity water have been transformed by excellent techniques and high quality data.

Figure 2-15
Examples of High Quality Data

2.6 Mechanics

The mechanics of cracks in components should always be understood and considered. Weld residual stresses, stresses on bolts, pressurization stresses, vibration and cyclic loading are important, but have significant differences. If the component experiences constant load, testing at constant load may also be considered appropriate. However, the change in K vs. crack advance is almost certainly very different in a test specimen compared to an actual component—sometimes much greater in the component and sometimes greater in the specimen.

Similarly, constant displacement loads from bolting or weld residual stress have often been viewed as affecting SCC less than active (for example, pressurization) loads. But this optimistic view is incorrect; one constant displacement configuration (for example, residual stress in a weld) may have little resemblance to that in a laboratory specimen where the compliance/ stiffness of the overall system can continue to maintain high load as the crack advances. Conversely, large diameter pipes and components can have large stresses from weld shrinkage or from ovalization issues (that is, large hydraulic jacks may have been used to align two piping pieces during welding). As a result, large, far-field stresses behave differently than local weld residual stresses. Laboratory system-to-system differences can be very large. The 'load path' can be long and circuitous with a smaller/thinner linkage and frame, while other systems can have a very short load path with a large/stiff linkage and frame.

The nature of crack advance from a small defect on a nominally smooth surface (for example, a pipe wall) is different than that of a CT specimen with a notch and fatigue crack, with the crack depth (a) measured from the load-line. Since K is proportional to $\sigma\sqrt{a}$, when cracks are small, K rises very rapidly with crack advance (Figure 2-4). This is especially true of weld residual stresses, where both σ and a contribute to the initial rapid rise in K. Some cracks exhibit a peak in K, then experience a slow decrease as the crack grows. In other cases, the K rises and has somewhat of a plateau and then rises fairly rapidly after growing beyond ~75% of the thickness. CT specimens show a comparatively small change in K until the crack length becomes long, for example, $a/W > 0.75$ (Figure 2-4). The ability to achieve both constant K as well as controlled change in K with crack advance ($\pm dK/da$) is important, but it involves a lot more sophisticated software and relies on a high resolution/precise DCPD crack length measurement and crack fronts that are as straight and uniform as possible. This is because K, crack length and crack growth rate are increasingly ambiguous as the crack front becomes more uneven.

2.7 Metallurgy

The spectrum of structural materials used in LWRs is not that large, with most falling into categories of plain CS and LAS; SS and weld metals; and nickel alloys and weld metals. Some precipitation hardened SSs and nickel alloys are used for bolts, springs, and so on, such as Type 630 SS (also known at 17-4PH), A286 SS, and nickel Alloy X-750 and Alloy 718.

Among the key issues is composition (minor compositional variations may not be as important as imagined), microstructural homogeneity/anisotropy, sensitization (grain boundary Cr depletion), changes in yield strength (for example, from irradiation or precipitation hardening), and unevenly distributed cold work. Nominal material specifications may not accurately represent in-service materials. This is in part, because material specifications rarely ensure homogeneity

and uniform properties, and because “deviations and exceptions” are often used to accept materials that do not meet specifications. Figure 2-16 shows an example of Alloy X-750 material that was considered to be “homogeneous” that was supplied to an LWR plant that had significant carbide banding [23, 24].

Surface preparation from fabrication and grinding can have a large impact on crack initiation and plant component surfaces are not always consistently manufactured. But crack growth depends on the interior, through-wall characteristics. Welding is a primary issue because of weld residual stresses and weld residual strains (Figure 2-17) in combination with mechanical forces used to align components prior to welding. Additionally, the rapid heating and cooling cycle during welding transforms the HAZ of LAS to martensite and a post-weld heat treatment (PWHT) must be used to temper the martensite. The PWHT does not restore the original hardness and specialized welding techniques often used for weld repairs (for example, temper bead welding) generally produce an even higher hardness. Data show an effect of yield strength (or hardness) even when there is only a limited increase above the baseline value. Importantly, PWHT is often referred to as a “stress relief”, which is a misnomer – it has only a limited effect on weld residual stresses, and less effect on “far-field” (mechanical) stresses.

Plain CS and LAS, especially historical steels, have high sulfur (S) content (broadly considered as greater than 0.010 wt.% S), with S present primarily as MnS inclusions. These inclusions slowly dissolve in high temperature water and can create a “high sulfur” crack chemistry that significantly accelerates environmental cracking. “High sulfur” conditions depend on the sulfur content, MnS morphology, yield strength, corrosion potential, and other factors [25, 26].

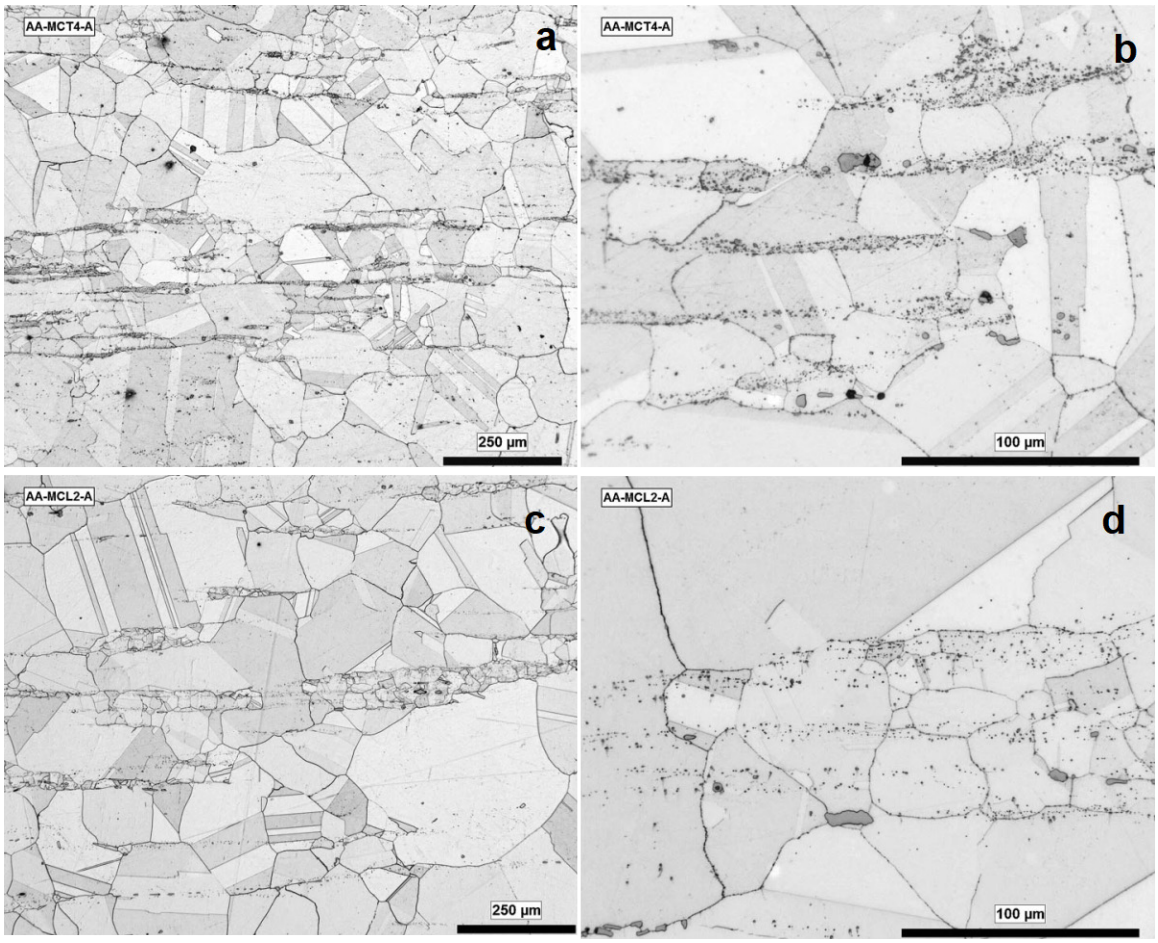

Figure 2-16
Optical Micrographs Showing Carbide Banding in an Alloy X-750 Component Delivered to an LWR Plant [23, 24]

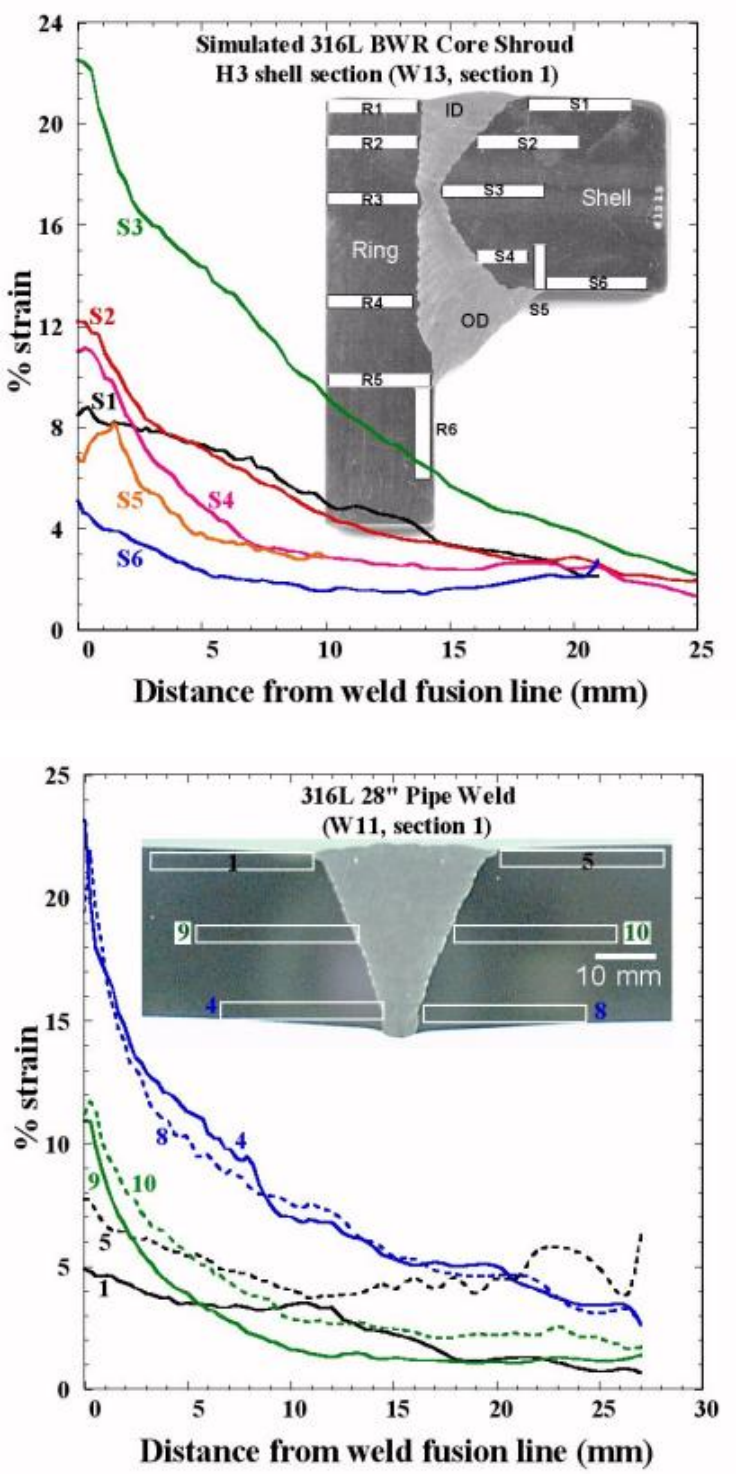

Note: The peak strain always occurs near the fusion line and at the root of the weld, with values of 20–30% being common both in SS and Alloy 600.

Figure 2-17
Weld Residual Strains in the HAZ Adjacent to the Weld Fusion Line as Determined from Electron Back-Scattered Diffraction

3
CONTROL AND MONITORING OF THE ENVIRONMENT

Environmental effects on cracking are often large. Great care is needed to control and measure all relevant parameters in the autoclave inlet to outlet paths, including impurities; solution conductivity and pH; temperature; dissolved gases (and all other oxidizing and reducing species); corrosion potential; and flow rate. The effects of water chemistry must always be considered in the context of the materials of interest recognizing that, in general, water chemistry effects are more pronounced on lower Cr materials like sensitized SS or LAS compared to high Cr materials like Alloy 690. There are interactions among the water chemistry parameters; for example, at low corrosion potential, all materials exhibit a higher tolerance to the impurity level in the bulk water. The benefit associated with a water chemistry change is also complex as it depends on other water chemistry parameters, the material, and loading (Figure 3-1).

The water chemistry emphasis is on the conditions at the test specimen, which are better reflected by the outlet water from the autoclave than the inlet water to the autoclave. Basic targets for BWR and primary PWR chemistry are given in Table 3-1 and Table 3-2, respectively, but there are situations in which these targets can be relaxed, and other situations when they are inadequate. For example, chloride levels as low as 2 ppb have been found to enhance the growth rate in LASs in BWR normal water chemistry; therefore, any study of impurity effects should ensure that the concentration of other impurities is low compared to the impurity under study. In fully deaerated water (that is, low corrosion potential), the tolerance to impurities is generally at least an order of magnitude greater than at high corrosion potential.

In most tests, adequate control of water purity and dissolved gas chemistry can only be achieved in a flowing system, an example of which is shown in Figure 3-2. An adequate refresh rate varies greatly with the target water chemistry. Tests in deaerated water can generally be performed at less than 1 autoclave volume exchange per hour. But, tests in finite but low oxygen and/or at intentionally low impurity levels (where the difference between outlet vs. inlet chemistry must be small), or tests in highly oxygenated water (where outlet conductivity can be significantly higher than the inlet conductivity due to an increase from oxidation of Cr_2O_3 to CrO_4^{2-}) may require more than 10 volume exchanges per hour, depending in part on the autoclave materials of construction. Such high volume exchange rates are best achieved with small autoclaves. If the hydrogen fugacity can be controlled (for example, with an Ag/Pd membrane, through which hydrogen diffuses very rapidly), static autoclave testing might be adequate in, for example, pH buffered PWR primary water, although it must be demonstrated that impurity levels do not rise too high. This is never the case in high purity water, with or without oxidants. In pure water, impurity levels down to ~2 ppb can be detected by solution conductivity; in PWR water, the baseline conductivity is too high to detect meaningful concentrations of impurities.

Critical elements of a refreshed system include (see Figure 3-2):

- Excellent baseline make-up water purity, usually deaerated, to which known, controlled ionic impurities or dissolved gases may be added
- Characterization instrumentation for inlet and outlet chemistry, for example, solution conductivity, dissolved oxygen and hydrogen, specific ions, and so on
- High pressure pump and accumulator (or, a pulse dampener to prevent pressure/load oscillations from the internal pressure acting on the pull rod and thereby on the specimen)
- Coaxial heat exchanger, coaxial water cooler, autoclave, and back pressure regulator

A final pre-heater is often desirable so that the inlet water is at the desired autoclave temperature, especially if the water is directed at the specimen. Digital temperature controllers are preferable because of their better temperature regulation capability than their analog equivalents and this is especially important for potential drop measurements of crack length. Full flow demineralization of the autoclave effluent, and its re-use as the inlet water, is often desirable because the organic and bacterial content of this water can usually be controlled much better compared to adding new make-up water.

The foremost safety concern in working with high temperature water is its vapor pressure and volume expansion (below the triple point of about 374.2°C, water is essentially incompressible), for which values are listed in Table 3-3. When working with supercritical water or steam, consideration must always be given to the conditions at intermediate temperatures.

Table 3-1
Basic Targets for BWR Water Chemistry

Parameter	Target	Achievable
Temperature fluctuation[1]	±1°C	±0.1°C
Autoclave outlet conductivity[2]	< 0.1 μS/cm	< 0.07 μS/cm
Autoclave inlet conductivity	< 0.06 μS/cm	0.055 μS/cm
Autoclave outlet dissolved O_2	> 80% of inlet	> 95% of inlet
Autoclave outlet SO_4, Cl, F	< 5 ppb	< 1 ppb
Total organic carbon, inlet & outlet	< 10 ppb	< 5 ppb

Notes:
1. Relevant temperatures include 274°C (most structural materials are exposed after the feed water is mixed in), and 288°C (the temperature in and above the core, until the feed water is mixed in). Temperature fluctuations affect SCC growth rates and noise in crack monitoring.
2. The outlet water is more representative of the water to which the specimen is exposed.

Table 3-2
Basic Targets for Primary PWR Water Chemistry

Parameter	Target	Achievable
Temperature fluctuation[1]	±1°C	±0.1°C
B, Li, conductivity and pH[2]	–	–
Dissolved H_2	25–40 cc/kg (2.2–3.6 ppm)	–
Autoclave inlet dissolved O_2	< 5 ppb	< 1 ppb
Autoclave outlet SO_4, Cl, F	< 50 ppb	< 1 ppb
Total organic carbon, inlet & outlet	< 20 ppb	< 5 ppb

Notes:
1. Relevant temperatures include ~290°C (core inlet), ~325°C (core outlet), ~343°C (pressurizer), and ~360°C (accelerated testing). Temperature fluctuations affect SCC growth rates and noise in crack monitoring.
2. The B and Li (or K) levels vary during the fuel cycle from ~1,500 ppm B and ~2 ppm Li (beginning of cycle) to less than 10 ppm B and ~0.25 ppm Li (end of cycle); different pH_T targets are used.

Table 3-3
Absolute Vapor Pressure and Volume Expansion of Water vs. Temperature

Temperature (°C)	25	100	200	250	280	300	320	340	360	370
Vapor pressure (psia)	0.031	14.77	225	576	930	1,245	1,636	2,117	2,706	3,050
Vapor pressure (MPa)	0.00021	0.1018	1.551	3.971	6.412	8.584	11.28	14.60	18.66	21.03
Vapor pressure, bar (absolute)	~0	1.02	15.5	39.7	64.1	85.8	112.8	146.0	186.6	210.3
Volume expansion	1.00	1.043	1.156	1.251	1.332	1.404	1.498	1.637	1.894	2.207

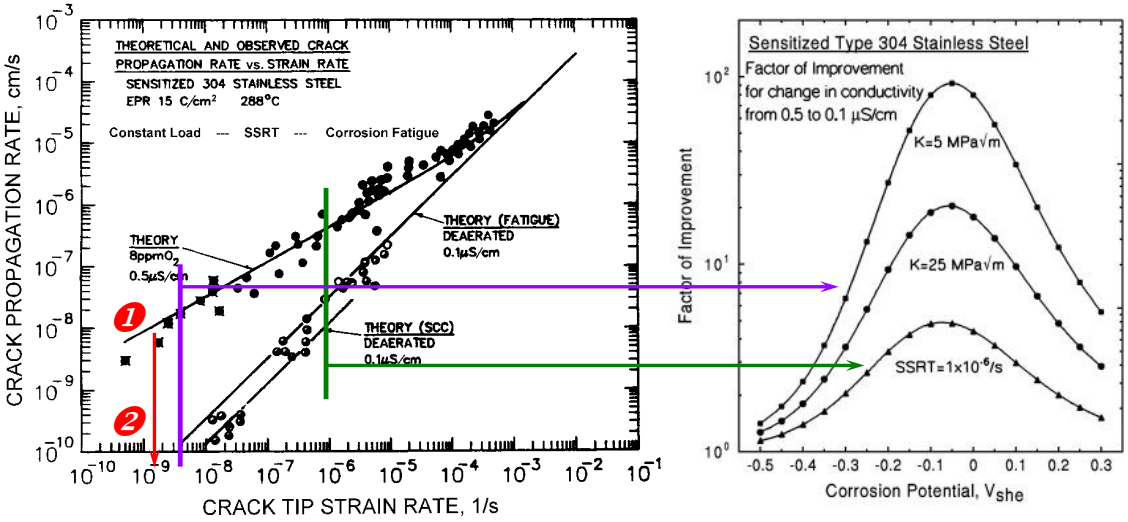

Note: The benefits of a material or water chemistry change depends on the loading, material and chemistry. The left graph shows that the benefit of a change in chemistry or material is greatest at lower strain rate (K, ΔK, frequency, and so on). The right graph shows that the benefit from purer water depends on corrosion potential and loading.

Figure 3-1
Benefits of a Material or Water Chemistry Change

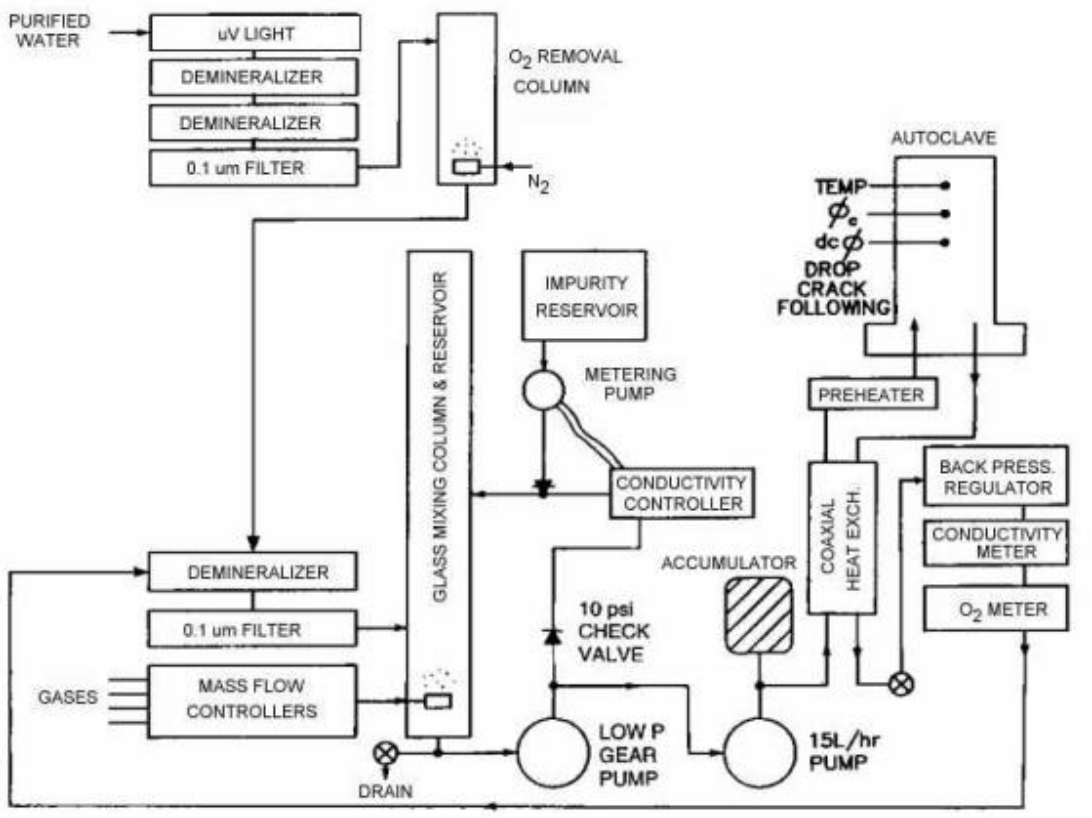

Figure 3-2
Schematic of Water Supply System Used on Each SCC System

3.1 Water Purity and Intentional/Unintentional Impurities

Water purity is very critical to most experiments in hot water since modern BWRs operate within the approximate conductivity range of 0.09–0.11 μS/cm, corresponding to ~10 ppb of total ionic impurities, with chloride and sulfate levels below 1 ppb. PWRs also have strict limits on impurities like chloride and sulfate, and generally operate with concentrations below a few ppb. EPRI provides Water Chemistry Guidelines for utilities that define Action Levels 1, 2 and 3 for actions that must be taken as the plant chemistry deviates from the preferred values [27, 28, 29], which are updated periodically. Other countries have similar water chemistry guidelines.

At room temperature, the conductivity of water is a very sensitive measure of ionic impurities. Conductivity is always measured using AC signals (typically 60 Hz or 1,000 Hz), because DC signals will produce polarization of the electrodes and incorrect values for the solution conductivity. Conductivity varies substantially with cation type (primarily H^+ vs. other cations), and typical conductivity values are shown in Table 3-4 for several anions when added to high purity water. Table 3-4 also compares NaCl and HCl on the basis of concentration in normality, N (charge equivalents per liter), and shows that the acidic form yields much higher conductivity than the salt form (about 3 times higher, once the conductivity is somewhat higher than pure water and enters a linear regime vs. Cl concentration) (Figure 3-3). The relationship between conductivity and pH for HCl, NaCl and NaOH is shown in Figure 3-3, which defines "domains of reality" – that is, it is impossible to have a pH(25°C) of 6.0 at a conductivity of 0.1 μS/cm because there is simply not enough H^+ and Cl^- at 0.1 μS/cm to have an activity of H^+ equal to 10^{-6} ($pH = -\log [H^+]$).

Carbon dioxide in the air is soluble in water and dissociates to form H^+ and HCO_3^-, raising the conductivity of pure water at 25°C from 0.0549 μS/cm to about 1 μS/cm, thus precluding the use of grab samples for measurement of conductivity for pure water. A much more pronounced effect is observed if the autoclave is not purged with inert gas and the air space is compressed by 100 atmospheres or more.

Table 3-5 lists the equivalent conductance and μS/cm per ppb for a variety of ions when added to high purity water. Note, because of the high mobility of H^+, the minimum value of conductivity does not occur in pure water, but rather for water containing ~0.188 ppb of LiOH, which drops the conductivity from 0.0549 to 0.0544 μS/cm. Despite the very small decrease in conductivity, the addition of Li^+ or other impurities should not be construed as beneficial.

The conductivity of pure water varies substantially with temperature (Figure 3-4), as a result of changes both in the dissociation constant of water (which produces a pH equal to 7.0 at 25°C, 6.14 at 100°C, and 5.63 at 288°C, Figure 3-5) and from increased mobility of the various ions. The conductivity of theoretical pure water increases from 0.0549 μS/cm at 25°C to about 4 μS/cm at 250°C, which is an increase of about a factor of 75, with the majority of that increase accounted for by the decrease in pH (that is, a factor of 22 increase in the H^+ and OH^- concentrations). While high temperature conductivity measurements are interesting, the high baseline conductivity of pure water at 288°C masks the effects of impurities on conductivity more than at room temperature. Thus, concentrations below 10^{-7} N can be measured and controlled by conductivity at 25°C, whereas at 288°C only concentrations of about 10^{-5} N can be detected.

Intentionally added impurities can be controlled by dilution of an injected solution into the main flow before or after the high-pressure pump or controlled by modulating their injection rate based on the autoclave inlet conductivity. In the former case, the impurity reservoir must have a known, controlled concentration, and the injection flow and autoclave flow rates must be known and stable. This approach is essential for non-ionic impurities and for very low levels of impurities. Table 3-4 shows that adding 10 ppb of chloride HCl shifts the conductivity from 0.055 to 0.110 μS/cm. This should be accurately detectable and controllable by conductivity meters, provided that the demineralizer used in the closed-loop system continues to produce 0.055 μS/cm water that returns to the reservoir and the reservoir maintains that water purity. Most conductivity meters have set point capability so that an injection pump can be triggered as the conductivity decreases below the set point. Some oscillation in the autoclave inlet conductivity from such an on-off controller is usually not an issue because the oscillation is highly damped by the volume of the autoclave. Below 5–10 ppb of ionic impurity, control by conductivity is less precise and the dilution approach should be used. For continuous online NobleChem™ [30, 31], Pt levels as low as 1 part per trillion have been injected in this fashion.

In PWR primary water (with B and Li, or B and K), there will be a slow drift upwards in conductivity in a closed-loop system because the primary impurity, when more than about 0.5 ppm of dissolved hydrogen is present, is Fe^{2+}, and as it is ion-exchanged in the demineralizer, H^+ and some Li^+ is released. Li^+ has a strong effect on conductivity and pH. To correct for this, the conductivity meter can be set to inject when the conductivity rises above the setpoint with the impurity reservoir containing only B at the desired level. A second demineralizer can also be switched in to absorb the excess Li^+, but this generally provides less stable, continuous control of conductivity and chemistry. While the drift in conductivity and pH is not rapid, and can be corrected manually every few weeks, it can have an effect on other measurements, including the DCPD. But such observations are only observed when segmented ceramic (ZrO_2) is used for wire insulation inside the autoclave. Below about 300°C, continuous PTFE Teflon can be used to insulate the DCPD wires which should be continuous from outside the autoclave to the specimen. This is discussed in more detail in Section 4 on crack monitoring.

Water grab samples should be taken during each test, at least once, and perhaps several times, depending on the length of the test and historical experience, for relevant cations and anions, such as Cl, SO_4, NO_3, Cr, Fe, K, Na, Mn, Ni and Si (and B and Li for PWR conditions), as well as total organic carbon.

Table 3-4
Solution Conductivity vs. Species and Concentration

Anion, ppb	0	3	10	30	100	300
μN, Cl	0	0.0846	0.282	0.846	2.82	8.46
μS/cm for NaCl	0.0549	0.0656	0.0906	0.162	0.412	1.125
μS/cm for HCl	0.0549	0.0725	0.110	0.367	1.205	3.609
μS/cm for HF	0.0549	0.0905	0.223	0.642	2.130	6.386
μS/cm for H_2SO_4	0.0549	0.0672	0.112	0.277	0.730	2.687
μS/cm for HNO_3	0.0549	0.0636	0.0942	0.215	0.683	2.040

Table 3-5
Equivalent Conductance and μS/cm per ppb vs. Species Added to Pure Water

Cation	Equivalent Conductance	μS/cm per ppb	Anion	Equivalent Conductance	μS/cm per ppb
H^+	350	0.346535	OH^-	199	0.011699
Li^+	38.69	0.005575	F^-	54.40	0.002863
Na^+	50.11	0.002180	Cl^-	76.35	0.002154
K^+	73.50	0.001880	Br^-	78.10	0.000977
Rb^+	77.80	0.000910	I^-	76.80	0.000605
Cs^+	77.30	0.000582	NO_2^-	71.80	0.001561
NH_4^+	73.50	0.004074	NO_3^-	71.40	0.001152
Mg^{2+}	53.06	0.004363	HCO_3^-	44.50	0.000729
Ca^{2+}	59.50	0.002969	$HS0_4^-$	50.00	0.000515
Sr^{2+}	59.46	0.001357	$H_2PO_4^-$	33.00	0.000340
Ba^{2+}	63.90	0.000931	$HS0_3^-$	50.00	0.000617
Cr^{3+}	67.00	0.003866	$C_2H_3O_2^-$	40.90	0.000693
Mn^{2+}	53.50	0.001948	HS^-	65.00	0.001966
Fe^{2+}	54.00	0.001933	CO_3^{2-}	72.00	0.002400
Fe^{3+}	68.00	0.003652	PO_4^{3-}	69.00	0.002179
Co^{2+}	53.00	0.001798	HPO_4^{2-}	57.00	0.001188
Ni^{2+}	50.00	0.001703	SO_3^{2-}	79.90	0.001996
Cu^{2+}	55.00	0.001731	SO_4^{2-}	80.00	0.001666
Zn^{2+}	52.80	0.001615	$C_2O_4^{2-}$	74.20	0.001686
Pb^{2+}	71.00	0.000685	$HCrO_4^-$	48.00	0.000410
$ZnOH^+$	26.40	0.000320	CrO_4^{2-}	84.50	0.001457

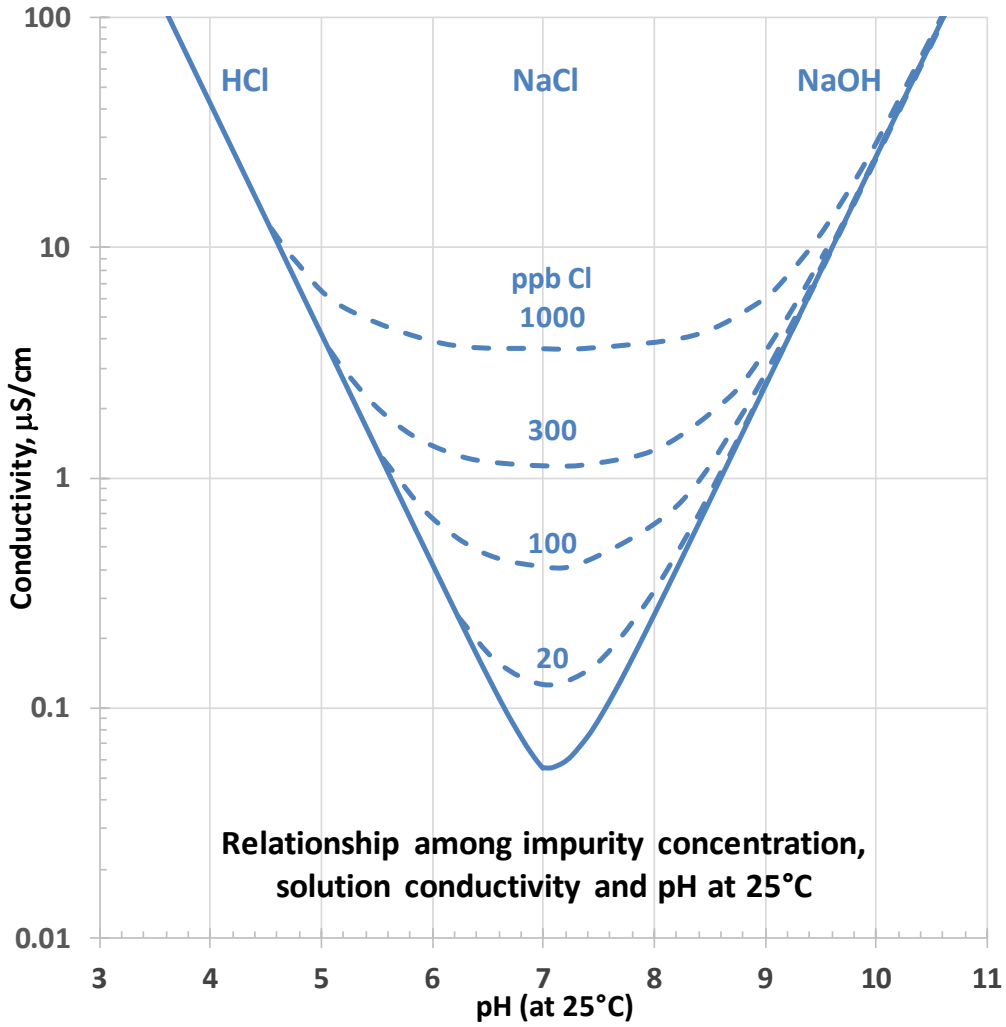

Note: The region below the outer curve is unachievable.

Figure 3-3
Relationship Between pH and Conductivity for the Spectrum of HCl, NaCl and NaOH

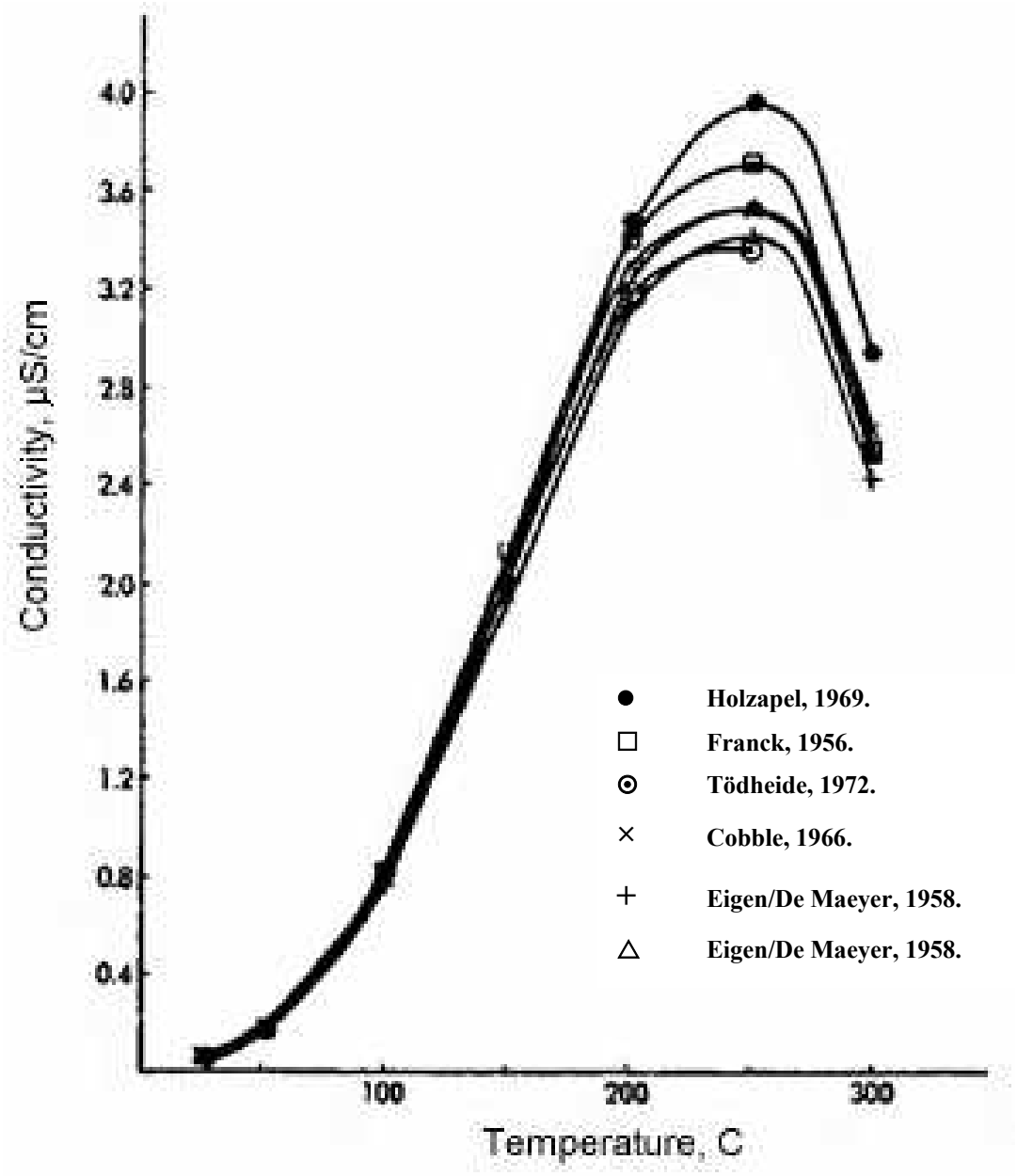

Figure 3-4
Conductivity of Pure Water vs. Temperature

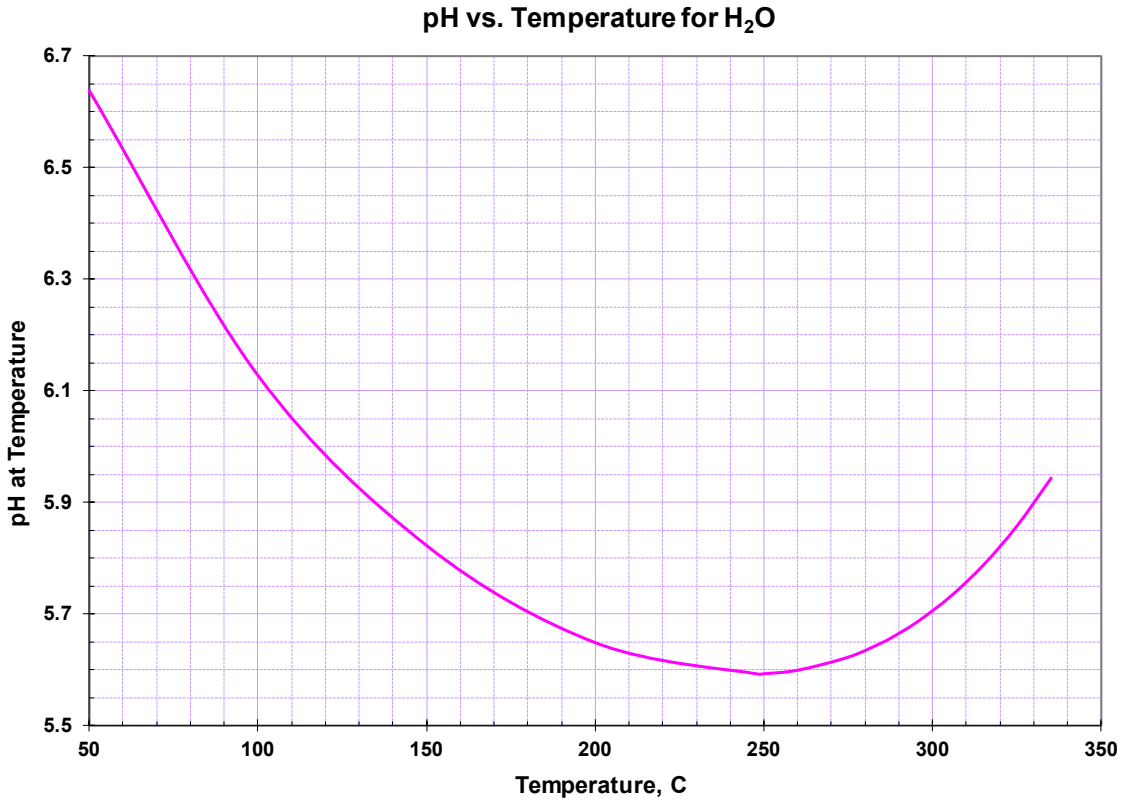

Note: The pK_W is double the pH, and this has a large effect on the pH of alkaline solutions because $[H^+] \times [OH^-] = pK_W$. The pH of $[OH^-] = 1$ is pK_W, which varies from 14 at 25°C to 11.2 at 250°C.

Figure 3-5
pH vs. Temperature for Pure Water

3.2 Asymmetric Water Chemistry Response

Asymmetric response to changes in water chemistry can be observed whenever there is a potential or thermal gradient present in the crack; that is, a driving force for concentrating anions into the crack creates an asymmetric response for rising vs. falling concentrations of impurities [32]. If only ordinary diffusion is operative, symmetry in chemistry is observed, but the growth rate might be sensitive to the lower range of concentrations. For example, if the growth rate is sensitive to 100 ppb of Cl in the crack and the ordinary diffusion transient is from 0 to 10,000 ppb of Cl, then the growth rate can be asymmetric. A far more significant asymmetry can occur with sulfur species because iron and nickel sulfides readily form in the crack at sulfur levels above about 2 ppm. As a result, a transient involving 20 ppm sulfur will continue to pump in sulfur, especially if a potential gradient also exists, which precipitates as a metal sulfide and maintains the dissolved sulfur level in the crack (often HS^-) to about 2 ppm. After extensive metal sulfide formation, when the transient ends, it can take significantly longer for HS^- to diffuse out when the interior concentration is limited (and held) at ~2 ppm. The presence of a potential gradient will of course add to the asymmetry. The dependence of the crack-tip strain rate and crevice water chemistry (for LAS, exposure of dissolvable MnS by the growing crack) on crack growth rate are other further reasons for the asymmetric SCC crack growth response during water chemistry transients.

3.3 Zinc Additions

Zinc (Zn) additions are used in BWRs and PWRs primarily to reduce the shutdown dose rate, although SCC mitigation is also a benefit [59]. Zn is preferentially incorporated into the tetrahedral (+2 oxidation state) sites in spinel oxides (such as Fe_3O_4), and thus tends to displace Co^{+2}, Ni^{+2} and other radioactive species. Zn also makes the oxide more protective and thinner. Since spinel oxides form on free surfaces of both nickel and iron alloys, a consistent benefit on SCC and CF initiation is observed [54]. For SCC growth, benefits have only consistently been observed for stainless steel, not for nickel alloys. The most likely explanation is that, unlike stainless steels, in nickel alloys such as Alloy 600 and Alloy 182/82 weld metals, the prevailing oxide near the crack is an NiO structure rather than spinel.

Monitoring and controlling Zn additions is challenging because some forms of Zn (like ZnO) do not affect the room temperature conductivity of pure water too significantly and because neither ZnO nor Zn acetate, at relevant concentrations, effect the conductivity or pH of B/Li solutions. PWRs generally inject Zn acetate while BWRs use pellets of ZnO through which a side-stream of heated water flows. For BWR tests, laboratory experiments often use fumed, nm-sized ZnO, which readily dissolves (or remains suspended as nano-sized particles) in room temperature water. Many BWRs, and a few PWRs, use depleted Zn where ^{64}Zn is reduced from 49.2% to less than 1%; ^{64}Zn activates to ^{65}Zn and is a 1.115 million electron volts (MeV) gamma emitter with a half-life of 244 days and contributes to operating and shutdown dose rates.

In laboratory tests, a known Zn concentration at the autoclave inlet is a poor measure of what the specimen is experiencing because Zn is initially absorbed by all oxide films in the system. Typically, the autoclave outlet Zn level lags far behind the inlet for weeks depending on the Zn level injected, the flow rate and the surface area of the specimens, autoclave, tubing, and so on. A further complication is related to Zn diffusion into cracks or crevices where the diffusional supply is limited in a tight crack or crevice and Zn is first absorbed into the oxides near the crevice/crack mouth while the crack is growing and creating new surface area. Zn will be removed by the demineralizer in a closed-loop system so there are several approaches to introducing and controlling the Zn concentration. One approach is to bypass the demineralizer so that Zn is not removed; in this case, Zn must be added until the oxides films throughout the system are equilibrated to the desired Zn level. This can only be determined by analysis of the autoclave outlet water for Zn. It is not uncommon to "spike" the Zn to higher levels to accelerate its absorption into the films and into the crack/crevice. A second approach is to leave the closed-loop system demineralizer in place and continuously inject Zn into the autoclave inlet water using the flow "dilution" approach described above. In this approach, the initial Zn concentration can also be "spiked" to accelerate its absorption.

Zn occupies the +2 valence (tetrahedral) sites in Fe_3O_4 type spinel oxides, where the $Fe^{2+}Fe^{3+}Fe^{+3}O_4$ can have Ni^{2+}, Co^{2+}, Zn^{2+}, Cr^{3+} and other substitutions. The Zn spinel has a lower free energy oxide than most other forms, creates a more dense, protective oxide, and reduces the level of Co^{2+} that get incorporated into the oxide. Co activates and is a major contributor to shutdown dose rate. The oxides on the free surface of Fe-Ni-Cr alloys always have a spinel structure and therefore, an SCC initiation benefit is observed for Fe and Ni alloys. Near the crack tip of nickel alloys, an NiO structure seems to predominate. There is no known benefit of Zn in non-spinel oxides such as NiO or Cr_2O_3, so no reduction in crack growth rate is expected (or, at least no reduction is consistently observed).

As the temperature drops Zn is released from the oxides. Thus, cycling temperature can accelerate the removal of Zn from laboratory systems, although a reduction from 10 or 20 ppb to less than 1 ppb can take a few weeks of temperature cycling at a few cycles per day.

3.4 Buffered Chemistries

Common buffered water chemistries include PWR primary water (a mix of H_3BO_3/LiOH), H_3BO_3/KOH (used in VVERs[1] and actively considered for western PWRs), NH_3, and LiOH (used in CANDU[2] reactors). The B concentration controls the reactivity through the PWR fuel cycle and a coordinated concentration of LiOH is used to maintain the desired pH. A typical beginning-of-fuel cycle chemistry is about 1,500 ppm B and 2 ppm Li and a typical end-of-cycle chemistry is less than 10 ppm of B and ~0.25 ppm of Li; the precise values and trajectory over the fuel cycle vary a bit. B/K chemistries always have Li from transmutation of B, and so should be considered B/K/Li. Designs that use NH_3 or LiOH target a similar high temperature pH, and typical values are ~15 ppm of NH_3 and ~0.25 ppm of Li as LiOH. B, Li and K are often reported in ppm, but additions are made as H_3BO_3, LiOH and KOH, which are factors of 5.72, 6.04 and 1.435 higher in formula weight, respectively. While H_3BO_3 is quite soluble in water, very little of it undergoes the first ionization to H^+ and $H_2BO_3^-$. Table 3-6 shows the pH at 300°C for various combinations of B and Li and Table 3-7 and Table 3-8 show the pH and conductivity at 25°C, respectively. The pH and conductivity are strongly controlled by the LiOH or KOH concentrations (Figure 3-6).

Mixed bed demineralizers can be equilibrated to the target chemistry using a simple room temperature set up involving the demineralizer, a pump and a beaker. The challenge is that a significant amount of chemical must be added before any changes are observed in the conductivity and pH, and then a very sudden change occurs (Figure 3-7). With one species (for example, NH3 or LiOH), solution, conductivity alone can define its concentration. With two species (B/Li or B/K), pH and conductivity are needed to define the concentrations. pH measurements near neutral pH are challenging and the presence of B can affect the pH electrodes. Temperature has a major effect on the pH of these solutions and a pH(25°C) of 9.56 for 0.25 ppm Li as LiOH becomes a pH(300°C) of 6.95. B/Li and B/K solutions change less between room temperature and ~300°C, but the differences are still large. Importantly, all solutions change pH with variations in high temperature, so the pH(300°C) and pH(320°C) and pH(340°C) differ in a non-linear fashion, primarily from changes in the dissociation constant of water (see Table 3-9 and Table 3-10 and Figure 3-5).

Care should be taken to avoid introducing oxidants with buffered chemistries as some materials exhibit much higher growth rates (Figure 3-8). The effect is more pronounced in lower Cr materials such as sensitized SS than in high Cr materials like Alloy 690.

[1] The water-water energetic reactor (WWER), or VVER (from Russian: водо-водяной энергетический реактор, which transliterates as vodo-vodyanoi energeticheskiy reaktor; water-water power reactor) is a series of PWR designs originally developed in the Soviet Union, and now Russia, by OKB Gidropress.

[2] The CANDU (Canada Deuterium Uranium) is a Canadian pressurized heavy-water reactor design used to generate electric power.

Table 3-6
pH at 300°C as a Function of B and Li Concentrations

pH =	6.7	6.8	6.9	7	7.1	7.2	7.3	7.4	7.5
B (ppm)	Li (ppm)								
0	0.14	0.18	0.22	0.28	0.36	0.45	0.57	0.73	0.92
50	0.18	0.23	0.29	0.37	0.46	0.59	0.75	0.95	1.21
100	0.22	0.28	0.36	0.45	0.57	0.73	0.92	1.17	1.49
150	0.27	0.34	0.43	0.54	0.69	0.87	1.10	1.40	1.79
200	0.31	0.39	0.50	0.63	0.80	1.01	1.28	1.63	2.08
250	0.35	0.45	0.57	0.72	0.91	1.15	1.47	1.87	2.38
300	0.40	0.50	0.64	0.81	1.02	1.30	1.65	2.10	2.68
400	0.48	0.61	0.78	0.99	1.25	1.59	2.03	2.59	3.30
500	0.57	0.73	0.92	1.17	1.49	1.89	2.41	3.08	3.93
600	0.66	0.84	1.07	1.36	1.73	2.20	2.80	3.58	4.58
700	0.75	0.96	1.22	1.55	1.97	2.51	3.20	4.09	5.24
800	0.85	1.08	1.37	1.74	2.21	2.82	3.60	4.61	5.91
900	0.94	1.19	1.52	1.93	2.46	3.14	4.02	5.14	
1,000	1.04	1.32	1.67	2.13	2.72	3.47	4.44	5.69	
1,100	1.13	1.44	1.83	2.33	2.97	3.80	4.86		
1,200	1.23	1.56	1.99	2.54	3.24	4.14	5.30		
1,300	1.33	1.69	2.15	2.74	3.50	4.48	5.75		
1,400	1.43	1.82	2.32	2.96	3.78	4.83			
1,500	1.53	1.95	2.48	3.17	4.05	5.19			
1,600	1.64	2.08	2.66	3.39	4.33	5.56			
1,700	1.74	2.22	2.83	3.61	4.62	5.93			
1,800	1.85	2.36	3.00	3.84	4.91				
1,900	1.96	2.49	3.18	4.07	5.21				
2,000	2.07	2.64	3.37	4.30	5.52				
2,100	2.18	2.78	3.55	4.54	5.82				
2,200	2.30	2.93	3.74	4.79					

Table 3-7
pH at 25°C as a Function of B and Li

B (ppm)	Li (ppm)												
	0	**0.5**	**1**	**1.5**	**2**	**2.5**	**3**	**3.5**	**4**	**4.5**	**5**	**5.5**	**6**
0	7.00	9.86	10.16	10.33	10.46	10.56	10.64	10.70	10.76	10.81	10.86	10.90	10.94
50	5.79	7.44	7.75	7.93	8.06	8.17	8.25	8.33	8.39	8.45	8.51	8.56	8.60
100	5.64	7.13	7.44	7.62	7.75	7.85	7.93	8.00	8.06	8.12	8.17	8.21	8.25
150	5.55	6.95	7.25	7.43	7.56	7.66	7.74	7.81	7.87	7.93	7.97	8.02	8.06
200	5.48	6.82	7.12	7.30	7.43	7.53	7.61	7.68	7.74	7.79	7.84	7.88	7.92
250	5.43	6.72	7.02	7.20	7.32	7.42	7.50	7.57	7.63	7.68	7.73	7.77	7.81
300	5.38	6.63	6.93	7.11	7.23	7.33	7.41	7.48	7.54	7.59	7.64	7.68	7.72
400	5.31	6.48	6.78	6.96	7.09	7.19	7.27	7.33	7.39	7.45	7.49	7.54	7.58
500	5.25	6.36	6.66	6.84	6.97	7.06	7.14	7.21	7.27	7.32	7.37	7.41	7.45
600	5.20	6.26	6.56	6.73	6.86	6.96	7.04	7.10	7.16	7.22	7.26	7.31	7.34
700	5.15	6.16	6.46	6.63	6.76	6.86	6.94	7.01	7.07	7.12	7.17	7.21	7.25
800	5.10	6.07	6.37	6.54	6.67	6.77	6.85	6.92	6.98	7.03	7.07	7.12	7.16
900	5.06	5.98	6.28	6.46	6.58	6.68	6.76	6.83	6.89	6.94	6.99	7.03	7.07
1,000	5.02	5.91	6.20	6.38	6.50	6.60	6.68	6.75	6.81	6.86	6.91	6.95	6.99
1,100	4.98	5.83	6.12	6.30	6.43	6.52	6.60	6.67	6.73	6.78	6.83	6.87	6.91
1,200	4.94	5.76	6.05	6.23	6.35	6.45	6.53	6.60	6.66	6.71	6.76	6.80	6.84
1,300	4.91	5.69	5.98	6.16	6.28	6.38	6.46	6.53	6.59	6.64	6.69	6.73	6.77
1,400	4.87	5.62	5.91	6.09	6.21	6.31	6.39	6.46	6.52	6.57	6.62	6.66	6.70
1,500	4.84	5.56	5.85	6.02	6.15	6.25	6.33	6.39	6.45	6.51	6.55	6.60	6.63

Table 3-7 (continued)
pH at 25°C as a Function of B and Li

B (ppm)	Li (ppm)												
	0	**0.5**	**1**	**1.5**	**2**	**2.5**	**3**	**3.5**	**4**	**4.5**	**5**	**5.5**	**6**
1,600	4.81	5.50	5.79	5.96	6.09	6.18	6.26	6.33	6.39	6.44	6.49	6.53	6.57
1,800	4.75	5.39	5.67	5.84	5.97	6.07	6.15	6.21	6.27	6.32	6.37	6.41	6.45
1,900	4.72	5.33	5.61	5.79	5.91	6.01	6.09	6.16	6.22	6.27	6.31	6.36	6.40
2,000	4.70	5.28	5.56	5.73	5.86	5.95	6.03	6.10	6.16	6.21	6.26	6.30	6.34
2,100	4.67	5.23	5.51	5.68	5.81	5.90	5.98	6.05	6.11	6.16	6.21	6.25	6.29
2,200	4.64	5.19	5.46	5.63	5.75	5.85	5.93	6.00	6.06	6.11	6.16	6.20	6.24

Table 3-8
Conductivity in μS/cm at 25°C as a Function of B and Li

B (ppm)	Li (ppm)											
	0	**0.5**	**1**	**1.5**	**2**	**2.5**	**3**	**3.5**	**4**	**4.5**	**5**	**5.5**
0	0.1	17.1	34.3	51.4	68.6	85.7	102.9	120.0	137.2	154.3	171.5	188.6
50	0.6	5.7	11.5	17.2	22.9	28.7	34.4	40.2	45.9	51.7	57.4	63.2
100	0.9	5.7	11.4	17.1	22.8	28.5	34.2	40.0	45.7	51.4	57.1	62.8
150	1.1	5.7	11.4	17.1	22.8	28.5	34.1	39.8	45.5	51.2	56.9	62.6
200	1.3	5.7	11.4	17.0	22.7	28.4	34.1	39.7	45.4	51.1	56.8	62.4
250	1.5	5.7	11.4	17.0	22.7	28.3	34.0	39.6	45.3	50.9	56.6	62.3
300	1.6	5.7	11.3	17.0	22.6	28.2	33.9	39.5	45.1	50.8	56.4	62.1
400	1.9	5.7	11.3	16.8	22.4	28.0	33.6	39.2	44.8	50.4	56.0	61.6
500	2.2	5.7	11.2	16.7	22.3	27.8	33.4	38.9	44.5	50.0	55.6	61.1
600	2.5	5.7	11.1	16.6	22.1	27.6	33.1	38.6	44.1	49.6	55.1	60.6
700	2.7	5.7	11.0	16.5	21.9	27.3	32.8	38.2	43.7	49.2	54.6	60.1
800	3.0	5.7	11.0	16.3	21.7	27.1	32.5	37.9	43.3	48.7	54.1	59.5
900	3.4	5.8	10.9	16.2	21.5	26.9	32.2	37.6	42.9	48.3	53.7	59.0
1,000	3.7	5.8	10.9	16.1	21.4	26.7	32.0	37.3	42.6	47.9	53.2	58.5
1,100	4.0	5.8	10.8	16.0	21.2	26.5	31.7	37.0	42.2	47.5	52.8	58.1
1,200	4.4	5.9	10.8	15.9	21.1	26.3	31.5	36.7	41.9	47.2	52.4	57.6
1,300	4.7	6.0	10.8	15.8	21.0	26.1	31.3	36.5	41.7	46.8	52.0	57.2
1,400	5.1	6.1	10.8	15.8	20.9	26.0	31.1	36.3	41.4	46.6	51.7	56.9
1,500	5.5	6.2	10.8	15.7	20.8	25.9	31.0	36.1	41.2	46.3	51.4	56.5

Table 3-8 (continued)
Conductivity in μS/cm at 25°C as a Function of B and Li

B (ppm)	Li (ppm)											
	0	**0.5**	**1**	**1.5**	**2**	**2.5**	**3**	**3.5**	**4**	**4.5**	**5**	**5.5**
1,600	5.9	6.3	10.8	15.7	20.7	25.8	30.8	35.9	41.0	46.1	51.1	56.2
1,800	6.8	6.6	10.9	15.7	20.6	25.6	30.6	35.6	40.6	45.7	50.7	55.7
1,900	7.2	6.8	11.0	15.7	20.6	25.5	30.5	35.5	40.5	45.5	50.5	55.5
2,000	7.7	7.0	11.1	15.7	20.6	25.5	30.4	35.4	40.4	45.3	50.3	55.3
2,100	8.1	7.2	11.2	15.8	20.6	25.4	30.4	35.3	40.3	45.2	50.2	55.2
2,200	8.6	7.5	11.3	15.8	20.6	25.4	30.3	35.2	40.2	45.1	50.1	55.0

Table 3-9
***pK*$_W$ of Water vs. Temperature**

Temp. (°C)	25	100	150	200	250	300	310	320	330	340	350
pK_W	14.01	12.27	11.64	10.93	11.19	11.41	11.46	11.62	11.78	12.00	12.30
pH of 1N H^+	1.00	1.00	1.00	1.00	1.00	1.00	1.00	1.00	1.00	1.00	1.00
pH of pure water	7.006	6.136	5.822	5.464	5.596	5.703	5.729	5.810	5.892	6.001	6.150
pH of 1N OH^-	14.01	12.27	11.64	10.93	11.19	11.41	11.46	11.2	17.78	12.00	12.30

Table 3-10
pH of 1,500 ppm B, 2.6 ppm Li Solution vs. Temperature

Temp. (°C)	pH_T	ΔpH	$pK_W/2$	$\Delta pK_W/2$	Log[OH^-]
310	7.000	0	5.729	0	4.458
320	7.146	0.146	5.810	0.162	4.474
330	7.327	0.327	5.892	0.326	4.457
340	7.557	0.557	6.002	0.544	4.445
350	7.867	0.867	6.150	0.842	4.433

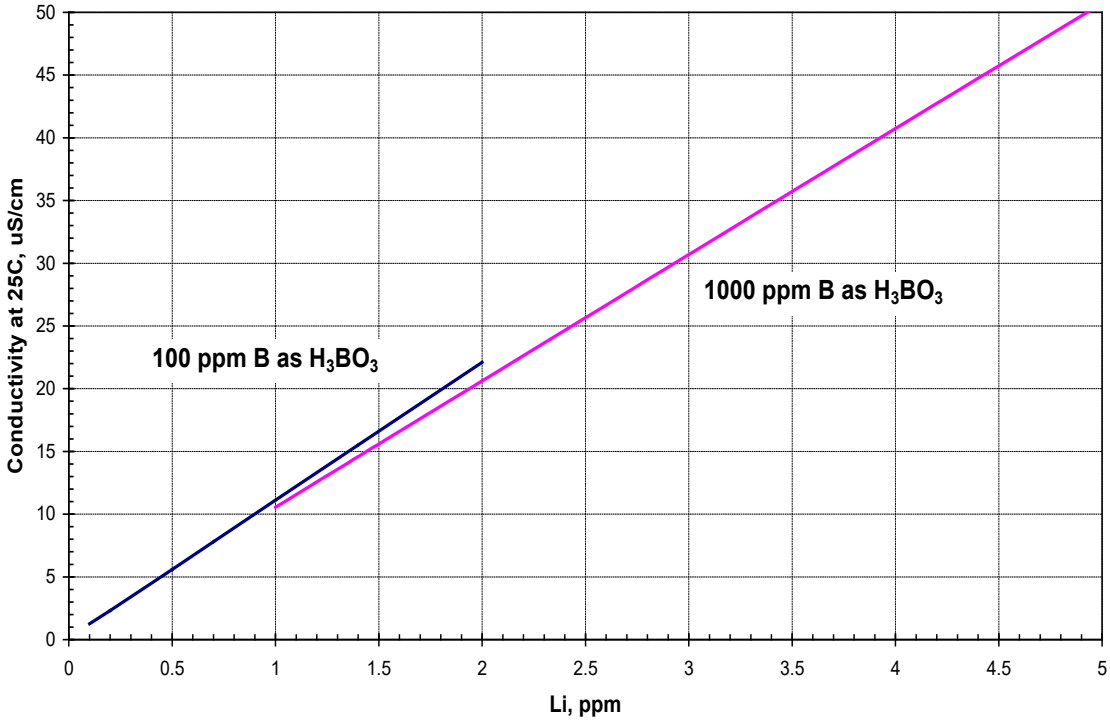

Note: The conductivity (and pH) of B/Li solutions is most strongly affected by the Li concentration because very little of the H_3BO_3 ionizes to H^+ and H_2BO_3. At 1,000 ppm B and 2 ppm Li, about 99.43% of the H_3BO_3 remains unionized at 25°C, and 99.7% at 300°C.

Figure 3-6
Conductivity as a Function of Lithium Content

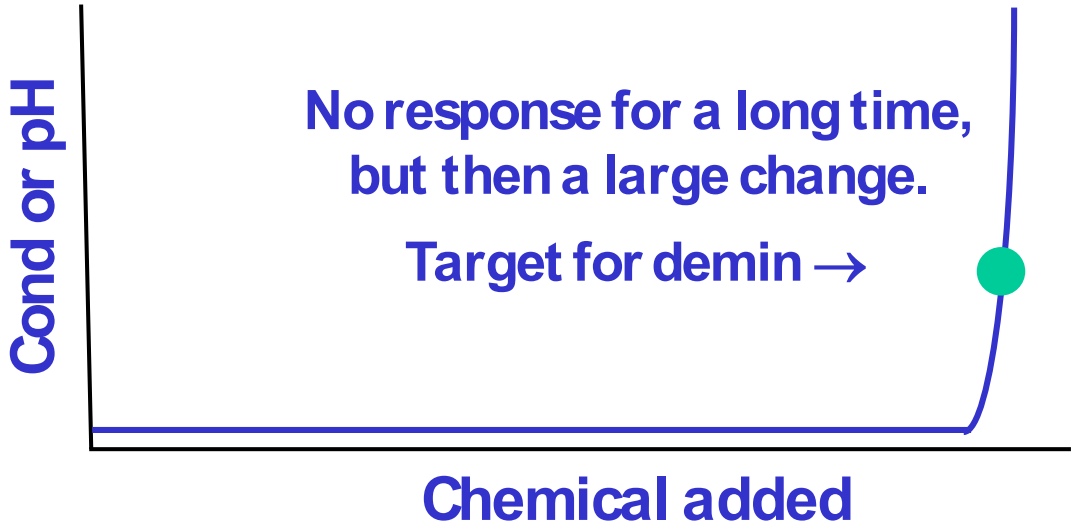

Figure 3-7
Schematic of the Challenge of Equilibrating Mixed-Bed Demineralizers to the Desired Chemistry (for example, for B/Li, B/K, NH_3, and so on)

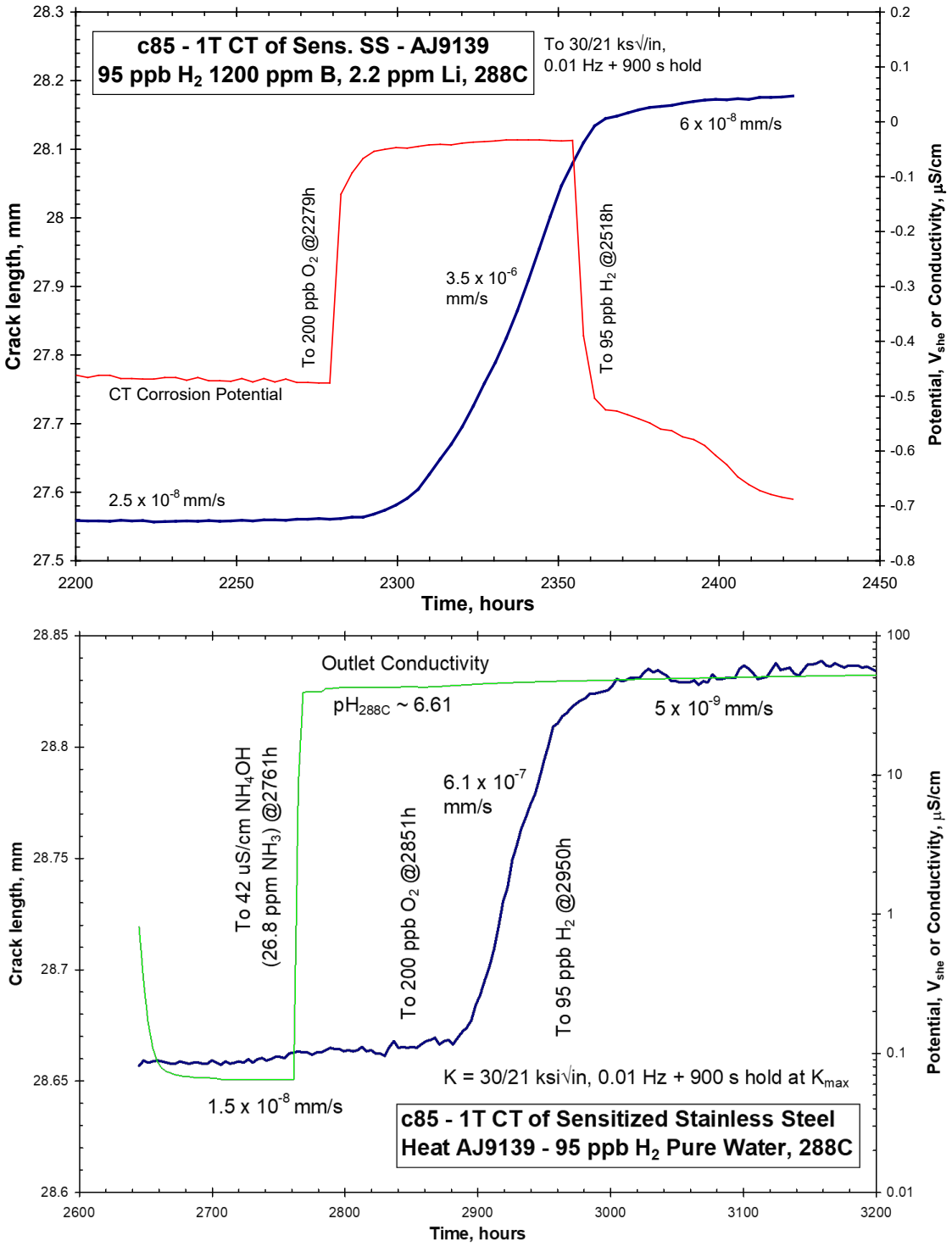

Figure 3-8
Crack length vs. Time for a 1T CT Specimen of Sensitized 304 SS Tested in Deaerated and Aerated Water with B/Li Additions (top) or NH_3 Additions (bottom)

3.5 High Temperature pH

The pH scale in high temperature water can be misleading for high values of pH. This is because many people are accustomed to thinking about pH at room temperature, where the pH of pure water is 7.0, so a H^+ activity equal to 1 yields pH equal to 0, and thus an OH^- activity of 1 yields a pH of 14 because the H^+ is 10^{-14}. The concentrations of H^+ and OH^- in water are linked by the K_W of water (where $K_W = [H^+] \times [OH^-]$), which is 10^{-14} at room temperature. However, at 250°C, the pH of pure water is 5.6 (see Table 3-9), so the pH(250°C) of a solution with an OH^- activity of 1 yields a pH of 11.2 because the activities of H^+ and OH^- in water are controlled by $[H^+] \times [OH^-] = K_W$, and K_W changes with temperature. So, while a pH(25°C) of 10 is not that aggressive, a pH(250°C) of 10 is very aggressive – as much as a factor of $10^{2.8} = 631$. Figure 3-9 shows examples of how the alkaline scale varies with temperature.

Table 3-11 shows that the change in pH vs. temperature of B/Li solutions is almost entirely unrelated to the change in the OH^- concentration, or pOH, but rather to the change in the K_W of water; thus, the pH scale is misleading on the alkaline side.

Table 3-11
Effect of Temperature on the pH_T of B and Li Solution

T (°C)	pK_W	ΔpK_W	1,500 ppm B 2.6 ppm Li pH_T	1,500 ppm B 2.6 ppm Li Delta pH	1,500 ppm B 2.6 ppm Li Log (OH^-)	pOH Log(OH^-)	$2pK_W$
310	5.729	0.000	7.000	0.000	4.458	11.458	11.458
320	5.810	0.162	7.146	0.146	4.474	11.620	11.620
330	5.892	0.326	7.327	0.327	4.457	11.784	11.784
340	6.001	0.544	7.557	0.557	4.445	12.002	12.002
350	6.150	0.842	7.867	0.867	4.433	12.300	12.300

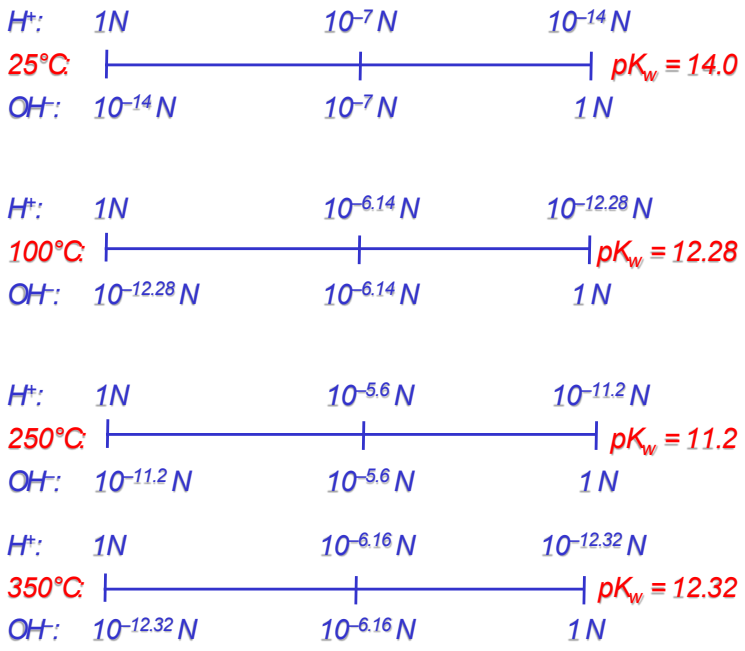

Figure 3-9
Examples of How the Change in K_W Affects the Alkaline Side of the pH Scale

3.6 Unintended Impurities

Unintended impurities can arise from many sources and are not adequately characterized by the conductivity of the autoclave inlet water because not all impurities are equally damaging or are even dissociated into ions. An example of a chemical that dissolves but does not dissociate into ions is sugar and chemicals like SiO_2, H_3BO_3 and ZnO only slightly dissociate in pure water. Many non-ionic impurities decompose at high temperature or under irradiation to form ionic species. For this reason, and because the source of impurities can be in the high temperature part of the system, autoclave outlet conductivity is a much better measure of the water purity to which the specimen is exposed to than the inlet conductivity.

Common sources of unintentional impurities and approaches to identify their origin and resolve the contamination are summarized below:

- Demineralizer resin fines, which decompose in hot water to produce (depending on the demineralizer) sulfate and nitrate, along with any impurity ions that exchanged into the resin. This source can be controlled by placing a sub-micron filter after every demineralizer resin or group of resins.
- Organics can come from the building water supply and can be present in water purified by distillation, demineralization, or reverse osmosis. Demineralizer resins are notorious for having very high organic content until they are flushed and cleaned. It is generally wise to flush out cartridges for several hours using high quality, bacteria-free water. Then the remaining organics can be cleaned by recirculating water through the demineralizer, a

sub-micron filter and an ultraviolet light for several days using a covered beaker to minimize the exposure to the CO_2 in the air (which forms HCO_3^- and will consume some of the demineralizer capacity). A cleaned resin that then sits for weeks or months will show higher organic content as leaching continues to occur from the resin beads.

- Organics in the building water supply are best controlled by isolating the ultra-high purity water system by running the in-coming water through a sub-micron filter (to trap debris, large bacteria, and so on) and an ultraviolet light designed and operated at the proper flow rates to decompose organics and kill bacteria. Careful cleaning of all components and tubing is also necessary since, for example, tubing often has residual lubricant, stampings, and so on. Final sterilization of the pure water system and distribution piping using hydrogen peroxide, chlorine bleach or iodine at the specified concentration and time is recommended.
- Usually it is preferable to design the autoclave water supply system to operate in a closed loop, with the autoclave effluent measured (for example, for conductivity), then demineralized, sub-micron filtered, and returned to a small reservoir for re-use. Smaller, non-metallic reservoirs are best, and tall, small diameter 'reservoirs' (for example, 2–3 inches [50.5–76.2 mm] in diameter × 60–80 inches [1,524–2,032 mm] tall glass tube) with gas bubblers at the bottom to promote rapid equilibration of dissolved gases are recommended.
- Bacteria originate from many sources, including the building water supply and human handling. Bacteria can often be identified by the slippery, slimy feeling they impart to surfaces, and sometimes by visible deposits. Bacteria is best controlled by:
  - Carefully cleaning the system and components (including prolonged soaking in iodine, chlorine bleach or hydrogen peroxide to kill known infestations)
  - Preventing ingress by avoiding handling, for example, of demineralizers and autoclave internals during assembly and specimen installation
  - Installing a bacteria trap at the building water supply system (involving a sub-micron filter and ultraviolet light, as noted previously)
- Leaching and breakdown of polymers, greases and oils. Greases and oils should be avoided in all parts of the water-wetted system. Manufacturers sometimes test pressure gages, accumulators and other instruments using oils, which are then shipped without cleaning. The high-pressure pump diaphragm can crack and permit oil to infiltrate the water side of the pump. Teflon diaphragms, changed every few years, have been the most reliable means of addressing this.
- Some polymers and elastomers contain plasticizers that leach contaminants into water and should be avoided. In high temperature water up to about 300°C, PTFE Teflon is satisfactory in low stress applications (for example, as electrical insulation around wires). Some leaching of fluoride usually occurs, but this is rarely a problem in refreshed systems, although it has produced cracking of non-Pt wires when they are encased in Teflon tubing that was not pre-exposed to hot water to release 'excess' fluorine. The pressure seal for wire feed-throughs and the pull rod can use Teflon, but it is usually possible to operate the Teflon below 200°C when the autoclave is inverted, and the seals are extended below the autoclave head. Using

Teflon or zirconia 'washers' to restrict the motion of water in the seal area of the autoclave head can also help. Most other polymers, including polyether ether ketone (PEEK) (a radiation resistant polymer) break down to a greater extent; PEEK remains structurally useful, but can elevate the outlet conductivity of 288°C water.

- Some reference electrodes (for example, Ag/AgCl) leach chloride. Apart from the obvious solution of avoiding these types of reference electrodes, approaches for controlling this contamination focus on reducing the diffusion rate of the chloride from the electrode. This can be done by reducing the chloride concentration in the electrode (for example, from 0.1 to 0.01 N KCl); using pure water (see Section 3.12 on reference electrodes); reducing the porosity of the ionic junction in the electrode; adding a secondary "isolation" chamber filled with pure water; or using a second ionic junction.
- Chromium containing materials will release soluble chromates (Cr^{+6} as CrO_4^{2-}) in high temperature water at high corrosion potential. Their contribution to conductivity is controlled by the surface area of chromium-containing materials exposed to hot water, the corrosion potential (for example, oxygen content), and autoclave refresh rate. Approaches to minimizing chromate contamination include using lower oxidant levels, changing to titanium tubing and internal autoclave parts for the hot portions of the system, increasing the flow rate, and decreasing the autoclave size (for example, pieces of titanium or PTFE Teflon can be used to reduce the water volume in an autoclave). A chromate transient is always observed when oxygen is added following exposure to deaerated or hydrogenated water, as chromium is oxidized from the outer parts of the films. Chromate can be distinguished from other contaminants by comparing the autoclave outlet conductivity in Ar or N_2 deaerated water, where other contaminants will still be present, to that in oxygen containing water, which primarily enhances the chromate contribution.
- Air saturated water contains carbon dioxide in sufficient concentration (that is, 0.040% and above) to raise the conductivity of pure water from 0.0549 μS/cm to about 1 μS/cm and decrease the pH from 7.0 to about 5.6. This precludes the use of grab samples for the measurement of conductivity, at least for solutions below about 20 μS/cm. It is also the reason why testing in air saturated water cannot be considered high purity water. Frequent water chemistry analysis should be done, since a few ppb of specific anions can affect the SCC behavior under oxidizing conditions, especially in CS and LAS.
- The use of copper, lead, mercury, arsenic, sulfur, and so on, should be completely avoided, since all these chemicals can affect SCC, and many can be very difficult to remove. Copper ion is an oxidant and sulfur, especially sulfide, inhibits repassivation and increases crack growth rate. Most contamination is inadvertent, for example, from lubricants such as molybdenum di-sulfide, anti-galling/anti-seize compounds (many contain copper, and all but graphite should be considered suspect in terms of impurities), brazes (copper and silver are common), graphoil seals, and so on.
- Silica is generally present at high levels in BWRs and PWRs (often between 100 and 1,000 ppb). Since silica dissociates sparingly, most is soluble in the non-ionic form; only about 1% ionizes at room temperature. High quality demineralizers can effectively remove silica. In turn, while few studies have been performed, most show no measurable effect of

silica on SCC. However, in metal alloys, silicon segregation to grain boundaries can cause high growth rates because silicon oxidizes at all relevant potentials in high temperature water and is reasonably soluble [16].

- Dissolution in hot water of many ceramic spacers and insulators is a concern. Dissolution of silica-based ceramics in hot water is relatively rapid. High purity alumina can often be used in pure 288°C water, although its dissolution rate can increase significantly in B/Li high temperature water. The most commonly used ceramic in hot water is zirconia, generally partially stabilized zirconia (for example, with 3% MgO).

Measurements of autoclave inlet and outlet conductivity should be continuously performed. pH and specific ionic chemistry should be periodically measured when intentional additives like B/Li are used but are generally not necessary in pure water where conductivity can define the maximum ion concentrations and pH shift. Nominally high quality chemicals (for example, boric acid) can also contain sufficient sulfur to increase cracking in LAS and CS materials. Special low sulfur grades of chemicals should be considered if significant concentrations of additives will be present, although closed-loop systems with demineralizers equilibrated to the desired B/Li level are a very effective way to control these contaminants.

Good water purity can be maintained during testing in closed-loop systems running with additives such as boric acid/lithium hydroxide, ammonia, and so on. While commercial demineralizers equilibrated to the target chemistry are available, the simplest approach involves conversion of standard mixed-bed demineralizers by flowing water at room temperature through them and adding the species of interest until, at steady state conditions, the demineralizer maintains the desired concentration (for example, 1,000 ppm B as H_3BO_3 and 1 ppm Li as LiOH). The challenge is that a significant amount of chemical must be added before any change in conductivity and pH is observed, and then a very sudden change occurs (Figure 3-7). After equilibration, the demineralizer will help maintain the desired concentration of additive as well as purify the solution of unwanted species. Shifts in the room or water temperature will alter the solution's affinity for B, Li, NH_3, and so on, and can cause some change in the water chemistry.

Diagnosis of water purity issues in the autoclave system must recognize that with oxygen present, Cr containing materials will release chromate into the water. Similarly, with increasing hydrogen, Fe^{+2} becomes more soluble. So, it is best to evaluate the basic system performance using nitrogen or Ar deaerated water (the presence of less than 100 ppb hydrogen is acceptable). With high purity (0.055 μS/cm) inlet water, the autoclave outlet should have a conductivity of less than 0.1 μS/cm, and ideally less than 0.060 μS/cm. Outlet conductivity is a measure of the contribution of residual oils and greases in the system, leaching of fluoride from Teflon, leakage of chloride from Ag/AgCl reference electrodes, breakdown of organics in the inlet water, and so on. With up to 2–3 ppm of hydrogen, the outlet conductivity should be less than 0.1 μS/cm, and with ~2 ppm of oxygen, it should be less than 0.15 μS/cm. Good systems can maintain an outlet conductivity of less than 0.07 μS/cm with ~2 ppm oxygen. The effect of 5 ppb chloride in the presence of 20+ ppb of other unknown and varying ionic species cannot be reasonably investigated. These criteria can be relaxed under some circumstances, such as testing in deaerated or hydrogenated water, where the sensitivity to less than 30 ppb of most impurities is low.

3.7 Dissolved Gases

Dissolved gas control and measurement are very important during SCC testing. Concerns include proper equilibration of gases, gas in-leakage, gas consumption in the autoclave, and proper measurement of dissolved gases. The concentration of dissolved gases in water varies with the gas, the pressure at which it is bubbled through water, temperature, and, to a lesser practical extent, with barometric pressure and dissolved solids. For pure oxygen or pure hydrogen bubbled through water, Table 3-12 shows the dissolved gas concentrations vs. water temperature [33], where the first rows of numbers assume that 1 atmosphere of gas partial pressure is maintained; the rows with an asterisk ("*") account for the increased vapor pressure of water vs. temperature for an open container where the total pressure is held constant at 1 atmosphere, so that the partial pressure of oxygen or hydrogen decreases with temperature. Variations in room temperature have a much larger effect on dissolved oxygen concentration than they have on dissolved hydrogen concentration. At very high solute concentrations, a "salting out" effect reduces the solubility of gases. For example, in 20°C sea water, the solubility of oxygen is ~21% lower than in pure water.

The solubility of the gas vs. water temperature in Table 3-12 is different than if gas is equilibrated in water at room temperature, then the water is pumped/pressurized, heated and passed through the autoclave. Since the concentration of gas in the water is fixed as the water is heated, it may be erroneously assumed that the fugacity is also fixed, but this is not true, especially above about 100°C [34, 35]. The fugacity of hydrogen vs. temperature is shown in Table 3-13 for 1 atmosphere of hydrogen dissolved in 25°C water (that is, 17.56 cc/kg, or 1.58 ppm hydrogen).

The composition of air is about 20.95% oxygen, 0.04% carbon dioxide, and 0.5 ppm hydrogen by volume. Therefore, when air is bubbled through (pure) water at 20°C, there is 9.07 ppm dissolved oxygen (8.23 ppm at 25°C), and carbon dioxide forms H^+ and HCO_3^- which raises the conductivity of pure water to about 1 μS/cm. Dissolved gases can be assumed to exhibit ideal behavior so that, for example, a mixture of 10% oxygen and 10% hydrogen in argon bubbled through 20°C water in an open container would yield 43.3 × 10% = 4.33 ppm oxygen and 1.58 × 10% = 0.158 ppm hydrogen. In turn, if pure oxygen is bubbled through 20°C water at 20 atmospheres partial pressure, the dissolved oxygen content is 44.3 × 20 = 886 ppm.

Achieving a very high concentration of dissolved oxygen or hydrogen is a challenge but such a concentration can be relevant to situations such as the pressurization to 160 atmospheres of trapped air in PWRs, which can produce more than 1,500 ppm oxygen. At 25°C, this would require an overpressure of ~35 atmospheres of pure oxygen, which requires a reservoir designed for high pressure in which to equilibrate the oxygen. An alternative is to bubble oxygen in the autoclave at a rate that exceeds its solubility in the flowing water at temperature and pressure. Table 3-14 shows that the solubility of oxygen rises significantly with temperature, and autoclaves are designed to handle the pressure better than room temperature reservoirs. Table 3-14 shows the dissolved oxygen achievable for a fixed system pressure of 2,250 psia (155.1 bar) and varying water temperature, which controls the vapor pressure of water and therefore the maximum partial pressure available for oxygen. To ensure oxygen saturated water, excess oxygen should be continuously flowed into the autoclave. This can be managed by positioning the water outlet tube near the top of the autoclave so that the oxygen bubble at the top of the autoclave only expands down to the location of the water outlet tube.

Equilibration of gases in water should be accomplished using continuous gas flow and fritted bubblers, which are much more efficient in equilibrating gases than a simple immersed tube, which in turn is much better than just controlling the gas space above a liquid. This is especially critical when the water flowing back into the reservoir has a different dissolved gas concentration than desired. This is often the case when low concentrations of oxygen (for example, less than 100 ppb) are used, mixtures of hydrogen and oxygen are used, or radiolysis occurs in the water loop. Mixtures of gases from two sources should be blended by mass flow controllers, which are much more precise and stable than simple needle valve/float-based flow meter schemes.

Since oxygen is consumed to varying degrees in the autoclave system, the autoclave outlet concentrations can vary substantially from the autoclave inlet, especially at low concentrations (for example, less than 100 ppb oxygen). The presence of hydrogen or impurities, which promotes corrosion and therefore consumption of oxygen, aggravates the problem. Controlling dissolved oxygen stable at levels below ~30 ppb is therefore very difficult. Conversely, since oxygen levels down to a few ppb have strong effects on corrosion potential and SCC, small amounts of residual oxygen can have a large effect on the resulting crack growth. To control fixed, low levels of dissolved oxygen, it is generally necessary to use a high flow (autoclave refresh) rate, a small autoclave volume, a minimum hot metal surface area, and/or titanium or titanium alloys on surfaces exposed to the hot water as much as possible. An experiment may be considered ambiguous and unacceptable when 100 ppb of oxygen exists at the autoclave inlet and 3 ppb of oxygen is measured at the autoclave outlet, and it is even more unacceptable to claim 50 ppb of oxygen, if present at the autoclave inlet, when there is essentially zero oxygen measured at the autoclave outlet.

Under low and “zero” oxygen conditions, special consideration must be given to sources of oxygen in-leakage. Common sources include air in-leakage on the suction side of pumps, especially if the inlet pressure dips sub-atmospheric; back-diffusion paths for oxygen into the reservoir; additions of non-deaerated water to the reservoir, for example, to alter the chemistry or raise the water level; or poor seals around sensors; sample lines, dead legs, and pulse dampeners that can act as “hide-out” locations for oxygen and impurities. Diffusion of gases through plastics must also be accounted for. For example, gas diffusivity can be problematical in clear, flexible Tygon® (silicone) tubing at room temperature at low gas flow rates. In high temperature water, gas diffusivity through Teflon and other plastics can be high, so Teflon tubing should be assumed to be a minimal barrier to gas diffusion. Forming a crevice with bulk Teflon is much more challenging in high temperature water.

To help insure “zero” oxygen concentration, all water should be highly deaerated before addition to the test reservoir or system, since the addition of even small amounts of air saturated water, which contains about 9 ppm oxygen, is capable of affecting a reservoir that contains low oxygen concentrations. The presence of small levels of hydrogen (for example, 1% hydrogen in argon, or about 16 ppb hydrogen at standard temperature and pressure [STP]) in the test reservoir also helps to ensure low potentials by reacting in hot water with the residual oxygen. Direct confirmation of inlet and outlet oxygen levels should be made and performed continuously if low, non-zero, dissolved oxygen levels are desired. Dissolved oxygen content is not the only concern, since various species such as hydrogen peroxide (which will be addressed later) and copper ions are also oxidants. Copper, along with the heavy metals previously mentioned, should be avoided entirely.

Measurement of dissolved oxygen can be accomplished by color comparison, with commercial kits available from CHEMetrics Inc. and other companies. Oxygen concentrations below about 9 ppm may be obtained by excluding contact of the sampled water with air, and values below about 50 ppb are difficult to measure reproducibly. In all cases, only limited resolution (for example, within 10% of full scale, which is about 200 ppb and 10,000 ppb) is possible by simple color comparison, although spectrophotometers provide more sensitivity. Many investigators use polarographic sensors for measurement of dissolved oxygen and hydrogen; these instruments measure the reduction or oxidation current from all of the oxygen (or hydrogen) that diffuses through a thin PTFE Teflon membrane. Other measurement technologies are also available. A wide variety of instruments are available that work reliably at high oxygen levels (for example, above 0.1 ppm); fewer instruments work reliably and accurately for oxygen and hydrogen at levels below about 20 ppb. Calibration should always include verifying a zero reading using Ar or N_2. Note that calibration need not be done in water in most cases, but can be done in gas using the ~3% correction for the contribution of the vapor pressure of water at room temperature; that is, in air, about 9.2 ppm of oxygen might be measured, but in air-saturated water, only about 8.9 ppm of oxygen may be measured depending on the effect of water temperature on both vapor pressure and oxygen solubility.

The control of hydrogen fugacity can be as important as oxygen, especially in PWRs, which use hydrogen over-pressure. Because the corrosion potential in deaerated water is controlled by the H^+/H_2 line, adjustment of the hydrogen fugacity provides a reliable mechanism for controlling the corrosion potential in deaerated water (Figure 3-10). Since hydrogen in the crack is not consumed by corrosion, like oxygen, nor does it consequentially diffuse into the metal, it also provides one of the few reliable methods for altering the potential at the crack tip. While the hydrogen concentration can readily be controlled by bubbling gases through room temperature water, the fugacity of hydrogen at fixed concentration begins to decrease significantly above about 100°C [34,35]. In deaerated water, hydrogen is often produced by corrosion, so the crack tip can be at somewhat a higher hydrogen level, and hydrogen can build up in static autoclaves if there are materials that corrode relatively rapidly. This is a concern in static autoclaves in PWR water that can be addressed, at least in part, using a Pd/Ag membrane with one side exposed to hot water and a pressure gage applied to the other side for measurement. However, a vacuum must first be created to remove the contribution of other gases to the measured pressure, or to a known pressure of hydrogen gas for control. Pd/Ag membranes have a high hydrogen permeability and can reliably measure or control the hydrogen fugacity in static or (slowly) flowing autoclaves without concern for the variation in fugacity with water temperature. This makes testing in static autoclaves feasible for some PWR primary tests, although impurities may build up and drift outside of an acceptable range.

Table 3-12
Solubility of Gases vs. the Water Temperature During Equilibration[1]

Temp (°C)	20	25	50	75	90	95	100	200	250	300
O2 (ppm)[2]	44.3	40.6	29.9	25.9	25.2	25.1	25.2	45.1	74.5	130
*O2 (ppm)[3]	43.3	39.3	26.3	16.0	7.77	3.17	0			
H2 (ppm)[2]	1.62	1.58	1.48	1.53	1.62	1.65	1.69	3.36	5.24	8.67
*H2 (ppm)[3]	1.58	1.53	1.30	1.00	0.50	0.21	0			

Notes:
1. 1 atmosphere of hydrogen = 1.58 ppm = 17.56 cc/kg (in water at 25°C).
2. Data based on maintaining 1 atmosphere partial pressure of oxygen or hydrogen.
3 Data based on 1 atmosphere total pressure (that is, an open container, so that the partial pressure of oxygen or hydrogen decreases as the vapor pressure of water rises).

Table 3-13
Fugacity of Hydrogen vs. Temperature (for 1 atmosphere of Pure H_2 dissolved in 25°C water)

Temp. (°C)	25	200	300	310	320	330	340	350	360	370
H_2 fugacity (atm.)	1.00	0.302	0.178	0.155	0.131	0.110	0.0885	0.0674	0.0478	0.0281
H_2 fugacity (MPa)	0.101	0.0306	0.0180	0.0157	0.0133	0.0111	0.00897	0.00683	0.00484	0.00285

Table 3-14
Change in Solubility of O_2 vs. Water Temperature During Equilibration (for 2,250 psia (155.1 bar) total system pressure and bubbling O_2 in the autoclave at test temperature)

Temp. (°C)	Total P (psia)	Vapor P (psia)	Available Over P (atm.)	Solubility of O_2 at temperature (ppm per atm. of O_2)	Using Air (ppm O_2)	Using O_2 (ppm O_2)
25	2,250	0.03	153.1	43	1,376	6,582
100	2,250	14.7	152.1	25.2	801	3,832
150	2,250	69	148.4	30.5	946	4,525
200	2,250	225	137.8	45.1	1,298	6,213
250	2,250	576	113.9	74.5	1,773	8,484
300	2,250	1,245	68.4	130	1,858	8,888

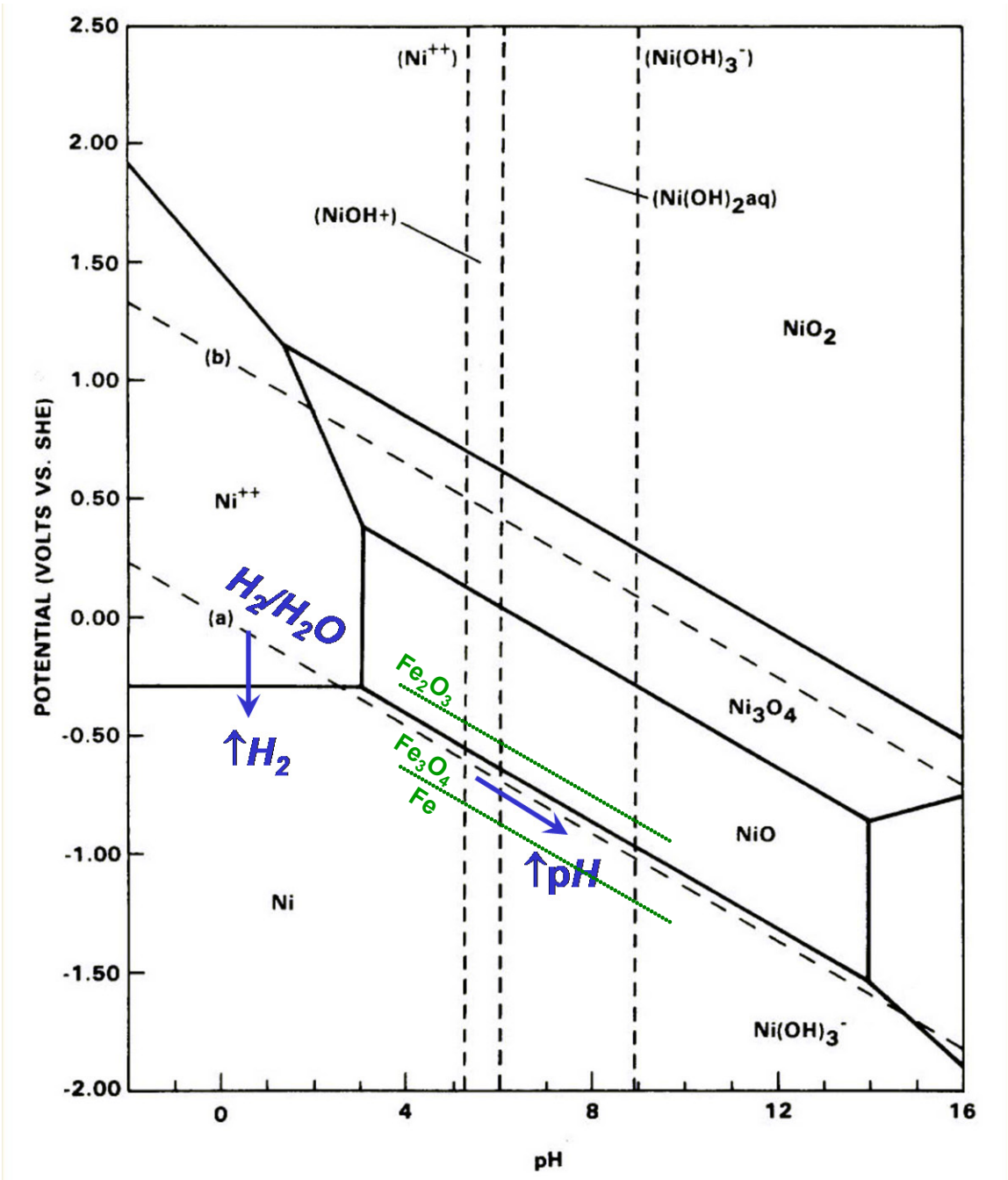

Note: The diagram shows that the Fe and Ni (and Cr) oxide stability lines are exactly parallel to the H^+/H_2 dashed line, which controls the corrosion potential in hydrogenated water without oxidants. Despite the large change in corrosion potential, changes in pH in deaerated water in the mid-pH range have little effect on SCC because the proximity to the metal oxides lines is not changed.

Figure 3-10
Pourbaix Diagram [36]

3.8 Hydrogen Peroxide

As much as ~400 ppb hydrogen peroxide is formed by radiolysis in BWRs, and some investigators add both dissolved oxygen and hydrogen peroxide to their tests to simulate BWR water. (This not a concern for PWRs since radiolysis is suppressed in PWRs, where the dissolved hydrogen is well above the critical level of roughly 400 ppb.) However, hydrogen peroxide is particularly difficult to control because its stability in high temperature water is low, and its decomposition to form oxygen and water is quite rapid on hot metal surfaces. Even when added to metal reservoirs at room temperature, hydrogen peroxide will decompose, which is why it is sold in plastic containers. It is common to find an absence of hydrogen peroxide at the autoclave outlet when adding as much as 100 ppb at the autoclave inlet. To minimize its decomposition as it passes through the autoclave, it is best to use a separate high pressure line of a slightly concentrated hydrogen peroxide solution that injects directly into the autoclave using small bore PTFE Teflon tubing (such as that used for ion chromatography, with a pressure seal applied to the Teflon tubing away from the hot autoclave using stainless steel tubing) or using PTFE Teflon coated stainless steel lines. Even with a separate PTFE Teflon line, it is not entirely reasonable to assume, based on the two relative flow rates going into the autoclave, that the target concentration of hydrogen peroxide exists at the specimen surface; a higher concentration might result from the injected stream, or a lower concentration may be present from decomposition. An approach occasionally used is to create a small, non-pressure-boundary PTFE Teflon chamber or box around the specimen to provide a "protected liquid volume".

Some investigators use a special sample line that is water cooled and/or blended with chilled pure water to quench the sample, so that the hydrogen peroxide has little opportunity to decompose in the sample line. Most analytical techniques for hydrogen peroxide measurement are based on color comparison; commercial kits are available from CHEMetrics Inc. and other companies.

3.9 Chemistry Changes

Gas equilibration is always much faster if the water reservoir is a tall, few-liter pipe with a small diameter tube compared to using a 200-liter metal tank. It is also much faster if the water reservoir is close to full (minimal gas space). Although, for very precise control of dissolved gases, the height of the water column (weight of water) changes the over-pressure at which the gas bubbles equilibrate. A well-designed system can achieve a 99.9% change in gas concentration in minutes; the overall change at the specimen is usually limited by the autoclave volume exchange rate, which is generally in the range of 2–5 per hour.

In most autoclaves, the chemistry change (dissolved gases or ions) follows a perfect mixing law, in which the change follows the exponential of the number of volume exchanges. When decreasing from 1,000 to 0 ppb oxygen or chloride, after one volume exchange, the chemistry drops to exp(-1) = 0.368, or 368 ppb, and after five volume exchanges, it drops to exp(-5), or 0.67 ppb (Table 3-15). When increasing from 0 to 1,000 ppb, after one volume exchange, the autoclave concentration increases to [1–exp(-1)] = 0.632, or 632 ppb (Table 3-15). The decreasing chemistry situation is usually the limiting case because very small levels of residual oxygen can have a large effect on corrosion potential, as discussed in Section 3.10. An increase

in corrosion potential of hundreds of millivolts can be seen at a concentration of a few ppb of dissolved oxygen, so when dropping from 10 ppm oxygen to 0 ppb, 10 volume exchanges are needed to drop the autoclave oxygen level to below 1 ppb; this of course assumes that the water reservoir dropped at time zero to very low levels of oxygen.

Table 3-15
Change in Autoclave Chemistry vs. Volume Exchanges Based on Perfect Mixing

# of Autoclave Volume Exchanges	0.2	0.5	1	2	3	5	8	10
Time (minutes)[1]	12	30	60	120	180	300	480	600
Increasing from 0 to 1,000 ppb	181	393	632	865	950	993	999.7	999.95
Decreasing from 1,000 to 0 ppb	819	607	368	135	50	6.7	0.34	0.045

Note:
1. Time based on a 6-liter autoclave and 100 cc/min (6 liter/hr) refresh rate.

3.10 Corrosion Potentials

Measurement of electrochemical potentials should be performed using a high impedance digital voltmeter (DVM) with an input impedance of greater than 10^9 ohms or an electrometer with an input impedance of about 10^{15} ohms. Many reference electrodes, and the reactions in high temperature water and the conductivity of high temperature water, involve relatively high impedances, for example, 10^4–10^6 ohms. If the measuring device and wiring path is only 10^7 ohms, it biases the reading significantly. Additionally, if the measurement is made continuously, or over extended periods of time, it will eventually damage the reference electrode because it uses its "capacity", somewhat like a battery. For occasional, brief measurements (say, less than every 10 minutes), high quality DVMs, whose input impedance is greater than 10^9 ohms, are generally acceptable. However, in some circumstances such as ZrO_2 membrane electrodes used below ~225°C, whose impedance increases exponentially at lower temperatures, an electrometer must be used. Electrometers generally have in input impedance of ~10^{15} ohms, but the instrument specifications must be matched by the entire circuit path; the wiring, any multiplexer switches, contaminants, proximity of connections/terminals, breaks in the wire insulation, or low quality wire insulation can dramatically reduce the effective input impedance.

Modern DVMs that have an input bias current are better than those that have an input resistance or impedance. That is, an instrument with 10^9 ohms input impedance might have an input bias current of 10^{-9} amp, which is drawn during the measurement independent of the measured voltage. Therefore, when the "source impedance" (of the reference electrode, and so on) is 10^6 ohms, a bias current of 10^{-9} amp would produce a 10^{-3} V (1 mV) error (based on $V = IR$) [3]. If the input bias current is 10^{-7} amp, the error is 100 mV. For an electrometer with an input bias current of 10^{-15} amp, the bias is unmeasurably small. The best instruments bias the measurement to a much greater extent when the full-scale voltage range used for the measurement is above ~10 V because resistor dividers are used at the input. Thus, a 10^9 ohm device can become a 10^6 ohm device.

[3] This equation is less commonly defined as $U = IR$ in some parts of Europe.

The conventional measurement is to attach the negative input of the DVM or electrometer to the reference electrode, and the positive input of the DVM to the electrode being measured. When two reference electrodes are measured vs. each other, one must be chosen as the "reference". Conversion from the raw measurements to volts standard hydrogen electrode (V_{SHE}), which is the standard scale for reporting electrochemical potentials; this is addressed in Section 3.12 on reference electrodes.

During ECP measurements, it is often wise to stop the flow of DCPD current for a few seconds for the reasons discussed in Section 4.8 on electrochemical effects of DCPD. Once a reliable reference electrode is developed, ECP measurements should be straightforward. However, an EPRI – Swedish Nuclear Power Inspectorate (SKI) round robin involving five labs, considered at the time to be among the best in the world that all tested specimens provided from a common source, showed very large data scatter (Figure 3-9). This persisted even when the reference electrodes were supplied by one laboratory, pointing to significant measurement issues. These discrepancies were never resolved, but they likely resulted from a combination of poor wiring insulation, instruments with insufficient high input impedance, and/or potential differences that develop in the autoclave water between the reference and working electrodes, which contribute to the measured voltage.

Potential measurements on both the test specimen and Pt are recommended. In hydrogenated water, the Pt potential should confirm the reference electrode integrity and in water with oxidants, it reflects the stability of the chemistry conditions much better than the test specimen (for example, an Fe-Ni-Cr alloy), whose potential evolves over time as the film forms or transforms. Note that electrochemists will often object to referring to an "ECP measurement on Pt", because Pt does not corrode, and thus "corrosion potential" has no meaning. However, in high temperature water, such criticism is not very relevant, in part because the term "ECP" is used for convenience, and in part because the potential of all common LWR materials and Pt is controlled primarily by the H_2 and O_2 reactions.

Corrosion potential is a more fundamental parameter in SCC than the concentrations of oxidants and reductants in solution, including when water radiolysis occurs during irradiation. This is best shown in Figure 3-11, where a rapid drop in corrosion potential and crack growth rate occurred on a Pd-coated CT specimen after changing from 200 ppb O_2 to a stoichiometric excess H_2 condition (greater than a 2:1 H:O molar ratio), despite the fact that the O_2 was increased from 200 to 500 ppb. Under certain conditions, particularly at low, but finite, oxidant concentrations (for example, less than 20 ppb oxygen), the corrosion potential can be very sensitive to small variations, such as dissolved gas concentration and flow rate (Figure 3-12). There are also significant effects of surface preparation, exposure time (pre-filming), material heat, and so on, as discussed below, so it is always important to measure the corrosion potential directly on the test specimen rather than on some nominally identical material in a different location.

The corrosion potential is formed by a kinetic balance among various oxidation (primarily hydrogen and metal) and reduction (primarily O_2 and H_2O_2) reactions (Figure 3-13). In higher Cr materials, like SSs and Alloy 600, the contribution of metal oxidation/corrosion is small, and the corrosion potential is controlled primarily by the water-gas and H_2O_2 reactions. In water containing O_2 and H_2, the corrosion potential is primarily defined by the intersection of the O_2 reduction curve and H_2 oxidation curve. The presence of even small amounts of O_2 on a metal surface produces an immediate contribution of the O_2 reduction reaction, and thus very low levels of O_2 can have a large effect on the corrosion potential (Figure 3-13). When corrosion

reactions, or the catalytic reaction of O_2 and H_2, occur on the specimen surface faster than O_2 can diffuse through the stagnant liquid boundary layer to the surface, the reaction is mass-transfer limited, and the corrosion potential drops to the H^+/H_2 line, as represented by the vertical drop-off of the O_2 reduction curve. The O_2 at which this drop-off occurs depends on the O_2 diffusion rate (which is affected by temperature), the flow rate (and the stagnant boundary layer thickness), the O_2 consumption rate from corrosion (which is affected by temperature), and the reaction of O_2 with any reducing species (like H_2) on the metal surface.

There are subtleties in the corrosion potential response related to, for example, the differences in the corrosion reaction as the potential changes. At low potential the corrosion rate is somewhat higher than at high corrosion potential, such that as O_2 is decreased toward zero, there can be a rapid decrease in potential at a concentration of 5 ppb O_2. After maintaining a low potential for some time, as O_2 is then slowly increased, a subsequent rise in the potential might be observed at a concentration of 15 ppb O_2. This hysteresis is real and is related to the different O_2 consumption rates from different corrosion rates.

The presence of O_2 triggers an O_2 reduction reaction. An increase in O_2 concentration increases the equilibrium O_2 potential (intersection with the Y-axis) and overcomes mass transport limited kinetics (that is, the diffusion of O_2 becomes much faster than its consumption rate from corrosion). Additions of, or increases in, H_2, even at relatively low levels, always reduce the corrosion potential. Flow rate has a large effect on corrosion potential when the O_2 reduction reaction is controlled by mass transport because the stagnant boundary layer through which O_2 must diffuse to the metal surface becomes thinner with increased convection. Flow-rate induced increases in corrosion potential have no effect on SCC growth rate [37], for reasons described in Section 3.14 on flow velocity effects.

Because ECPs and mixed potentials (that is, corrosion potentials) form at the metal-solution interface, different materials and different regions of one material can have different corrosion potentials despite exposure to the same bulk water. Thus, the corrosion potential on a cracked specimen exposed to water containing O_2 can vary widely, with the surface at perhaps $+100\ mV_{SHE}$, while the deaerated crack tip might be at $-500\ mV_{SHE}$. This again underscores the importance of measuring corrosion potential on the test specimen, ideally in the vicinity of the crack mouth where the corrosion potential has the largest effect on crack chemistry.

The ability to galvanically influence the corrosion potential of the specimen (for example, of loading linkage made of a different material) is very limited in pure water because the conductivity of water is low, so the coupling current is low. As the conductivity of the solution increases, more ionic current can flow and thus the corrosion potential of a specimen exposed to sea water can be strongly affected by galvanic coupling. This issue is also discussed in connection with DCPD, where the voltage drop along the wiring can have a large effect on the measurement of corrosion potential vs. the actual corrosion potential. There are two phenomena of concern associated with galvanic coupling between the specimen and the loading linkage or the autoclave:

- One is a real shift in the corrosion potential of the specimen surface.
- The other is an apparent shift in corrosion potential associated with a mis-measurement of corrosion potential from the voltage (*IR*) drop in the solution as ionic current flows. The magnitude of the error depends on the reference electrode placement and the solution conductivity.

In pure water, the ability of a galvanic couple to shift the corrosion potential of the specimen is quite limited. This was evaluated using Pd strips on a SS specimen under excess hydrogen conditions [30,31], where shifts of hundreds of millivolts in the local corrosion potential, as measured using a micro-reference electrode placed near the specimen surface, occurred over a distance of about 1 mm. The low galvanic current that can flow in pure water is insufficient to alter the corrosion potential at distances above about one millimeter, and perhaps much less. Note that, in a more typical measurement where the reference electrode is tens of millimeters away, the difference in the local potentials on a specimen surface are averaged together. This also applies if several specimens with different corrosion potentials are electrically connected. The potential registered by the reference electrode is a weighted average of all potentials, with surfaces of larger area and/or closer proximity to the reference electrode making a larger contribution.

If the galvanic couple, or voltage difference, is physically separated rather than existing on the specimen surface as with the Pd strips, and the reference electrode is between them, as would likely occur for a specimen and an autoclave, then a different measurement-related problem arises. As stated before, for galvanic coupling or voltage differences in pure water, the high resistivity (R) of water (even at 288°C) limits the ionic current flow (I). The voltage difference is primarily dissipated as "*IR* drop", with the water path being a continuous resistor, and the reference electrode "looking through" part or all of the *IR* drop to "see" the potential on the metal surface. Simplistically, if there is a 1 V drop between the autoclave and the specimen, and the reference electrode is half-way in between the two, it will mis-measure the corrosion potential by 0.5 V. More often, the reference electrode will measure a larger fraction than half. See Section 4.8 on electrochemical effects of DCPD for additional discussion.

Therefore, it is essential either to electrically isolate the specimen from the linkage and surrounding metal surfaces, or to place the reference electrode much closer to the test specimen than other electrically connected metal surfaces. However, an average surface potential is always measured, and it is the corrosion potential close to crack mouth that controls SCC growth. In most cases, the potential does not vary that significantly along the exposed surface of the specimen because the potential is low in the crack due to O_2 consumption by corrosion. However, on partially catalytic surfaces [30,31], there can be large variations in corrosion potential when there is a stoichiometric excess of H_2 (for the reaction of $2H_2 + O_2 = 2H_2O$) because where Pt particles exist, the potential is very low (less than –500 mV_{SHE}). Thus, an average potential of –300 mV_{SHE} may represent 50% of the surface at –500 mV_{SHE} and 50% at –100 mV_{SHE}.

The most reliable potential measurements in 250°C or hotter water are made on a Pt electrode in deaerated water containing greater than 10 ppb H_2 where the theoretical potential is well defined (see Section 3.11). The potential is less well-defined on Pt in water containing only O_2 at greater than 1 ppm, and still less well-defined on high alloy materials (SS, Alloy 600, and so on) for water containing only O_2 at greater than 1 ppm O_2. A key reason for choosing O_2 levels greater than 1 ppm is to help ensure that the dissolved O_2 concentration in the autoclave outlet is a very high fraction of the inlet value. In O_2-only solutions, the potential of Pt is perhaps 100 mV higher than SS with typical potentials in 1 ppm O_2 on the order of ~300 mV_{SHE} for Pt and ~175–200 mV_{SHE} for SS. The potential on unoxidized SS evolves (that is, rises) over the first 5–14 days.

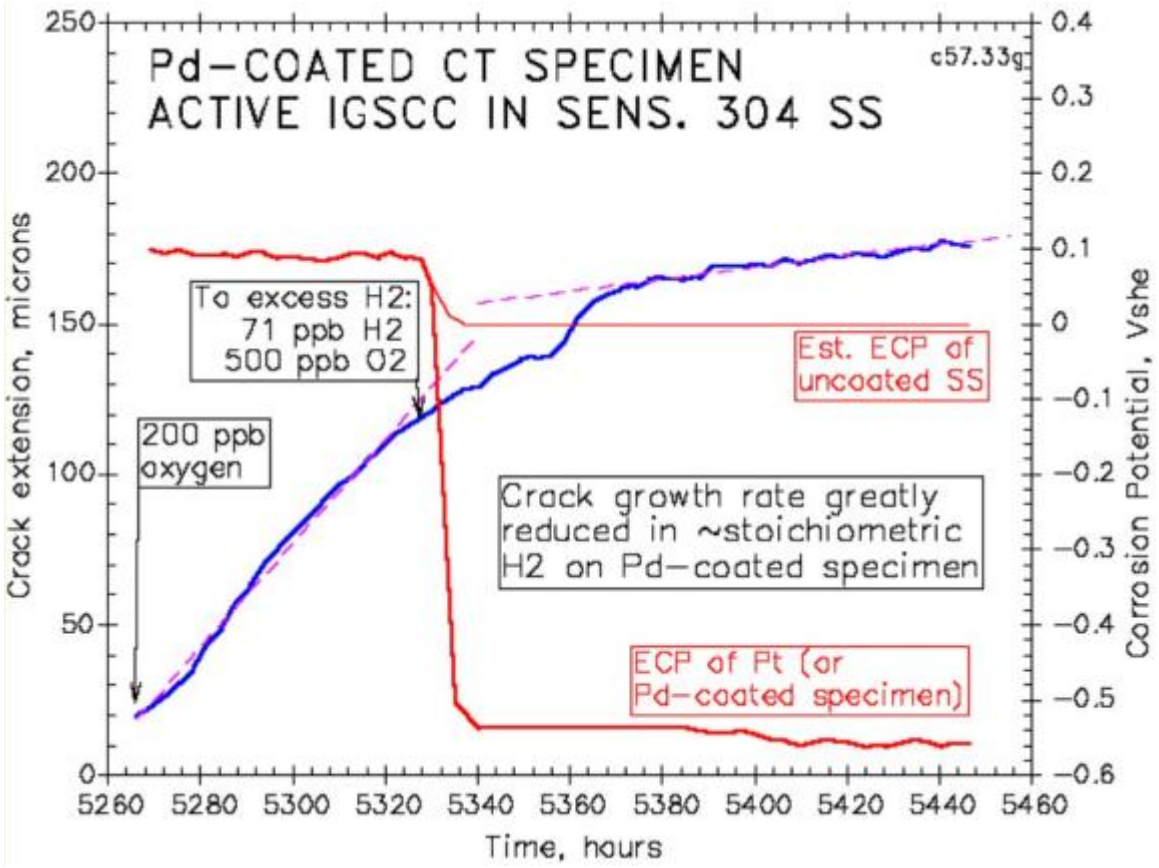

Note: The plot shows the rapid drop in corrosion potential and crack growth rate on a Pd-coated CT specimen on changing from 200 ppb O_2 to stoichiometric excess H_2 (greater than 2:1 H:O molar ratio), despite the increase in O_2 from 200 to 500 ppb O_2.

Figure 3-11
Crack Length and Corrosion Potential vs. Time

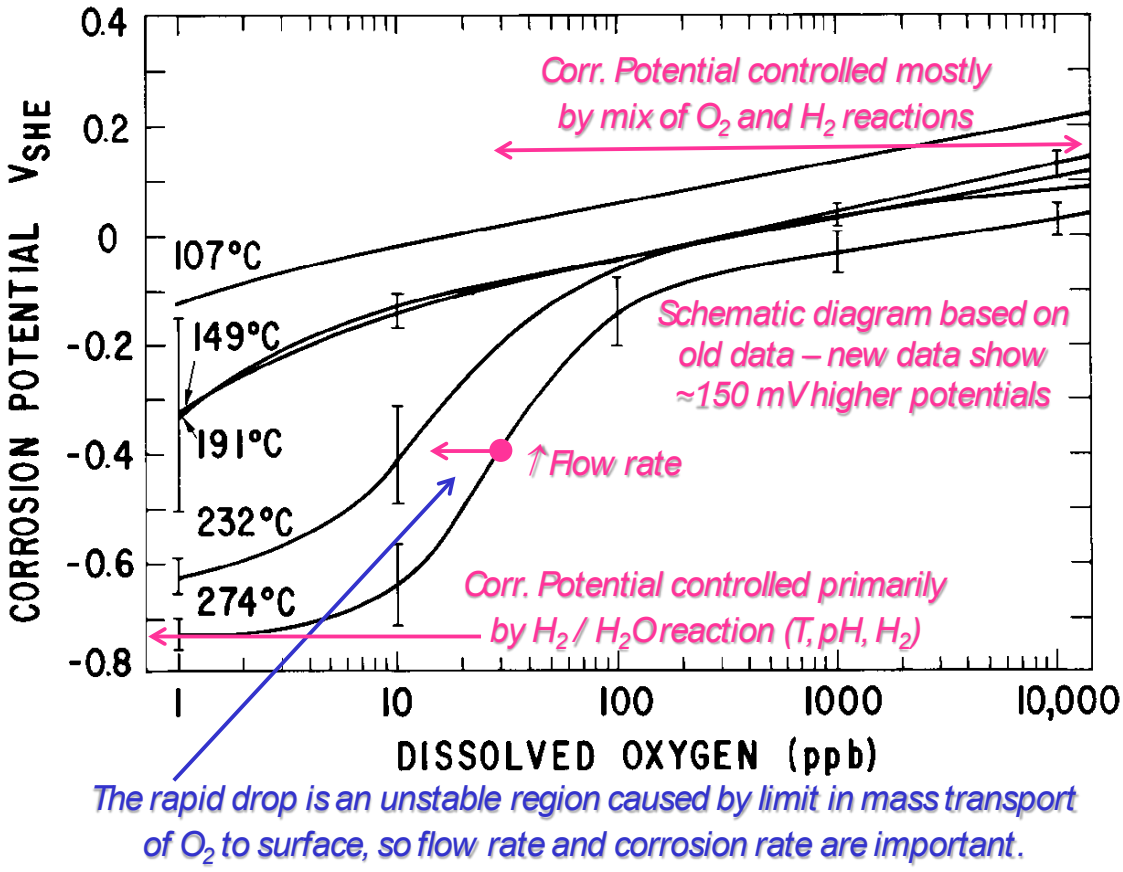

Note: At low dissolved O_2 concentrations (for example, less than 10–50 ppb), there is rapid shift in corrosion potential with O_2 that is associated with mass transport of O_2 to the metal surface and consumption of O_2 by corrosion, and the corrosion potential is very sensitive to flow rate. At lower temperatures, the corrosion rate is lower, and the drop off in potential is shifted to lower O_2 concentrations.

Figure 3-12
Corrosion Potential vs. the Logarithm of Dissolved Oxygen Concentration in 288°C Water

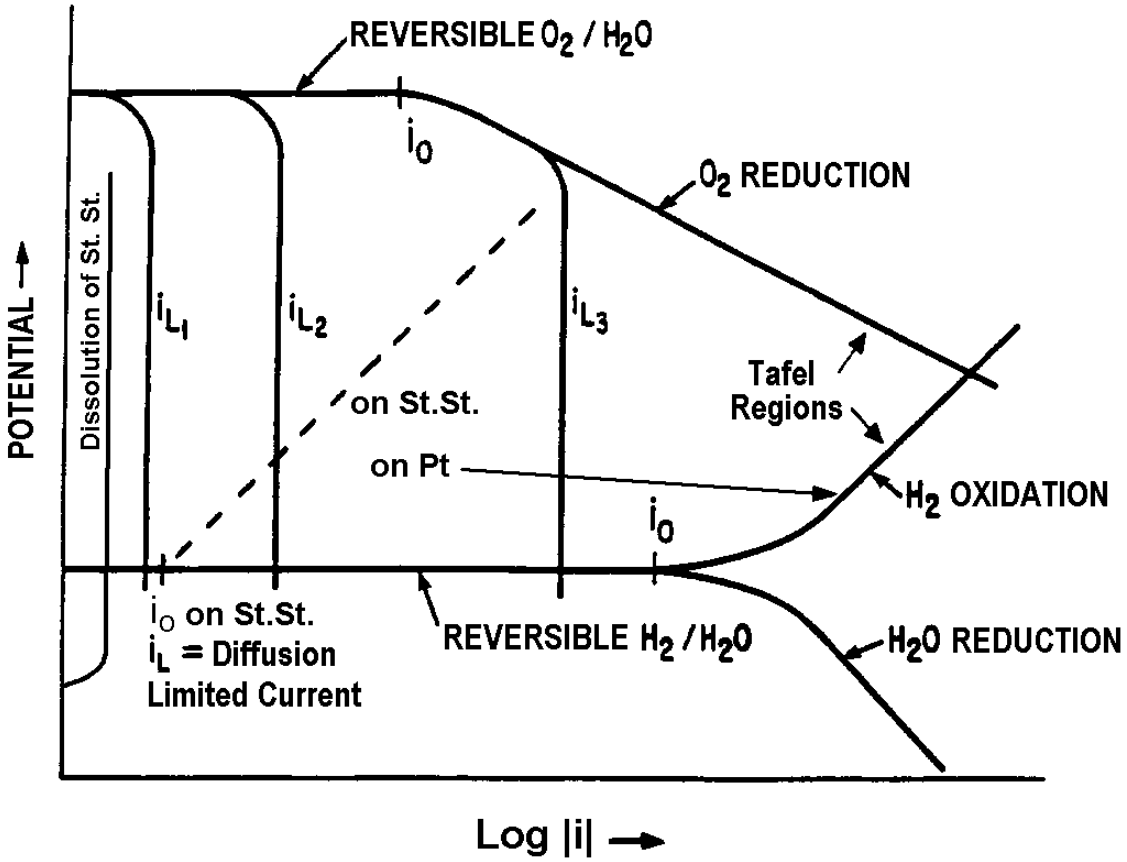

Note: The figure show log |i| curves, where i is the absolute value of current density, showing the interaction of H_2 and O_2 on a catalytically active surface such as Pt or Pd. i_o, the exchange current density, is a measure of the reversibility of the reaction.

Figure 3-13
Schematic Evan's Diagram – E (potential) vs. the Logarithm of the Absolute Value of the Current Density

3.11 Calculating Potentials vs. Temperature, pH and Hydrogen

This section focuses on thermodynamic calculations of potentials in water, and in particular on the redox potential on Pt in hydrogenated water (no oxidants). The Nernst Equation derives from Gibb's Free Energy:

$$\Delta G = \Delta G^0 + RT\ ln(Q) \qquad \textbf{Eq. 3-1}$$

where ΔG is the free energy of reaction (of products to reactants), ΔG^0 is the standard free energy, R is the gas constant, T is temperature in Kelvin, and Q is the ratio of the activity of products and reactants. For a simple reaction, such as $NaCl + AgNO_3 = NaNO_3 + AgCl$, Q is defined as follows (where the bracketed terms represent the activity of each substance):

$$Q = \text{ratio of the activities} = [NaNO_3] \times [AgCl]/(\,[NaCl] \times [AgNO_3]\,) \qquad \textbf{Eq. 3-2}$$

For a more general reaction involving aA + bB = cC + dD, where the upper case is the chemical and the lower case is the number of moles:

$$Q = [\mathrm{C}]^{\mathrm{c}} \times [\mathrm{D}]^{\mathrm{d}} / \left([\mathrm{A}]^{\mathrm{a}} \times [\mathrm{B}]^{\mathrm{b}} \right) \quad \textbf{Eq. 3-3}$$

Then:

$$\Delta G = -nFE \quad \textbf{Eq. 3-4}$$

where n is the number of electrons involved in an electrochemical reaction, F is Faraday's constant (96,500 coulombs/equivalent), and E is the electrochemical potential of the reaction.

Substituting for ΔG gives:

$$-nFE = -nFE^0 + RT\ ln(Q), \text{ or} \quad \textbf{Eq. 3-5}$$

$$E = E^0 - \left({}^{RT}/_{nF}\right) ln(Q) \qquad \text{(the Nernst Equation)} \quad \textbf{Eq. 3-6}$$

By convention, potentials are defined for the reduction reaction. The reference or standard potential of 0 V is assigned to the hydrogen reaction ($2H^+ + 2e^- \rightarrow H_2$) at all temperatures based on $[H^+] = 1$ (pH = 0) and H_2 fugacity equals 1:

$$2H^+ + 2e^- = H_2 \qquad E = 0 - \left({}^{RT}/_{nF}\right) ln\left(\frac{[H_2]}{[H^+]^2}\right) \quad \textbf{Eq. 3-7}$$

Converting *ln* to *log* involves 2.303, so:

$$E = -2.303\left({}^{RT}/_{nF}\right) log\left(\frac{[H_2]}{[H^+]^2}\right) \quad \textbf{Eq. 3-8}$$

The potential on Pt in deaerated solutions is controlled by the hydrogen reaction. At 25°C (298.15 K), and with pH = –log $[H^+]$ this becomes:

$$E = -0.02958\ log[H_2] - 0.05916\ pH \quad \textbf{Eq. 3-9}$$

For 1 atmosphere H_2 and 1N H^+ (pH 0), E = 0 V.

Note that the slope of potential vs. pH is twice that of *log* $[H_2]$. The dependency on both pH and H_2 scales with absolute temperature, so at 300°C (573.15 K):

$$\Delta E = 0.059\left(\frac{573.15}{298.15}\right)\Delta pH = 0.1137\Delta pH \quad \textbf{Eq. 3-10}$$

(or 113.7mV per pH unit for a 10X change in H^+)

$$\Delta E = 0.0569\ log[H_2] \quad \textbf{Eq. 3-11}$$

(or 56.9 mV for a 10X change in H_2)

At 300°C, with 1 atmosphere fugacity of H_2 in pure water (pH = 5.70):

$$E = -0.0569\ log[H_2] - 0.1137\ pH \quad \textbf{Eq. 3-12}$$

$$\boldsymbol{E} = 0 - 0.1137 \times 5.70 = -0.6481\ V \quad \textbf{Eq. 3-13}$$

At pH = 7.0 and 300°C and 1 atmosphere H_2 fugacity:

$$E = 0 - 0.1137 \times 7.0 = -0.7959\ V \quad \textbf{Eq. 3-14}$$

Note that 1 atmosphere fugacity is not the same as 1 atmosphere partial pressure of H_2 at elevated temperatures, because temperature has a significant effect (Figure 3-14) [36].

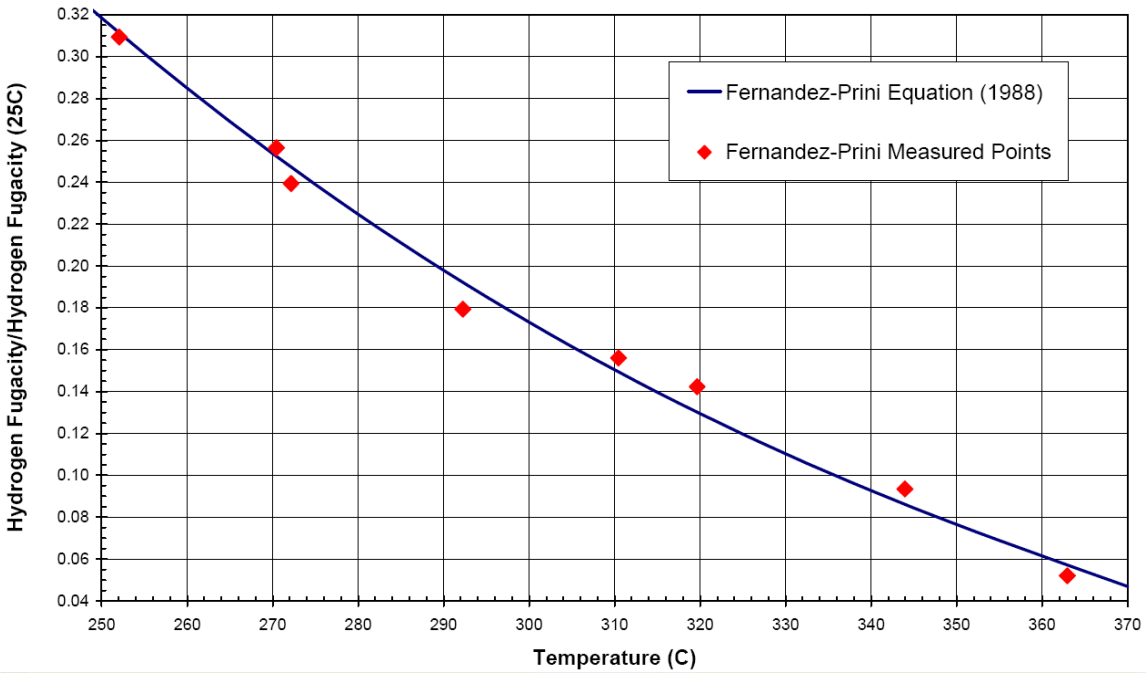

Figure 3-14
H_2 Fugacity at Temperature Divided by H_2 Fugacity at Room Temperature [36]

3.12 Reference Electrodes

Reference electrodes of many types and designs have been developed for measurement of potentials during testing in high temperature water. Measurement of ECPs is addressed in Section 3.10 on corrosion potentials. When converting from a measured voltage of, for example, 1.1 V using a $ZrO_2/Fe_3O_4/Fe$ electrode whose reference potential in the test environment is -0.80 V_{SHE}, a simple linear scale is often helpful (Figure 3-15). The 1.1 V measured potential would be +0.30 V_{SHE}.

The most common reference electrodes include:

- Pt coupons, which provide thermodynamic potentials only in the presence of stoichiometric excess hydrogen for the reaction of $2H_2 + O_2 = 2H_2O$. Ideally a molar ratio of H:O greater than 5 is desired, so that any oxidant present will react to form water on the catalytic surface and the corrosion potential will remain low. A Pt coupon's reference half-cell potential is a function of temperature, pH, and hydrogen fugacity, as discussed in the previous section.
- External Ag/AgCl reference electrodes, which are pressure balanced electrodes (that is, they operate at the autoclave pressure) that extend outside the autoclave so that the reference half-cell reaction is at room temperature [37-43]. These electrodes typically use an electrolyte of 0.1 or 0.01 N KCl but have been found to give stable potentials when filled only with pure water (which relies on the ~10^{-6} N solubility of AgCl at room temperature). For correction to the SHE scale, a calibration with Pt and a known H_2 concertation should be performed. All the Ag/AgCl electrodes show some drift with time, and junctions may produce some junction potentials. Since PTFE Teflon is commonly used in construction, these electrodes are limited

to about 300°C, although construction materials like zirconia and oxidized zirconium have been used. Reference electrode drift from loss of, and autoclave contamination by, chloride is largely determined by the quality (that is, adequate by limited porosity) of the ionic junction at the tip of the electrode, which is usually porous zirconia.

- Internal Ag/AgCl reference electrodes, in which the entire electrode is exposed to the autoclave pressure and temperature [43-45]. As with external Ag/AgCl electrodes, electrolytes of 0.1 or 0.01 N KCl are most common; pure water versions are more common than in external electrodes because the solubility of AgCl at 300°C is higher at ~10^{-3} N. Problems with electrode drift from loss of, and autoclave contamination by, chloride are common, as is their eventual malfunction in solutions that contain high hydrogen because of the reduction of AgCl to Ag, thereby changing the reference half-cell potential and/or plugging the porous ion junction. This can occur relatively rapidly at high hydrogen levels. Since PTFE Teflon is commonly used in construction, these electrodes are also limited to about 300°C, although electrodes made from oxidized zirconium tubing or zirconia with an integral ionic junction tip have been used.
  - Very simple designs have been devised (Figure 3-16) that apply to both external and internal Ag/AgCl electrodes, although they are limited to ~300°C because they use PTFE Teflon. In most cases, tests in PWR primary water are performed at higher temperatures, which is hydrogenated, and thus Pt can function as a reference electrode. Figure 3-17 and Figure 3-18 provide the reference potentials of common external and internal Ag/AgCl electrode designs.
- Zirconia membrane reference electrodes, which operate like standard glass pH electrodes but rely on oxygen anion conductivity in the zirconia ceramic at elevated temperatures (Figure 3-19) [46]. These electrodes are fundamentally identical to O_2 electrodes used to monitor fuel-air mixtures in the exhaust of cars. They are sealed, fully inert electrodes with no ionic junction, and are properly identified as pH electrodes because of the dependency of their half-cell potential on pH. At constant or known pH, the electrodes provide a stable thermodynamic reference potential that does not depend on dissolved oxygen or hydrogen. The half-cell potential varies with the internal fill of the electrode, which can be Cu_2O/Cu, Fe_3O_4/Fe, Hg_2O/Hg, and so on. The impedance of the reference electrode below about 200°C is so high that it is only usable with extreme shielding (that is, a "Faraday cage") and electrometers. Zirconia membrane reference electrodes are the preferred solution in most applications with excellent long-term stability and reproducibility, as well as no chloride contamination. The quality of the zirconia is important; a low SiO_2 content and low other impurity levels are crucial. Grain boundary silicate phases can be formed that dissolve in high temperature water and provide a leakage path for water to the inner part and even failure of the tube.

The half-cell potential for a Cu_2O/Cu junction in V_{SHE} is $0.175 - 0.0015585 \times T$ (where T is in °C) and must be corrected for any difference from a pH of 5.65 at temperature. So, in 330°C water with a pH(330°C) of 7.65, the half-cell potential is $0.175 - 0.0015585 \times 330 = -0.339$ V, which is then corrected for 2 pH units (7.65–5.65) at 0.1197 V/pH at 330°C to a value of -0.578 V_{SHE}. When in doubt about the effect of H_2 or pH on potential, reference can be made to the H^+/H_2 reaction, labeled "(a)" on a Pourbaix diagram (Figure 3-10) [36].

Similarly, the half-cell potential for a Fe_3O_4/Fe junction in V_{SHE} is:

$$-0.537076 - 0.0001064T - 0.00000292286T^2 \qquad \textbf{Eq. 3-15}$$

where T is in °C and must be corrected for pH in the same fashion (Figure 3-20).

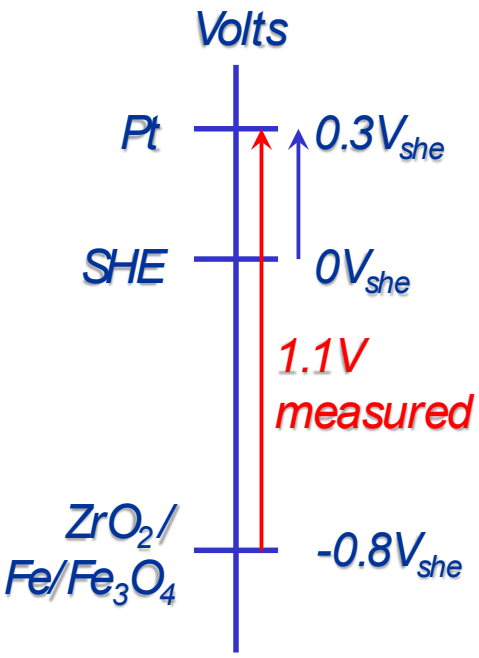

Note: A linear scale is often the simplest way to envision conversion of the measured potential (for example, on Pt of 1.1 V) using a reference electrode to the standard hydrogen electrode voltage (V_{SHE}). If the reference potential is -0.8 V_{SHE}, then the Pt potential is 0.3 V_{SHE}. Measurements should be made with the negative (-) terminal of the voltmeter connected to the reference electrode, and the positive (+) terminal to the Pt (or other electrode of interest).

Figure 3-15
Conversion of Measured Potential

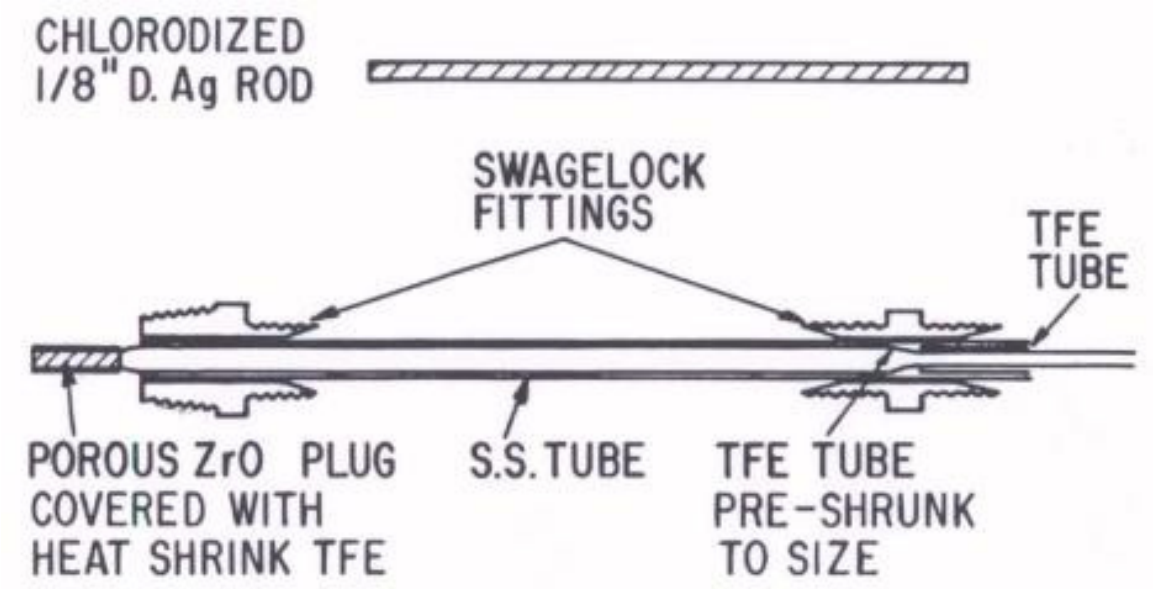

Figure 3-16
Schematic of a Simplified External Ag/AgCl Reference Electrode

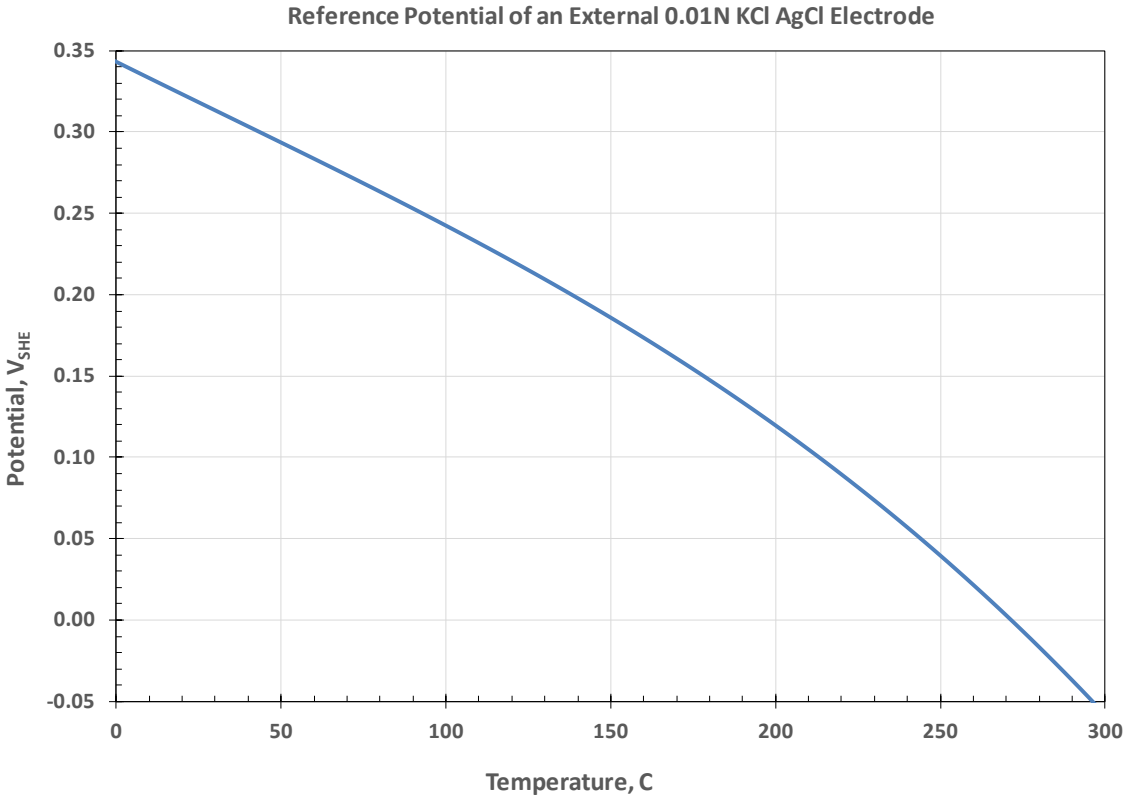

Figure 3-17
Half-Cell Potential vs. Temperature for an External Ag/AgCl Electrode with 0.01 N KCl

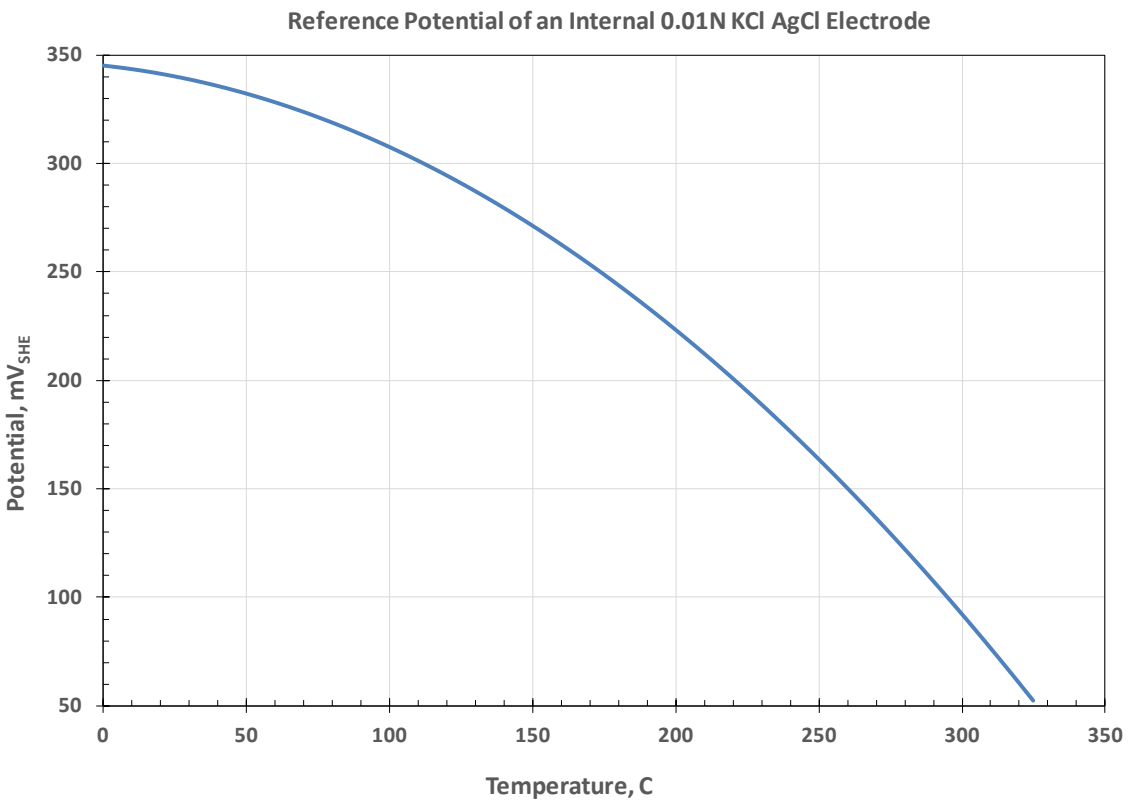

Figure 3-18
Half-Cell Potential vs. Temperature for an Internal Ag/AgCl Electrode with 0.01 N KCl

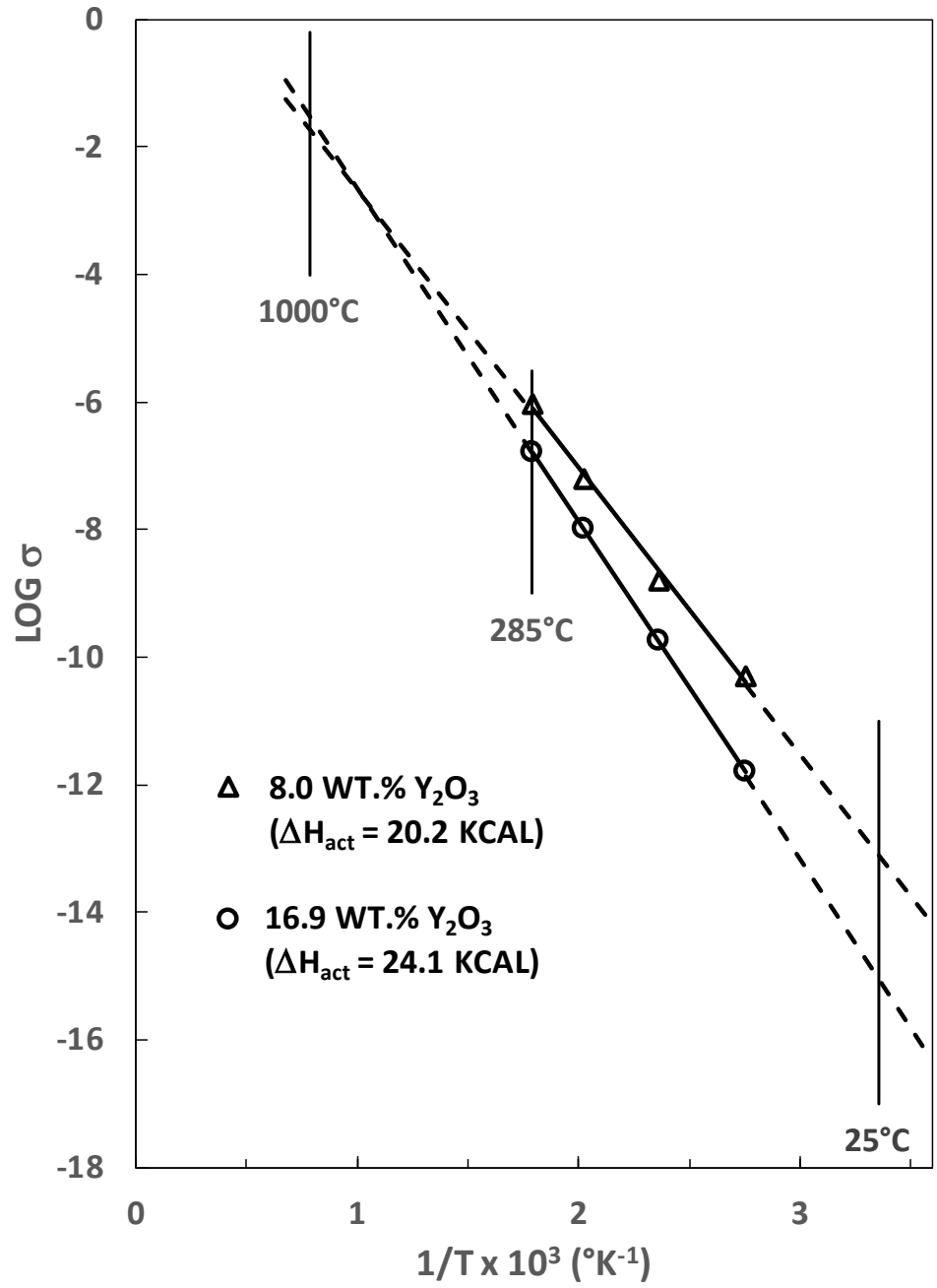

Figure 3-19
Conductivity of Yttria Stabilized ZrO_2 vs. Temperature [43]

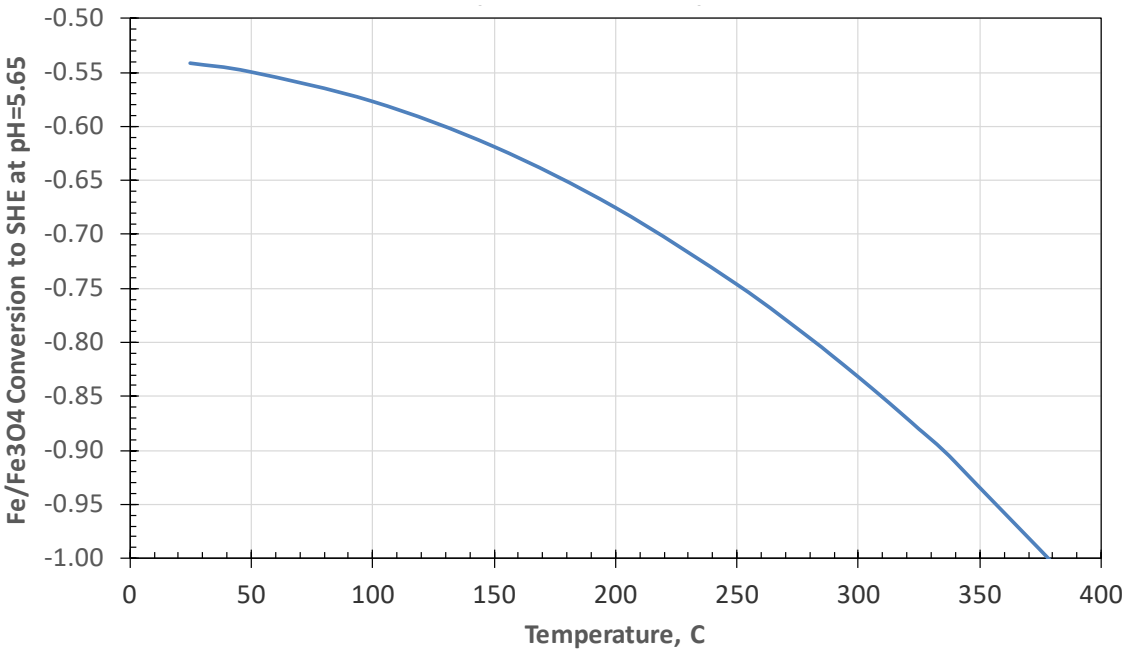

Figure 3-20
Potential for an $ZrO_2/Fe_3O_4/Fe$ Reference Electrode vs. Temperature

3.13 Potentiostatic Control

Potentiostatic control of the specimen potential is complex and is not recommended for most investigators and studies, especially in high temperature water. While a potentiostat is capable of controlling the measured specimen surface potential to a specific value measured by the reference electrode, there are many opportunities for errors and anomalies that can result from:

- ***IR* errors, which are associated with high resistivity media and/or high current flow.** As described earlier, the solution acts like a continuous resistor and current flow causes a continuous potential (*IR*) drop in the solution. Depending on the solution resistivity, current density, specimen geometry, and so on, these *IR* potentials can be very large (hundreds of millivolts or even greater than 50 V). For a reference electrode placement half-way between the specimen and the counter electrode, and assuming identical electrode geometries, the reference electrode will not only register the potential of the specimen, but it also will measure half of the *IR* potential. Placing the reference electrode closer to the specimen does not help, because, for a cylindrical specimen surrounded by a counter electrode, half of the total *IR* drop occurs in the solution within a distance of one specimen radius. Thus, placement and mechanical stability become extremely critical, and it is still not possible to eliminate a significant portion of the *IR* drop. Similarly, electronic *IR* correction techniques, such as current interruption and low amplitude AC superposition, are very difficult to implement correctly in pure water because more than 99% of the potential change measured by the reference electrode can be attributed to *IR* drop; expertise and development are required.
- **A reversal of surface reactions and local pH shifts.** In solutions containing oxygen, the reaction on the external surface is cathodic (that is, oxygen reduction to form OH^-). In the crack, oxygen is rapidly consumed and the solution in most of the crack becomes deaerated. Thus, the primary anodic reactions are metal dissolution/oxidation which forms H_2, because

Fe-Ni-Cr ions are not very soluble and undergo hydrolysis. If a potentiostat is used to polarize the specimen to more positive potentials, it must make the surface of the specimen anodic, causing oxidation reactions to become predominant on the metal surface. This alters the local concentration of OH^- and the local pH.

- **An inability to polarize most crack tips in pure water.** Projecting polarizing current down a long, tight metal crack is effectively impossible. Thus, any connection between the applied potential and the potential at the crack tip is indirect because the crack tip potential is changed primarily by shifts in the pH of the crack chemistry from the differential aeration crevice cell or other differences in potential or thermal gradients. Thus, assuming cathodic polarization is evidence of hydrogen embrittlement is inappropriate. As an example, in one instance it was shown that an increase in crack growth rate from cathodic polarization was not associated with hydrogen, but rather with reduction of sulfate to sulfide on the specimen surface, followed by its diffusion into the crack; sulfide is known to significantly reduce repassivation kinetics and thereby enhance crack growth rates.

3.14 Flow Velocity Effects

Flow velocity can have an effect on SCC growth rate, but it is not common. There is a beneficial effect of high flow rate on EAC initiation from smooth surfaces in LAS. A primary impact of flow rate on SCC in high temperature water is observed when the flow disrupts crack chemistry, and this requires that a distinct crack chemistry develop in a given environment. This occurs primarily in oxidizing environments (Figure 3-21) or when boiling or thermal gradients are present. In deaerated water without thermal gradients, there is no consequential driving force to create an altered crack chemistry, although a distinct crack chemistry can be formed in deaerated water from dissolution of MnS inclusions, which is most relevant in CS and LAS materials (Figure 3-22).

As cracks develop on smooth surfaces, flow rate can inhibit the formation of an altered crack chemistry in very shallow cracks. As cracks become deeper, flow rate effects that influence the crack tip are limited to TG cracks that are partly or fully aligned with the direction of flow. IG cracks are complex and create too many turns for flow to penetrate very deep into the crack, and many in-service plant component cracks are full of oxide. If flow is perpendicular to the crack mouth, counterflow eddies develop, and the velocity in each eddy drops rapidly with crack depth (Figure 3-23). If flow is parallel to the crack mouth, then flow can penetrate deep into the crack (Figure 3-24), but only if the crack sides are relatively flat and are not heavily oxidized. In such isolated cases, flow velocity is beneficial in eliminating the altered crack chemistry. The displacement of the altered crack chemistry by bulk water containing oxygen is beneficial, as shown in Figure 3-25 where the displacement of the crack chemistry is accomplished by rapid sampling of the crack tip chemistry. The fact that oxygen present at the crack tip does not accelerate growth rates shows that the supply of cathodic current at the crack tip is not limiting.

In the laboratory it is much easier for flow rate to affect crack growth. Most tests are performed using CT specimens where the crack is open on three sides. This is essentially never the case with cracks in plant components which are almost always open only on one face. Therefore, undertaking relevant flow rate effects using CT specimens is unwise, and surface cracks should be used. One approach is described in Reference [47].

Deleterious effects of flow velocity have been proposed, primarily where there is an elevation in corrosion potential by flow velocity at low dissolved oxygen levels (Figure 3-12); and the consumption of oxygen by metal corrosion outpaces the diffusion of the oxygen through the stagnant liquid boundary layer. Increasing flow rate reduces the boundary layer thickness and increases the supply of oxygen to the surface, thus increasing the corrosion potential markedly. However, it has been recognized in some experiments [47] that, in the convection field near the crack mouth, mass transport by ion migration is overwhelmed by convection, and can only begin to have a role as convection vanishes. This is where ion migration begins to create an altered crack chemistry and thus, the increase in corrosion potential from flow velocity does not affect crack chemistry or environmental cracking.

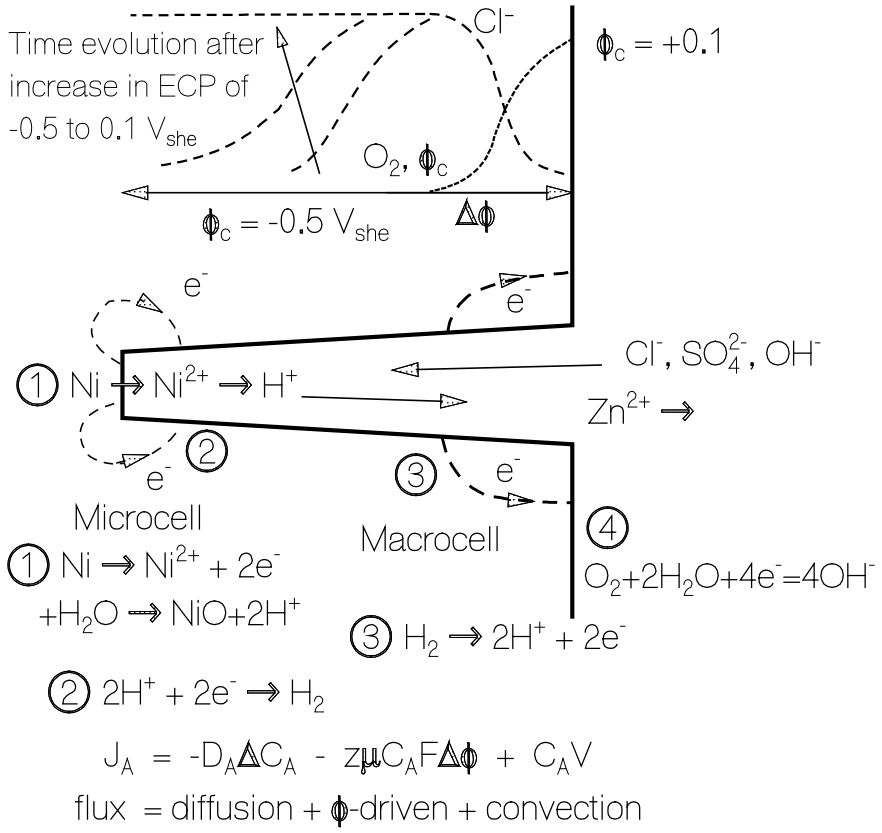

Figure 3-21
Schematic of the Formation of Crack Chemistry

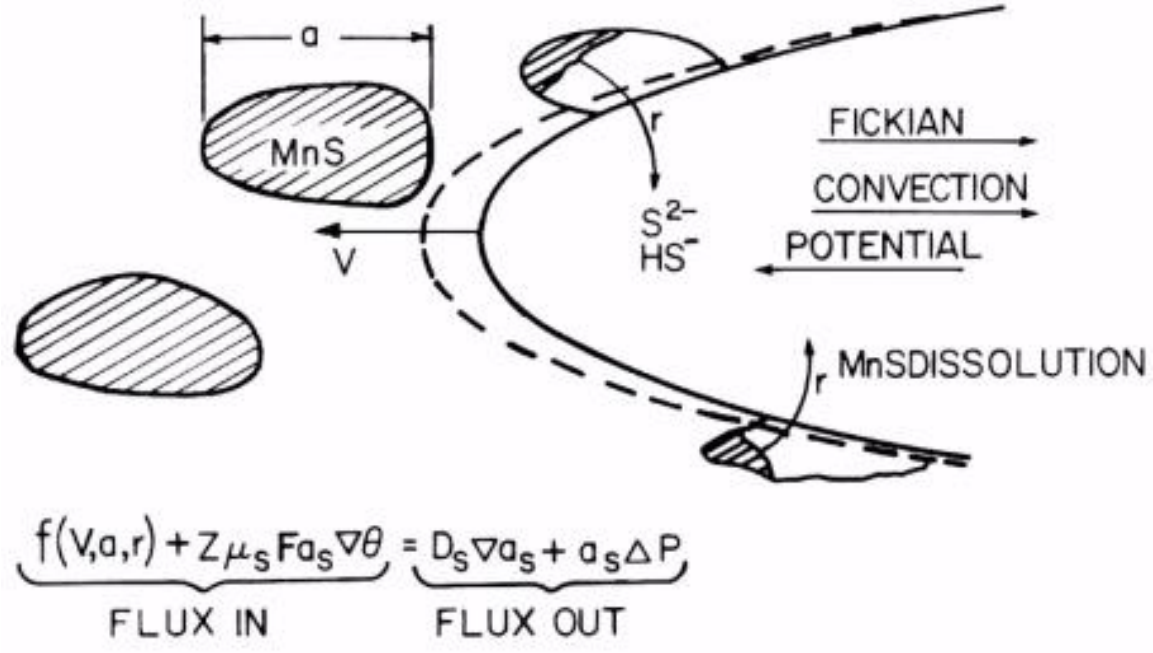

Figure 3-22
MnS Effects on Crack Chemistry

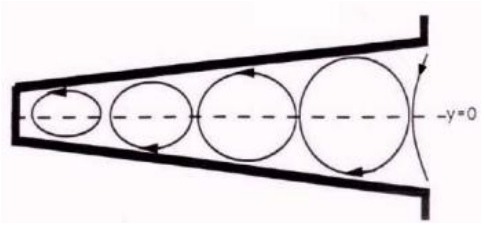

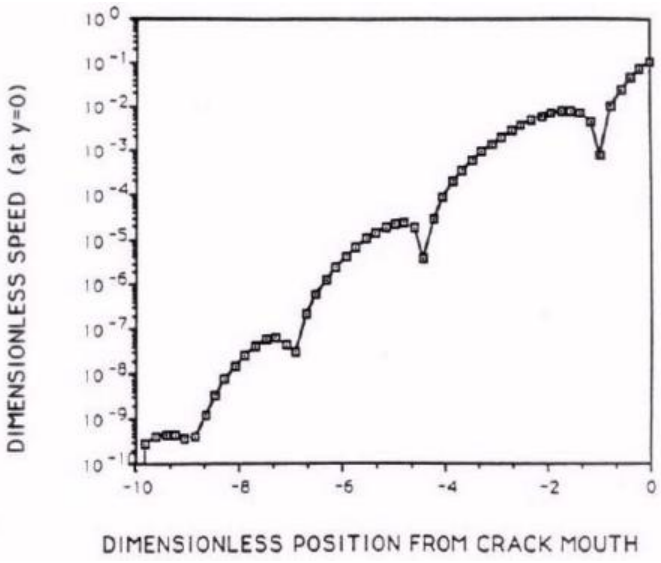

Note: Convection for flow perpendicular to the crack creates a series of counterflow eddies that produce a rapid drop in flow velocity.

Figure 3-23
Convection Modeling for Flow Velocity Perpendicular to the Crack Mouth

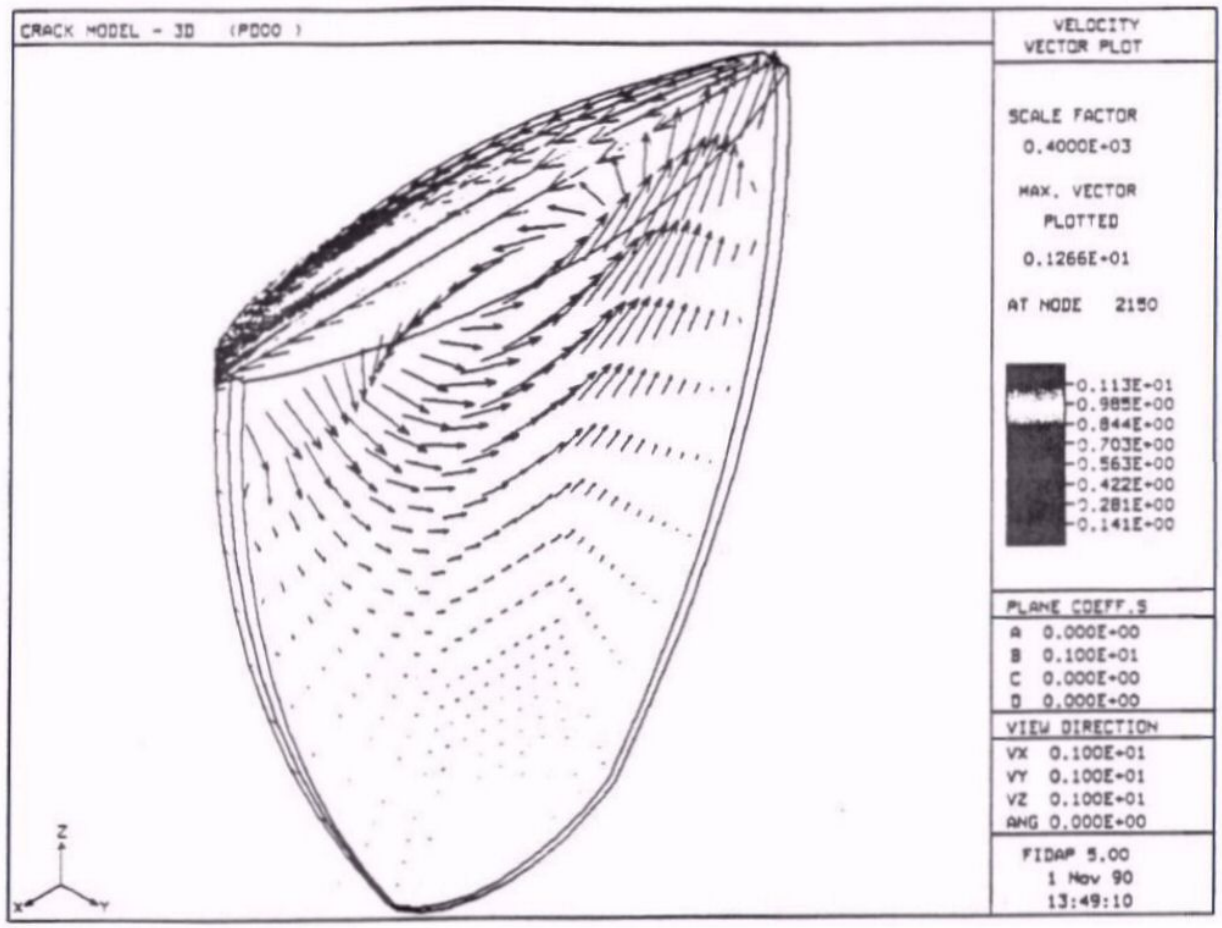

Note: Convection for flow parallel to the crack can create convection deep into the crack, but only if the crack sides are smooth and parallel.

Figure 3-24
Convection Modeling for Flow Velocity Parallel to the Crack Mouth

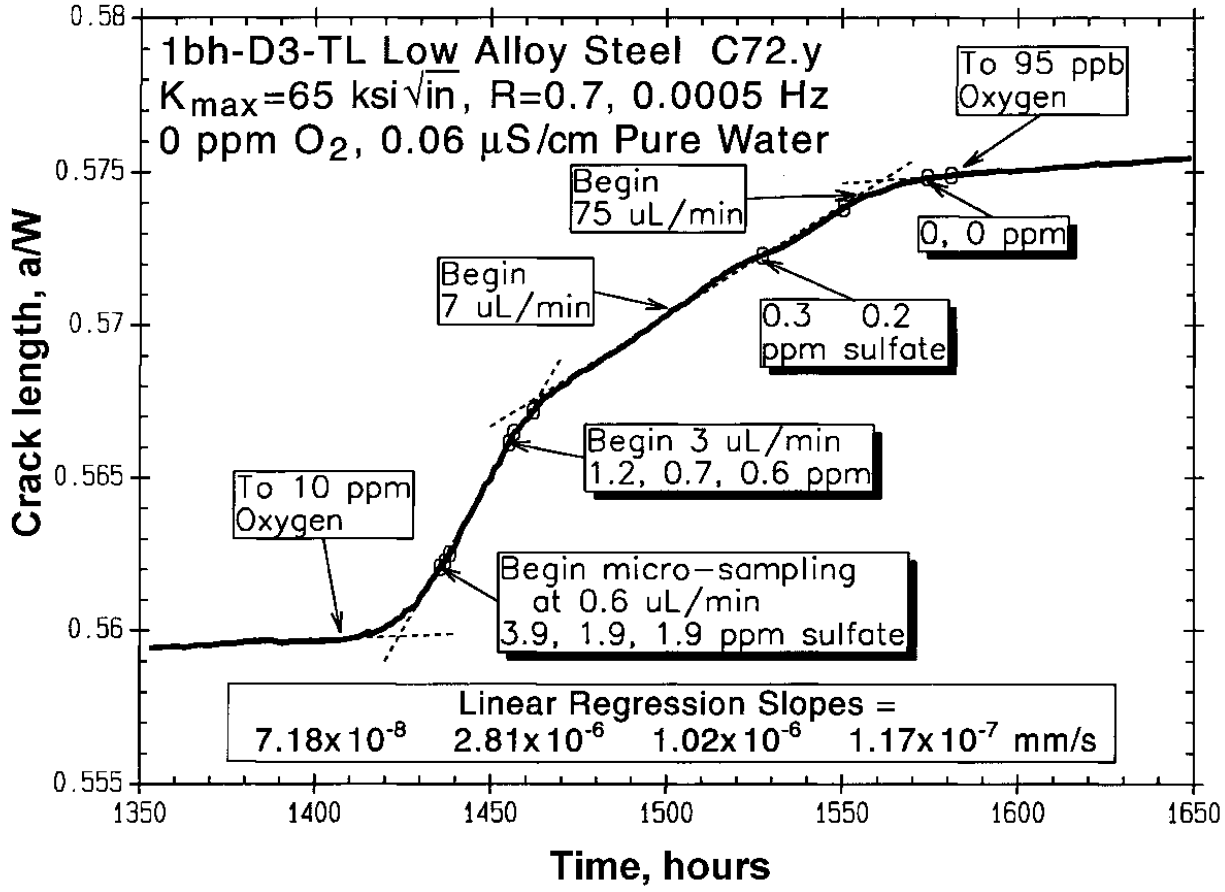

Note: The figure shows that, as the crack tip solution is replaced by the bulk solution containing oxygen, the growth rate drops because the altered chemistry controls the growth rate, not the availability of cathodic current.

Figure 3-25
Effect of Crack Tip Liquid Sample Rate on LAS Crack Growth Rate

4
CRACK MONITORING

While some useful SCC data can be obtained using unmonitored specimens, there are major limitations. For example, SCC can begin to develop at less than 20% of the time-to-failure, and without monitoring, even the time-to-failure can only be determined based on the usually long intervals used between test interruptions. Similarly, for SCC growth rate data, applying a fixed load for thousands of hours to an unmonitored fatigue pre-cracked specimen (often known as a single-condition test) provides no information on when the cracking transitions from TG fatigue to IGSCC. There is value in knowing during testing that there was no cyclic loading or change in test conditions. However, there are large drawbacks when little or no crack advance occurs from the fatigue pre-crack, because no conclusions can be drawn without extensive observations showing that transitioned data consistently produces sustained crack advance when no growth is observed without transitioning. Additionally, while any IG growth would have occurred during the single-condition exposure, it is not known whether cracking commenced early or late in the exposure. In general, high resolution crack monitoring is more valuable than single-condition, unmonitored tests, but they should be considered complementary.

The simplest form of crack monitoring is to investigate for failure, which is of limited value. Monitoring actuator motion, specimen elongation or crack opening displacement is somewhat more helpful but is imprecise and is not adequate for good transitioning or detailed crack growth data. Quantitative crack growth monitoring is usually accomplished with DCPD or unloading compliance. Unloading compliance works best with cantilever loaded, through-crack specimens such as a CT specimen, where there are well-defined relationships between the change in load and the crack in crack mouth opening displacement [2, 48]. Measuring crack opening displacement in high temperature water is not trivial, but there are linear variable differential transformer (LVDT), capacitance, and eddy current sensors available. A major disadvantage is that unloading is essential, and this generally perturbates the SCC growth response. Compliance is never as high in resolution as good DCPD implementations. If there is contact in the wake of the crack (for example, from oxides, cracking around and rotation of grains, Mode II or Mode III loading that causes the matching fracture surfaces to fail to mate during unloading) compliance can exhibit significant errors; however, in many cases, these errors can be detected by non-linearity in the load vs. displacement curve. Friction between the pins and clevis (in particular with insulations) are also an issue for unloading compliance, as are creep contributions under static load.

Potential drop measurement techniques rely on the change in resistance as cracks nucleate and grow. In most cases, a constant current is used, and the evolution in voltage is monitored. Both DC and AC approaches have been used. However, AC potential drop is more complex and expensive, and its primary benefit is the skin effect on smooth specimens for crack initiation whereby high frequency AC flows primarily near the specimen surface. Good implementations of DCPD more than offset this advantage by their superior noise rejection and resolution.

4.1 An Overview of DCPD

Early incarnations of DCPD used 50–100 amp power supplies that could generate more than 50 mV of potential difference in a 1T CT specimen, and the resulting signal was often recorded on a strip chart recorder. The noise level for such setups was quite high, as was the possibility of electrochemical effects on the specimen and electrolysis of water (above ~0.8 V) caused by the voltage drop in the current leads. For the last four decades or so, DCPD has evolved to using generally less than 5 amps of current and ~100 μV of voltage drop for a 1T CT specimen, which can be readily measured by DVMs that can resolve ~1 nV (with averaging). Since thermoelectric voltages at metal-to-metal contacts often exceed 1 mV, the current is reversed after one or several readings to eliminate their contribution.

In most implementations, a constant current from a precision power supply is reversed periodically using a solid state relay bridge (Figure 4-1). Solenoid (mechanical contact) relays are not recommended because of the large number of current reversals throughout years of testing (perhaps three million per year). DC-DC solid state relays conduct in the "forward" direction and only conduct in the reverse direction when activated, usually by a control voltage above ~3.2 V. The current reversal is coordinated by a computer that reads the nanovoltmeter, averages the data, and uses one or more algorithms to compute a crack length. The net result is that crack growth rates below 10^{-9} mm/s can be measured and monitored (Figure 4-2).

While different current attachment points on a CT specimen may be used, an attachment toward the back of the CT specimen has several advantages, including less sensitivity to uneven crack fronts and more stable reference potentials (both of these issues will be discussed later). However, such advantages are not large. The preferred implementation positions the current connection in the center of the top and bottom of the CT specimen about 9.5 mm (0.374 inch) from the back of a 1T CT specimen (Figure 4-3). When reference probes are necessary, they should be located on the back face of the CT specimen about one-third and two-thirds of the distance from the crack plane to the top (or bottom) of the CT specimen. A stable contact is crucial, as minor shifts in the contact area can have large effects on the measured potentials. While many types of wire can be used, the integrity and stability of the spot weld are bigger issues with nickel, nickel alloy or stainless steel wires than with Pt wires. While Pt is costly, it's a one-time investment that can avoid a significant amount of wasted time repairing failed spot welds. Typically, 0.75 mm (0.030 inch) diameter Pt wire is used for the current leads, and 0.25 to 0.50 mm (0.010–0.020 inch) diameter Pt wire is used for the potential leads.

The DC potential leads are typically attached on the front of the CT specimen across the notch; unlike the current connections, the location and contact stability are much less critical. It is best to strain-relieve the leads at the specimen to avoid stress and fatigue on the attachments, which are usually connected by spot welding. The leads generally must be insulated to avoid contact with other leads or the autoclave internals. Below ~300°C, it is best to use continuous PTFE Teflon from the CT specimen through the seal and outside the autoclave (as discussed later). Above 300°C, it is best to use partially stabilized zirconia (for example, 3% MgO). High purity alumina can also work in pure water, but at higher pH levels (for example, B/Li chemistries), alumina slowly dissolves.

Multi-wire seals, such as Conax 2-, 4- or 8-wire seals with PTFE Teflon, are generally used because there are generally two or more current leads and two or more potential leads. For multiple specimens and reference probes, it is not unusual to use a dozen or more leads. Current leads should use a different seal than the potential leads unless continuous PTFE Teflon is used from outside the autoclave to the specimen. It is possible to use the autoclave structures to carry the current, since metal-to-metal threads, even when oxidized in high temperature water, are a very low resistance path. Success requires that the only possible current path is through the specimen(s), as discussed elsewhere.

The solution conductivity is rarely an issue, although in concentrated solutions like sea water, there is some error in crack monitoring by DCPD associated with solution conductivity in the tight crack. However, this is likely a limited error compared to the typical errors (for example, from unevenness in the crack front) of 10–30%. Liquid metals pose a problem, although if oxidation of the cracked metal surfaces occurs, use of these might be manageable. The use of DCPD for non-conductive ceramics, glasses or polymers can sometimes be managed using conductive films applied to the specimen surface.

In general, an inverted autoclave is preferred because, with the PTFE Teflon seals beneath the autoclave, the seals remain much cooler than if they are located above the autoclave. The Conax, or similar, wire seals can also be extended a small distance away from the autoclave head. This approach is routinely used for autoclave temperatures of 500°C and higher (for example, in steam or supercritical water).

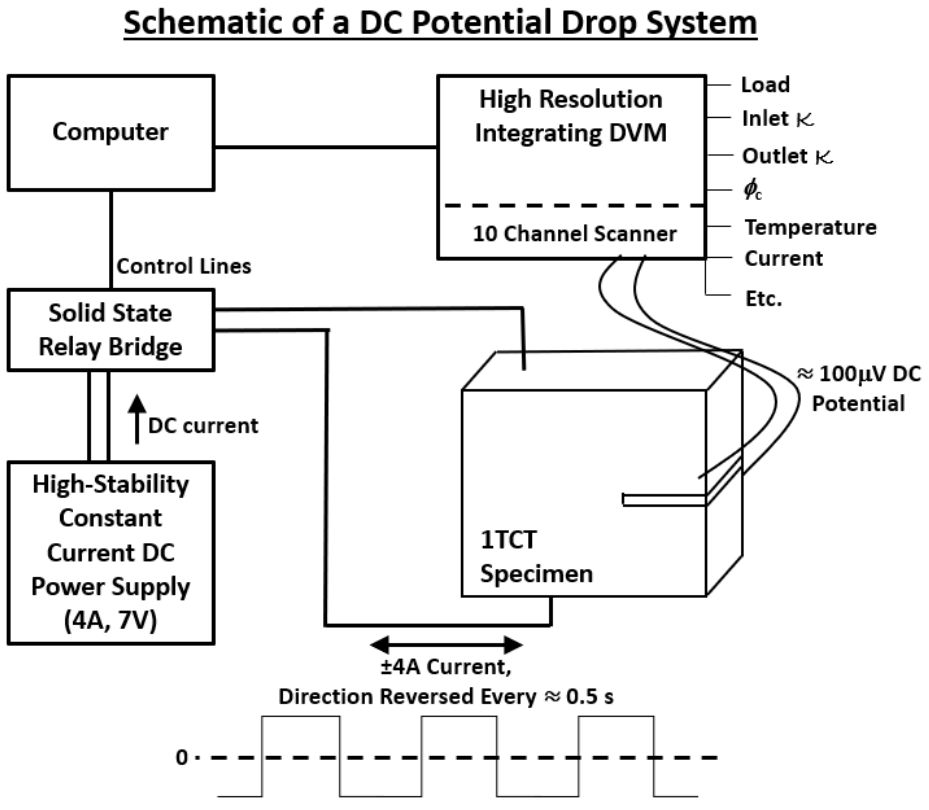

Figure 4-1
Schematic of a Typical DCPD Crack Monitoring System for Either Crack Growth or Crack Initiation Testing

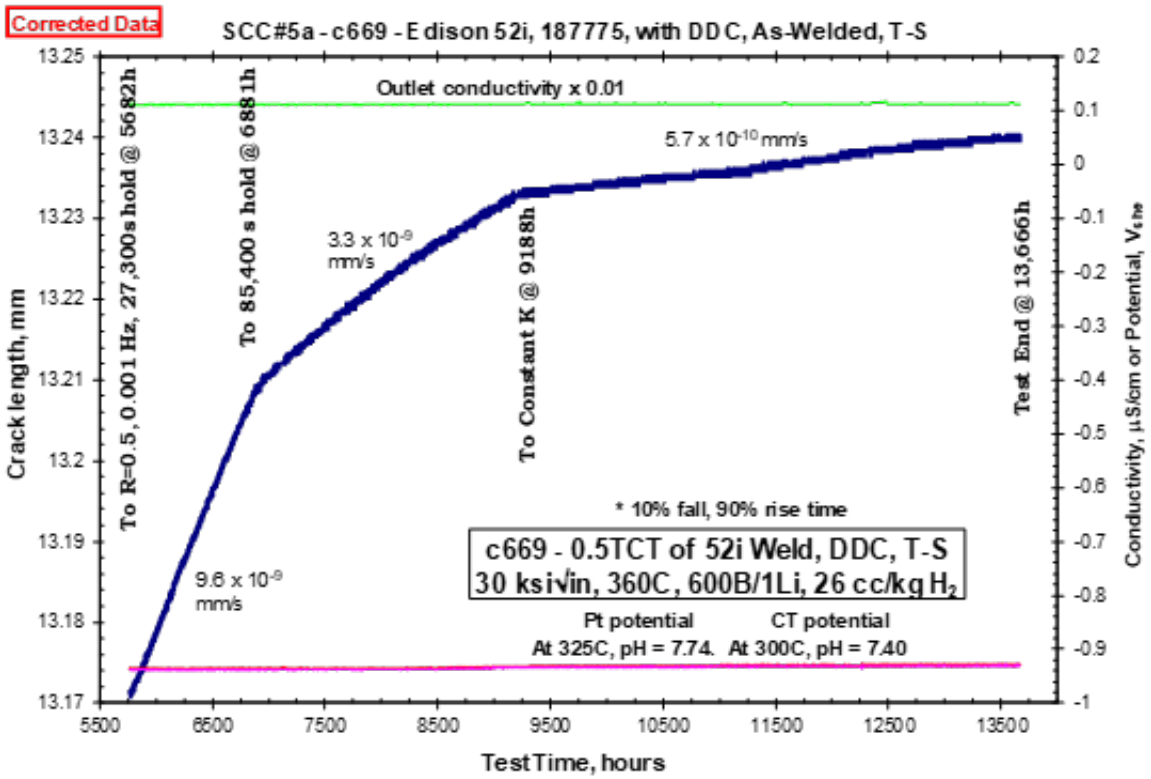

Note: High crack depth resolution is often obtained using high quality DCPD implementations that address all DCPD optimizations.

Figure 4-2
High Crack Depth Resolution Below 10^{-9} mm/s

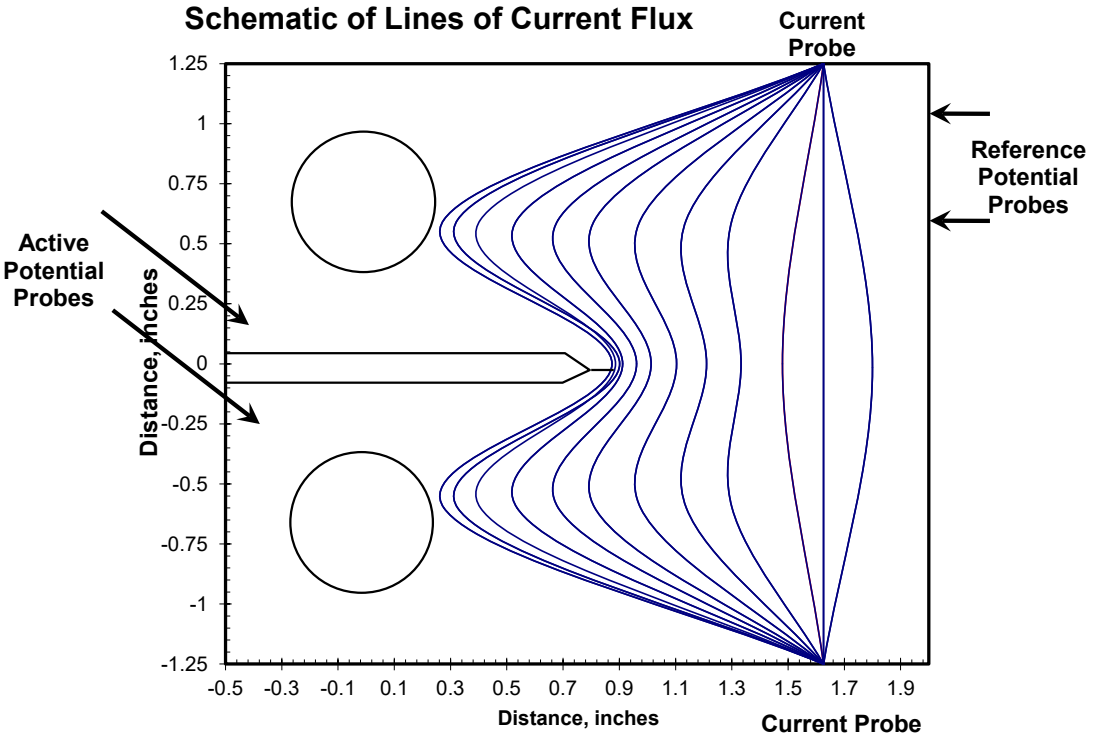

Note: On this 1T CT specimen, the current wires are positioned 9.5 mm from the back-face. The active potential location is at the front of the CT (the exact location is not critical), but the spot welds were made near the corner of alternate faces. The reference probe location is 0.6 and 1.1 inch (15.2 and 28 mm) above the centerline on the back face. These dimensions can be scaled with the size of the CT specimen.

Figure 4-3
Schematic of the Distribution of Current Flowing through a Homogeneous CT Specimen

4.2 DCPD Instrumentation

Commercially available DCPD systems have never achieved the resolution that have been achieved in custom system designs; the issues range from their design to the inexperience of the user. There are many key elements in achieving high resolution DCPD data, but among the most important are current reversal and integrating nanovoltmeters. An integrating voltmeter averages all fluctuations in the DC signal over a given time period. The period should be set to an integral number of the power line cycle (PLC) (where 1 PLC, which is at 60 Hz, is 16.67 ms), because the vast majority of noise comes from 60 Hz sources. For example, at 20 PLC, for the Keysight 34420A nanovoltmeter in the normal mode (noise only on the "+" input to the DVM), noise rejection is 100 decibels (dB), which is a noise rejection factor of 100,000. Even at 1 PLC, the noise rejection is 60 dB, which is a factor of 1,000. At less than 1 PLC, the normal mode rejection ratio is 0 dB (that is, none). The common mode rejection ratio (CMRR), where the same noise occurs on both "+" and "–" DVM inputs, is 140 dB for DC (or, a factor of 10,000,000) and only 70 dB for AC (a factor of ~3,000). This is a major reason why DCPD has an advantage over AC potential drop and can achieve very high crack length resolution.

A nanovoltmeter is needed because, for a signal level of ~100 μV and a desired resolution of 1 part in 10,000 or 100,000, the voltmeter must read 10 nV or 1 nV, respectively. Because potential drop readings are ratioed to an initial reading, accuracy is not as important as stability. If the voltmeter is 10% off on all readings, it has no effect on potential drop. If the voltmeter can only resolve 1 μV (1,000 nV), then the crack monitoring will be low resolution and noisy. No nanovoltmeter is both accurate and stable at either a 1 nV or 10 nV level, and this is where data averaging is important. When crack growth rates below about 10^{-8} mm/s must be monitored with confidence, often 1,000–5,000 pairs of ± current readings are averaged to obtain a single data point and acquiring DCPD data generally represents roughly 99% of the readings made. Voltmeters with 5 digits of resolution, whose lowest scale is only 100 mV, can only represent, on the lowest digit, 10 μV. Averaging cannot improve that by factors of 1,000 or 10,000 (down to 10 nV or 1 nV). Instrumentation amplifiers have been used to boost the signal level, but none are near as good as carefully designed nanovoltmeters. DVMs from Keysight (for example, Model 34420A) and Keithley are two examples of good nanovoltmeters.

The alternative design used in almost all desktop computer board-level voltmeters and many moderately priced voltmeters is "sample-and-hold." Sample-and-hold devices take a sample of the voltage, often using a window of < 1 μs, then perform an analog-to-digital conversion on this sample with varying speed and resolution. However, a 20 bit (about 5½ digits) or a 24 bit (about 7 digits) resolution is not useful when it is based on a very short time sample window of, say, 0.1 μs, because this brief window will sample only a random point of the signal and noise. If 1,000 such readings are averaged over a 1-second period, this only represents a total sample time of 0.1 ms, or one ten-thousandth of the overall PLC time period. An integrating voltmeter monitors the entire signal over the integration time period and offers significant benefits in noise reduction. This discussion ignores the fact that 20 and 24 bit analog-to-digital converters are rarely monotonic in their lowest 1–3 bits; that is, a slow, continuously rising analog signal will not yield a uniformly increasing digital conversion.

A second consideration is the stability of the power supply to provide a constant current when the power line voltage or room temperature varies. The power supply specifications should ensure that there is less than about a 0.01% variation with line voltage and temperature. The Keysight Model 6611C (which is no longer manufactured, but is still available used, or many alternatives with similar specifications are available) lists a variation of 0.5 mA for a 5 amps full-scale output over the entire power line input range, which is 0.01%. This same power supply has a temperature coefficient of 0.01% + 20 μA per °C change. (Note that many instruments will exhibit some greater initial drift for the first ~1 hour after power up, which should be considered when starting tests.) These specifications encourage operation at a relatively high fraction of the full scale, since some sources of noise and variation are a small percentage of full scale. Thus, using a 20A power supply at 1A output is unwise. There is no sudden degradation, but at lower fractions of the full scale output, more noise and variation will exist.

There is generally a need to monitor more than one or two signals. The Keysight 34420A nanovoltmeter has two input channels, so it can handle two DCPD signals and all other measurements (load, temperature, water conductivity, and so on) must be handled by other instruments. However, it is not uncommon to require measurement of 5, 10 or 15 DCPD channels and purchasing 3, 5 or 8 nanovoltmeters is very expensive. Multiplexers of many types can be used, but many are unsuitable for low level signals. For example, solid state switches often have high contact potentials (for example, on the mV level) and noise, so they are

unacceptable for high resolution measurements. Sealed, reed relay switches are often adequate, such as Keysight 34901A (20 channel) or 34902A (16 channel) multiplexer cards with a Keysight 34901A Multiplexer. Very expensive, ultra-low noise multiplexers are available (similar to those that exist in the two-channel Keysight 34420A), but they do not provide any significant benefit.

DC-DC solid state relays (SSR) are standard, common devices, most available brands are reliable, although it's possible they can age differently over time. An example is a Crydom CMX60D20 SSR, a 20-amp device controlled by a 3–10 V signal. Heat is always a major issue, so typically 40-amp relays are used despite rarely using them at current levels over 5 amps. Modern SSRs have very high conductivity channels, but it is still recommended to use devices that are rated for at least twice the current at which they will be used.

4.3 Optimization of DCPD

There are a variety of design and implementation optimizations that should be addressed in all DCPD systems. Testing laboratories that fail to address these issues often achieve poor crack length resolution, for example, greater than 1 mm of noise. Laboratories that successfully address all of these issues achieve a resolution of ~ 1 μm on a 1T CT specimen (that is, 1 part in ~50,000). Not all of the optimization issues discussed below are critical in every case, but experimentalists should understand why they may all be important in some circumstances.

Reference probes have been used to correct for fluctuations in the test temperature, current and other test parameters, but it is much better to resolve these issues at their source, that is, eliminate temperature fluctuations by tuning the controller PID values, use very stable current supplies, and so on. The only unavoidable issue is metal resistivity drift during testing (Figure 4-4), and reference probes are necessary to compensate for this, as discussed later. Reference probes can be implemented in various ways, but it is essential that they reflect the same material, material condition and prior exposure as the material undergoing crack advance. This can pose challenges if the specimen is not homogeneous (for example, comprised of some mix of base metal, weld metal, dissimilar metals, and so on), or possibly even machined from only weld metal, since the homogeneity of welds is uncertain (especially if multiple heats of weld wire were used to produce the weld). Back-face reference probes can be used on CT specimens, or a separate unloaded CT specimen or simple small bar or rod of material can be monitored.

There are many factors that can be optimized to produce high resolution DCPD crack monitoring, although it is not clear which of the following will make the largest impact in a given laboratory:

- Use of a very stable current source, preferably operated at greater than 50% of the full scale output, not a factor of 20 below it. Noise and fluctuations are often overcome using appropriate specifications that are expressed as a fraction of the full scale, as their relative contribution rises at lower outputs.
- Use of current reversal between DCPD readings to eliminate thermoelectric voltages, which develop at all metal contacts/junctions.
- Maintenance of very stable autoclave temperature (ideally ± 0.1°C) and room temperature (ideally ± 1°C). It is also best to avoid allowing sunshine exposure on all instruments, which can produce localized heating.

- Use of Pt wire leads on specimens (~0.5 mm [0.020 inch] for voltage readings, and ~0.75 mm [0.030 inch] for current readings) that allow up to 5 amps of applied current and ensuring high quality spot welds of the leads to the specimen. A very stable current attachment area is very important. Often a strain relief (for example, a metal strap over the Teflon or ZrO_2 insulator that is spot-welded to the specimen) helps to ensure that stress and fatigue do not affect the integrity of the lead spot welds. When new, or with use, Pt wires can become stiff, but they can be flame-annealed in air.
- Use of a very stable attachment for the current leads on the specimen. DCPD is very sensitive to the entry point of current into the specimen, even if part of the spot weld area becomes compromised. A 1–2 mm (0.040–0.080 inch) diameter wire or rod welded to the specimen may be used so that the entry point of the current is very stable.
- Avoid alternate current paths in the specimen. Because the current entry points and distribution in the specimen is very important, there must not be any alternate paths for current to flow through the specimen. For example, if the loading linkage is not insulated from the specimen, current can flow into one loading pin and around to the other loading pin. While some labs use a sleeve type of insulator on the loading pins and thin ceramic or PTFE Teflon between the clevis and specimen, it is adequate to insulate the end of the pull rod, inside or outside the autoclave, to eliminate the alternate current path.
- Avoid issues related to current flow through the Pt wires. A variety of occasionally significant issues can arise from the current flow through the Pt wires. In many cases, the voltage (*IR*) drop created as current flows in the Pt wires inside the autoclave can be greater than 0.5 or 1 V. Some of these issues are discussed later in Section 4.8 on electrochemical effects and polarization. Using the autoclave structure and pull rods to carry the current works very well, despite the presence of oxidation in threads and other contacts. The primary issue with this approach is to ensure that the current enters and flows through the specimen exactly as intended. This can be achieved using clevises that are fully insulated from the CT specimen, with a small link of Pt wire from the clevis to the CT specimen to carry the current. Clearance between the pull rod and the autoclave head near the seal must be adequate to ensure there is no contact. While algorithms that introduce the current using the loading pins have been developed, the average point of current entry changes with load, cycling, crack advance, and time.
- Use of a shielded, twisted pair for DC potential leads with the shield grounded at one end. The cable used for DCPD should be high quality instrumentation cable, with two twisted conductors in a foil shield. Multiple twisted pairs with individual shields in one cable is fine. The shield should be earth grounded at one location, not at both ends of the cable, and this is ideally done at the multiplexer card, or the DVM if no multiplexer is used. The fewer connectors in the signal path, the better, and for DCPD, a single instrumentation cable is generally used from the multiplexer card to the Pt wires. Screw terminals can oxidize with time, so the Pt wires should extend away from the autoclave several hundred millimeters. Using spot welds to connect the wires reduces the chance of contact problems developing over time.
- Ensure that all DCPD instruments are plugged into high quality power with a third-conductor ground that is earth-grounded at the laboratory (for example, using a metal post anchored several feet into the ground).

- Use of continuous Teflon insulation from outside autoclave to the specimen, if possible. Above ~300°C, zirconia must be used in the autoclave, but it is best to run the PTFE Teflon through the seal and extending up about 0.5 inch (12.7 mm), using an overlap a piece of ZrO_2 long enough to extend an inch or two (25–50 mm) above the head. Ideally, a long piece of ZrO_2 reaching near the specimen is best but this is not always possible.
- Careful lead routing. The current and potential leads should be routed in separate feed-throughs/seals and inside the autoclave. While this can be avoided if there is continuous PTFE Teflon on all leads from outside the autoclave to the specimen, cracks can develop in the PTFE Teflon, especially heat shrink PTFE Teflon. For this reason, it is best to avoid heat shrink PTFE Teflon. Heat guns should be avoided because they will inevitably over-heat the PTFE Teflon. Alternatively, use of a controlled temperature furnace is preferred. Non-heat-shrink PTFE Teflon tubing close to the desired size is best. Heat shrinkable PTFE Teflon with a final diameter that is not much smaller than the wire it surrounds is a second-best alternative.
  - An alternative is to use the autoclave structures rather than wires to carry the DCPD current. Oxidized, threaded contacts in high temperature water in the autoclave are a relatively low resistance path. Current can be passed through the autoclave structure, the loading posts, an interior loading plate and down through a string of ~12 threaded initiation specimens and through the pull rod, provided it is insulated outside the autoclave. The same approach can be used with crack growth specimens using the linkage and clevises to carry the current, with short Pt wires from the clevises to the desired location on the specimen. To succeed, there must be excellent insulation at the loading pins/clevises such that the current enters and exits the specimen via the Pt wires. Additionally, the pull rod extending through pressure seal must be insulated from the autoclave and actuator so that the only path for the current is through the CT specimen. In turn, the ground-isolated power supply can be connected to the autoclave structure and to the insulated pull rod.
- The laboratory should be a low-AC noise environment, with “zero crossing” solid state temperature controllers. Such controllers eliminate electric arcing and large noise bursts associated with interrupting the current using mechanical relays. Large motors, opening and closing electrical power contactors, and other noisy equipment should be kept distant from the test and instrumentation.
- Careful lead routing. The DCPD and load cell leads should be routed away from heaters and other AC power and servo-motor control lines. Consider using ferrite cores to suppress noise on both the sources of noise, the DCPD leads and the load cell cable.
- Manage all wire contacts, including keeping all screw or connector contacts cool (away from the autoclave), secure and unoxidized. Contacts should be periodically re-established by loosening and tightening screw connections or by breaking and making sliding contacts.
- Use of a high-quality DVM. The nanovoltmeter DVM must be very high quality to read ~100 V with ~1 nV resolution by integration over more than one PLC.
- Use of low noise, low thermal offset reed relay multiplexer switches. Such switches are essential for DCPD. Solid state switches are not acceptable for such low level signals, although they may be used for signals above ~0.1 V.

- Use of capable data acquisition software. The data acquisition program must average as many DCPD readings as possible, consistent with data frequency requirements. For example, during fatigue pre-cracking at 10^{-4} mm/s, only 50 ± pairs might be appropriate, while at 10^{-9} mm/s, perhaps 5,000 ± pairs might be optimal.
- Use of resistivity correction. For some materials, there is a resistivity shift during exposure to high temperature water that is also observed in water, air or argon (Figure 4-4). The most pronounced effects have been observed in nickel alloys, with some effect observed below 300°C for non-cold-worked materials, and below 270°C for greater than 10% cold-worked materials. At higher temperatures or cold work levels, the approach to an equilibrium value is quicker, but the effect early in the test is larger. The importance of resistivity correction depends on the magnitude of the resistivity drift and the magnitude of the crack growth rate being observed. At 10^{-6} mm/s, resistivity drift is a small issue in almost all materials, but at 10^{-9} mm/s, resistivity drift is an issue in many materials. Resistivity drift is also a small issue in high purity materials while the largest effects have been observed in commercial purity Alloy 600. To resolve this issue, a resistivity correction must be used. This correction can be accomplished using a separate coupon, with the exact same heat treatment, cold work and exposure history as the test specimen, or on the test specimen itself. This is discussed in more detail in Section 4.7 on resistivity drift on metals.
- Consider Ni stability issues. There are issues with Ni metal stability in nickel alloys with sufficient dissolved hydrogen to make Ni metal stable or in inert environments where metals do not oxidize. In such cases, the DCPD current shorts across the crack flanks, just as it does when the crack front is very uneven, or there are islands of uncracked metal in the wake of the crack. Crack closure effects on DCPD during cycling can be minimized using a threshold setting for load or load ratio below which DCPD readings are not taken.
- Use of an uninterruptible power supply. An uninterruptible power supply for the system is recommended, although it is more challenging for the heaters and high pressure pump. There is a risk of overloading the specimen if power is lost and the actuator remains in a fixed position while the temperature drops.

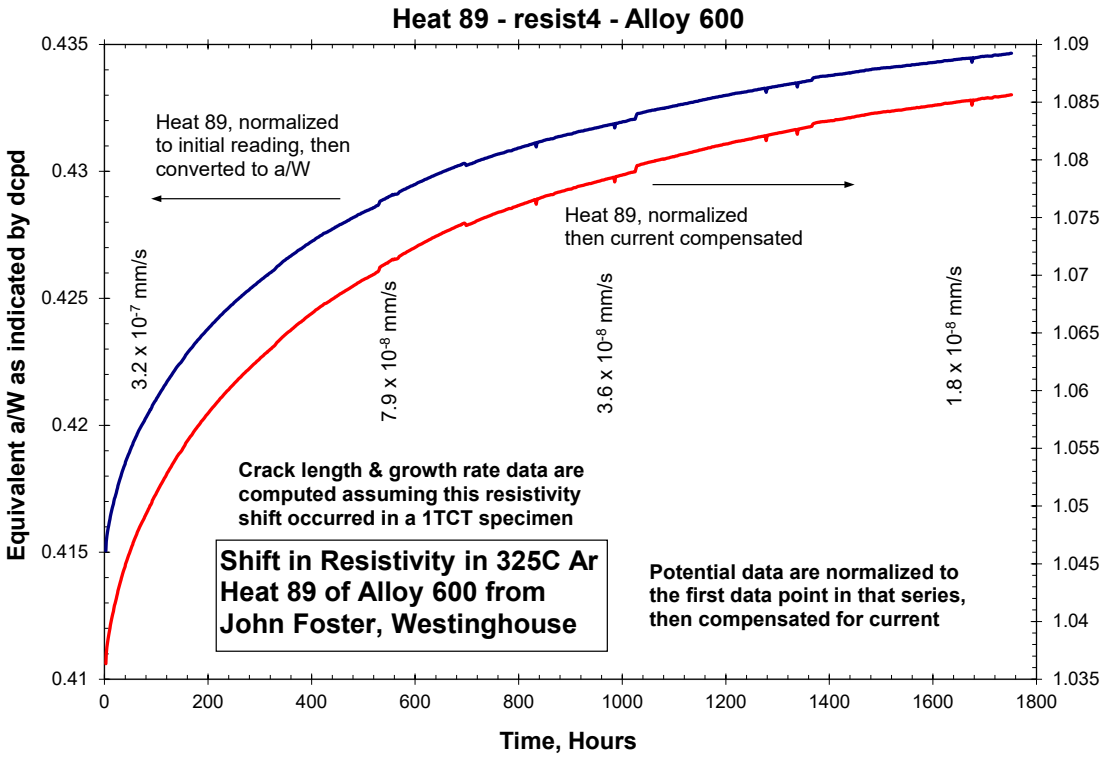

Note: The overall change in resistivity depends on the alloy, heat and processing. The resistivity asymptotically approaches a steady-state value faster at higher temperatures and for cold worked materials. The growth rates represent the apparent values from the resistivity drift.

Figure 4-4
Example of the Drift in Resistivity in Alloy 600 vs. Time

4.4 Calculating Crack Length from DCPD

Crack monitoring by DCPD uses a ratio of an initial potential to each subsequent specimen potential during the test, where each potential is an average of many potential pairs obtained as the current is reversed. When starting a test with a specimen that has a machined notch of known depth, the specimen should be installed, heated and loaded to about the maximum loading that will be used for testing to obtain an initial set of averaged potentials (V_0). Then, throughout the test, other averaged potentials (V) are obtained, and the ratio is calculated as V/V_0.

If reference probes are needed (for example, to correct for resistivity drift), their measurements are also ratioed (Ref/Ref_0), and the overall potential ratio is $(V/V_0)/(Ref/Ref_0)$.

The algorithm used to convert from potential ratio to a/W in a crack growth rate specimen must be known or created for different specimen geometries, just as different equations are used for K vs. load and a/W. For specimens that are scaled in size, such as a 0.5T, 1T and 2T CT specimens, the same algorithm can be used. This applies independent of specimen thickness, material resistivity (for example, Cu vs. CS vs. SS), and the DCPD current. The measured potentials measured will vary, but the ratios will not.

Most DCPD algorithms are created from finite element models (FEMs), but they can also be created by running an air fatigue test and altering the loading conditions to create beach marks on the fracture surface while recording the DC potential data. Beach marking can generally be accomplished by making a large change in ΔK, often by changing the load ratio (R), for example, from an R value of 0.1 to a value of 0.7, followed by growing the crack a short distance at an R value of 0.7 before returning to an R value of 0.1. The algorithms are based on the calculated or measured potential and represent a parallel scale to the measured potentials. The determination of crack length (a/W) is made by:

- Using the known (for example, as-machined) a/W and determining the associated FEM potential (F_0).
- Heating and loading the specimen and acquiring a set of initial averaged potentials (V_0).
- Running the test and accumulating a series of later, averaged potentials (V).
- Computing each potential ratio (V/V_0), then applying that ratio to the initial FEM potential (F_0), to obtain a new FEM potential, F, computed as $F_0 \times (V/V_0)$. If reference probes are used, then $F = F_0 \times (V/V_0)/(Ref/Ref_0)$.
- Using the new FEM potential to determine the new crack length (a/W) via the algorithm.
- The best FEM algorithm is one that is "reversible", that is, you can calculate F_0 from the initial a/W, or a/W from F. Otherwise, an iterative calculation is needed to get an accurate F_0 from the initial a/W.

For DCPD probe locations on a CT specimen, the following FEM algorithm can be used, which can be directly solved to compute the DCPD potential from a/W. Figure 4-5 shows the change in DCPD potential for the active and reference probes. Because there is no location on a CT specimen where the potential is unaffected by crack length, the division by reference ratio (Ref/Ref_0) alters the relationship between DCPD and a/W, and thus a separate algorithm can be used when a back-face reference is used. The difference is small for $a/W < 0.6$.

$$a/W = 1.0763072 - 1.5762256\, e^{(-0.37278571(dcpd)^{0.61018004})} \qquad \textbf{Eq. 4-1}$$

$$dcpd = \left(\frac{\left[ln \frac{1.0763072 - \frac{a}{W}}{1.5762256} \right]}{-0.37278571} \right)^{1.638860557} \qquad \textbf{Eq. 4-2}$$

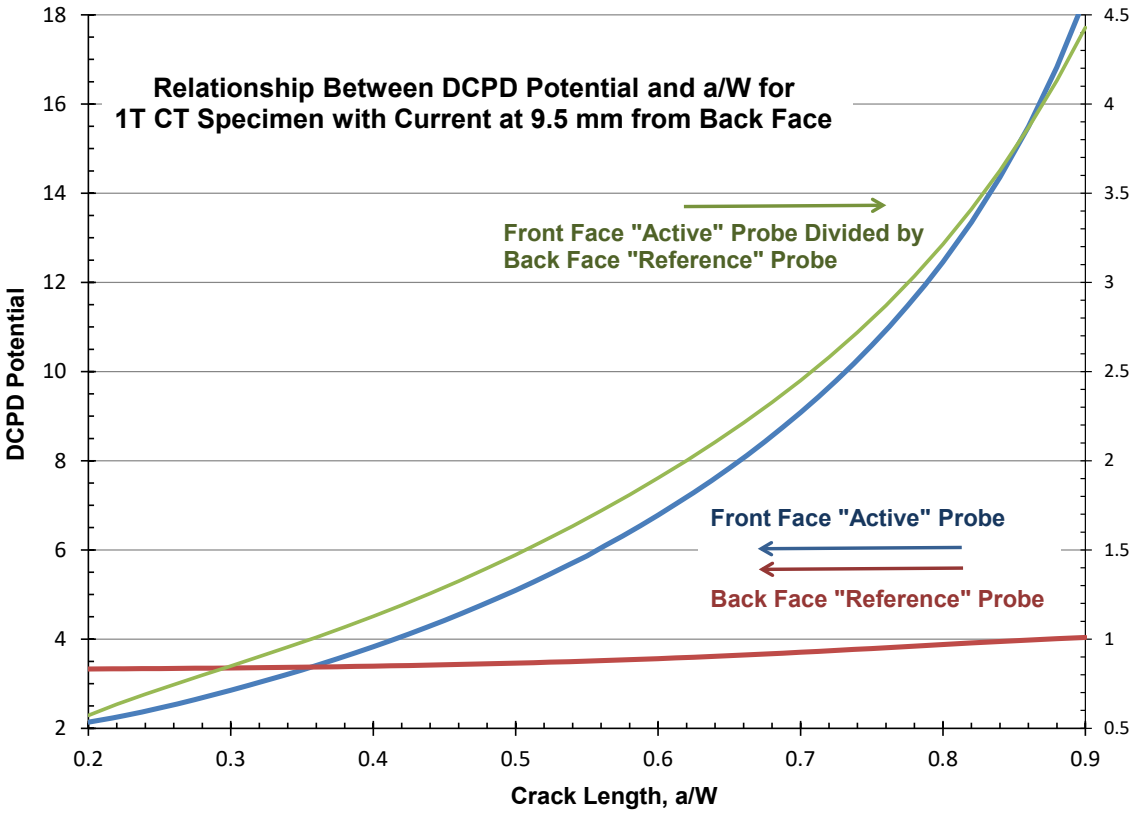

Note: The back face reference probe is not independent of crack length, especially above $a/W = 0.6$, so if they are used, a separate algorithm (the green line) is used.

Figure 4-5
Finite Element Analysis of the Front Face (active) and Back Face (reference) DCPD Potentials

4.5 DCPD Software Capabilities

Averaging the measured DCPD potentials while reversing the current is not complex. However, optimizing measurement throughput often requires low-level control of the DVM and multiplexer so that they directly interact to sequence through the multiplexer channels. It is also important so the DVM avoids an extra auto-zero measurement, which may not be helpful because the current is reversed and thereby self-corrects for any small offsets in the DVM. Additionally, there are many key elements needed beyond this very basic capability, including:

- Operation at variable PLC integration (more than 1 PLC, often 2, 10, 20 or 100 PLC)
- Maximizing acquisition of the DCPD data
- Reversing the current between readings
- Equilibration and initialization, including easily changing the initial a/W and DC potentials
- Algorithms to compute a/W from DC potentials, and DC potentials from the initial a/W
- Multiple algorithms for back-face reference, different specimen geometries, and so on
- The ability to handle DCPD reference probes on the specimen back-face or on separate coupons

- The ability to handle multiple specimens
- The ability to read DCPD data only at or near peak load
- The ability to reject out-of-specification DCPD readings, for example, using a moving average of prior readings
- The ability to calculate K vs. a/W and load for various specimen geometries
- The ability to account for the internal tare load from the autoclave pressure
- The ability for the user to change the load, load ratio, K, frequency, waveform and symmetry, and/or hold time
- The ability to compute and control load to maintain constant K as the crack grows
- The ability to incorporate program steps so that conditions automatically change, which is especially important during rapid crack growth, for example, during fatigue pre-cracking
- The ability to control of $\pm dK/da$ profiles to simulate the way cracks grow in components
- The ability to embed user and automated load-correction comments for a unified data file
- Use of ASCII (text) data files for easy review, editing, and importing to analysis and plotting software
- Use of a variable number of DCPD averages
- The ability to read other key data, for example, temperature, corrosion potentials, inlet/outlet conductivities, load, and so on
- The ability to compute statistics (for example, standard deviation) for key measurements
- The ability to create secondary detailed (debug) files so that testing issues can be diagnosed
- The ability to create files that document errors (error logs), out-of-specification DCPD readings, and so on

4.6 Specimen Homogeneity

Standard DCPD algorithms work for any homogeneous material at any temperature for any applied current. Inhomogeneities pose problems for the base algorithms and the resistivity correction. Materials like SS, most nickel alloys and their weld metals, are all sufficiently similar in resistivity that specimens made of a combination of these materials can be treated as homogeneous. However, if resistivity correction is involved, the resistivity correction can become complex because the active DCPD probes may reflect current flowing through materials of varying resistivity drift and the reference probes may not be positioned to reflect the same mix of materials as the active probes.

A classic example is a specimen comprised of Alloy 600 (or SS, Alloy 690, or their weld metals) and LAS. If the interface between the two materials is parallel to the crack plane, then the current flux lines (Figure 4-3) are not changed, although the DCPD voltage will be lower, and the DCPD algorithm remains accurate. Conversely, if the interface is perpendicular to the crack plane and ahead of the crack, as is relevant to the configuration in Figure 4-6, the current partitions preferentially to the higher conductivity metal. For this example, the CS has about a factor of

5 times higher conductivity at room temperature and ~3 times higher at ~300°C compared to the Alloy 600 material. As the crack nears the material interface, there is a large effect on the relationship between DCPD and *a*/*W* (Figure 4-7) and special algorithms are required. If the interface is some distance behind the crack front, the effect of the different resistivity materials is limited because a very limited fraction of the current flows out of the specimen near or around the loading pin holes. Resistivity correction must reflect the dominant source of the resistivity change. In this example, if the crack is some distance into the Alloy 600 from the material interface, the resistivity shift in Alloy 600 will have a large contribution. If the crack has advanced beyond the material interface well into the LAS, the resistivity shift in Alloy 600 will have minimal effect.

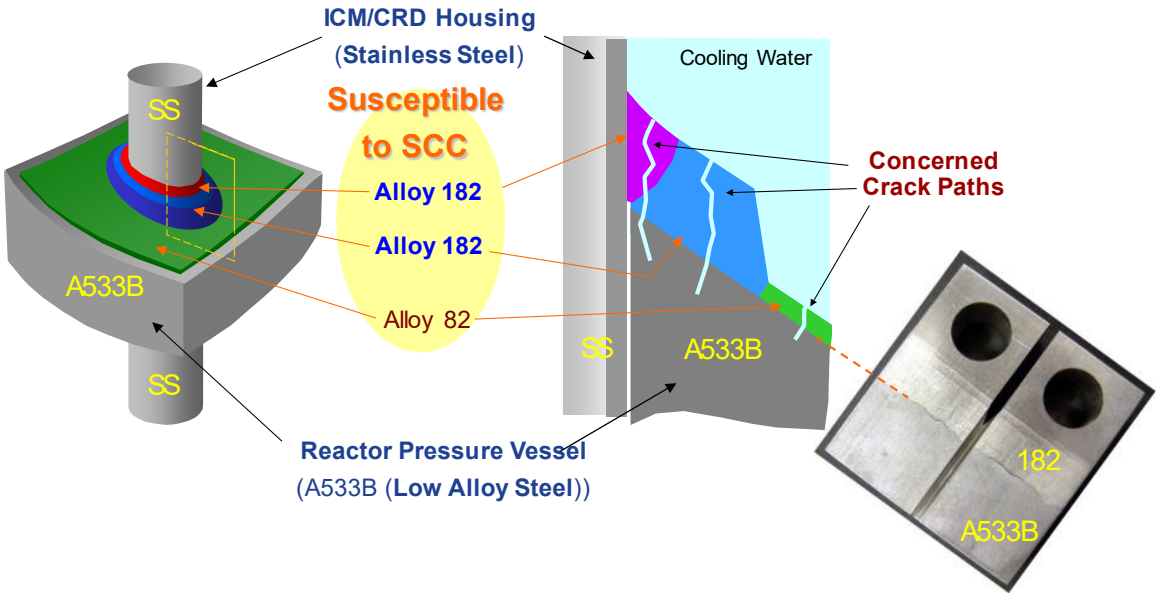

Note: LAS and CS are 3–5 times more conductive than nickel alloys and SS.

Figure 4-6
An Example of the Relevance of Composite Specimens Fabricated from Multiple Materials

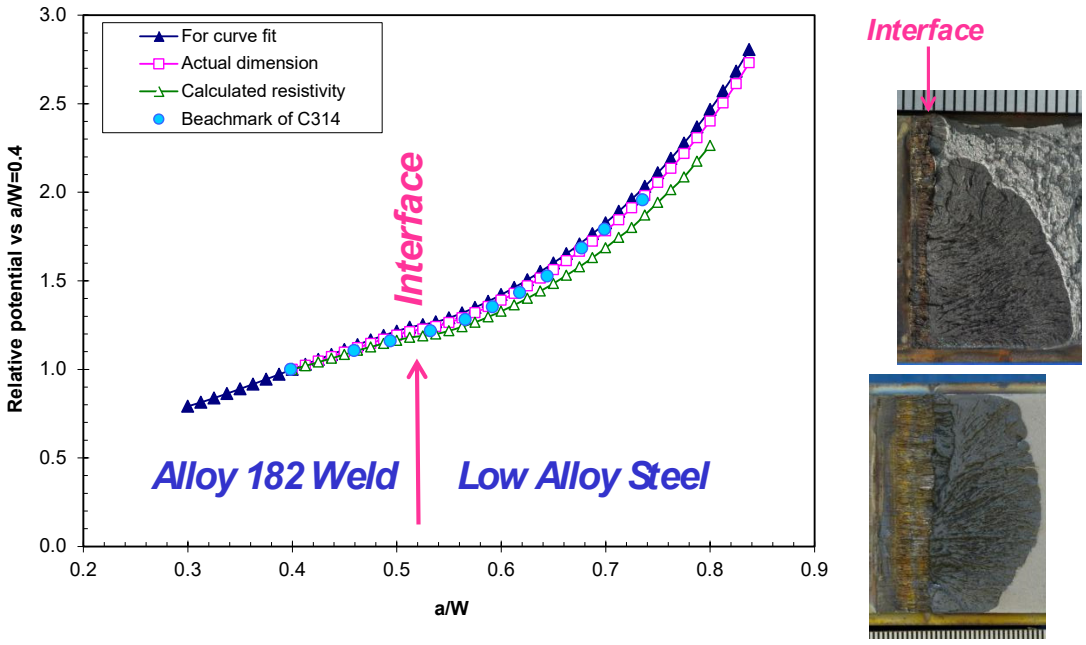

Note: As the crack approaches the interface, the DC potentials remain relatively unchanged, then begin to increase again as the crack moves into the LAS. At 288°C, the resistivity of Alloy 182 is ~3 times higher than LAS.

Figure 4-7
Finite Element Analysis for a Composite Specimen of Alloy 182 Weld Metal and LAS

4.7 Resistivity Drift in Metals

In 1989, Andresen found that supposed crack growth was occurring in Alloy 600 in high temperature water at very low load, and observed that it decayed with time, asymptotically approaching an equilibrium value. This was then evaluated in water of varying dissolved oxygen and hydrogen contents, and in air and argon at various temperatures. The crack growth was instead determined to be unrelated to the environment, but rather represented a drift in metal resistivity vs. time (Figure 4-4). At 360°C, the resistivity approached saturation faster, and thus the initial slope was greater. However, at lower temperatures (for example, below 300°C), the change in resistivity took longer, but it still approached roughly the same saturation value. Cold work accelerated the effect in a similar fashion to temperature, so that a 20% cold-worked specimen shows the same resistivity drift at 280°C as a non-cold-worked specimen at 300°C. If the resistivity drift is erroneously attributed to crack growth, it would reflect a crack growth rate higher than 3×10^{-7} mm/s during early exposure, decaying vs. time. Indeed, various investigators have claimed that the growth rate in Alloy 600 steadily slowed over the first one or two thousand hours at 325°C, which is entirely consistent with the resistivity drift.

Each alloy, heat and weld metal behave differently with respect to resistivity drift. High purity Alloy 600 shows essentially no resistivity drift, leading to the conclusion that the resistivity drift is caused by impurity segregation to the grain boundaries. Broadly speaking, among common Ni alloys used in LWRs, commercial purity Alloy 600 exhibits the highest shift, followed by Alloy 182/82 weld metals, Alloy X-750, Alloy 690 and Alloy 152/52 weld metals, but this is a

very general categorization. Equally important when studying low crack growth rates, even very small shifts in metal resistivity can have a large effect. For example, the 3×10^{-7} mm/s apparent crack growth mentioned in the previous paragraph is important when measuring growth rates in the range of 10^{-7} mm/s or lower, but a factor of 100 times lower resistivity drift becomes important if the growth rate of interest is in the vicinity of 10^{-9} mm/s or lower.

Importantly, when resistivity compensation is used, the material, which may sometimes be a separate coupon, must be exactly the same material with exactly the same heat treatment and processing, and exactly the same exposure history as the SCC specimen. While there appears to be some small effect of cooling and reheating, it does not reset the resistivity drift response.

There is one careful study on the variations in resistivity drift in one heat at various locations, which can be consequential. Thus, the resistivity correction based on different areas of the same material must be viewed as possibly imperfect. In multi-pass welds, including possible changes in the heat of the weld wire used during welding, there is no guarantee that the resistivity response in the vicinity of the reference probes will be identical to the response near the crack. It must also be recognized that these are not point or line measurements. Rather, the DCPD potentials measured on both the active and reference probes represent averages of the potential created as current flows in three dimensions throughout the volume of the specimen. Fortunately, SCC growth rates are rarely reproducible within a factor of two, so resistivity variations, which are also expected to be within a factor of two, should not be a dominant factor. Additionally, the largest ambiguity often occurs at low and very low crack growth rates (for example, less than 5×10^{-9} mm/s), where, in the opinion of most experts, the growth rate is sufficiently low such that it does not affect predicted component lifetimes of 80 years or more.

4.8 Electrochemical Effects of DCPD

Concern for electrochemical effects on SCC and CF from DCPD have been considered from the outset. There are several categories of concern:

- **Polarization between the crack wake surfaces**, which produces accelerated dissolution of MnS and temporarily enhances growth rates, then potentially reduces growth rates as the intersection rate of new MnS is insufficiently fast to sustain the high sulfur crack chemistry.
- **Polarization of the free surface of the specimen**, which produces a different crack chemistry and difference SCC response.
- **Errors in corrosion potential measurements** related to *IR* voltage drops in solution that are unrelated to actual polarization of the specimen surface.
- **Electrolysis of water** across the current leads, which produces oxygen and hydrogen evolution if the voltage difference between the leads is high enough (perhaps larger than 0.7 V for solutions containing little or no oxygen).

Polarization Between the Crack Wake Surfaces is very unlikely but has been claimed in at least one case. The effect of MnS dissolution on crack chemistry and crack growth is primarily limited to CS and LAS, where the composition of MnS renders it more prone to dissolution and the effect of dissolved sulfur species in the crack (primarily HS^-) is greater than in higher alloy

materials like SS.[4] An effect of DCPD on CF behavior was identified by Lee James in tests on LAS in ammoniated water at ~300°C. When DCPD was operating, there was a period where the crack continued growing more rapidly, then it slowed to a rate consistent with low sulfur behavior. Without DCPD, the elevated crack growth rate was sustained. Assuming these results were correctly interpreted, there are two factors that may have contributed in this situation: 1) the surface crack specimen that was used created a very tight crack (that is, small crack opening displacement), and 2) the presence of ammonia enhanced the conductivity of the solution and therefore the electrochemical coupling. An additional factor is the unknown current level used and associated DC potential created, which might have been high.

Other extensive measurements by many testing organizations on LAS, SS and nickel alloys showed no such bias from DCPD measurements. Even in controlled experiments where DCPD was shut down for many days, then restarted, the growth rate proceeded at the same rate. These include tests in pure water and in primary PWR (B/Li) water. It is important to recognize that the typical potential measured at the crack mouth using the active probes is 30–200 μV. The lower end of this scale is applicable for LAS, which is more conductive than SS or nickel alloys. If the potential probes were moved along the crack flanks toward the crack tip, the potential difference would drop dramatically. At less than 1 mm from the crack tip, the potential difference from the upper crack surface to the lower crack surface would be less than 10 μV and reversing about every second. Additionally, the high specific resistance of the water further limits the current densities through the crack crevice environment between the crack flanks. This is a very small value, and concerns for these effects in modern DCPD implementations should be viewed as very unlikely. But, as with dozens of other aspects of experiments in high temperature water, the investigator should be aware of and watch for such anomalies.

Polarization of the Free Surface of the Specimen and Errors in Corrosion Potential Measurements are related issues, in that both result from the voltage drop in the DCPD current leads inside the autoclave. Figure 4-8 outlines the issue, which is based on the fact that a ~1 V drop along each current lead acts like a battery. Thus, if there is an ionic path near the autoclave seal, then there will be some polarization applied to the specimen. This polarization is due to the fact that there is a resistor divider involving a possibly lower resistance ionic path between one current lead and the autoclave head (R_1), and a second (likely higher resistance) ionic path between the autoclave body and the specimen (R_2). If there is a 1 V drop along the current wire leading to the specimen, then the voltage drop between the autoclave wall and the specimen is $1\ V \times R_2/(R_1+R_2)$, which is close to 1 V if R_2 is much larger than R_1.

Polarization can cause two problems. First, if the reference electrode is located close to the autoclave wall, as it "looks toward" the specimen to measure the corrosion potential, it must "look through" the *IR* drop in the fairly low conductivity water. In general, attempts to polarize a specimen in pure water, or B/Li or other LWR primary water chemistries, result in a large *IR*

[4] MnS is readily soluble in high-temperature water, FeS and NiS are somewhat less soluble, and CrS is "sparingly" soluble. The formed sulfide anions in the crevice environment strongly affect the repassivation rate after oxide film rupture, in particular in low Cr CS and LAS, and the repassivation rate strongly increases with Cr content. Furthermore, especially in the older nuclear plants, CS and LAS can have quite high sulfur contents.

drop because moving ionic current in high resistivity solutions requires a significant amount of voltage. One laboratory that measured the corrosion potential during DCPD operation showed a change by about ±1 V, from about +1 V to –1 V (Figure 4-9). The actual voltage induced was probably higher, but the electrolysis reaction limited the value to about ±1 V.

Even very small leakage causes problems for ECP noise measurements, which often evaluate mV level changes in corrosion potential to identify crack initiation. The quality of the insulation along the current wires must be excellent to avoid each current reversal producing a 1 to 20 mV or more change in the apparent corrosion potential.

Since most of the voltage occurs as an *IR* drop in solution, specimen surface polarization is limited. In turn, in a CT specimen, the majority of the crack mouth often exists in the notch of the specimen, vs. along the exposed edges of the specimen, and these areas are polarized even less. This is not a reason to ignore the concern, but it does make it less likely to be problematic. Note that in typical PWR (B/Li) primary water, the conductivity of the water is not nearly as different, relative to pure water, at ~300°C compared to room temperature. At room temperature, the conductivity of pure water is 0.055 μS/cm, which increases to ~4 μS/cm at 250°C, then decreases somewhat at higher temperatures. A B concentration of 1,000 ppm and 1 ppm Li has a conductivity of 10.6 μS/cm at room temperature and 71.7 μS/cm at 250°C. So, the difference between the two chemistries is a factor of 193 at room temperature, but only a factor of 18 at 250°C.

If the current leakage path of the two current leads is identical and the voltage drop is the same in each wire, then from the perspective of polarizing the specimen, the two contributions will cancel each other. The proper way to view this is that there is a “battery” with a positive voltage on the current lead going to the specimen and an equivalent “battery” with a negative voltage on the current lead coming back from the specimen. However, the chance that the two contributions of current leakage near the autoclave seal are identical is very low. Another way to look at this is that, relative to the specimen, at the seal one wire is +1 V and the other wire is –1 V, so no net current will flow to the autoclave, but current will flow between the current wires.

Electrolysis of Water is always a concern for O_2 (and H_2) evolution when there is a large voltage drop in the autoclave. In general, the concern is much higher for O_2 evolution because the corrosion potential in nitrogen or argon deaerated water remains quite low (that is, at the water line). When ppb levels of oxygen become present, the oxygen reduction reaction arises and its half-cell potential, depending on the oxygen concentration, is 700 to 1000 mV higher. Thus, when a potential difference of that magnitude is present, and there is an ionic path, electrolysis of water will occur. Often the difference in the potential of the current leads at the seal, representing the voltage drop in one Pt wire, through the specimen(s) and back in another Pt wire, is greater than 1V. So, if there is a break in the insulation near the seal, or closer to the seal than the specimen, oxygen evolution may be occurring. At the specimen, the voltage drop is small, perhaps a few mV between the entry point and exit point of the current; most of the voltage drop occurs in the wires that carry the current. If there is a very limited ionic path because the wires are nearly fully insulated, the breaks in the insulation are separated, or the wires penetrate separate seals, then the voltage drop is mostly dissipated as an *IR* voltage drop, and very little oxygen is evolved. If both current wires are exposed near the seal, there would be a significant amount of electrolysis. The fact that the current reverses every second or so does not help the situation; it only means that oxygen evolution occurs alternately at one wire, then the other.

One solution to electrolysis is to use larger Pt wires such that the voltage drop along the two wires is below ~0.5 V, or to ensure that the wires are continuously insulated from outside the autoclave to the specimen. This is impossible above ~310°C because zirconia insulation, with at least some breaks including at the wire seal, must be used in place of PTFE Teflon. Another solution is to use the autoclave structures rather than wires to carry the DCPD current. (Note: there has been concern that the various threaded contacts in high temperature water could oxidize and become somewhat, or highly, resistive, but this concern has not been experienced.) The total voltage drop through the autoclave head, the loading posts, the interior loading plate and down through a string of ~12 threaded initiation specimens is typically in the vicinity of 40 mV. The same approach can be used with crack growth specimens using the linkage and clevises to carry the current, then using a short Pt wire to introduce the current at the desired location on the specimen. To succeed, there must be excellent insulation at the loading pins/clevises so that the current enters and exits the specimen via the Pt wires. Additionally, the pull rod extending through the pressure seal must be insulated from the autoclave and actuator so that the only path for the current to flow is through the CT specimen. In turn, the ground-isolated power supply can be connected to the autoclave structure and to the insulated pull rod.

The concern for water electrolysis has been confirmed when using Pt current wires in early initiation tests where a specimen failure occurred, and the current path was interrupted. In modern power supplies, this causes a "cross-over" into constant voltage mode, which is usually set to a relatively high voltage (greater than 5 V) to make sure there is sufficient voltage to maintain constant current. Under these specimen failure conditions, it was observed that some current flow continued because of electrolysis of water, producing O_2 and H_2. In these tests, the current was carried by the autoclave structures and down through the string of initiation specimens, so the problem was fully resolved by adjusting the power supply so that its maximum output voltage (for example, after specimen failure) was less than 0.4 V. However, if the current was instead carried by wires, the problem would have persisted.

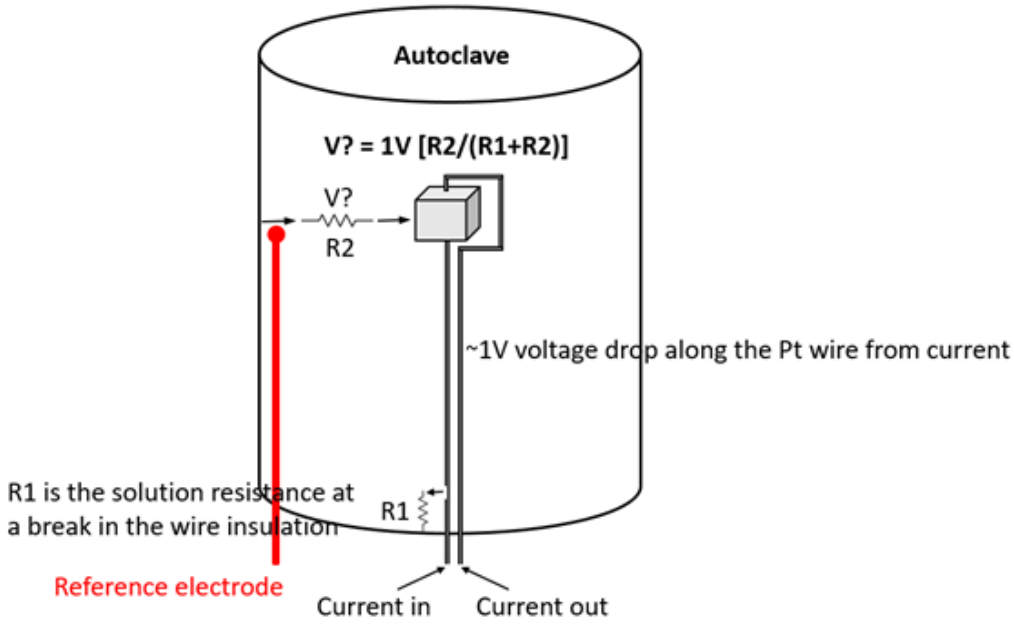

Figure 4-8
Schematic of the Equivalent Circuit that Exists if There is an Ionic Path (R1) from Incomplete Insulation on the Current Wires Near the Seal

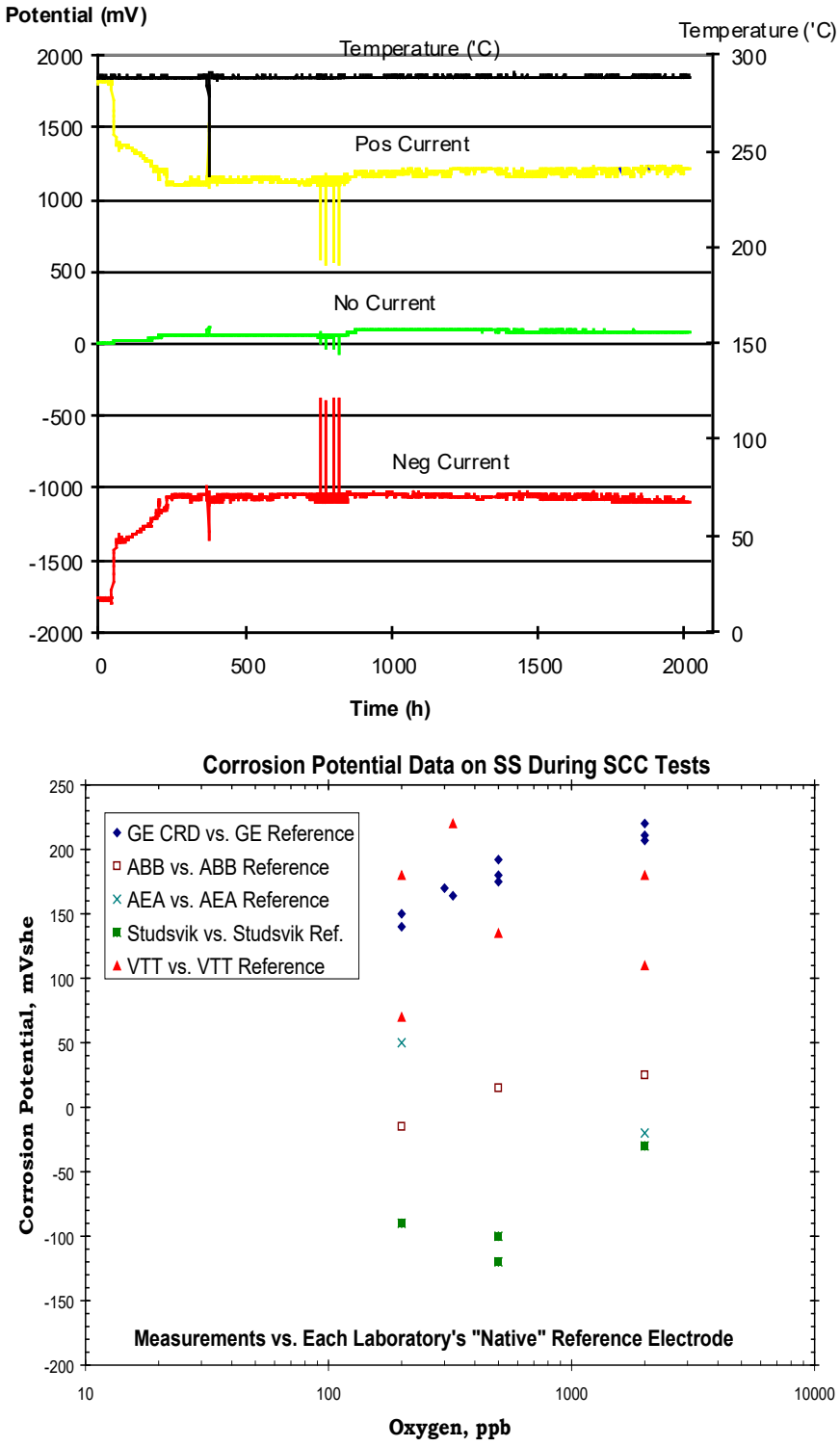

Note: (Top) The effect of DCPD on corrosion potential measurements when the current wires are not well insulated. (Bottom) The variation in corrosion potential measured at different labs on the same material in the same water chemistry.

Figure 4-9
Variations in Corrosion Potential Measurements

4.9 Crack Front Unevenness and Other Sources of DCPD Error

Despite its very high resolution capability, DCPD can suffer from significant errors, usually under-estimation, in measurements of crack depth. When evaluated in air fatigue tests where the crack is TG and a single, planar crack exists, DCPD is usually very accurate (for example, within ±5% of the crack growth increment). However, if the crack front is very uneven, islands of uncracked material exist in the wake of the crack, extensive branching occurs, or there is contact in the wake of the crack through which DC current can flow, DCPD can have significant measurement error. This is also true with unloading compliance.

Errors in DCPD occur for the same basic reason; there is an alternate (that is, shorting) path for the DC current because the current flux lines bulge out toward the loading pins. This issue is even more pronounced if the current entry point is shifted toward the front of the CT specimen. This situation becomes more extreme if the current inputs are located at the front face of the specimen (although the sensitivity, or higher increase in potential for a given crack growth increment, is higher for straight crack fronts). The current flux lines become dense near the crack tip (Figure 4-3), and if there is a path for the current in the wake of the crack, it has a large effect.

Errors in DCPD measurements have been evaluated using a series of Pt wire spot welds across the wake of the crack and the specimen notch, which produced a significantly stronger effect than is consistently observed using an area average for the current conduction path. It has also been evaluated by FEM (Figure 4-10), which evaluated various idealized versions of uneven crack fronts, and showed that DCPD is strongly influenced by the region of shortest crack advance. Examples of uneven cracks are shown in Figure 4-11.

For different reasons, nickel alloy weld metals and irradiated SS can exhibit large DCPD errors, more than a factor of 10 in some cases. For weld metals, growth from the machined notch or the fatigue pre-crack may not occur along the entire crack front, despite extensive crack advance along most of the crack front. Dendrites can also rotate out of the fracture surface and remain connected to the upper and lower wake of the crack (Figure 4-11). For irradiated SS, the crack can be non-uniform, the susceptibility is often high, and cracking occurs around most grains, which can rotate and remain attached to both the upper and lower wake of the crack. Non-uniformity of the crack front is more pronounced if the test is run for long periods at constant *K*/load. The unevenness may increase or decrease during a test and can result in periods of lower and/or higher SCC rates.

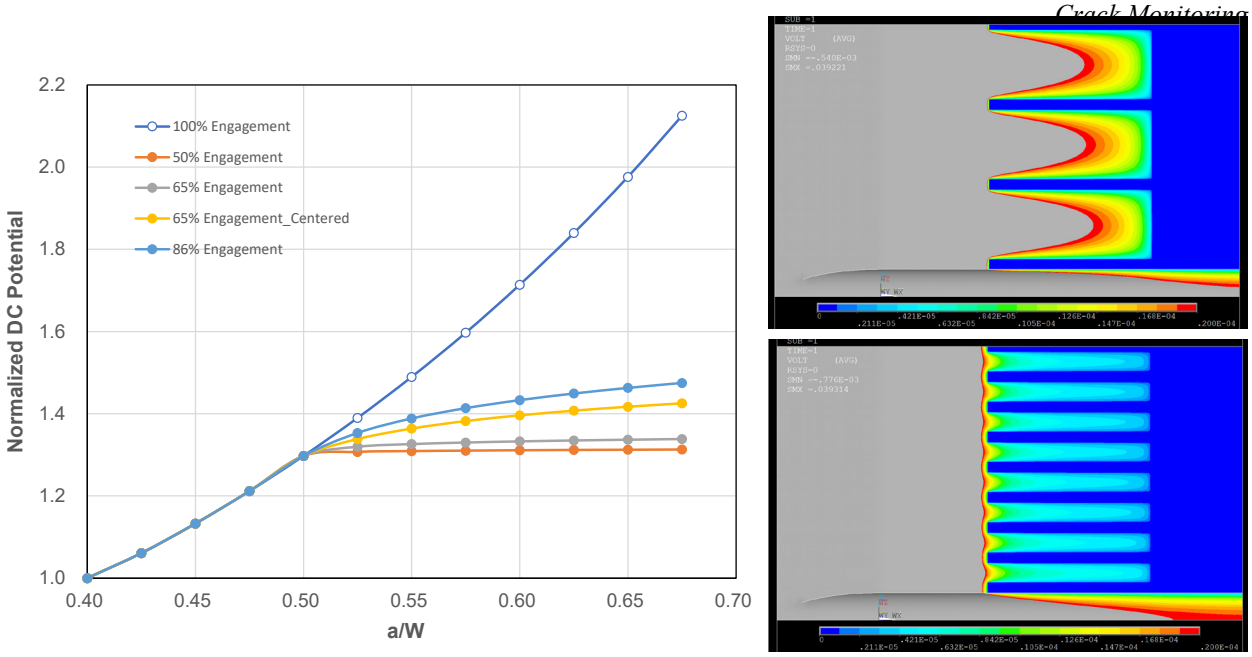

Note: The figures on the right represent a crack growing to the right for 65% engagement (bottom) and 86% engagement (top), where the bright blue represents uncracked regions. Courtesy of personal communication with Katsuhiko Kumagai (TEPCO).

Figure 4-10
Finite Element Analysis of the Strong Effect of an Uneven Crack Front Starting at an *a*/*W* of 0.5 on DCPD

Note: (Left) Very uneven crack growth in a composite CT specimen of Alloy 182 weld metal (bottom) and LAS. (Right) Very uneven crack growth in Alloy 182 weld metal showing dendrite rotation that maintains metal contact between the upper and lower faces of the crack wake.

Figure 4-11
Examples of Uneven Crack Growth

4.10 Post-Test Correction

After testing in high temperature water, the specimen should be fatigued apart in air to create a clearly visible distinction between the water oxidized fracture surface and the shiny, air-fatigue surface. The post-test fatigue conditions (K_{max}, R-ratio) should be selected to avoid the destruction of micro-fractographic details by crack closure or excessive crack-tip plasticity, especially if further post-test metallographic/fractographic investigations are intended. CS and LAS, or other body-centered cubic (bcc) alloys, can be very efficiently opened by brittle fracture after cooling in liquid nitrogen by mechanical overloading. While 10- and 20-line averages have been recommended to determine the average crack depth, it is easier and better to take a macro photograph and estimate (or perform area mapping) to determine the average crack depth. In almost all cases, it is more relevant to correct to the average crack depth than it is to correct the maximum crack depth. While leakage of coolant will occur in actual components based on the maximum crack depth, there are many reasons why only some regions of the microstructure will grow faster, then later other regions will grow faster. The consensus among experts is that the average crack depth is the most relevant.

The exception to averaging the crack depth across the entire specimen thickness is when there is no crack advance from the machined notch or the fatigue pre-crack. This is because there is voluminous data to show that there are many reasons why SCC does not quickly/easily develop from the notch or pre-crack, and none of the reasons are relevant to plant components. In such cases, experts have agreed that the best approach is as follows:

- Average the areas where the crack has engaged/grown from the machined notch or fatigue pre-crack, provided the crack has engaged along at least a 35–50% of the crack front. Below that level, the data are less credible, but it is still worth reporting the local maximum growth rates.[5]
- If there are large regions of engaged area that are at a similar crack depth, then only those areas should be used to determine the average crack depth (the areas of shallower growth should not be included in the average).

The preferred method for post-test corrections is to attribute the correction linearly throughout the duration of the test. Many investigators will perform separate linear corrections for the TG fatigue pre-crack and the IG crack, when it occurs. There is some justification for a non-linear correction, because as unevenness initially develops, the correction is smaller than when the unevenness increases; the greater the difference between the average crack depth and the minimum crack depth, the bigger the error can be. However, it is not possible to know when or how the unevenness developed; if such details were known, a more sophisticated correction methodology would be justified. Such details are never known, so a simple linear correction is strongly recommended.

[5] Experience indicates that the local rates with very uneven crack fronts are often in a similar range as in specimens with full engagement and even crack fronts under otherwise identical conditions, although perhaps lower because more stress is carried by the uncracked portions of the crack. For CS and LAS, SCC/EAC can spread like a fan from a large MnS-inclusion (or clusters/stingers of MnS) that is intersected by the crack front/specimen surface. Under some conditions, these cracks can spread over large areas after long periods, so the local crack growth direction can strongly deviate from the main crack growth direction in CT specimens. In plant components, this behavior can result in through wall semi-elliptical cracks that result in leakage. Such situations should be treated differently.

Post-test correction can be accomplished by linearly adjusting DC potentials, then converting the potentials to a/W or linearly adjusting a/W; the differences are not large. However, it is equally important to correct the K, especially when there has been extensive crack advance, because for a given load, K rises rapidly with a/W (Figure 4-12). In addition to this correction in K, consideration should be given to decrease the corrected K because the uncracked ligaments carry a disproportionate fraction of the applied load, so the portions of the crack front are extending are at a low "K" (although K is not a local, microscopic parameter.)

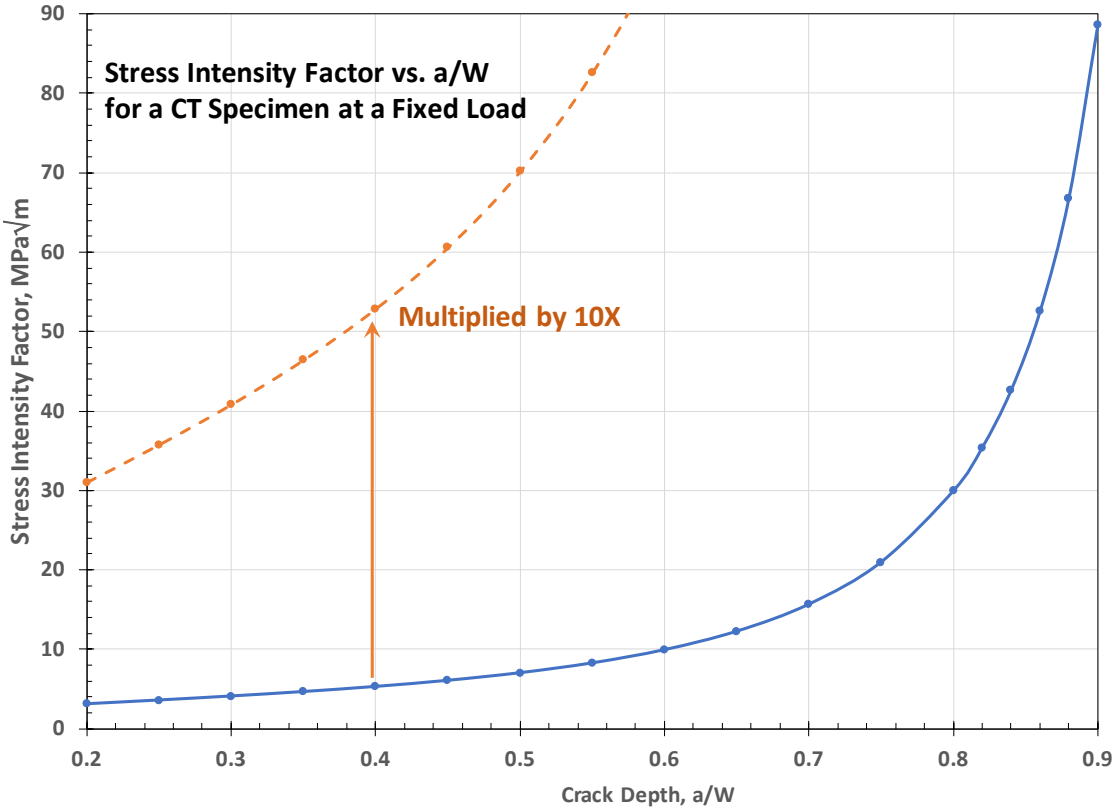

Figure 4-12
Relationship of *K* vs. *a/W* for a Fixed Load Applied to a CT Specimen

4.11 Anticipatory Correction

With some experience, a reasonable estimate of the DCPD error that will develop during testing can be made. A valuable feature of data acquisition software is anticipatory correction, whereby any change in DC potential above a specific value, V_s, (typically the potential after fatigue pre-cracking or transitioning and before SCC testing) is increased by an anticipator correction, V_{corr}, value of AC (for example, using values of 1.5, 2, 3, and so on). In other words, $V_{corr} = V + AC\,(V - V_s)$, and then the ratio of V_{corr}/V_0 is performed. This could also be accomplished using a reference value in a/W and increasing that in a proportional fashion. This improves the estimate of crack depth and crack growth rate and permits the test to run close to constant K conditions.

4.12 Limiting DCPD During Unloading

DCPD can show a lower potential during unloading cycles. Often the fracture surfaces do not re-mate perfectly, and/or the (semi-conducting) oxide on the fracture surface is insufficiently insulating and the unloading process produces contact that alters the current distribution. Occasionally this causes a very strong effect of unloading on DCPD. The data acquisition software can incorporate a load limit, or ratio to the maximum load, like the *R*-ratio, below which DCPD measurements are not taken.

4.13 Effect of Test Temperature Changes on DCPD

While temperature fluctuations in the autoclave are best addressed by better PID tuning of the temperature controller, there are occasions when temperature is intentionally changed during a test. Even with reference probes, the compensation is imperfect. The best approach is to make the temperature change as rapidly as possible which usually can be accomplished in an hour or two. Then the initial DCPD potential (V_0) can be changed so that the new/current DCPD potential gives the same potential ratio (V/V_0, or a/W). This change is equivalent to starting and running the test at the new temperature.

There are alternative specimen designs and DCPD methods that are very insensitive to temperature [49]. One is a DCB specimen, where the DCPD current is introduced at the ends of the arms and potential probes are positioned along the arms in the wake of the crack. When the potentials are plotted vs. distance along the arm, the linear fit can be extrapolated to 0 V, which corresponds to a fixed offset from the crack tip. As the current, temperature, or resistivity changes, all potentials change proportionately, and the extrapolation to 0 V occurs at the same point.

4.14 Effect of Chemistry Changes on DCPD

As noted in Section 4.8 on electrochemical effects of DCPD, DCPD can create voltage drops that induce ionic current flow when there is incomplete insulation along the DCPD leads. Another side-effect is that the measured DCPD potentials can change with the water chemistry. This is not a significant issue for very small changes in conductivity, such as from pure water to 10–30 ppb chloride or sulfate; these have a very limited effect on high temperature conductivity. It can be a consequential effect if significant changes are made in PWR primary water, whether because of a slow drift in chemistry or an intentional change.

Figure 4-13 shows an example of a slow drift in PWR conductivity, measured at 25°C, that was corrected back to the target values. The correction resulted in a significant change in DCPD potentials and the associated apparent crack length. The underlying issue is that in hydrogenated water, the primary impurity is often Fe^{2+}, which is ion-exchanged in the B/Li equilibrated demineralizer with H^+ and some Li^+. An increase in Li^+ results in an increase in pH and conductivity (Figure 3-6). As the conductivity rises, there is cross-talk or interference between the various DCPD leads which, above ~300°C, must be insulated with segments of zirconia; this is not observed if continuous PTFE Teflon is used from outside the autoclave to the specimen. Some DCPD potentials increase and some decrease. Careful wire routing, minimizing the number and size of gaps in the insulation, and staggering the insulation breaks can reduce the effect.

The best resolution for these issues is to maintain a stable chemistry. This is best accomplished by using a conductivity meter to control the injection of a solution containing only the desired B concentration where the conductivity meter is set to inject as the conductivity rises. In these situations, some limited increase in solution level in the reservoir (or overflow from the reservoir) will occur. This approach can automatically maintain the B/Li levels to very stable levels as a function of time.

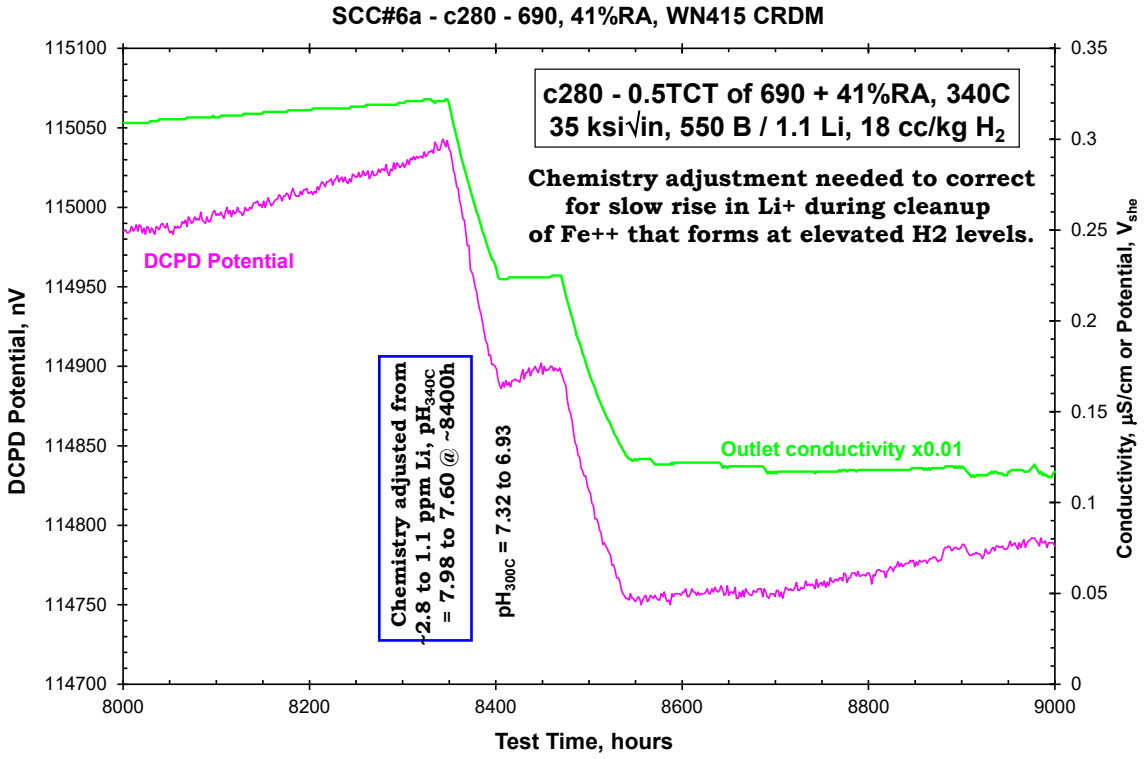

Note: The long-term drift upward in conductivity, usually from ion exchanging Li^{+} for Fe^{2+}, can have an effect on DCPD potentials. At about 8,350 and 8,450 hours, manual corrections were made to bring the B/Li levels to the desired levels (550 ppm B and 1.1 ppm Li), which caused a significant effect on DCPD potentials. In some cases, the effect is smaller or negative.

Figure 4-13
Long Term Drift Upward in Conductivity

4.15 DCPD for Monitoring Initiation; Specimens vs. Components; FAC/Corrosion

DCPD is capable of monitoring a wide array of phenomena from incipient cracking to crack advance, to wall thinning, to metal resistivity changes, to providing size/shape information for cracks in specimens and components. Potential drop tomography has been developed for geo-physics and medical uses under various names, such as electric current computed tomography, electrical resistivity tomography, electrical resistivity imaging, and electrical impedance tomography, among others. General Electric (GE) developed tomographic DCPD ~35 years ago to monitor crack growth and shape from the outside surface of components like piping and safe ends.

GE performed the first growth rate tests on irradiated SS [50], and later used DCPD to measure crack growth rates in both the recirculation loop and in-core components in various BWRs [51]. They also worked with the variable energy cyclotron at the United Kingdom Atomic Energy Authority at Harwell and the test reactors at the Massachusetts Institute of Technology and the Halden Reactor Project.

In the laboratory setting, somewhat different approaches are used for studying crack initiation from smooth surfaces, crack growth on specimens with surface cracks, crack growth on defected specimens (for example, CT specimens) and wall thinning from flow accelerated corrosion or general corrosion. The more well-defined the area of damage is, the more precise DCPD can be. DCPD works extraordinarily well for notched or CT specimens (Figure 4-14 and Figure 4-15) and it works almost as well for surface cracks if the potential probes are positioned near the crack (Figure 4-16 and Figure 4-17). DCPD also can detect very small cracks initiating in notched bars (Figure 4-18). For round tensile specimens without notches or defects, the potential probes are usually placed on the radius or shoulders of the specimen and must identify incipient cracking “at a distance” (Figure 4-19). Under these conditions, it is essentially impossible to know whether the crack is long and shallow, narrow and deep, or if there are multiple cracks. It is often possible to detect cracks that are ~0.01% of the specimen area, but this also depends on the length of the gage section (that is, the distance between the potential probes). Arbitrarily small cracks can be detected as the probes get closer together and the gage diameter becomes small. In most cases for this geometry, the current is introduced at the ends of the specimen.

In large specimens or components, whether monitoring for cracking or wall thinning, it is not feasible to introduce current at the ends of the component; for example, a large diameter pipe or safe end. In such cases, current is best introduced somewhat local to the potential probes or potential probe array.

In smooth specimens at elevated temperatures, creep also occurs. In addition to monitoring creep cracking, DCPD has long been used to measure creep rates, where the measured potential increases as the specimen elongates and the diameter shrinks because of the overall resistance change. This change in potential is proportional to $\rho L/A$, where ρ is the resistivity of the specimen material, L is the specimen length and A is the specimen cross-sectional area. The measured potential also depends on the current (I) flowing through the specimen, so that:

$$V = I \times \rho L/A \qquad \textbf{Eq. 4-3}$$

Conservation of volume ($A \times L$) as the specimen elongates dictates that $A = (Volume)/L$, so:

$$V = I \times \frac{\rho L}{A} = I \times \rho L^2/(Volume) \quad \textbf{Eq. 4-4}$$

Since ratios of V/V_0 are used, the constants (current, resistivity and volume) cancel:

$$V/V_0 = (L/L_0)^2 \quad \text{or} \quad L/L_0 = (V/V_0)^{0.5} \quad \textbf{Eq. 4-5}$$

Conversion to strain is straightforward based on the ratio of the initial potential to subsequently measured potentials (V/V_0). True strain, ε, is equal to ln (L/L_0), so:

$$\varepsilon = ln(V/V_0)^{0.5} = 0.5ln(V/V_0) \quad \textbf{Eq. 4-6}$$

Reference probe resistivity compensation (R) uses the usual reference-normalized voltage:

$$(V/V_0)/(Ref/Ref_0) \quad \textbf{Eq. 4-7}$$

So, the equation becomes:

$$\varepsilon = 0.5ln[(V/V_0)/(Ref/Ref_0)] \quad \textbf{Eq. 4-8}$$

These equations apply for uniform elongation and are not appropriate for situations where necking or a non-uniform density of cracks develop. In practice, the value in converting to strain is greatest for creep testing. Converting to strain is rarely critical for initiation testing because the increasing potential from crack initiation disrupts the relationship between potential and strain; that is, initiation can be estimated from the intersection of the earlier slope of the potential and strain and the subsequent higher slope of the potential and strain as cracks form. Strain can be used to evaluate yielding during loading but, this is often not helpful because all specimens may not be monitored and the yield strength varies slightly from specimen to specimen and region to region in the specimen, especially in alloys with significant inhomogeneity, which most commercial materials possess. If yielding is evaluated in 30% of the specimens and loading is stopped at that point, yielding might not occur in some other specimens. Testing is normally performed at a predetermined value of yield strength, for example, 102%, where yielding in all specimens is likely. Note also it has been observed that initiation occurs at 90% of the yield strength in some tests, which is a common crack initiation observation, so testing above 100% yield strength is not essential for either some plastic strain or crack initiation to occur.

Detection of crack initiation is based on the deviation from the evolution in potential or reference-normalized potential (V/R). In most cases, the differences are not very significant. The reference-normalized potential has a somewhat lower slope as a function of time because the resistivity drift is removed, but the creep rate contribution remains. In most cases, the deflection in slope is quite pronounced as SCC initiation occurs, as noted in Figure 4-19. Detection of initiation on the finest scale would be slightly enhanced using reference-normalized potentials, but much less than the benefit of using a smaller diameter or shorter specimen or localizing the initiation site and potential probe placement using a notch or other defect.

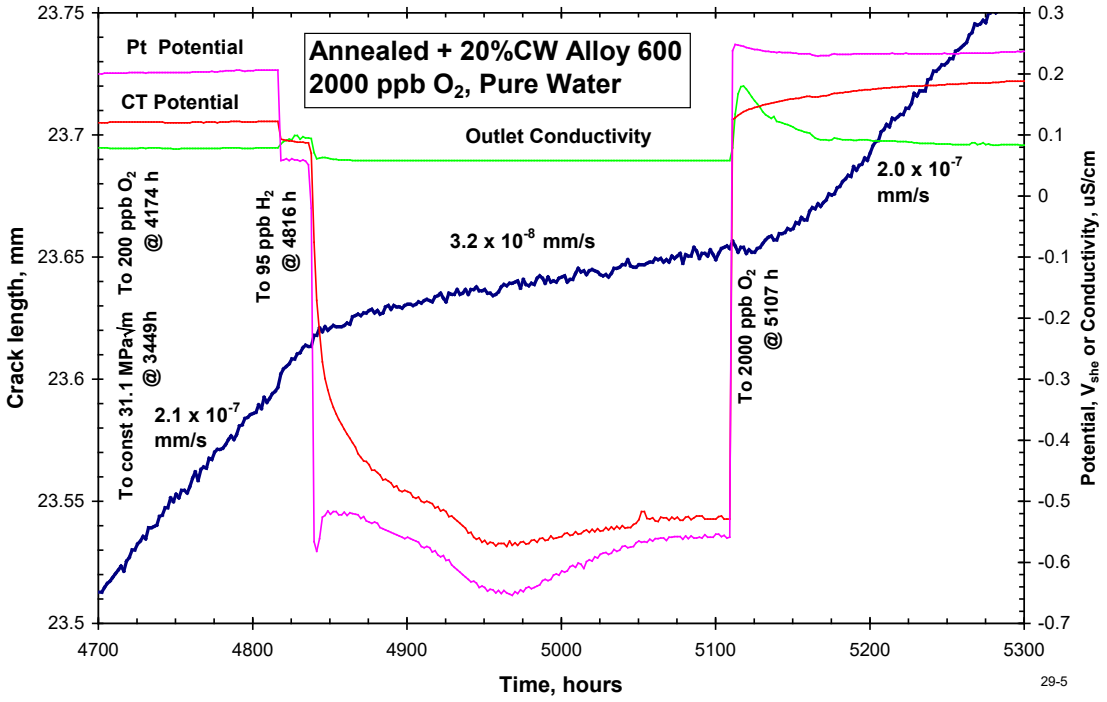

Figure 4-14
Crack Length vs. Time Showing the Crack Length Resolution, the Effects of "On-the-Fly" Changes in Water Chemistry, and Growth Rate Repeatability

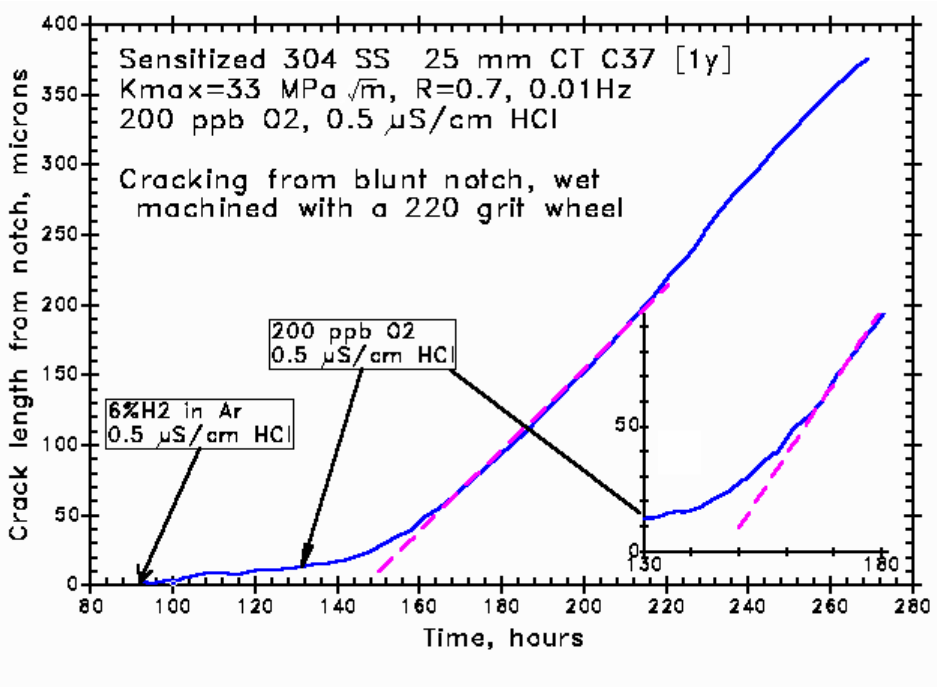

Figure 4-15
Detection of Crack Nucleation and Growth from a CT Specimen with a Blunt Notch in Place of the Machined Notch

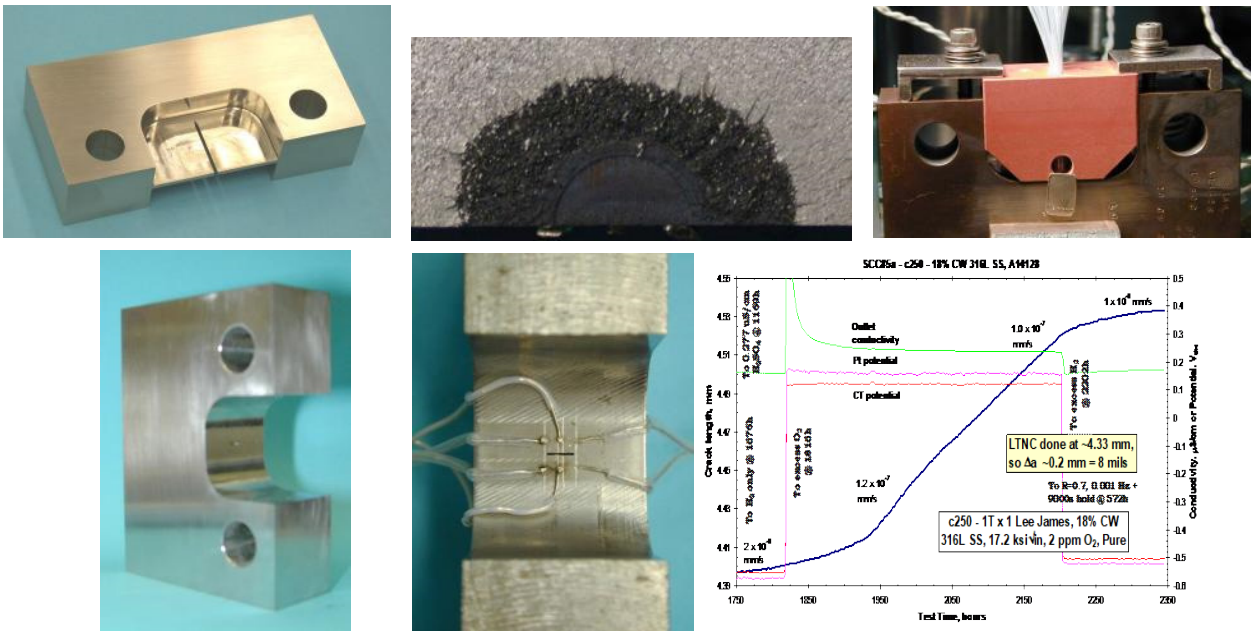

Note: Current is introduced at the top and bottom of the specimen, and the potential probes are positioned near the crack.

Figure 4-16
Surface Crack Specimen for Use to Study Flow Rate Effects

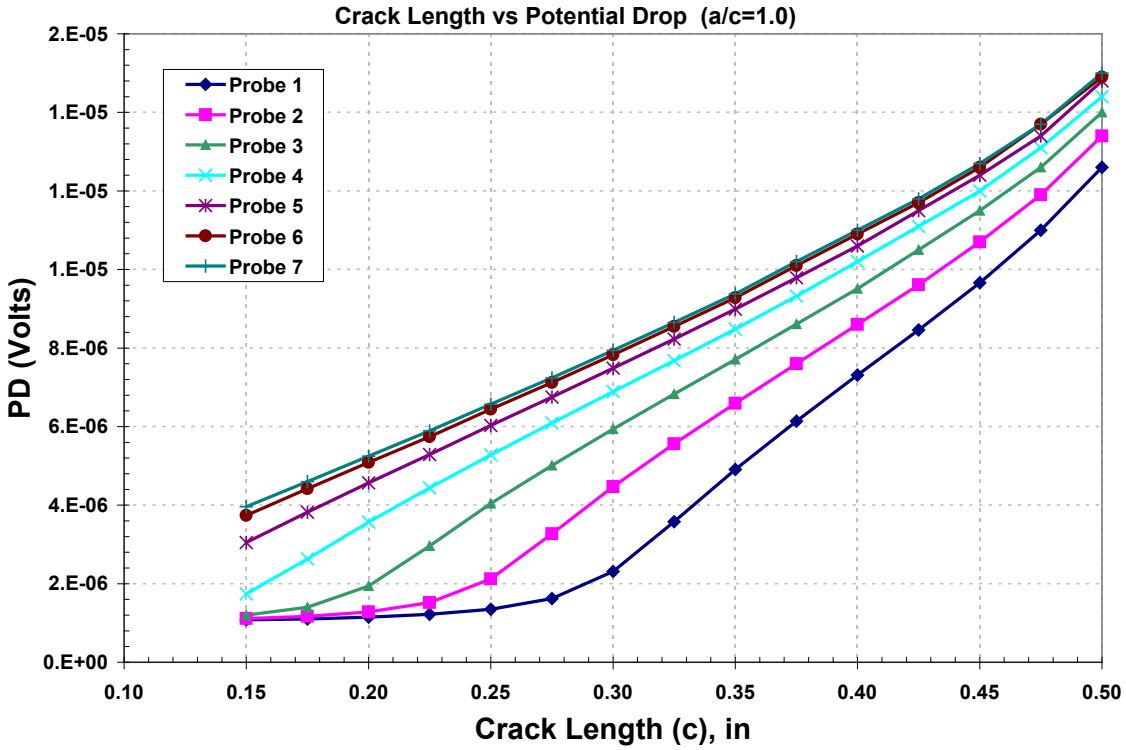

Figure 4-17
DC Potential vs. Surface Crack Length in the Specimen in Figure 4-16

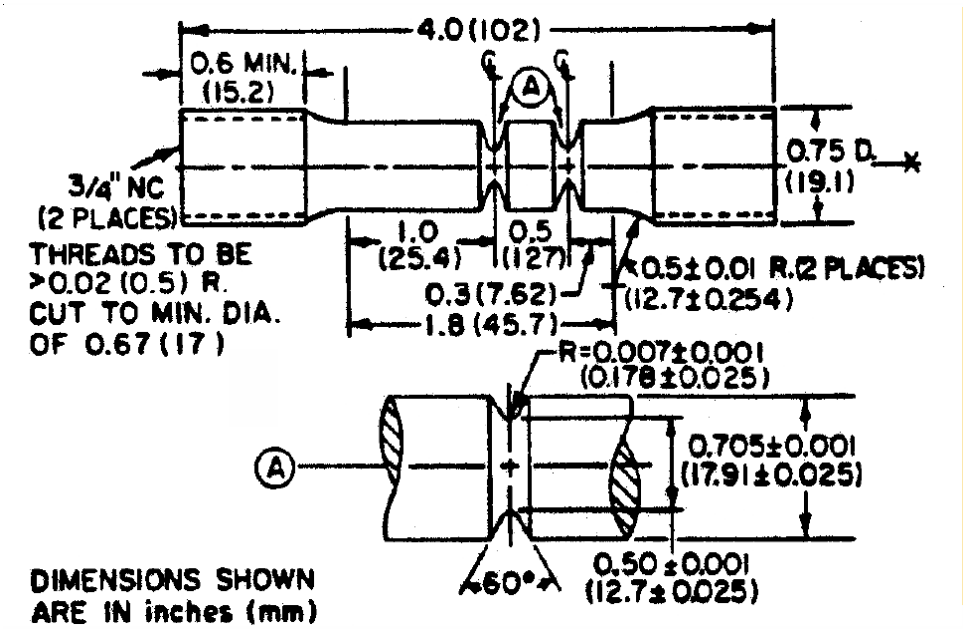

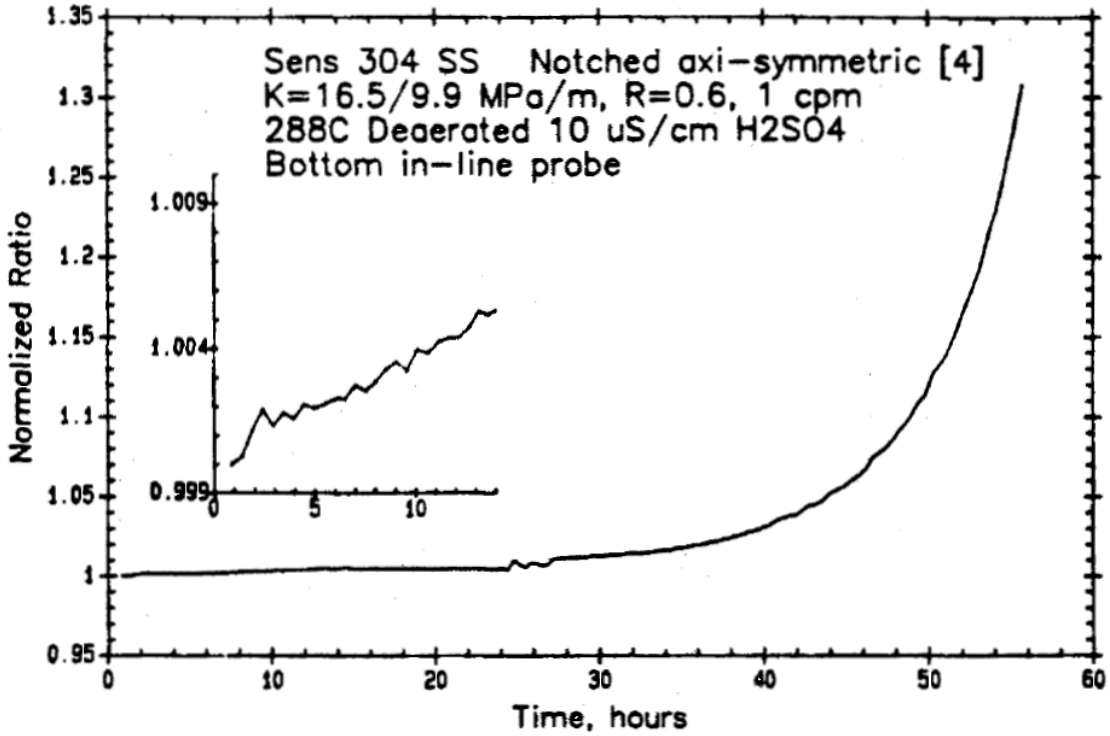

Note: In this instance, cracking initiates from time zero, as indicated by the inset diagram.

Figure 4-18
Development of Cracking in Circumferential Notches

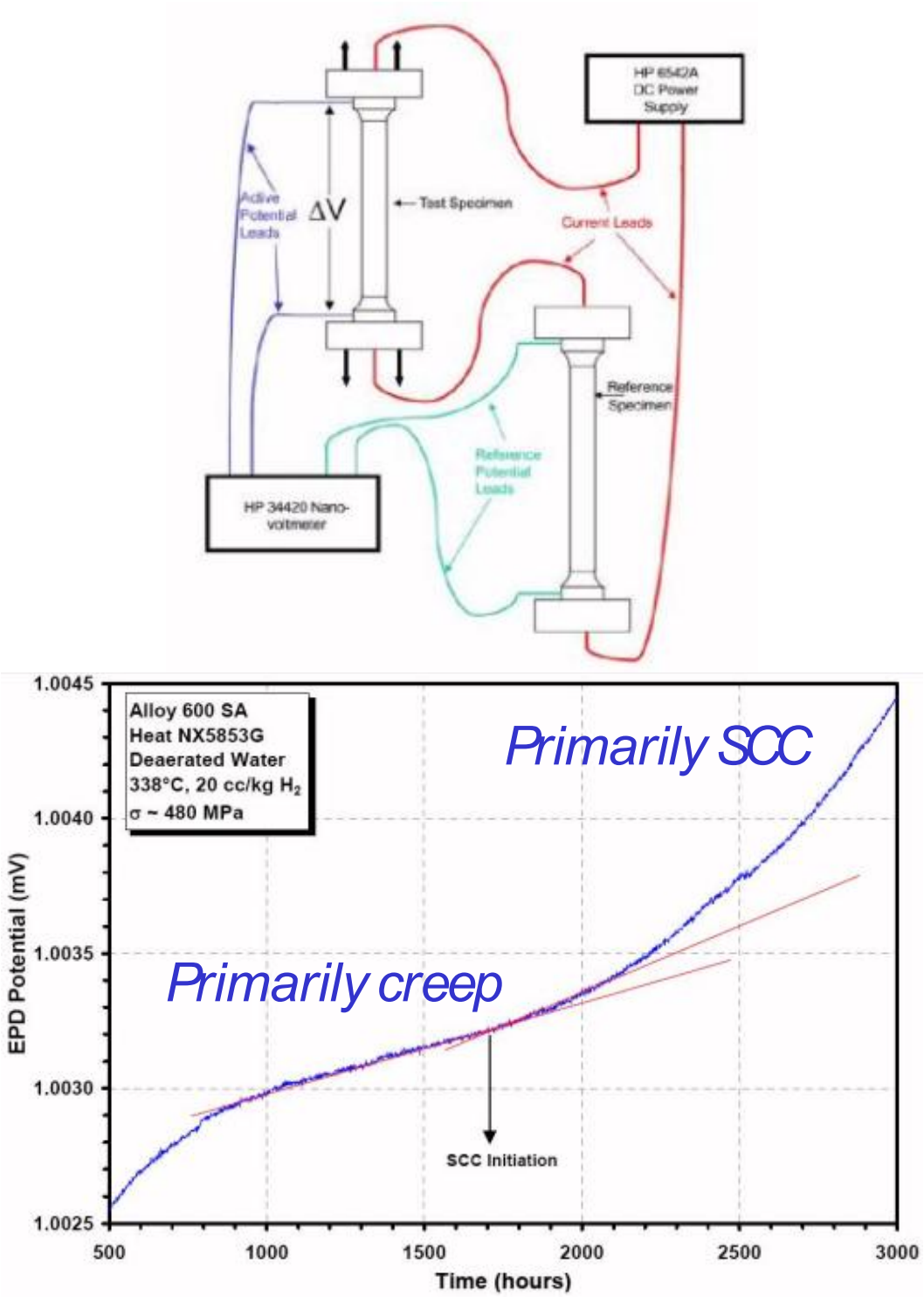

Note: DCPD can monitor creep in the specimen, and the development of SCC is reflected by a deviation from the original potential trajectory vs. time.

Figure 4-19
An Example of an Arrangement Used for Testing for Crack Initiation in Smooth Specimens

5
CRACK INITIATION TESTING

5.1 Introduction to Crack Initiation

Cracks must initiate to grow, but there are many complexities surrounding the understanding of crack initiation. For many reasons, crack initiation experiments are less definitive than crack growth experiments, and certain elements should be considered in determining the balance of crack initiation and crack growth studies. SCC initiation shares many common elements and dependencies with SCC growth, but there are also many distinctive elements.

Fe and Ni alloys are thermodynamically unstable in water and, without a passive film, they react very rapidly in high temperature water. In CF crack initiation and environmental crack growth, it is generally accepted that cracking behavior is controlled by dynamic strain, which produces shear strains that disrupt the protective (passive) film. The importance of dynamic strain has been identified from plant component data where, for example, identically manufactured and installed PWR baffle former bolts exhibit a higher cracking incidence in plants that employ load-following (controlled and planned changes in plant power) [52]. Thus, SCC initiation is not always controlled by the static nature of the passive film, but rather the kinetics of film repair following shear strain.

Crack initiation is the basis for most design codes and criteria in the nuclear industry, but there is no consistent or accepted definition of initiation in terms of crack depth or fraction of wall thickness. For example, the ASME Code defines fatigue crack initiation in terms of 25% load drop in strain controlled tests in small-scale laboratory specimens. Initiation is inherently affected by near surface microstructure and stresses/strains, which are variable and not well known for structural components. SCC initiation is strongly affected by processing and fabrication, including grain boundary oxidation during heat treatment, aggressive machining, severe grinding, sharp corners, weld defects, weld residual and applied stresses, and so on. Other factors that create challenges in measuring and using laboratory SCC initiation data in plant applications include:

- Time is inherently important in environmental cracking and it is not feasible to evaluate crack initiation without significantly limiting the test time relative to component design lives, resulting in acceleration factors between 50–1,000. The acceleration factor in a given laboratory test is not known so deriving a plant-relevant time to initiation is not possible. The effect on crack initiation of specific changes in water chemistry, stress, temperature, dissolved hydrogen, heat treatments (for example, grain boundary carbides), surface treatments, and so on, can be obtained, but it is unclear how meaningful they are given acceleration factors of 50–1,000X.

- Many initiation tests are designed for "experimental convenience" more than to simulate plant component conditions. For example, U-bends and reverse U-bends induce high strains that vary through-thickness, and many such tests have been performed by simply clamping or bolting the U-bend in place, which causes issues related to creep stress relaxation and changes in the modulus of elasticity with temperature.
- SSRTs impose dynamic strain, which does not exist in most structural components, and such tests are rarely run for more than a few weeks.
- SSRTs are performed using "position control" by moving an actuator very slowly vs. time. Thermal expansion of the loading path from a few degrees variation in room temperature produces load oscillations, sometimes large, on an hourly, daily and weekly time scale, so the loading does not monotonically increase. Other loading anomalies can occur when multiple specimens are tested in series or parallel. The failure of one specimen can affect the load on other specimens and the test interruption to remove a specimen may affect crack initiation on other specimens.
- SCC initiation can occur by more than one mechanism, such as pitting, grain boundary oxidation/attack, grain boundary sliding, flaws in the passive film, and so on. However, a given test may not be sensitive to all of these possible mechanisms, including those that may occur in actual components during plant startup or after very long-term exposure to the environment.
- Testing rarely uses a large number of loading cycles, whereas plant components may have millions of cycles. Testing almost always uses small specimens relative to much larger plant components, with limited surface area and a rapid change in net section stress as the crack develops. Only recently has it become more common to employ on-line detection of the time to initiation, or even failure; interrupting a test every 2,000 hours creates a large ambiguity in the time to initiation.
- Initiation is inherently variable (that is, stochastic), but the distribution is strongly affected by inhomogeneities in microstructure, welding, grinding, and so on. Some Alloy 182 weld metal specimens have exhibited very rapid initiation [53], which is consistent with weld defects but is not consistent with the initiation distribution in the remaining specimens. The greatest concern in actual components is for the first initiation, which is inherently an extreme value statistics issue. For example, in steam generators (a hugely parallel system with well controlled surfaces compared to structural components), the distribution vs. time is more important. For Alloy 600 steam generator tubes, there have been a large number of crack indications, and good initiation statistics can be obtained from such plant data.

Given the extent and diversity of issues related to crack initiation testing, it is not surprising that design codes and laboratory testing have not been successful in preventing crack initiation. This section is not intended to discourage efforts to understand and quantify initiation, but rather is intended to portray the challenges in acquiring and using initiation data.

5.2 Definition and Mechanisms of Crack Initiation

A precise, universally accepted definition of SCC initiation does not exist. To a utility engineer, a satisfactory definition might be detection by ultrasonic or other inspection methods, which often requires a crack to be at least 20% of wall thickness for many actual components. In simplistic laboratory tests, SCC initiation might be failure (fracture) of a U-bend or SSRT specimen or visual observation of cracks during periodic test interruption every 2,000 hours. In more sophisticated laboratory tests with on-line monitoring, SCC initiation can be cracks extending through one or a few grains of the material. In very small specimen tests, which are rarely performed, cracks can be detected at sizes below 10 μm. A detailed evaluation of the definition of SCC initiation and the characteristics and processes in the laboratory and in situ is presented in Reference [54], which proposes a functional definition of initiation as the "*formation of a mechanical distinct geometry that grows in preference to its surroundings*". The latter element of this definition is important because there are often instances of crack-like observations that do not continue to grow, at least for long periods of subsequent exposure to loads and the environment.

In turn, defining the transition from crack "initiation" to "growth" is ambiguous, variably thought of in terms of material grain size dimensions, to fully develop crack chemistry, a transition to long crack growth rates, and so on. The evolution of cracking is generally portrayed in terms of precursor phenomena, crack initiation, crack coalescence (in cases where multiple cracks initiate near each other), and crack growth (Figure 5-1)[6]. These are conceptual stages, not well-defined processes and phenomena that inherently apply to all cracks.

Different mechanisms can be involved in crack initiation, including pitting, grain boundary oxidation/attack, grain boundary sliding, and so on, as well as aggravating factors from crevices, stagnant regions, sharp corners, weld defects, grain boundary oxidation during heat treatment, aggressive machining, severe grinding, cold work, and so on. For example, pitting is a dominant factor in SCC initiation in CS and LAS, and it generally develops during lower temperature exposure. The aggravating factors like sharp corners, crevices, and bulk cold work are now controlled better than in early-vintage nuclear plants, but when cracks in plant components are evaluated, there is often evidence of undesirable surface conditions (Figure 5-2 and Figure 5-3 [55]).

The fraction of time spent in each stage varies significantly with the nature of the specimen or component, the loading, the material, the environment, and so on. Modeling of actual components in BWRs has been very successful based on the assumption of early initiation and a slow evolution in crack advance as the K increases [21, 56], even for bolts. On the other hand, it is reasonable to assume that some component lifetimes are dominated by initiation, but the nature of the expected evolution of cracking vs. time is such that very sensitive techniques are required to distinguish initiation from the growth of small cracks. The nature of the component or specimen design and loading is also important, as many specimens, and some components, have a significant increase in net section stress as the crack develops.

[6] In 2008, Kilian [60] presented a version of Figure 5-1 that included a pre-operating phase ("-I"). This phase includes design, fabrication, manufacturing, surface contamination, and so on, which are important elements in the construction of new nuclear power plants.

For initiation tests performed with U-bends or other constant displacement methods, there is always a decrease in load at the test temperature because of changes in the elastic modulus, but a loss of more than 75% of the load can occur from creep relaxation in some cases. For actively loaded specimens, there is always an unusually large increase in net section stress as cracks develop, that is, the loss of area from crack advance increases the stress on the uncracked materials. This leads to an artificially increasing stress vs. time which is rarely representative of actual plant components. The most unrealistic test is the SSRT, as no components are designed to undergo continuous straining vs. time, and such imposed strain rates mask the innate material response to stress.

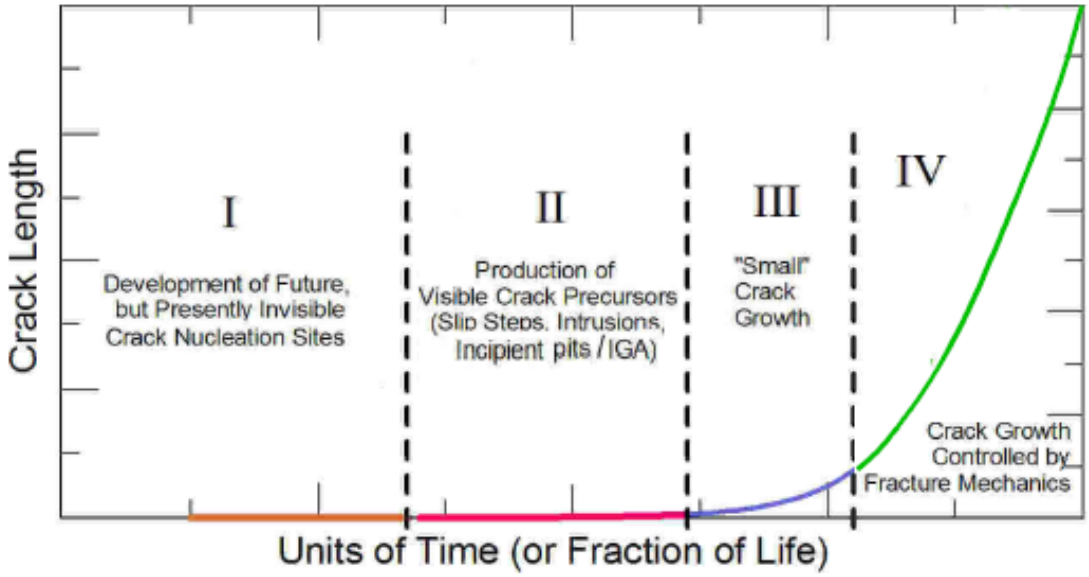

Figure 5-1
Segmentation of Stages in the Development of EAC Degradation [54]

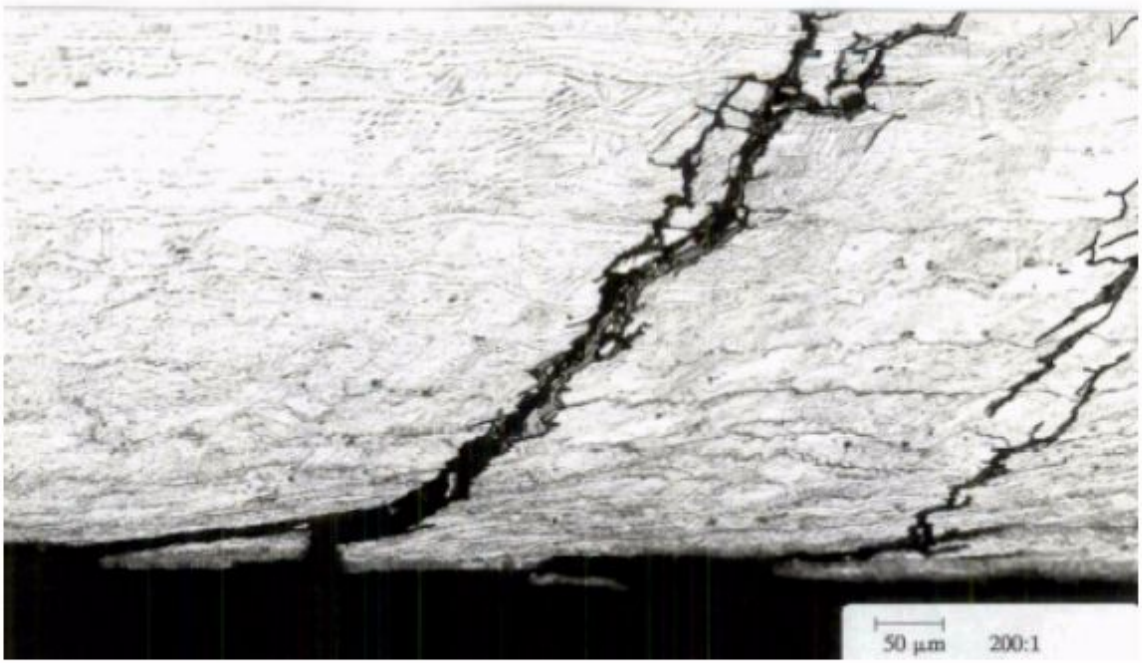

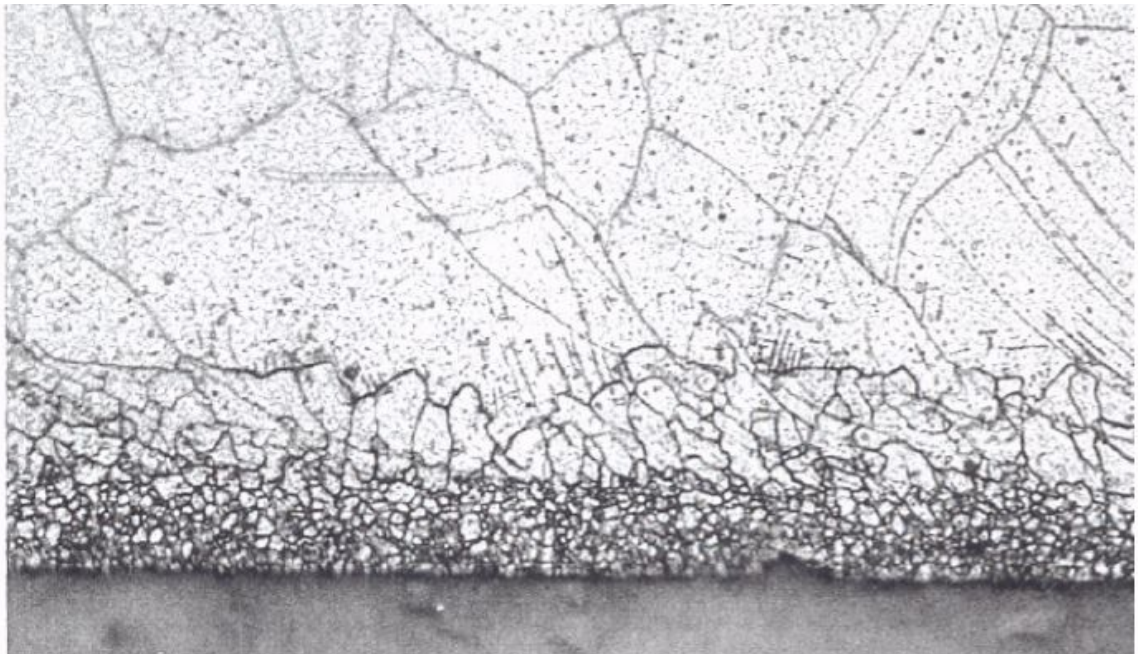

Figure 5-2
Examples of Plant Component Surfaces Where SCC Initiated

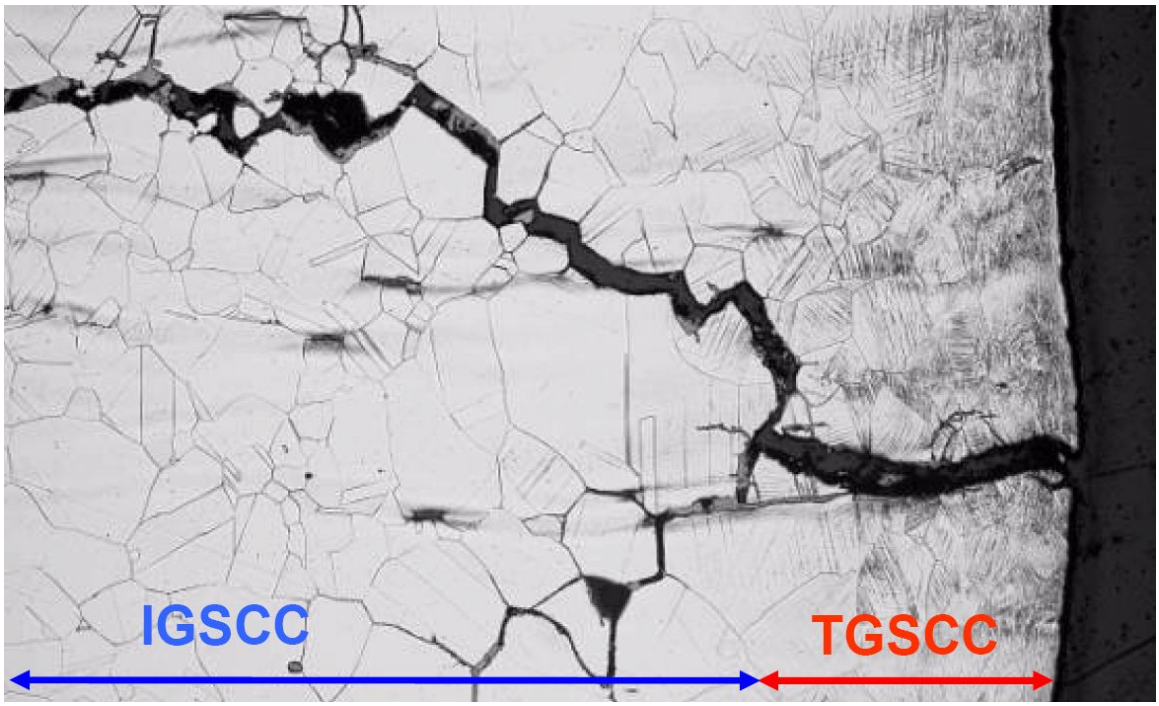

Figure 5-3
Another Example of Plant Component Surfaces Where SCC Initiated
Republished with permission of the Japan Society of Maintenology from [55]

5.3 Challenges in the Statistics and Plant Relevance of SCC Initiation Testing

The biggest statistical issues in initiation measurement in the laboratory are the small area of each specimen, limited replicates, and often poor detection of crack initiation. For example, the ambiguity of the time to initiation in tests interrupted every 2,000 hours is significant. Plant components provide an almost infinite number of opportunities for crack initiation when compared to laboratory specimens, and oftentimes little is known about the details of the plant surfaces and the applied stresses. The effect of weld defects/flaws is always more significant in small laboratory specimens, but their likelihood is significantly higher, by exposed surface area, in plant components. The same holds true for microstructural inhomogeneities.

Laboratory tests are often designed with a few to ten replicates, and this yields weak statistics, which is an issue that is severely aggravated by the inhomogeneities mentioned in the previous paragraph. A great deal of optimism and selective analysis can be applied to statistical evaluation, and it is wiser to intuitively integrate the effect of the many and diverse issues than to focus on a narrow analysis of a few observations.

Initiation data likely will never provide the statistical confidence or insights available from crack growth rate tests, given that the latter tests:

- Provide thousands to tens-of-thousands of observations per specimen (vs. one for initiation).
- Allow evaluation of reproducibility within one specimen (not possible for initiation).

- Use “on-the-fly” changes to examine factors such as water chemistry and temperature, and also the effect of material microstructure and composition in “gradient structures” (not possible for initiation).
- Allow for extensive microstructure examination (which is not possible for initiation testing).
- Can be highly representative of plant components, including material, environment and stress, without test acceleration over most of the relevant range of crack depth (initiation tests generally must accelerate testing by factors of 50–1,000).

The value of laboratory initiation data is therefore primarily limited to the effects of factors like grain boundary carbides, grain boundary Cr depletion, oxidizing water chemistry, temperature, stress, and so on. Even in these cases, it is necessary to assume that the 50–1,000X test acceleration does not change the factor of improvement, which is an uncertain assumption.

By contrast, the statistics of SCC available from some plant components can be compelling:

- There has been extensive SCC in Alloy 600 steam generator tubing, and there is a very large, statistically significant population with modern steam generators that are comprised of more than 15,000 long tubes, with a variety of crevices, bends, tube expansion and seal welding factors. The nature of the surfaces and the stresses are also much more highly controlled and known than in most other structural components. Measured crack indications obtained from eddy current inspections or instances of leakage cover the full spectrum of crack depths in the thin tubes.
- Scott et al. [52] evaluated SCC in bolts manufactured from the same heat, at the same time, installed in the same way, using the same initial torque, in plants that were operated differently. Plants that employed load following had a more statistically significant distribution of cracking than those that did not. Again, the extent to which this data represent initiation is somewhat speculative.

5.4 Crack Initiation Testing

Many types of crack initiation tests have been utilized and they can be categorized in terms of constant displacement (or constant displacement rate or slow strain rate), and constant load (or constant loading rate).

Examples of constant displacement or constant displacement rate or slow strain rate tests include:

- U-bend and reverse U-bend tests in which a strip or longitudinally split tube is bent. Historically, the ends of the U-bends were held/loaded with a bolt or fixture but, in the last decade or two, springs have been used to reduce load relaxation at temperature. In some materials and at temperatures above 300°C, 75% load relaxation have been observed in some U-bend tests. Additionally, all constant displacement loading tests suffer from a load reduction because of the change in elastic modulus with temperature which is often in the range of 10–13% at about 300°C. The use of springs can resolve load relaxation issues but not modulus changes with temperature. Almost all such tests are unmonitored and evaluations for cracking are done by test interruption, often at 500–5,000 hour intervals.

This leads to a large uncertainty in the time to initiation and reduces the statistical confidence of the results. The levels of plastic strain in the outer fiber of U-bend specimens can be high, and even higher in reverse U-bend specimens, thus raising concerns for their relevance to plant components.

- Crevice bent beam tests (Figure 5-4) are typically performed using matching (convex and concave) radius blocks, between which is placed a flat specimen, and the two blocks are bolted together. Load relaxation can be an issue in some tests, although less at 288°C, where such tests have been more widely used, than at 340 or 360°C. In some cases, material such as graphite wool is used between the radius blocks and the specimen to promote the formation of a crevice. Unfortunately, materials like graphite wool release a significant amount of impurities and those impurities in the presence of a crevice, coupled with oxidants in the bulk water, produce very high and unrealistic levels of damaging anions that promote significant cracking. The levels of plastic strain in the outer fiber of bent specimens can be high, raising concerns for their relevance to plant components.
- SSRTs became popular in the 1970s as an accelerated test that identified circumstances where SCC susceptibility is high. Most SSRTs are done on tensile specimens and a small proportion have been monitored by periodic interruption (Figure 5-5) to determine if cracking developed [58]. As materials and water chemistries have improved in LWRs, SSRTs have been much less useful in identifying SCC susceptibility and discriminating the effects of water chemistry and other factors. Depending on the strain rate, austenitic Fe-Ni-Cr materials will undergo some or all TG cracking, but SCC in such materials in LWRs and in SCC growth rate testing has been highly IG. The imposed strain rate is poorly representative of any plant component, and the actual strain rate on the specimen can be cyclic because room temperature fluctuations affect the thermal expansion along the load path. Monitoring SSRTs by DCPD is complicated by the expected change from elongation, and reduced area, during straining. The combination of these factors has significantly reduced the value of SSRTs.

Examples of constant load or constant loading rate tests include:

- Constant load tests on tensile specimens, with the loading actively applied by a servo loading system, differential pressure (Figure 5-6), springs, and so on. Dozens of specimens can be tested at the same load and, perhaps different stresses if the gage diameter is different, and monitoring is straightforward. Examples of Weibull statistical analyses for constant load tests are shown in Figure 5-7, where it is important to recognize that, with a limited number of specimens, the confidence bands often produce overlap among the different conditions.
- A variation of constant load tests is tests where the load is very slowly and monotonically increased or cycled. Unlike constant displacement or displacement rate tests, the load relaxation and cycling can be eliminated.
- Another variation of constant load tests is tests where 3- or 4-point bend specimens are used.
- Still another variation of constant load tests is tests that use a notch (Figure 4-18) to examine stress concentrations or localize where cracking will develop.

- Blunt notch (controlled radius) CT specimens (Figure 5-8) can be used, typically using the same techniques used for crack growth rate tests. There are well-developed, pseudo-stress calculations that characterize the stresses in a blunt notch relative to a smooth specimen ($\sigma = 2K/\sqrt{\pi\rho}$, where σ is the stress at the notch, ρ is the notch radius, and K is the stress intensity factor assuming the notch is sharp).

All SCC initiation tests must be carefully designed. For example, the benefit of surface improvements such as water jet or shot peening must address the effects of initial loading and plastic strain, plant startup and shutdown conditions, differential thermal strains, and so on, since surface benefits are often eroded by any, even very localized, plasticity. Stability of the testing conditions is more critical for SCC initiation since there is no way to monitor of the effects of test instability as is possible in crack growth testing.

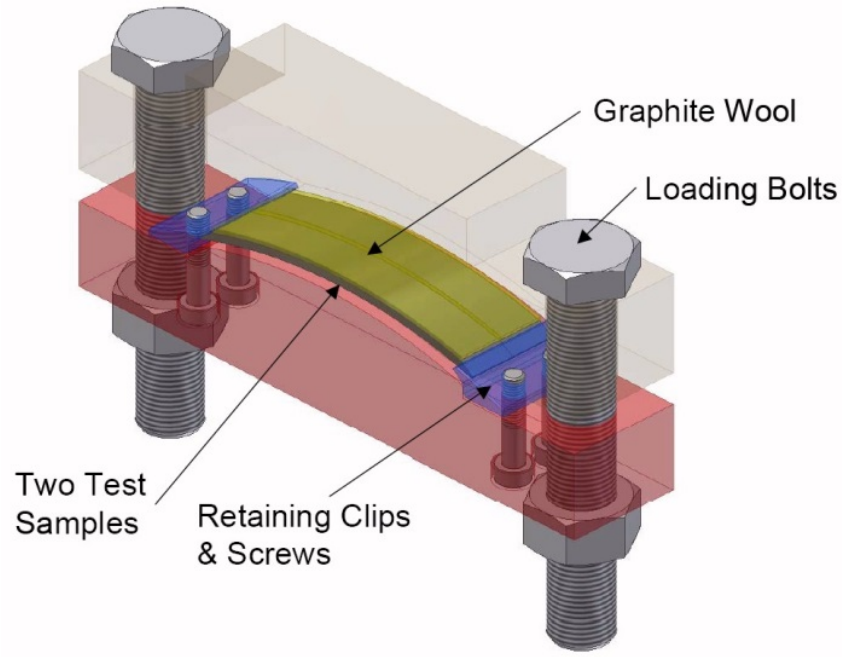

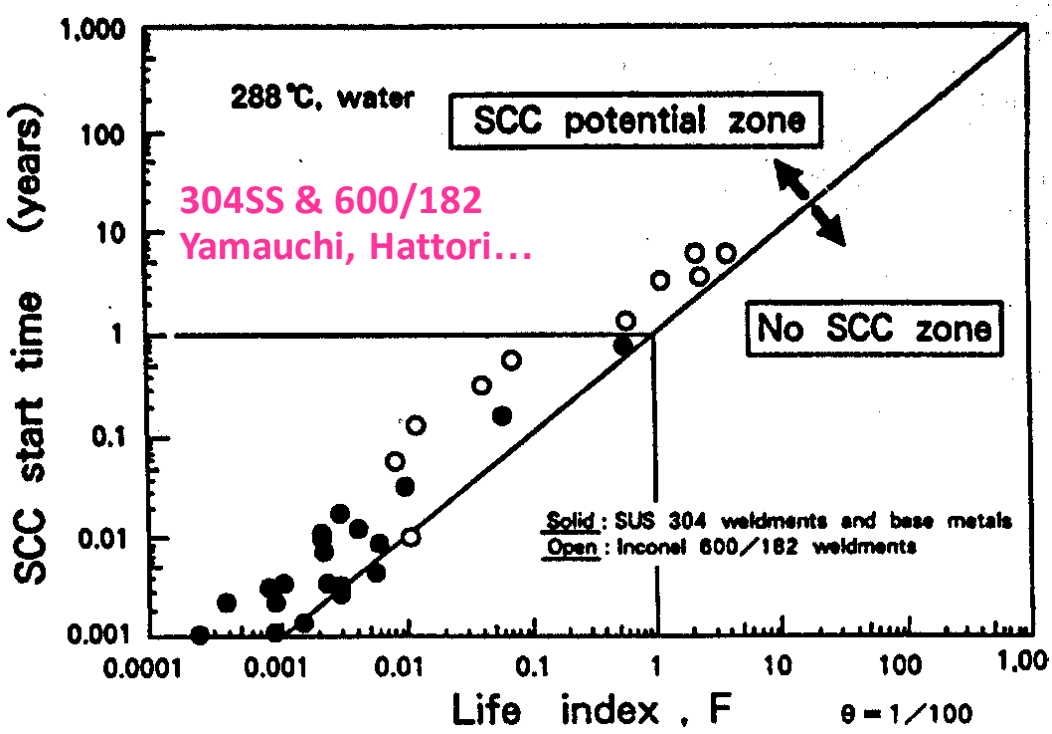

Note: A crevice bent beam test in which a flat specimen is bent to conform to two radius blocks. In most cases, a graphite wool was used to enhance the crevice (limit O_2 transport), which releases high levels of impurities.

Figure 5-4
Crevice Bent Beam (CBB) Tests
Republished with permission of NACE International from [57]; permission conveyed through Copyright Clearance Center, Inc.

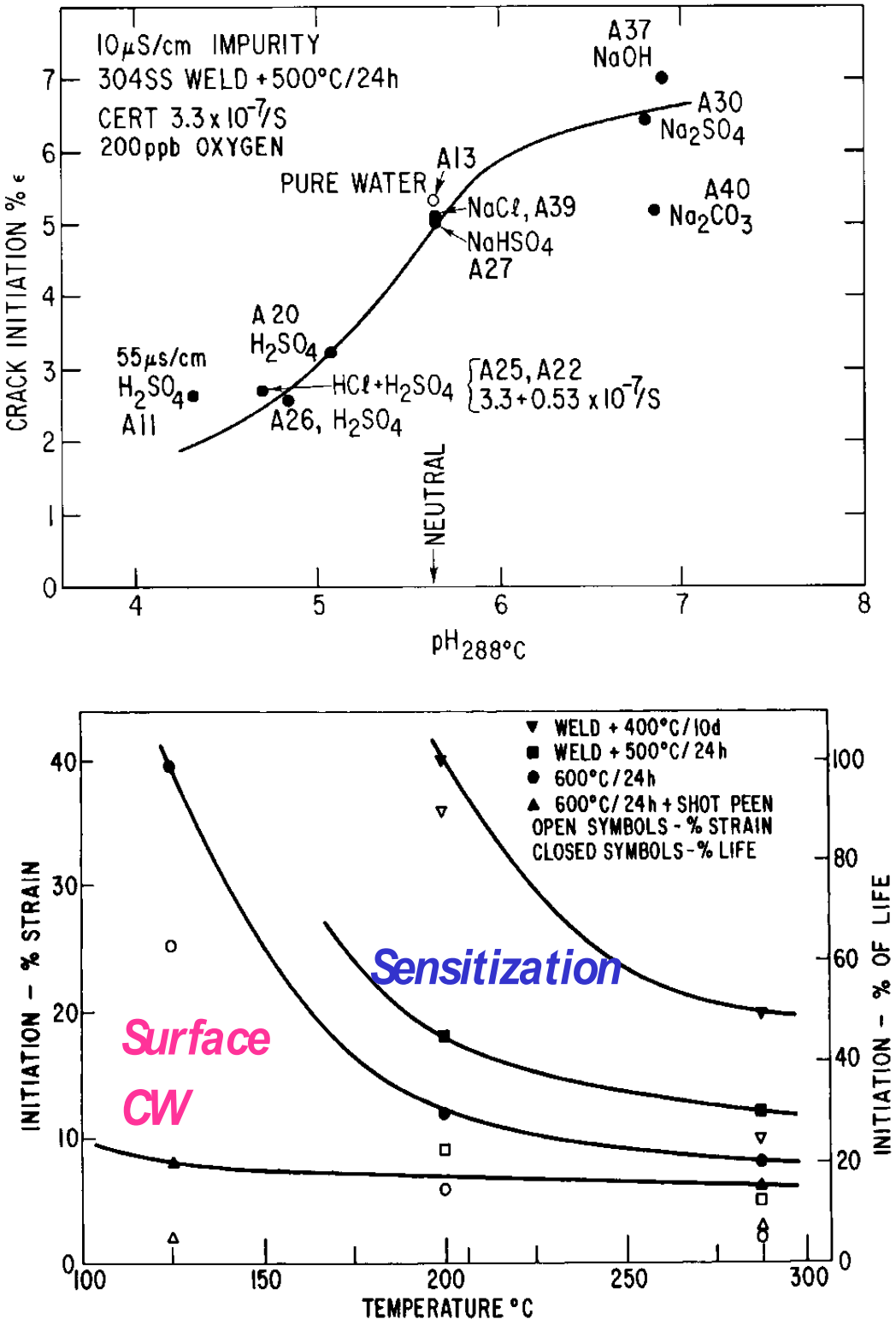

Figure 5-5
SSRTs That Were Interrupted at Every ~0.5% Strain Increment to Evaluate Crack Initiation

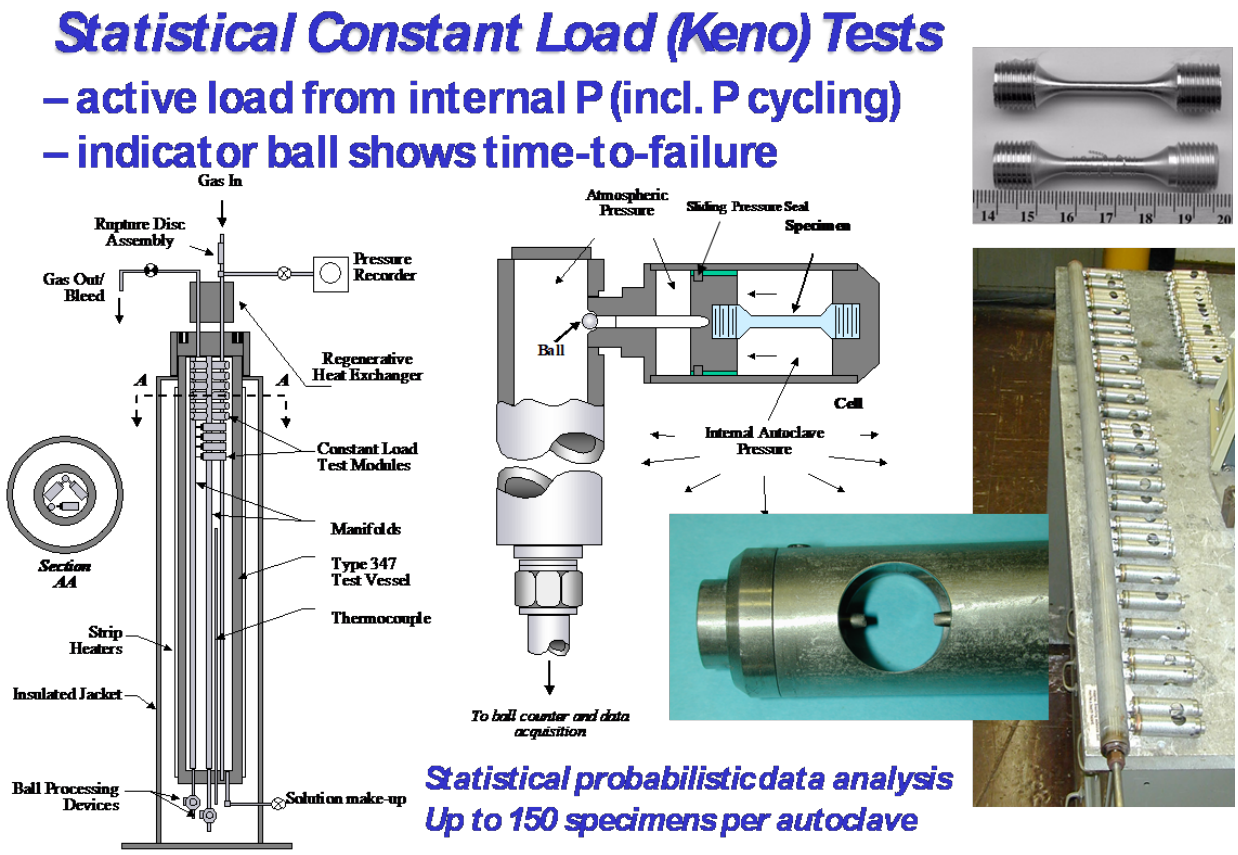

Note: This differential pressure loading system can evaluate 150 specimens simultaneously. Failure is detected by ejection of a number stainless steel ball.

Figure 5-6
Differential Pressure Loading System

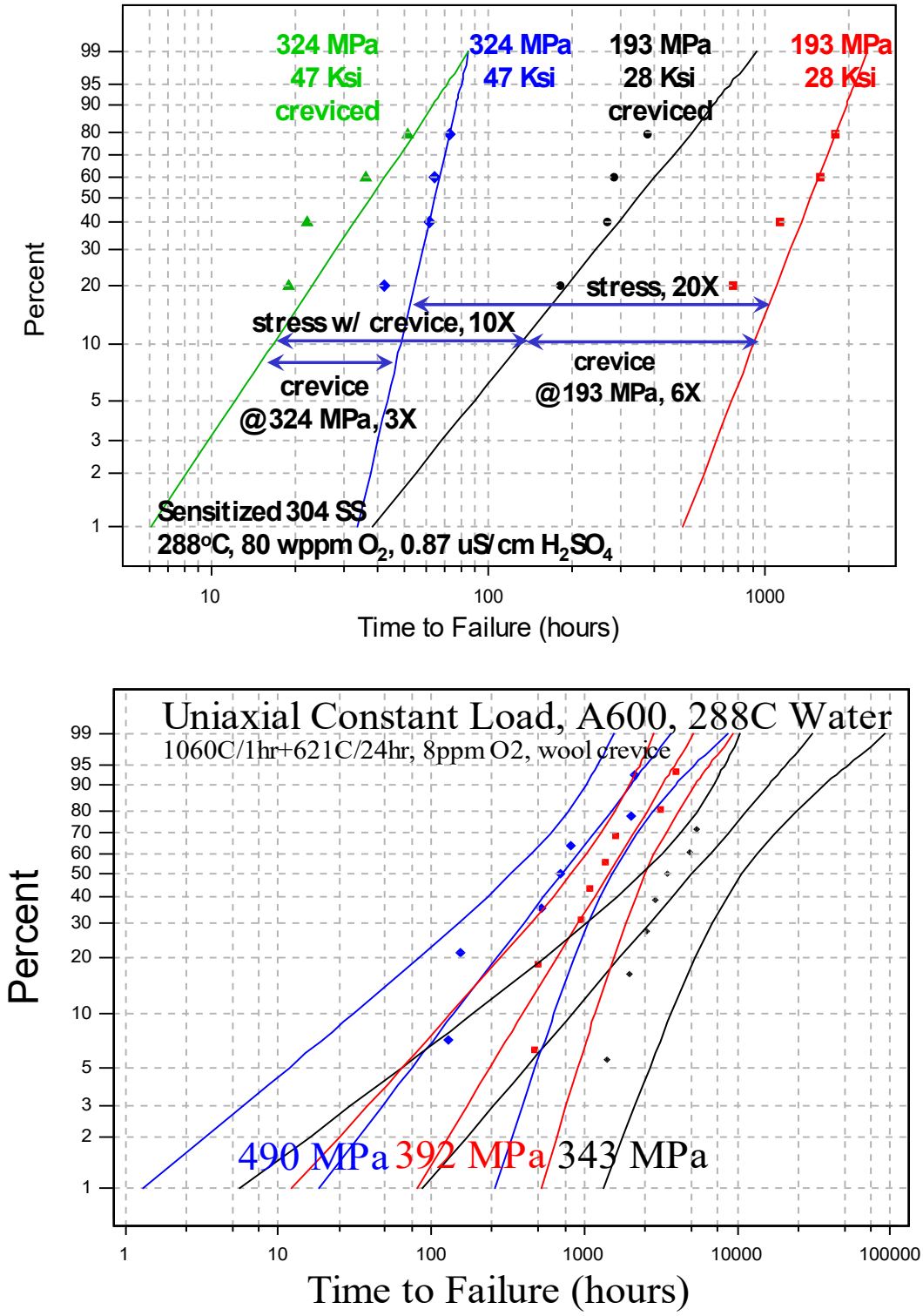

Figure 5-7
Examples of the Use of Weibull Statistics to Evaluate Different Stresses and Conditions

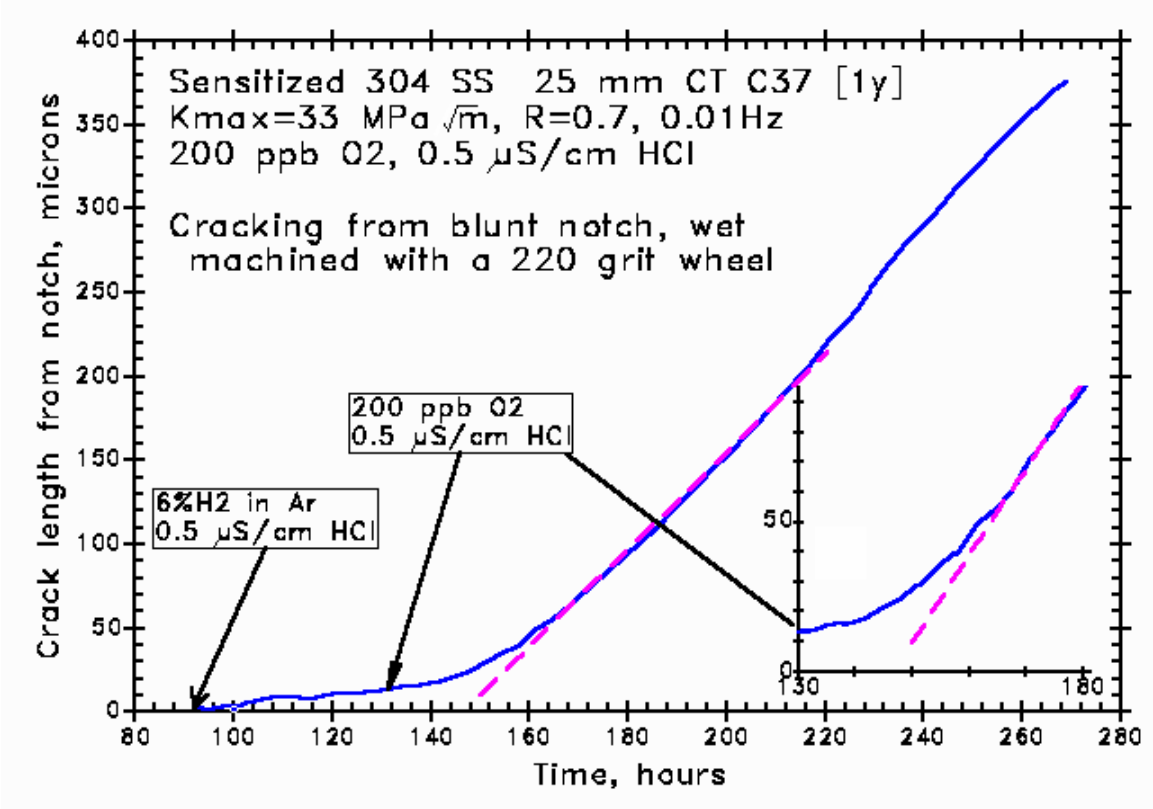

Note: The results shown in this figure indicate that initiation is promoted by dynamic strain (increasing stress).

Figure 5-8
DCPD Monitoring of a Blunt Notch CT Specimen

5.5 Methods of Crack Initiation Monitoring

Specimen initiation, or at least failure, is ideally detected on-line; otherwise, the uncertainty in initiation or failure time between test interruptions (for example, every 500–2,000 hours) can significantly impact the statistical confidence in the data. "Keno" systems (Figure 5-6) eject a numbered SS ball that indicates the time and identity of each failure. Test interruption is simple, but the cool-down, heat-up, and inspection processes are time consuming and can perturb the initiation data. There are many methods that have been used to monitor crack initiation, including:

- On-Line Failure Detection or Test Interruption is simplest, but may not be easy, and can yield imprecise or biased data. In simple one-specimen tests, such as SSRTs, failure detection is easy. Detecting the early stages of initiation is possible but requires accurate displacement measurement and stable room temperature. The most common historical initiation test employs a collection of U-bend or reverse U-bend specimens that were unmonitored, so the test was interrupted every 500, 1,000, 2,000+ hours to observe what had occurred. This leads to a large uncertainty in time to initiation, in addition to ambiguities in the actual stress vs. time.

- DCPD can provide very high resolution detection of cracking, but a stable current must be directed through the specimen(s), and potential leads across the gage section are needed for each specimen (Figure 4-19). Compared to AC potential drop, DCPD is far simpler to implement, much less sensitive to layout, is less expensive, and has much better noise rejection. Details of DCPD implementations for crack growth and initiation are covered in Section 4 on crack monitoring.
- AC potential drop is more expensive than DCPD and is very sensitive to lead placement. The main benefit of AC potential drop testing is the "skin" effect where the applied current to the specimen flows mostly near surface, which increases the sensitivity to cracking. Both DCPD and AC potential drop methods have been used for more than 40 years with no identified advantage of AC potential drop over DCPD.
- Electrochemical Noise (ECN) requires sensing electrodes to be very close to the crack area, requires stable conditions (for example, ECP), is sensitive to laboratory electromagnetic noise, and often depends on finding a data analysis approach that is correlated with SCC. SCC initiation detection by ECN (in particular, potential noise) in high temperature water works best in oxidizing conditions where the is a large potential difference between the active surface defect (low potential) and the remaining surface (high potential, but the reference electrode has to be placed very close to the initiation location, for example, notched specimens). In hydrogenated water, this potential difference is small and probably overwhelmed by the H2/H20 reaction with high exchange current density. The higher conductivity in PWR water relaxes the distance issue.
- Electrochemical impedance spectroscopy (EIS) is a variation of ECN monitoring. In both techniques, interesting changes in response must be shown to be a result of SCC. Figure 5-9 shows an example of increasing ECN in a SSRT when plastic strain commences.
- Acoustic Emission (AE) requires good coupling to the specimen, is susceptible to noise (for example, seal stiction or clock ticks), and assumes large steps in brittle or discontinuous crack advance. GE performed AE evaluations on SS specimens that extended from the autoclave. There was no evidence that SCC in hot water involves brittle fracture, at least until cracks become large, where unevenness in growth along the crack front can develop and create uncracked ligaments that might suddenly grow.

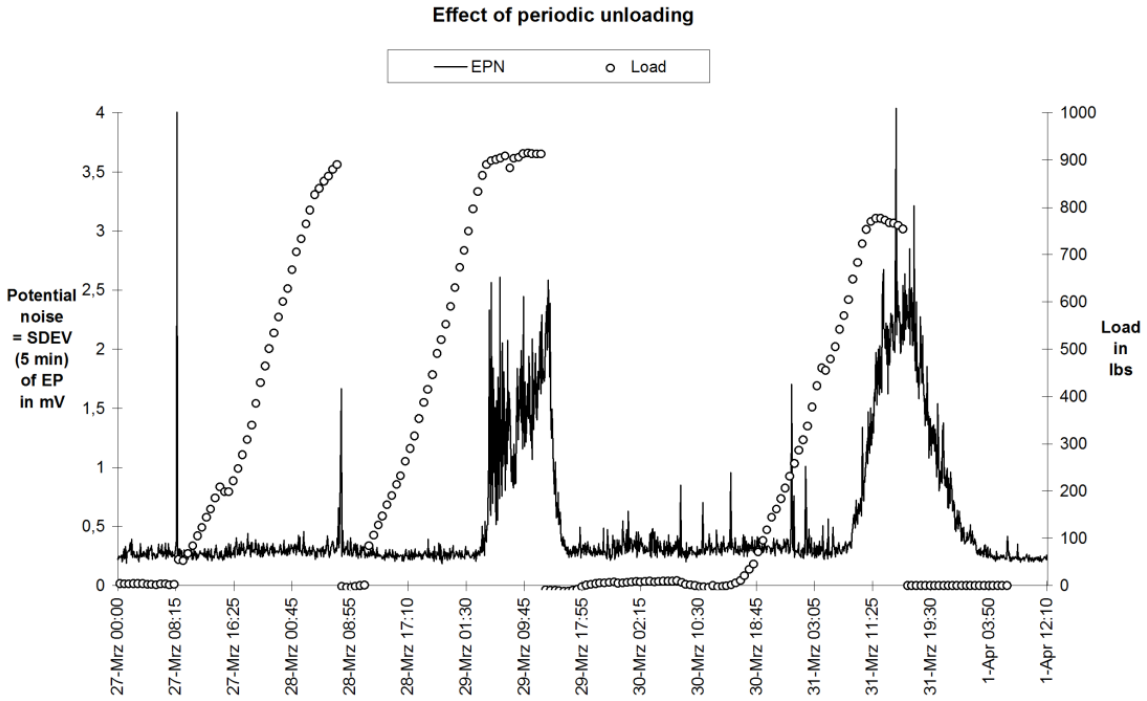

Note: Unloading caused the ECN to decrease, and re-straining caused the ECN to increase. The ECN potential noise was measured by electrodes placed very close to the SCC specimen.

Figure 5-9
Electrochemical Noise (ECN) Monitoring of a SSRT specimen Showing a Large Increase in ECN as Plastic Strain Occurs

6
SUMMARY AND CONCLUSIONS

Evaluation of EAC response is complex in any environment but is especially challenging in high temperature water. The incentive to quantify the kinetics and dependencies of EAC in high temperature water is high given the need for reliable, long-lifetime and safe LWR operation. This guideline is designed to provide essential information, reference data and guidance for conducting SCC and CF tests in high temperature water. Crack growth rate testing is a major emphasis, but a section is included on SCC initiation testing. While focused on high temperature water, much of this report is also applicable to EAC testing in other environments.

This report is a "guideline" for testing and not a "standard", which implies that high quality data will be ensured by following defined procedures. EAC is very different than ordinary mechanical or fatigue testing because there are many complex inter-dependencies and large effects of subtle testing differences. Addressing all testing subtleties and nuances is far beyond the scope of a document of this size, and it strives to identify important issues and best practices and provide basic reference data. Its underlying intent is to alert the experimentalist to observe carefully, question and steadily improve techniques and observations, repeat experiments, interact with international colleagues, and optimize test management.

7
REFERENCES

1. "Standard Test for Plane-Strain Fracture Toughness of Metallic Materials", E399-17, ASTM, 2017.
2. "Standard Test Method for Constant Load Amplitude Fatigue Crack Growth Rates", E647-15e1, ASTM, 2015.
3. "Standard Test Method for Determining a Threshold Stress Intensity Factor for Environment-Assisted Cracking of Metallic Materials Under Constant Load", E1681-03, ASTM, 2013.
4. "Standard Test Method for Measurement of Fracture Toughness", E1820-18ae1, ASTM, 2018.
5. P. L. Andresen, "SCC Testing and Data Quality Consideration", *Proc. Ninth Int. Symp. on Env. Degradation of Materials in Nuclear Power Systems – Water Reactors*, AIME, pp. 411, 1999.
6. P. L. Andresen, "Effects of Testing Characteristics on Observed SCC Behavior in BWRs", Paper 98137, *Corrosion/98*, NACE, 1998.
7. P. L. Andresen, K. Gott and J. L. Nelson, "Stress Corrosion Cracking of Sensitized Type 304 Stainless Steel in 288C Water: A Five Laboratory Round Robin", *Proc. Ninth Int. Symp. on Environmental Degradation of Materials in Nuclear Power Systems – Water Reactors*, AIME, p. 423, 1999.
8. P. L. Andresen, "ICG-EAC Experimental Quality Guidelines for SCC Testing", GE CRD, Schenectady, Jan. 30, 1998.
9. P. M. Scott, "Recommended Test Procedure for Studies on Crack Growth in Simulated LWR Water Environments", *Proc. Third Intl. Atomic Energy Agency Specialists Mtg on Subcritical Crack Growth*, Moscow, USSR, May 1990, NRC NUREG/CP-0112 (ANL-90/22), Vol. 1, pp. 117-128.
10. P. L. Andresen and M. M. Morra, "Effect of Rising and Falling K Profiles on SCC Growth Rates in High Temperature Water", *Journal of Pressure Vessel Technology*, Volume 129, Issue 3, pp. 488-506, August 2007.
11. J. A. Sutliff, "An Investigation of Plastic Strain in Copper by Automated-EBSP", *Microscopy and Microanalysis*, Vol. 5. Supp. 2, 1999, p. 236 (*Proc: Microscopy and Microanalysis '99*).
12. M. A. Othon and M. M. Morra, "EBSD Characterization of the Deformation Behavior of Alloy 182 Weld Metal", *Microscopy and Microanalysis (2005)*, 11 (Suppl 2):522-523CD Cambridge University Press, 2005. doi:10.1017/S1431927605506949.
13. T. M. Angeliu, P. L. Andresen, J. A. Sutliff and R. M. Horn, "Intergranular Stress Corrosion Cracking of Unsensitized Stainless Steels in BWR Environments", *Proc. 9th Int. Symp. on Environmental Degradation of Materials in Nuclear Power Systems - Water Reactors*, AIME, 1999.

14. T. M. Angeliu, P. L. Andresen, E. Hall, J. A. Sutliff, S. Sitzman, "Strain and Microstructure Characterization of Austenitic SS Weld HAZs", *Corrosion/2000*, Paper 00186, NACE, 2000.

15. P. L. Andresen and M. M. Morra, "SCC of Stainless Steels and Ni Alloys in High Temperature Water", Corrosion Vol. 64, pp. 15-29, 2008.

16. P. L. Andresen, P. W. Emigh, M. M. Morra and R. M. Horn, "Effects of Yield Strength, Corrosion Potential, Stress Intensity Factor, Silicon and Grain Boundary Character on the SCC of Stainless Steels", *Proc. 11th Int. Symp. on Environmental Degradation of Materials in Nuclear Power Systems – Water Reactors*, ANS, 2003.

17. E. Richey, D. S. Morton and W. C. Moshier, "Influence of Specimen Size on the SCC Growth Rate of Ni-Alloys Exposed to High Temperature Water", Paper 06513, *Corrosion/06*, NACE, Houston, 2006.

18. P. L. Andresen, "K/Size Effects on SCC in Irradiated, Cold Worked and Unirradiated Stainless Steel", *Proc. of 11th Int. Symp. on Environmental Degradation of Materials in Nuclear Power Systems - Water Reactors*, ANS, 2003.

19. A. Jenssen, Peter Chou, C. Topbasi, "Effect of Specimen Size on the Crack Growth Rate Behavior of Irradiated Type 304 Stainless Steel", *Proc. of 18th Int. Symp. on Environmental Degradation of Materials in Nuclear Power Systems - Water Reactors*, TMS, 2017.

20. P. L. Andresen, R. B. Rebak, E. J. Dolley, "SCC Growth Rate of Irradiated and Unirradiated High Cr Ferritic Steels", *Proc 17th Environmental Degradation of Materials in Nuclear Power Systems*, CNS, 2015.

21. R. G. Ballinger, R. M. Latanision, W. C. Moshier, and R. M. Pelloux, *The Effect of Heat Treatment and Environment on Corrosion Fatigue – Volume 2: Alloy 600*. Research Project RP1166-3, Final Report, EPRI, Palo Alto, CA. 1987.

22. F. P. Ford and P. L. Andresen, "Corrosion in Nuclear Systems: Environmentally Assisted Cracking in Light Water Reactors", in *Corrosion Mechanisms*, Ed. P. Marcus and J. Ouder, Marcel Dekker, pp. 501-546, 1994.

23. P. L. Andresen, J. Flores-Preciado, M. M. Morra and R. Carter, "Microstructure and SCC of Alloy X-750", *Proc. 15th Int. Symp. on Environmental Degradation of Materials in Nuclear Power Systems – Water Reactors*, The Metallurgical Society, August 2011.

24. *BWRVIP-240: BWR Vessel and Internals Project, Metallurgical Analyses and Macro- and Microstructural Mapping of Alloy X-750 and Alloy XM-19 Plates*. EPRI, Palo Alto, CA: 2010. 1021003.

25. H. P. Seifert, S. Ritter, "Research and Service Experience with Environmentally-Assisted Cracking of Carbon & Low-Alloy Steels in High-Temperature Water", SKI-Report 2005:60, ISSN 1104-1374, SKI, Stockholm, Sweden, 2006. (available at www.stralsakerhetsmyndigheten.se).

26. H. P. Seifert, S. Ritter, "Environmentally-Assisted Cracking of Carbon and Low-alloy Steels in Light Water Reactors," in: S. Ritter (Ed.), Nuclear Corrosion: Research, Progress and Challenges, EFC Publications No. 69, Woodhead Publishing, 2020 (in press).

27. *BWRVIP-190 Revision 1: BWR Vessel and Internals Project, Volume 1: BWR Water Chemistry Guidelines – Mandatory, Needed, and Good Practice Guidance*. EPRI, Palo Alto, CA: 2014. 3002002623.

28. *Pressurized Water Reactor Secondary Water Chemistry Guidelines—Revision 8*. EPRI, Palo Alto, CA: 2017. 3002010645.

29. *Pressurized Water Reactor Primary Water Chemistry Guidelines: Revision 7, Volumes 1 and 2*. EPRI, Palo Alto, CA: 2014. 3002000505.

30. P. L. Andresen, T. P. Diaz and S. Hettiarachchi, "Effect on Stress Corrosion Cracking of Electrocatalysis and Its Distribution Within Cracks", *Proc. of 11th Int. Symp. on Environmental Degradation of Materials in Nuclear Power Systems – Water Reactors*, ANS, 2003.

31. P. L. Andresen and Y. J. Kim, "Developments in SCC Mitigation by Electrocatalysis", *Proc. 15th Int. Symp. on Environmental Degradation of Materials in Nuclear Power Systems – Water Reactors*, The Metallurgical Society, August 2011.

32. P. L. Andresen, "SCC Growth Rate Behavior in BWR Water of Increasing Purity", *Proc. 8th Int. Symp. on Environmental Degradation of Materials in Nuclear Power Systems - Water Reactors*, p. 675, ANS, 1998.

33. D. M. Himmelblau, *J. Chem. Eng. Data 5*, 10, 1960.

34. J. Alvarez, R. Crovetto and R. Fernandez-Prini, "The Dissolution of N_2 and of H_2 in Water from Room Temperature to 640 K", *Ber. Bunsenges. Phys. Chem. 92*, pp. 935-940, 1988.

35. W. C. Moshier and R. C. Witt, unpublished data, 2002. Referenced in S.A. Attanasio and D. S. Morton, "Measurement of the Ni/NiO Transition in Ni-Cr-Fe Alloys and Updated Data and Correlations to Quantify the Effect of Aqueous Hydrogen and Primary Water SCC", *Proc. 11th Int. Conf. on Environmental Degradation of Materials in Nuclear Power Systems – Water Reactors*, ANS, 2003.

36. *Materials Reliability Program: Mitigation of PWSCC in Nickel-Base Alloys by Optimizing Hydrogen in the Primary Water (MRP-213)*. EPRI, Palo Alto, CA: 2007. 1015288.

37. P. L. Andresen and L. M. Young, "Characterization of the Roles of Electrochemistry, Convection and Crack Chemistry in Stress Corrosion Cracking", *Proc. 7th Int. Symp. on Environmental Degradation of Materials in Nuclear Power Systems - Water Reactors*, NACE, pp. 579-596, 1995.

38. D. F. Taylor, "Thermodynamic Properties of Metal-Water Systems at Elevated Temperatures", *J. Electrochem. Soc.*, Vol. 125, No. 5, p. 808, 1978.

39. R. S. Greeley, W. T. Smith, Jr., R. W. Stoughton and T. J. Lietzke, *J. Phys Chem.*, Vol. 64, p. 652, 1960.

40. M. J. Danielson, "The Construction and Thermodynamic Performance of an Ag/AgCl Reference Electrode for Use in High Temperature Aqueous Environments Containing H_2 and H_2S", *Corrosion*, 35, p. 200, 1979.

41. D. D. Macdonald, A. C. Scott, and P. Wentrcek, "Silver – Silver Chloride Thermocells and Thermal Liquid Junction Potentials for Potassium Chloride Solutions at Elevated Temperatures", *J. Electrochem. Soc. 126*, 9, p. 1618, 1969.

42. D. D. Macdonald, A.C. Scott, and P. Wentrcek, "External Reference Electrode for Use in High Temperature Aqueous Systems", *J. Electrochem. Soc. 126*, 9, p. 908, 1969.

43. P. L. Andresen, "Innovations in Experimental Techniques for Testing in High Temperature Aqueous Environments", GE CRD Report No. 81CRD088, May 1981.

44. M. E. Indig and A. R. McIlree, *Corrosion* 35, p. 201, 1979.

45. J. Leibovitz, W. R. Kassen, W. L. Pearl and S. G. Sawochka, "Improved Electrodes for BWR In-Plant ECP Monitoring", Project 706-1, EPRI, 1983.

46. L. W. Niedrach, "A New Membrane Type pH Sensor for Use in High Temperature – High Pressure Water", *J. Electrochem. Soc*., 127, p. 2122, 1970.

47. P. L. Andresen, A. Ayhan, G. M. Catlin, W. R. Catlin, "Development and Use of a Lee James Surface Cracked Specimen for Evaluating Chemistry and Flow Rate Effects in Realistic Cracks", Paper #04567, Corrosion/04, NACE, 2004.

48. A. Saxena, and S. J. Hudak, Jr., "Review and Extension of Compliance Information for Common Crack Growth Specimens," *International Journal of Fracture*, Vol. 14, No. 5, October 1978.

49. H. D. Solomon and W. R. Catlin, "Method for Calculating Crack Lengths of Conductive Sensors," U.S. Patent US4924708A, 1989.

50. P. L. Andresen, F. P. Ford, J. P. Higgins, I. Suzuki, M. Koyama, M. Akiyama, T. Okubo, Y. Mishima, S. Hattori, H. Anzai, H. Chujo, Y. Kanazawa, "Life Prediction of Boiling Water Reactor Internals", *Proc. International Conference on Nuclear Engineering (ICONE-4)*, ASME, 1996.

51. P. L. Andresen, F. P. Ford, S. M. Murphy, J. M. Perks, "State of Knowledge of Radiation Effects on Environmental Cracking in Light Water Reactor Core Materials", Invited Review Paper, *Proc. 4th Int. Symp. on Environmental Degradation of Materials in Nuclear Power Systems - Water Reactors*, Jekyll Island, NACE, pp. 1-83 to 1-121, 1990.

52. P. M. Scott, M-C. Meunier, D. Deydier, S. Silvestre, A. Trenty, "An analysis of baffle/former bolt cracking in French PWRs", ASTM STP 1401, *Environmentally Assisted Cracking: Predictive Methods for Risk Assessment and Evaluation of Materials, Equipment and Structures*, Ed. R.D. Kane, ASTM 2000, pp. 210-223.

53. M. Toloczko; Z. Zhai, K. Kruska, S. Bruemmer, "SCC Initiation Behavior of Alloy 182 in PWR Primary Water", *Proc. 18th Int. Symp. On Environmental Degradation of Materials in Nuclear Power Systems – Water Reactors*, TMS, August 2017.

54. P. M. Scott, P. Combrade, R. Kilian, A. Roth, P. L. Andresen, Y-J Kim, "Status Review of Initiation of Environmentally Assisted Cracking and Short Crack Growth", Final Report, October 2005, EPRI, Palo Alto, CA. 1011788.

55. S. Suzuki, K. Takamori, K. Kumagai, A. Sakashita, N. Yamashita, C. Shitara, and Y. Okamura, "Stress Corrosion Cracking in Low Carbon Stainless Steel Components in BWRs," *E-Journal of Advanced Maintenance*, Japan Society of Maintenology, Vol. 1, No. 1-29, 2009.

56. P. L. Andresen and F. P. Ford, "Life Prediction by Mechanistic Modelling and System Monitoring of Environmental Cracking of Fe and Ni Alloys in Aqueous Systems", *Materials Science and Engineering*, A103, pp. 167–183, 1988.

57. K. Yamauchi, S. Hattori, J. Kuniya, T. Asami, "Methodology for Formulating Predictions of Degradation of Plant Components Induced by Synergistic Effect of Various Influencing Factors", *Proc. Int. Symp. On Plant Aging and Life Predictions of Corrodible Structures*, Sapporo, Japan, 1995, NACE 1997, p. 69.

58. P. L. Andresen, "Effect of Material and Environmental Variables on SCC Initiation in Slow Strain Rate Tests on Type 304 Stainless Steel", *Symp. on Environmental Sensitive Fracture: Evaluation and Comparison of Test Methods*, April 1982, STP 821, ASTM, Philadelphia, 1984, pp. 271-287.

59. *Materials Reliability Program: Mitigation of Stress Corrosion Crack Growth in Nickel-Based Alloys in Primary Water by Hydrogen Optimization and Zinc Addition (MRP-280)*. EPRI, Palo Alto, CA: 2010. 1021013.

60. R. Kilian, "Crack Initiation as seen from Field Experience," *Workshop on Detection, Avoidance, Mechanisms, Modeling, and Prediction of SCC Initiation in Water-Cooled Nuclear Reactor Plants, Beaune, France – September 7-12, 2008*, EPRI, Palo Alto, CA: 2009. 1018908.

A
TRANSLATED TABLE OF CONTENTS

DISCLAIMER OF WARRANTIES AND LIMITATION OF LIABILITIES

應力腐蝕開裂試驗指南

以高溫水為重點

3002018265

最終報告，2020年8月

EPRI專案經理
G. Stevens

EPRI

核子質量保證方案的所有或部分要件適用於本產品。

YES (NO)

美國電力研究院
地址：3420 Hillview Avenue, Palo Alto, California 94304-1338 ▪ PO Box 10412, Palo Alto, California 94303-0813 ▪ USA
+1 800.313.3774 ▪ +1 650.855.2121 ▪ askepri@epri.com ▪ www.epri.com

可交付產品編號：3002018265

產品類型：技術報告

產品名稱：應力腐蝕開裂試驗指南以高溫水為重點

主要受眾 ：專注於環境裂紋擴展速率試驗的研究者

次要受眾：對環境裂紋擴展速率試驗和相關研究感興趣的項目工程師

重要研究問題

可為高溫水中開展應力腐蝕開裂（SCC）試驗提供哪些指導？

研究概述

本報告目標如下：

- 為在高溫水中開展應力腐蝕開裂（SCC）試驗和腐蝕疲勞（CF）試驗提供關鍵資訊、參考資料和指導。
- 依據目前對最佳應力腐蝕開裂（SCC）試驗和腐蝕疲勞（CF）試驗技術的瞭解，突出關鍵問題。
- 作為應力腐蝕開裂（SCC）試驗和腐蝕疲勞（CF）試驗最佳做法的知識傳遞文檔。
- 提供有關水化學、溫度控制、直流電位元降技術與優化、試樣類型、應力腐蝕裂紋擴展速率和裂紋萌生試驗、機器控制（軟體要求）、腐蝕電位理論與測量、以及試驗技術的指導。

報告重點關注不銹鋼和鎳合金中的SCC（裂紋擴展）和晶間應力腐蝕裂紋（IGSCC），同時適用於碳鋼和低合金鋼的應力腐蝕開裂（SCC）試驗以及腐蝕疲勞（CF）試驗。報告中大部分內容也適用于高溫水以外環境中的應力腐蝕開裂（SCC）試驗和腐蝕疲勞（CF）試驗。在SCC研究中實驗問題只是作為補充，而本報告卻側重於實驗問題，而非對應力腐蝕開裂（SCC）的理解和相關性。因此，本報告不適用於初學者，讀者需具備一定的背景知識。

重要發現

- 任何環境中對環境敏感開裂（EAC）反應的評估都比較複雜，高溫水環境尤為具有挑戰性。鑒於輕水反應堆運行可靠性、長使用壽命和安全性需求，需要高度量化高溫水中環境敏感開裂（EAC）的動力學和依賴性。
- 本指南旨在為高溫水中開展應力腐蝕開裂（SCC）試驗和腐蝕疲勞（CF）試驗提供重要資訊、參考資料和指導。重點介紹裂紋擴展率試驗，其中一章介紹了應力腐蝕裂紋（SCC）萌生試驗。本報告以高溫水為重點，大部分內容也適用於其他環境中的環境敏感開裂（EAC）試驗。

- 環境敏感開裂（EAC）與普通的機械或疲勞試驗大為不同，存在許多複雜的相互依賴關係和較大的細微試驗差異影響。本報告未涵蓋所有試驗細節和細微差別；但卻明確了

重要問題和最佳做法，提供基本參考資料，意在提醒實驗人員仔細觀察，提出質疑並穩步提高技術和觀察結果，重複實驗，與國際同行互動，並優化試驗管理。

為何重要

目前存在五十多年的應力腐蝕開裂（SCC）和腐蝕疲勞（CF）資料可用於核工業，其較大的分散性和有限的複現性表明某些實驗技術存在重大缺陷。此類缺陷無法通過試驗之後專家評估資料加以解決，而需要在試驗之前和試驗期間解決。由於在應力腐蝕開裂（SCC）和腐蝕疲勞（CF）的研究和試驗方面擁有數百年的經驗，且大多數國際實驗室之間存在重要互動，目前已收集許多重要背景資料，可用於制定全面的指導方案，為未來在高溫水中開展應力腐蝕開裂（SCC）和腐蝕疲勞（CF）試驗
提供相關指導。本報告匯總了此類重要資訊，旨在為研究者對未來試驗工作提供相關指導，儘量減少試驗成果缺陷。

如何應用結果

本報告可供實驗人員參考，幫助其開展試驗活動。本報告明確了關鍵問題和最佳做法，提供了基本參考資料，並強調實驗人員必須仔細觀察和管控的問題。鼓勵讀者質疑試驗技術和觀察結果、重現試驗結果、與國際同行互動、並學會管理試驗活動。本報告可為在高溫水中開展或計畫開展應力腐蝕開裂（SCC）試驗且追求高品質資料的研究人員提供有用綱要。

學習和參與機會

- 國際研究技術會議，例如國際環境敏感開裂合作小組（ICG-EAC）
- 核動力系統-水反應堆材料環境退化會議
- 材料可靠性計畫以及沸水反應堆（BWR）容器和內部構件項目會議

EPRI連絡人：Gary L. Stevens，技術主管，gstevens@epri.com

計畫： “核動力”， P41；“沸水反應堆容器和內部構件（BWRVIP）”，P41.01.03；“壓水堆材料可靠性（MRP）”， P41.01.04

執行類別： 參考文獻

目錄

插圖列表

表格列表

应力腐蚀开裂试验指南

以高温水为重点

3002018265

最终报告，2020 年 8 月

EPRI 项目经理
G. Stevens

所有或部分 EPRI 核能质量保证项目要求适用于本产品。

YES (NO)

ELECTRIC POWER RESEARCH INSTITUTE
3420 Hillview Avenue, Palo Alto, California 94304-1338 ▪ PO Box 10412, Palo Alto, California 94303-0813 ▪ USA
+1.800.313.3774 ▪ +1.650.855.2121 ▪ askepri@epri.com ▪ www.epri.com

可交付产品编号：3002018265

产品类型：技术报告

产品名称： 应力腐蚀开裂试验指南以高温水为重点

主要受众： 专注于环境裂纹扩展速率试验的研究者

次要受众： 对环境裂纹扩展速率试验和相关研究感兴趣的项目工程师

主要研究问题

可为高温水中开展应力腐蚀开裂（SCC）试验提供哪些指导？

研究概述

本报告目标如下：

- 为在高温水中开展应力腐蚀开裂（SCC）试验和腐蚀疲劳（CF）试验提供关键信息、参考数据和指导。
- 依据目前对最佳应力腐蚀开裂（SCC）试验和腐蚀疲劳（CF）试验技术的了解，突出关键问题。
- 作为应力腐蚀开裂（SCC）试验和腐蚀疲劳（CF）试验最佳做法的知识传递文档。
- 提供有关水化学、温度控制、直流电位降技术与优化、试样类型、应力腐蚀裂纹扩展速率和裂纹萌生试验、机器控制（软件要求）、腐蚀电位理论与测量、以及试验技术的指导。

报告重点关注不锈钢和镍合金中的 SCC（裂纹扩展）和晶间应力腐蚀裂纹（IGSCC），同时适用于碳钢和低合金钢的应力腐蚀开裂（SCC）试验以及腐蚀疲劳（CF）试验。报告中大部分内容也适用于高温水以外环境中的应力腐蚀开裂（SCC）试验和腐蚀疲劳（CF）试验。在 SCC 研究中实验问题只是作为补充，而本报告却侧重于实验问题，而非对应力腐蚀开裂（SCC）的理解和相关性。因此，本报告不适用于初学者，读者需具备一定的背景知识。

主要发现

- 任何环境中对环境敏感开裂（EAC）反应的评估都比较复杂，高温水环境尤为具有挑战性。鉴于对轻水反应堆运行可靠性、长使用寿命和安全性的需求，需要高度量化高温水中环境敏感开裂（EAC）的动力学和依赖性。
- 本指南旨在为高温水中开展应力腐蚀开裂（SCC）试验和腐蚀疲劳（CF）试验提供重要信息、参考数据和指导。重点介绍裂纹扩展率试验，其中一章介绍了应力腐蚀裂纹（SCC）萌生试验。本报告以高温水为重点，大部分内容也适用于其他环境中的环境敏感开裂（EAC）试验。

- 环境敏感开裂（EAC）与普通的机械或疲劳试验大为不同，存在许多复杂的相互依赖关系和较大的细微试验差异影响。本报告未涵盖所有试验细节和细微差别；但却明确了

重要问题和最佳做法，提供基本参考数据，旨在提醒实验人员仔细观察，提出质疑并稳步提高技术和观察结果，重复实验，与国际同行互动，并优化试验管理。

为什么重要?

目前存在五十多年的应力腐蚀开裂（SCC）和腐蚀疲劳（CF）数据可用于核工业，其较大的分散性和有限的复现性表明某些实验技术存在重大缺陷。此类缺陷无法通过试验之后专家评估数据加以解决，而需要在试验之前和试验期间解决。由于在应力腐蚀开裂（SCC）和腐蚀疲劳（CF）的研究和试验方面拥有数百年的系统经验，且大多数国际实验室之间存在重要互动，目前已收集许多重要背景资料，可用于制定全面的指导方案，为未来在高温水中开展应力腐蚀开裂（SCC）和腐蚀疲劳（CF）试验提供相关指导。本报告汇总了此类重要信息，旨在为研究者对未来试验工作提供相关指导，尽量减少试验成果缺陷。

如何应用这些成果？

本报告可供实验人员参考，帮助其开展试验活动。本报告明确了关键问题和最佳做法，提供了基本参考数据，并强调实验人员必须仔细观察和管控的问题。鼓励读者质疑试验技术和观察结果、重现试验结果、与国际同行互动、并学会管理试验活动。本报告可为在高温水中开展或计划开展应力腐蚀开裂（SCC）试验且追求高质量数据的研究人员提供有用纲要。

学习和参与机会

- 国际研究技术会议，例如国际环境敏感开裂合作小组（ICG-EAC）
- 核动力系统-水反应堆材料环境退化会议
- 材料可靠性计划以及沸水反应堆（BWR）容器和内部构件项目会议

EPRI 联系人：Gary L. Stevens，技术主管，gstevens@epri.com

计划： “核动力”， P41；“沸水反应堆容器和内部构件（BWRVIP）”，P41.01.03；“压水堆材料可靠性（MRP）”， P41.01.04

执行类别：参考文献

目录

插图清单

表格目录

Lignes directrices pour les essais de fissuration par corrosion sous contrainte

Avec une température élevée de l'eau

3002018265

Rapport final, août 2020

Chef de projet EPRI
G. Stevens

La totalité ou une partie des exigences du programme d'assurance qualité nucléaire EPRI (EPRI Nuclear Quality Assurance Program) s'appliquent à ce produit.

YES  NO

ELECTRIC POWER RESEARCH INSTITUTE
3420 Hillview Avenue, Palo Alto, California 94304-1338 ▪ PO Box 10412, Palo Alto, California 94303-0813 ▪ États-Unis
(+1) 800.313.3774 ▪ (+1) 650.855.2121 ▪ askepri@epri.com ▪ www.epri.com

Numéro de livrable : 3002018265

Type de produit : Rapport technique

Titre de produit : Lignes directrices pour les essais de fissuration par corrosion sous contrainte avec une température élevée de l'eau

PRINCIPAL PUBLIC VISE : Chercheurs réalisant des essais sur le taux de croissance des fissures environnementales

PUBLIC SECONDAIRE VISE : Ingénieurs de programme intéressés par les essais sur le taux de croissance des fissures environnementales et d'autres études connexes

OBJET ESSENTIEL DE LA RECHERCHE

Quelles lignes directrices sont disponibles pour mener des essais de fissuration par corrosion sous contrainte (SCC) en eau à température élevée ?

PRÉSENTATION DE LA RECHERCHE

Les objectifs du présent rapport sont les suivants :

- Fournir des informations essentielles, des données de référence et une orientation pour mener des essais SCC et de fatigue par la corrosion (CF) en eau à température élevée.
- Mettre en évidence les principaux problèmes en fonction des connaissances actuelles sur les techniques optimales pour les essais SCC et CF.
- Servir de document de transfert des connaissances pour les bonnes pratiques des essais SCC et CF.
- Fournir une orientation sur la composition chimique de l'eau, la régulation de la température, les techniques de chute de tension de courant continu et leur optimisation, les types d'éprouvettes, les essais du taux de croissance et d'amorçage SCC, le contrôle informatique (logiciels requis), la théorie du potentiel de corrosion et les mesures correspondantes, ainsi que les techniques d'essai.

Le rapport aborde avant tout la croissance des fissures (SCC) et la fissuration par corrosion sous contrainte intergranulaire (IGSCC) dans les aciers inoxydables et les alliages de nickel. Il est également utile pour les essais SCC d'acier au carbone et d'acier faiblement allié, de même que pour les essais CF. Une grande partie des informations figurant dans le rapport est également applicable aux essais SCC et CF dans des milieux autres que l'eau à température élevée. Le rapport ne cherche pas à examiner en détail la SCC et ses dépendances, mais traite avant tout de questions expérimentales, bien que ces dernières constituent des enjeux complémentaires dans toute étude SCC. De ce fait, il n'est pas destiné aux débutants, mais à des professionnels expérimentés.

PRINCIPALES CONCLUSIONS

- Si l'évaluation de la réponse de la fissuration environnementale (EAC) est complexe dans tout milieu, c'est tout particulièrement le cas en eau à température élevée. Il existe de nombreuses raisons motivant la quantification des effets cinétiques et des dépendances de l'EAC en eau à température élevée, compte tenu de la nécessité d'assurer une exploitation fiable, prolongée et sûre des réacteurs à eau légère.
- Les lignes directrices visent à fournir des informations essentielles, des données de référence et une orientation pour mener des essais SCC et CF en eau à température élevée. L'étude attache une importance toute particulière au taux de croissance et comprend également une section sur les essais d'amorçage de SCC. Bien que le rapport se penche essentiellement sur

les milieux d'eau à température élevée, une grande partie des informations y figurant est également applicable aux essais EAC dans d'autres milieux.

- Un essai EAC est très différent des essais mécaniques ou de fatigue ordinaires, car il existe de nombreuses interdépendances complexes et de subtiles différences peuvent avoir des effets considérables. Le présent rapport ne cherche pas à examiner toutes ces subtilités et nuances. En revanche, il vise à identifier les enjeux les plus importants et les bonnes pratiques tout en fournissant des données de référence de base dans le but de pousser les chercheurs à faire des observations minutieuses, à se remettre en question, à améliorer leurs techniques et leurs observations, à répéter leurs expériences, à échanger avec des collègues internationaux et à optimiser la gestion des essais.

POURQUOI EST-CE IMPORTANT ?

Cela fait plus de cinquante ans que le secteur nucléaire génère des données SCC et CF. Les coefficients de dispersion élevés et la reproductibilité limitée de certaines techniques expérimentales témoignent de lacunes importantes. Ces lacunes ne peuvent être corrigées par des évaluations postérieures des données, mais doivent être prises en charge avant et durant les essais. Avec plusieurs centaines d'années-système d'expérience dans les études et les essais SCC et CF, conjuguées à de nombreux échanges entre la plupart des laboratoires internationaux, les informations substantielles recueillies permettent de créer une orientation complète pour les futurs essais SCC et CF en eau à température élevée.

Le rapport synthétise ces informations clés dans le but de fournir aux chercheurs une orientation qui, lors de leurs futurs essais, les aidera à réduire les lacunes des résultats obtenus.

COMMENT APPLIQUER LES RÉSULTATS

Le rapport peut être utilisé par les chercheurs comme référence pour leurs activités d'essai. Il identifie les principaux enjeux et les bonnes pratiques, fournit des données de référence de base et met en évidence les aspects que les chercheurs devraient observer et gérer avec soin. De plus, il encourage les lecteurs à remettre en question leurs techniques et leurs observations, à reproduire les résultats expérimentaux, à échanger avec leurs collègues internationaux et à apprendre à gérer leurs activités d'essai. Enfin, il constitue un outil de référence qui aidera les chercheurs souhaitant obtenir des données de grande qualité dans les essais SCC en eau à température élevée qu'ils réalisent ou prévoient de réaliser.

POSSIBILITÉS D'APPRENTISSAGE ET D'ENGAGEMENT

- Conférences techniques de recherche internationale, par exemple International Cooperative Group on Environmentally Assisted Cracking (ICG-EAC)
- Conference on Environmental Degradation of Materials in Nuclear Power Systems-Water Reactors
- Réunions du Programme de fiabilité des matériaux et du Projet relatif aux équipements internes et aux cuves des BWR

CONTACT EPRI : Gary L. Stevens, responsable technique, gstevens@epri.com

PROGRAMMES : Nuclear Power, P41 ; Boiling Water Reactor Vessels and Internals (BWRVIP), P41.01.03 ; Pressurized Water Reactor Materials Reliability (MRP), P41.01.04

CATEGORIE DE MISE EN ŒUVRE : Référence

TABLE DES MATIERES

LISTE DES FIGURES

LISTE DES TABLEAUX

Richtlinien für die Prüfung von Spannungsrisskorrosion

Mit Schwerpunkt auf Hochtemperaturwasser

3002018265

Abschlussbericht, August 2020

EPRI-Projektmanager
G. Stevens

Für dieses Produkt gelten alle oder ein Teil der Anforderungen des EPRI Nuclear Quality Assurance-Programms.

YES NO

ELECTRIC POWER RESEARCH INSTITUTE
3420 Hillview Avenue, Palo Alto, California 94304-1338 ▪ PO Box 10412, Palo Alto, California 94303-0813 ▪ USA
+1.800.313.3774 ▪ +1.650.855.2121 ▪ askepri@epri.com ▪ www.epri.com

Ergebnisnummer: 3002018265

Produkttyp: Technischer Bericht

Produkttitel: Richtlinien für die Prüfung von Spannungsrisskorrosion mit Schwerpunkt auf Hochtemperaturwasser

PRIMÄRE ZIELGRUPPE: Auf die Prüfung der Risswachstumsrate unter Umgebungsbedingungen spezialisierte Forscher

SEKUNDÄRE ZIELGRUPPE: Programmingenieure, die sich für die Prüfung der Risswachstumsrate unter Umgebungsbedingungen und verwandte Studien interessieren

WICHTIGE FORSCHUNGSFRAGE

Welche Richtlinien gibt es für die Durchführung von Spannungsrisskorrosionsprüfungen (stress corrosion cracking, SCC) in Hochtemperaturwasser?

FORSCHUNGSÜBERSICHT

Die Ziele dieses Berichts sind folgende:

- Bereitstellung wichtiger Informationen, Referenzdaten und Richtlinien für die Durchführung von SCC- und Korrosionsermüdungsprüfungen (corrosion fatigue, CF) in Hochtemperaturwasser.
- Hervorhebung von Schlüsselfragen auf der Grundlage des aktuellen Wissensstandes über optimale SCC- und CF-Prüftechniken.
- Verwendung als Wissenstransferdokument für SCC- und CF-Prüfverfahren.
- Bereitstellung von Anleitungen speziell zu Wasserchemie, Temperaturregelung, Gleichspannungspotentialabfall- (DCPD-)Techniken und -Optimierung, Probentypen, SCC-Wachstumsraten- und Einleitungsprüfung, Maschinensteuerung (Softwareanforderungen), Korrosionspotenzialtheorie und -messungen sowie Prüftechniken.

Der Schwerpunkt des Berichts liegt auf SCC (Risswachstum) und meist interkristalliner Spannungsrisskorrosion (IGSCC) in rostfreien Stählen und Nickellegierungen, außerdem ist er für SCC-Prüfungen von Kohlenstoffstahl und niedrig legiertem Stahl sowie für CF-Prüfungen relevant. Ein Großteil des Berichts ist auch auf SCC- und CF-Prüfungen in anderen Umgebungen als Hochtemperaturwasser anwendbar. Der Bericht konzentriert sich nicht auf das Verständnis und die Abhängigkeiten der SCC, sondern eher auf experimentelle Fragen, obwohl dies komplementäre Elemente in jeder SCC-Studie sind. Daher ist der Bericht nicht für Neulinge auf diesem Gebiet gedacht, und es wird ein gewisses Hintergrundwissen der Leser vorausgesetzt.

WICHTIGSTE ERKENNTNISSE

- Die Bewertung der Reaktion auf umgebungsbedingte Risse (environmentally assisted cracking, EAC) ist in jeder Umgebung komplex, stellt jedoch in Hochtemperaturwasser eine besondere Herausforderung dar. Der Anreiz, die Kinetik und die Abhängigkeiten von EAC in Hochtemperaturwasser zu quantifizieren, ist angesichts des Bedarfs an einem zuverlässigen, langlebigen und sicheren Leichtwasserreaktorbetrieb hoch.
- Diese Richtlinie soll wichtige Informationen, Referenzdaten und Richtlinien für die Durchführung von SCC- und CF-Prüfungen in Hochtemperaturwasser liefern. Die Prüfung der Risswachstumsrate ist ein wichtiger Schwerpunkt, und ein Abschnitt widmet sich der SCC-Einleitungsprüfung. Der Schwerpunkt des Berichts liegt zwar auf Hochtemperaturwasser, jedoch ist ein Großteil des Berichts auch auf EAC-Prüfungen in anderen Umgebungen anwendbar.

- EAC unterscheidet sich sehr von gewöhnlichen mechanischen oder Ermüdungsprüfungen, da es viele komplexe Abhängigkeiten und starke Auswirkungen von subtilen Prüfunterschieden gibt. Die Auseinandersetzung mit allen Feinheiten und Nuancen der Prüfung sprengt den Rahmen des Berichts; vielmehr ist er bestrebt, wichtige Fragen und bewährte Verfahren aufzuzeigen sowie grundlegende Referenzdaten bereitzustellen, mit der Absicht, den Experimentator darauf aufmerksam zu machen, sorgfältig zu beobachten, Techniken und Beobachtungen zu hinterfragen und stetig zu verbessern, Experimente zu wiederholen, mit internationalen Kollegen zu interagieren und das Prüfmanagement zu optimieren.

WARUM DAS WICHTIG IST

Über fünf Jahrzehnte lang wurden SCC- und CF-Daten für die Verwendung in der Nuklearindustrie erzeugt, und die große Streuung und begrenzte Reproduzierbarkeit weisen auf erhebliche Mängel in einigen der Versuchstechniken hin. Die Mängel können nicht einfach durch eine Bewertung der Daten nach der Prüfung durch Experten behoben werden; sie müssen vielmehr vor und während der Prüfung behoben werden. Mit Hunderten von Systemjahren an Erfahrung in der Untersuchung und Prüfung auf SCC und CF sowie einer bedeutenden Interaktion zwischen den meisten internationalen Laboratorien wurde umfangreiches Hintergrundmaterial gesammelt, das zur Entwicklung einer umfassenden Richtlinie für zukünftige SCC- und CF-Prüfungen in Hochtemperaturwasser verwendet werden kann. Der Bericht fasst solche Schlüsselinformationen zusammen, um den Forschern eine Anleitung zu geben, die sie bei zukünftigen Prüfungen in Betracht ziehen können, um die Mängel der Prüfungsergebnisse zu minimieren.

DIE ANWENDUNG DER ERGEBNISSE

Der Bericht kann von Experimentatoren als Referenz verwendet werden, um sie bei ihren Prüfungen zu unterstützen. Der Bericht zeigt Schlüsselfragen und bewährte Praktiken auf, liefert grundlegende Referenzdaten und weist auf Aspekte hin, die der Experimentator sorgfältig beobachten und handhaben sollte. Der Bericht ermutigt die Leser, ihre Techniken und Beobachtungen zu hinterfragen, experimentelle Ergebnisse zu reproduzieren, mit internationalen Kollegen zu interagieren und zu lernen, ihre Prüfaktivitäten zu verwalten. Er ist ein nützliches Kompendium für Forscher, die SCC-Prüfungen in Hochtemperaturwasser durchführen oder diese planen und dabei nach qualitativ hochwertigen Daten streben.

MÖGLICHE LERN- UND GESCHÄFTSCHANCEN

- Internationale technische Forschungskonferenzen, zum Beispiel die International Cooperative Group on Environmentally Assisted Cracking (ICG-EAC)
- Konferenz über die umgebungsbedingte Verschlechterung von Materialien in Kernkraftwerk-Wasserreaktoren
- Material-Zuverlässigkeitsprogramm sowie Meetings der Boiling Water Reactor Vessel and Internals Project (BWRVIP) Gruppe

EPRI-KONTAKTPERSON: Gary L. Stevens, Technischer Geschäftsführer, gstevens@epri.com

PROGRAMME: Nuclear Power, P41; Boiling Water Reactor Vessels and Internals (BWRVIP), P41.01.03; Pressurized Water Reactor Materials Reliability (MRP), P41.01.04

UMSETZUNGSKATEGORIE: Referenz

INHALT

ABBILDUNGSVERZEICHNIS

TABELLENVERZEICHNIS

応力腐食割れ試験ガイドライン

特に高温水に関して

3002018265

2020 年 8 月　最終報告書

EPRI プロジェクトマネージャー
G. Stevens

本成果物には、EPRI 原子力品質保証プログラム（Nuclear Quality Assurance Program）の要件の全てまたは一部が適用される。

YES　NO

米国電力研究所
3420 Hillview Avenue, Palo Alto, California 94304-1338 ▪ PO Box 10412, Palo Alto, California 94303-0813 ▪ USA
+1.800.313.3774 ▪ +1.650.855.2121 ▪ askepri@epri.com ▪ www.epri.com

納品番号：3002018265

製品タイプ：技術報告書

製品タイトル：応力腐食割れ試験ガイドライン特に高温水に関して

主な対象読者：環境クラック進展速度試験を中心に研究している研究員

二次的な対象読者:環境クラック進展速度試験およびそれに関連する研究に関心のあるプログラムエンジニア

主な研究課題

高温水中で応力腐食割れ（SCC）試験を実施するために利用できるガイダンスは何か？

研究概要

本報告書の目的は次のとおりである。

- 高温水中で SCC および腐食疲労（CF）試験を実施するための重要な情報、参考データ、およびガイダンスを提供すること。
- 最適な SCC および CF の試験技術に関する知識の現状に基づいて、主要な問題に焦点を当てること。
- SCC および CF 試験のベストプラクティスに関する知識移転文書として機能すること。
- 水化学、温度制御、直流電位降下の技術と最適化、試験片タイプ、SCC 進展速度と発生に関する試験、機械制御（ソフトウェア要件）、腐食電位理論と測定、および試験技術に特有のガイダンスを提供すること。

本報告書は、SCC（クラック進展）と、主にステンレス鋼とニッケル合金の粒界応力腐食割れ（IGSCC）に焦点が置かれており、また炭素鋼と低合金鋼の SCC 試験、および CF 試験にも関連している。本報告書の大部分は、高温水以外の環境における SCC および CF 試験にも適用できる。本報告書は SCC の理解や依存関係ではなく、実験的な課題（これらは SCC 研究の補足的な要素ではあるが）に焦点を当てている。その結果、本報告書は初心者向けではなく、読者にはある程度の予備知識が必要とされる。

主な所見

- 環境誘起割れ（EAC）対応の評価は、どの環境でも複雑だが、高温水では特に困難を伴う。信頼性が高く、寿命が長く、安全な軽水炉運転の必要性を考えると、高温水における EAC の動特性と依存性を定量化する利点は大きいと言える。
- 本ガイドラインは、高温水中で SCC および CF 試験を実施するための重要な情報、参考データ、およびガイダンスを提供するよう設計されている。クラック進展速度試験に主な重点が置かれ、SCC 発生試験に関するセクションが含まれている。高温水に焦点が当てられているが、本報告書の大部分は、他の環境における EAC 試験にも適用することができる。

- EAC は、多くの複雑な相互依存関係と微妙な試験の違いに起因する大きな影響があるため、通常の機械的または疲労試験とは大きく異なる。すべての試験の繊細さや微妙な違いに対応することは、本報告書の範囲を超えているため、むしろ、ここでは重要な問題とベストプラクティスを特定し、基本的な参考データを提供することに努めている。これは、注意深く観察し、技術と観察に疑問を投げかけ、かつ着実に改善し、実験を繰り返し、国外の同業者と意見交換し、試験管理を最適化するよう実験担当者に注意を促すことを目的としたものである。

本文書の重要性

原子力業界で使用するために生成された SCC および CF データは 50 年分以上に上り、ばらつきが大きく、再現性が限られているため、一部の実験技術には重大な欠点があることがわかっている。それらの欠点は、専門家による試験後のデータ評価では解決できない。むしろ、試験前および試験中に対処する必要がある。システム年で数百年分に及ぶ SCC と CF に関する研究と試験の経験と、多数の国際的な研究所間の意義深い交流により、高温水中での将来的な SCC と CF 試験の包括的なガイドラインを開発するために使用できる相当量の参考資料が収集された。
本報告書は、そのような重要な情報を要約しており、研究者が試験結果の欠点を最小限に抑えるため将来の試験作業で検討すべきガイダンスを提供することを目的としている。

研究結果の使い方

実験担当者は、本報告書を、試験作業を支援するための参考文献として使用できる。本報告書では、主要な問題とベストプラクティスを特定し、基本的な参考データを提供し、実験担当者が注意深く観察および管理する必要がある問題に焦点を当てている。本報告書は、読者に技術と観察に疑問を投げかけ、実験結果を再現し、国外の同業者と意見交換し、試験作業の管理方法を習得することを推奨している。これは、高温水で SCC 試験を実施中または実施する計画を立てており、質の高いデータを求める研究者にとって有用な概要となっている。

学習および参加の機会

- International Cooperative Group on Environmentally Assisted Cracking (ICG-EAC)などのような国際研究技術学会
- Conference on Environmental Degradation of Materials in Nuclear Power Systems-Water Reactors
- 材料信頼性プログラムおよび BWR 容器と内部構造物プロジェクト会議

EPRI 連絡先： Gary L. Stevens (テクニカルエグゼクティブ)、gstevens@epri.com

プログラム： 原子力、P41、沸騰水型原子炉容器および内部構造物 (BWRVIP)、P41.01.03、加圧水型原子炉材料信頼性 (MRP)、P41.01.04

実施カテゴリー:参考文献

目次

図一覧

表一覧

응력부식균열 시험 지침서

고온냉각수를 중심으로

3002018265

최종 보고서, 2020 년 8 월

EPRI 프로젝트 매니저
G. Stevens

본 보고서에는 EPRI 원자력 품질 보증 프로그램의
요건이 전부 또는 일부 적용됩니다.

YES NO

미국 전력연구소(EPRI: ELECTRIC POWER RESEARCH INSTITUTE)
3420 Hillview Avenue, Palo Alto, California 94304-1338 ▪ PO Box 10412, Palo Alto, California 94303-0813 ▪ USA
+1.800.313.3774 ▪ +1.650.855.2121 ▪ askepri@epri.com ▪ www.epri.com

결과물 번호: 3002018265

결과물 유형: 기술 보고서

결과물 제목: 응력부식균열 시험 지침서 고온냉각수를 중심으로

1 차 대상: 환경에 의한 균열 성장률 시험에 중점을 둔 연구자

2 차 대상: 환경에 의한 균열 성장률 시험 및 관련 연구에 관심이 있는 프로그램 엔지니어

주요 연구 관련 질문

고온냉각수에서 응력부식균열(SCC) 시험을 수행할 때 어떤 지침을 이용할 수 있습니까?

연구 개요

본 보고서의 목적은 다음과 같습니다.

- 고온냉각수에서 SCC 및 부식 피로(CF) 시험 수행을 위한 중요 정보, 참고 자료 및 지침 제공
- 최적의 SCC 및 CF 시험 기법에 대한 현재 지식 상태를 기초로 핵심 사안 강조
- SCC 및 CF 시험 모범 사례에 대한 지식 전이 문서로 사용
- 냉각수 화학, 온도 제어, 직류 전위 강하 기법 및 최적화, 시편 유형, SCC 성장률 및 초기 시험, 기계 제어(소프트웨어 요건), 부식 전위 이론 및 측정 그리고 시험 기법에 대한 지침 제공

본 보고서의 중점은 SCC(균열 성장) 그리고 주로 스테인리스강 및 니켈 합금의 입계응력부식균열(IGSCC)에 있으며, 또한 탄소강 및 저합금강의 SCC 시험 그리고 CF 시험에도 관련됩니다. 보고서의 많은 부분은 고온냉각수 이외 환경에서 수행하는 SCC 및 CF 시험에도 적용할 수 있습니다. 본 보고서는 SCC 이해와 의존성에 중점을 두지 않으며, 비록 모든 SCC 연구에서 보완적인 요소이지만 실험적 사안에 중점을 둡니다. 결과적으로 본 보고서는 초보자를 위한 것이 아니며 독자의 배경 지식이 어느 정도 있다고 가정합니다.

주요 결과

- 환경유기균열(EAC) 반응의 평가는 어떤 환경에서도 복잡하지만 특히 고온냉각수에서 도전적입니다. 신뢰성 있고 수명이 길며 안전한 경수로 운전에 대한 필요성을 감안할 때 고온냉각수에서 EAC 의 동역학과 의존성을 정량화하는 인센티브가 높습니다.
- 본 지침은 고온냉각수에서 SCC 및 CF 시험의 수행을 위해 중요 정보, 참고 자료 및 지침을 제공하도록 고안되었습니다. 균열 성장률 시험이 중요한 강조사항이며 SCC 초기 시험에 대한 섹션이 포함되어 있습니다. 고온냉각수에 중점을 두고 있지만 본 보고서의 많은 부분은 다른 환경의 EAC 시험에도 적용할 수 있습니다.

- EAC 는 보편적인 기계적 시험 또는 피로 시험과 아주 다른데, 미묘한 시험 차이의 여러 복잡한 상호의존성과 큰 영향이 있기 때문입니다. 모든 시험 세부요소 및 미묘한 차이를 다루는 것은 본 보고서의 범위를 넘어서는 것이므로, 차라리 중요 사안과 모범 사례를

식별하고, 실험자에게 기법과 관찰사항을 주의해서 준수하고 의문을 가지며 꾸준히 개선하고, 실험을 반복하며 전세계 동료와 상호작용하며 시험 관리를 최적화하도록 충고하는 근원적인 의도와 함께 기본적인 참고 자료를 제공하기 위해 노력합니다.

이것이 중요한 이유

원자력 산업에서 사용하기 위해 생성된 50 년이 넘는 SCC 및 CF 데이터가 있으며, 큰 분산과 제한된 재현성은 일부 실험 기법의 의미심장한 단점을 시사합니다. 이 단점은 데이터에 대한 시험 후 전문가 평가로 해결할 수 없으며, 차라리 시험 전 및 시험 중에 다룰 필요가 있습니다. SCC 및 CF 에 대한 연구와 시험에서 수 백 시스템-연의 경험과 가장 국제적인 연구소들 사이의 중요한 상호작용으로, 고온냉각수에서 향후 SCC 및 CF 시험을 위한 포괄적 지침을 개발하기 위해 사용할 수 있는 상당한 배경 자료가 수집되었습니다. 본 보고서는 향후 시험에서 시험 결과의 단점을 최소화하고자 노력할 때 연구자가 고려할 지침을 제공하려는 의도로 관련 핵심 정보를 요약합니다.

결과 적용 방법

본 보고서는 실험자의 시험 활동을 지원하는 참고 자료로 사용할 수 있습니다. 본 보고서는 핵심 사안과 모범 사례를 식별하고 기본 참고 자료를 제공하며 실험자가 주의 깊게 준수하고 관리해야 할 사안을 강조합니다. 본 보고서는 독자가 자신의 기법과 관찰에 의문을 갖고, 실험 결과를 재현하고, 국제 동료들과 상호작용하며 자신의 시험 활동을 관리하는 방법을 학습하도록 장려합니다. 이것은 고온냉각수에서 SCC 시험을 시행하거나 시행을 계획하고 고품질의 데이터를 얻기 위해 애쓰는 연구자에게 유용한 개요서입니다.

학습 및 참여 기회

- 국제 연구 기술 컨퍼런스. 예, 환경유기균열 국제협력그룹(ICG-EAC)
- 원자력 시스템-수 원자로에서 물질의 환경적 열화에 관한 컨퍼런스
- 재료 신뢰성 프로그램 그리고 비등수형 원자로 및 내부구조물 프로젝트 회의

EPRI 연락처: Gary L. Stevens, Technical Executive, gstevens@epri.com

프로그램: 원자력, P41; 비등수형 원자로 용기 및 내부구조물 프로그램(BWRVIP), P41.01.03; 가압경수로 재료 신뢰성(MRP), P41.01.04

시행 범주: 참고문헌

목차

그림 목록

도표 목록

Diretrizes para testes de fragilização por corrosão sob tensão

Com ênfase em água em alta temperatura

3002018265

Relatório final, agosto de 2020

Gerente de projeto EPRI
G. Stevens

Os requisitos do Programa de Garantia de Qualidade Nuclear do EPRI se aplicam a este produto total ou parcialmente.

ELECTRIC POWER RESEARCH INSTITUTE
3420 Hillview Avenue, Palo Alto, Califórnia 94304-1338 ▪ PO Box 10412, Palo Alto, Califórnia 94303-0813 ▪ EUA
+1.800.313.3774 ▪ +1.650.855.2121 ▪ askepri@epri.com ▪ www.epri.com

Número do entregável: 3002018265

Tipo de produto: Relatório técnico

Título do produto: Diretrizes para testes de fragilização por corrosão sob tensão com ênfase em água em alta temperatura

---

PÚBLICO PRINCIPAL: Pesquisadores com foco em testes de crescimento de fissuras ambientais

PÚBLICO SECUNDÁRIO: Engenheiros de programa interessados em testes de crescimento de fissuras ambientais e estudos relacionados

QUESTÃO PRINCIPAL DE PESQUISA

Que orientações estão disponíveis para a realização de testes de fragilização por corrosão sob tensão (CST) em água em alta temperatura?

VISÃO GERAL DA PESQUISA

Os objetivos deste relatório são os seguintes:

- Fornecer informações essenciais, dados de referência, e orientações para a condução de testes de CST e fadiga de corrosão (FC) em água de alta temperatura.
- Destacar questões principais baseadas no estado atual do conhecimento sobre as técnicas ideais de testes de CST e FC.
- Servir como documento de transferência de conhecimento das boas práticas de testes de CST e FC.
- Oferecer orientações específicas quanto à química da água, controle de temperatura, técnicas e otimização de queda de potencial de corrente contínua, tipos de amostras, índice de crescimento de CST e testes de início de fissura, controle de máquinas (requisitos de software), teoria e medições de potencial de corrosão, e técnicas de testes.

O foco do relatório está no CST (crescimento de fissuras) e principalmente na fratura intergranular por corrosão sob tensão (*Intergranular Stress Corrosion Cracking* - IGSCC) em aço inoxidável e ligas de níquel. O relatório também é pertinente para os testes de CST em aço carbono e aço de baixa liga, além de testes de FC. Grande parte do relatório também se aplica a testes de CST e FC em ambientes diferentes da água em alta temperatura. O relatório não está focado no entendimento do CST e dependências, mas em questões experimentais, embora esses sejam elementos complementares em qualquer estudo de CST. Consequentemente, o relatório não se destina a iniciantes, e presume-se que haja algum nível de conhecimento do contexto por parte do leitor.

RESULTADOS PRINCIPAIS

- A avaliação da resposta de fratura assistida pelo ambiente (*Environmentally Assisted Cracking* - EAC) é complexa em qualquer ambiente, mas é especialmente difícil em água em alta temperatura. O incentivo para quantificar a cinética e as dependências da EAC em água em alta temperatura é alto, considerando-se a necessidade de operação confiável, de longa duração, e segura do reator de água.
- As diretrizes têm o objetivo de fornecer informações essenciais, dados de referência, e orientações para a condução de testes de CST e FC em água de alta temperatura. Os testes de índice de crescimento de fissura são uma grande ênfase, e é incluída uma seção sobre os testes de início de CST. Apesar do foco em água de alta temperatura, grande parte do relatório também se aplica a testes de CST e FC em outros ambientes.

- A EAC é bem diferente dos testes de fadiga ou mecânicos comuns, pois há muitas interdependências complexas e grandes efeitos de diferenças sutis entre os testes. O escopo deste relatório não inclui todas as diferenças sutis e nuances dos testes. Ele busca identificar questões importantes e boas práticas e oferece dados de referência básicos com a intenção subjacente de alertar os responsáveis pelos experimentos para que observe cuidadosamente, questione e aperfeiçoe constantemente técnicas e observações, repita experimentos, interaja com colegas internacionais, e otimize a gestão dos testes.

PORQUE ISSO É IMPORTANTE

Há mais de quatro décadas, são gerados dados sobre CST e FC para uso no setor nuclear. Entretanto, o fato de esses dados estarem espalhados e sua reprodutibilidade ser limitada indicam deficiências significativas em algumas das técnicas experimentais. As deficiências não podem ser resolvidas por avaliações pós-teste dos dados feitas por especialistas, e, pelo contrário, precisam ser tratadas antes e durante os testes. Com centenas de anos de sistemas de experiência no estudo e nos testes de CST e FC, e interação significativa entre a maioria dos laboratórios internacionais, coletou-se uma quantidade considerável de material de contexto que pode ser utilizado para desenvolver uma diretriz abrangente para futuros testes de CST e FC em água em alta temperatura. O relatório resume essas informações-chave com a intenção de oferecer orientações para pesquisadores levarem em consideração em testes futuros para minimizar as deficiências dos resultados dos testes.

COMO APLICAR OS RESULTADOS

O relatório pode ser utilizado pelos responsáveis pelos experimentos como referência para ajudá-los nas atividades de testes. O relatório identifica questões-chave e boas práticas, oferece dados de referência básicos, e destaca problemas que o responsável pelos experimentos deve observar e administrar cuidadosamente. O relatório incentiva os leitores a questionar suas técnicas e observações, reproduzir resultados experimentais, interagir com colegas internacionais, e aprender a gerenciar suas atividades de testes. É um compêndio útil para pesquisadores que realizam ou planejam realizar testes de CST em água em alta temperatura, e que buscam dados de alta qualidade.

OPORTUNIDADES DE APRENDIZADO E ENVOLVIMENTO

- Conferências técnicas de pesquisa internacionais, por exemplo, o Grupo colaborativo internacional sobre fratura assistida pelo ambiente (*International Cooperative Group on Environmentally Assisted Cracking* - ICG-EAC)
- Conferência sobre degradação ambiental de materiais em sistemas de energia nuclear - reatores a água
- Programa de confiabilidade dos materiais e reuniões do Projeto de vasos BWR e componentes internos

CONTATO DO EPRI: Gary L. Stevens, Executivo técnico, gstevens@epri.com

PROGRAMAS: Energia nuclear, P41; Vasos e partes internas de reatores de água fervente (BWRVIP), P41.01.03; Confiabilidade de materiais de reatores de água pressurizada (MRP), P41.01.04

CATEGORIA DE IMPLEMENTAÇÃO: Referência

ÍNDICE

LISTA DE FIGURAS

LISTA DE TABELAS

Guías sobre ensayos de fisuración por corrosión bajo tensión

Con énfasis en el agua a alta temperatura

3002018265

Informe final, agosto de 2020

Jefe de Proyecto de EPRI
G. Stevens

Este producto está sujeto a la totalidad o a parte de los requisitos del Programa de aseguramiento de la calidad nuclear de EPRI.

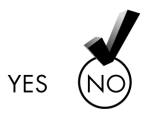

ELECTRIC POWER RESEARCH INSTITUTE
3420 Hillview Avenue, Palo Alto, California 94304-1338 ▪ PO Box 10412, Palo Alto, California 94303-0813 ▪ EE. UU.
+1.800.313.3774 ▪ +1.650.855.2121 ▪ askepri@epri.com ▪ www.epri.com

Número del documento para entregar: 3002018265

Tipo de producto: Informe técnico

Título del producto: Guías sobre ensayos de fisuración por corrosión bajo tensión con énfasis en el agua a alta temperatura

PÚBLICO PRINCIPAL: Investigadores centrados en ensayos de la tasa de crecimiento de las fisuras ambientales

PÚBLICO SECUNDARIO: Ingenieros de programa interesados en ensayos de la tasa de crecimiento de las fisuras ambientales y estudios relacionados

FUNDAMENTO DE LA INVESTIGACIÓN

¿Qué orientación hay disponible para realizar ensayos de fisuración por corrosión bajo tensión (SCC) en agua a alta temperatura?

RESUMEN DE LA INVESTIGACIÓN

Este informe tiene los siguientes objetivos:

- Ofrecer información crítica, datos de referencia y orientación para la realización de ensayos de fatiga por corrosión (CF) y de fisuración por corrosión bajo tensión en agua a alta temperatura.
- Destacar los principales problemas sobre la base de la situación actual de los conocimientos sobre las técnicas óptimas de ensayo de fisuración por corrosión bajo tensión y fatiga por corrosión.
- Servir como documento para la transferencia de conocimientos relativos a las buenas prácticas en los ensayos de fisuración por corrosión bajo tensión y fatiga por corrosión.
- Ofrecer orientación específica para la química del agua, el control de la temperatura, las técnicas y la optimización de la caída potencial de corriente continua, los tipos de muestras, la tasa de crecimiento de la fisuración por corrosión bajo tensión y las pruebas de inicio, el control de maquinaria (requisitos de software), la teoría y medición del potencial de corrosión y las técnicas de ensayo.

En este informe se presta atención a la fisuración por corrosión bajo tensión (crecimiento de la fisuración) y, sobre todo, a la fisuración por corrosión intergranular bajo tensión (IGSCC) en aceros inoxidables y aleaciones de níquel, y también es pertinente para los ensayos de fisuración por corrosión bajo tensión en aceros al carbono y aceros de baja aleación, así como los ensayos de fatiga por corrosión. Gran parte del informe es también aplicable a los ensayos de fisuración por corrosión bajo tensión y fatiga por corrosión en entornos distintos al agua a alta temperatura. Este informe no se centra en el conocimiento y las relaciones de dependencia de la fisuración por corrosión bajo tensión, sino en las cuestiones experimentales, aunque estas son elementos complementarios en cualquier estudio de fisuración por corrosión bajo tensión. Como resultado de ello, el informe no está destinado a principiantes y se asume que el lector posee ciertos conocimientos.

CONCLUSIONES PRINCIPALES

- La evaluación de la respuesta a la fisuración asistida por el ambiente (EAC) es compleja en cualquier entorno, pero es especialmente compleja en el agua a alta temperatura. El incentivo de cuantificar la cinética y las dependencias de la fisuración asistida por el ambiente en agua a alta temperatura es alto, dada la necesidad de un funcionamiento del reactor de agua ligera fiable, de larga duración y seguro.
- La guía está diseñada para ofrecer información esencial, datos de referencia y orientación para la realización de ensayos sobre fisuración por corrosión bajo tensión y fatiga por corrosión en

agua a alta temperatura. El ensayo de la tasa de crecimiento de las fisuras es una cuestión importante y se incluye un apartado sobre ensayos de iniciación de la fisuración por corrosión bajo tensión. Aunque se centra en el agua a alta temperatura, gran parte del informe también es aplicable a los ensayos de fisuración asistida por el ambiente en otros entornos.

- La fisuración asistida por el ambiente es muy distinta a otros ensayos mecánicos o de fatiga habituales, ya que hay muchas interdependencias complejas y grandes efectos en las sutiles diferencias entre los ensayos. Abordar todos los detalles y matices de los ensayos queda fuera del alcance de este informe que, en su lugar, pretende identificar problemas importantes y buenas prácticas, así como ofrecer datos de referencia básicos con una intención subyacente de avisar al responsable del ensayo para que observe detenidamente, pregunte y mejore constantemente las técnicas y observaciones, repita los experimentos, interactúe con compañeros a nivel internacional y optimice la gestión de los ensayos.

POR QUÉ ESTO ES IMPORTANTE

Han pasado casi cinco décadas de generación de datos sobre la fisuración por corrosión bajo tensión y la fatiga por corrosión en el sector nuclear, y ha habido una gran dispersión y una capacidad de reproducción limitada que apuntan a importantes defectos en algunas técnicas experimentales. Las deficiencias no pueden resolverse mediante la evaluación de los datos por parte del experto posterior a los ensayos. En lugar de ello, es necesario abordarlas antes y durante los ensayos. Con cientos de años de experiencia en el sistema, estudiando y ensayando la fisuración por corrosión bajo tensión y la fatiga por corrosión, así como una importante interacción entre la mayoría de laboratorios internacionales, se ha recopilado una importante cantidad de material que puede usarse para desarrollar una guía exhaustiva para los ensayos futuros de fisuración por corrosión bajo tensión y fatiga por corrosión en el agua a alta temperatura. El informe resume dicha información clave con la intención de ofrecer una orientación para que los investigadores la tengan en cuenta en futuros ensayos para minimizar las deficiencias en los resultados de las pruebas.

CÓMO USAR LOS RESULTADOS

Los responsables de los ensayos pueden usar el informe como referencia, que les ayudará en sus actividades de ensayo. El informe identifica los principales problemas y las buenas prácticas, ofrece datos de referencia básicos y destaca los problemas que los responsables de los ensayos deben observar y gestionar detenidamente. Asimismo, el informe anima a los lectores a cuestionar sus técnicas y observaciones, reproducir los resultados experimentales, interactuar con compañeros a nivel internacional y aprender a gestionar sus actividades de ensayo. Es un compendio útil para los investigadores que realizan o planean realizar ensayos de fisuración por corrosión bajo tensión y fatiga por corrosión en agua a alta temperatura y que tratan de obtener datos de gran calidad.

OPORTUNIDADES DE APRENDIZAJE Y PARTICIPACIÓN

- Conferencias técnicas internacionales sobre investigación, por ejemplo, el Grupo cooperativo internacional sobre fisuración asistida por el ambiente (ICG-EAC)
- Conferencia sobre la degradación ambiental de materiales en sistemas de energía nuclear y reactores de agua
- Reuniones sobre el programa de fiabilidad de los materiales y el proyecto de vasijas e internos del reactor de agua en ebullición

CONTACTO DE EPRI: Gary L. Stevens, ejecutivo técnico, gstevens@epri.com

PROGRAMAS: Energía nuclear, P41; Vasijas e internos del reactor de agua en ebullición (BWRVIP), P41.01.03; Fiabilidad de los materiales del reactor de agua a presión (MRP), P41.01.04

CATEGORÍA DE APLICACIÓN: REFERENCIA

CONTENIDO

LISTADO DE FIGURAS

LISTADO DE TABLAS

Riktlinjer för att testa sprickbildning till följd av spänningskorrosion

Med betoning på vatten med hög temperatur

3002018265

Slutrapport, augusti 2020

EPRI-projektansvarig
G. Stevens

Alla krav eller en del av kraven enligt EPRI:s kärnkvalitetssäkringsprogram gäller för denna produkt.

ELECTRIC POWER RESEARCH INSTITUTE
3420 Hillview Avenue, Palo Alto, Kalifornien 94304-1338 ▪ PO Box 10412, Palo Alto, Kalifornien 94303-0813 ▪ USA
+1.800.313.3774 ▪ +1.650.855.2121 ▪ askepri@epri.com ▪ www.epri.com

Leveransnummer: 3002018265

Produkttyp: Teknisk rapport

Produkttitel: Riktlinjer för att testa sprickbildning till följd av spänningskorrosion med betoning på vatten med hög temperatur

PRIMÄR MÅLGRUPP: Forskare fokuserade på tester av sprickbildning från miljöpåverkan

SEKUNDÄR MÅLGRUPP: Programingenjörer intresserade av tester av tillväxthastighet av sprickor i olika miljöer och relaterade studier

HUVUDSAKLIG FORSKNINGSFRÅGA

Vilken vägledning finns för tester av sprickbildning till följd av spänningskorrosion (SCC) i vatten med hög temperatur?

ÖVERSIKT ÖVER FORSKNINGEN

Syftet med denna rapport är följande:

- Att tillhandahålla kritisk information, referensdata och vägledning för utförande av SCC- och korrosionsutmattningstester (CF) i vatten med hög temperatur.
- Att lyfta fram viktiga frågor baserat på det nuvarande kunskapsläget om optimala SCC- och CF-testtekniker.
- Att fungera som ett dokument för kunskapsöverföring med bästa praxis för SCC- och CF-tester.
- För att tillhandahålla riktlinjer som är specifika för vattenkemi, temperaturkontroll, tekniker och optimering av potential vid likström, provtyper, SCC-tillväxthastighet och initieringstester, maskinkontroll (programvarukrav), teorier och mätningar av korrosionspotential samt testtekniker.

Fokus i rapporten läggs på SCC (spricktillväxt) och mestadels interkornsprickbildning till följd av spänningskorrosion (Intergranular Stress Corrosion Cracking, IGSCC) i rostfritt stål och nickellegeringar och är också relevant för SCC-tester av kolstål och låglegerat stål samt CF-tester. Stora delar av rapporten är också tillämplig på SCC- och CF-tester i andra miljöer än vatten med hög temperatur. Rapporten är inte fokuserad på SCC-förståelse och -beroenden utan snarare på experimentella frågor, även om dessa är kompletterande element i någon SCC-studie. Som ett resultat är rapporten inte avsedd för nybörjare och läsaren förutsätts ha en viss bakgrundskunskap.

HUVUDSAKLIGA SLUTSATSER

- Utvärderingen av EAC-respons (sprickbildning från miljöpåverkan) är komplex i alla miljöer men är särskilt utmanande i vatten med högt temperatur. Incitamentet att kvantifiera EAC:s kinetiska energi och beroenden av vatten med hög temperatur är hög med tanke på behovet av pålitlig och säker drift av lättvattenreaktorn med lång livslängd.
- Riktlinjerna är designade för att tillhandahålla grundläggande information, referensdata och vägledning för utförande av SCC- och CF-tester av korrosionsutmattning i vatten med hög temperatur. Tester av tillväxthastigheten av sprickor är en viktig betoning och

ett avsnitt SCC-initieringstester ingår. Medan den fokuserad på vatten med hög temperatur är stora delar av rapporten också tillämplig på EAC-tester i andra miljöer.

- EAC är väldigt annorlunda än vanliga mekaniska tester eller utmattningstester eftersom det finns många komplexa ömsesidiga beroenden och stora effekter av subtila testskillnader. Att vända sig till alla skillnader och nyanser i tester ligger utanför rapportens omfattning. Den strävar snarare efter att identifiera viktiga frågor och bästa praxis samt tillhandahålla grundläggande referensdata med en underliggande avsikt att varna de som experimenterar för att noggrant observera, ifrågasätta och ständigt förbättra tekniker och observationer, upprepa experiment, interagera med internationella kollegor och optimera testhantering.

PÅ VILKET SÄTT HAR DETTA BETYDELSE

Det har genererats över fem decennier av SCC- och CF-data för att användas inom kärnkraftsindustrin och stor spridning samt begränsad reproducerbarhet pekar på betydande brister i några av de experimentella teknikerna. Bristerna kan inte lösas genom expertutvärdering av uppgifterna efter tester. Snarare måste de adresseras före och under testerna. Med hundratals systemårig erfarenhet av att studera och testa SCC och CF och betydande interaktion mellan de flesta internationella laboratorier har betydande bakgrundsmaterial samlats in som kan användas för att utveckla en omfattande riktlinje för framtida SCC- och CF-tester i vatten med hög temperatur. Rapporten sammanfattar sådan viktig information med avsikten att tillhandahålla vägledning för forskare att överväga i framtida tester för att minimera bristerna i testresultaten.

TILLÄMPA RESULTATEN

Rapporten kan användas av de som experimenterar som referens för att hjälpa dem i sina testaktiviteter. Rapporten identifierar viktiga frågor och bästa praxis, tillhandahåller grundläggande referensdata och belyser frågor som de som experimentera noggrant bör följa och hantera. Rapporten uppmuntrar läsarna att ifrågasätta sina tekniker och observationer, återge experimentella resultat, interagera med internationella kollegor och lära sig att hantera sina testaktiviteter. Den är ett användbart kompendium för forskare som utför eller planerar att utföra SCC-tester i vatten med hög temperatur och strävar efter högkvalitativa data.

TILLFÄLLEN FÖR INLÄRNING OCH ENGAGEMANG

- Internationella tekniska forskningskonferenser såsom International Cooperative Group on Environmentally Assisted Cracking (ICG-EAC)
- Konferens om miljöförstöring av material i kärnkraftssystem med vattenreaktorer
- Program för materialpålitlighet och BWR-kärl samt interna projektmöten

Kontakt hos EPRI: Gary L. Stevens, teknisk chef, gstevens@epri.com

PROGRAM: Kärnkraft, P41; Kokvattenreaktorkärl och interna komponenter (BWRVIP), P41.01.03; Pålitligheten hos material i tryckvattenreaktorer (MRP), P41.01.04

GENOMFÖRANDEKATEGORI: Hänvisningar

INNEHÅLL

LISTA ÖVER BILDER

LISTA ÖVER TABELLER

Export Control Restrictions

Access to and use of this EPRI product is granted with the specific understanding and requirement that responsibility for ensuring full compliance with all applicable U.S. and foreign export laws and regulations is being undertaken by you and your company. This includes an obligation to ensure that any individual receiving access hereunder who is not a U.S. citizen or U.S. permanent resident is permitted access under applicable U.S. and foreign export laws and regulations.

In the event you are uncertain whether you or your company may lawfully obtain access to this EPRI product, you acknowledge that it is your obligation to consult with your company's legal counsel to determine whether this access is lawful. Although EPRI may make available on a case by case basis an informal assessment of the applicable U.S. export classification for specific EPRI products, you and your company acknowledge that this assessment is solely for informational purposes and not for reliance purposes.

Your obligations regarding U.S. export control requirements apply during and after you and your company's engagement with EPRI. To be clear, the obligations continue after your retirement or other departure from your company, and include any knowledge retained after gaining access to EPRI products.

You and your company understand and acknowledge your obligations to make a prompt report to EPRI and the appropriate authorities regarding any access to or use of this EPRI product hereunder that may be in violation of applicable U.S. or foreign export laws or regulations.

The Electric Power Research Institute, Inc. (EPRI, www.epri.com) conducts research and development relating to the generation, delivery and use of electricity for the benefit of the public. An independent, nonprofit organization, EPRI brings together its scientists and engineers as well as experts from academia and industry to help address challenges in electricity, including reliability, efficiency, affordability, health, safety and the environment. EPRI also provides technology, policy and economic analyses to drive long-range research and development planning, and supports research in emerging technologies. EPRI members represent 90% of the electricity generated and delivered in the United States with international participation extending to nearly 40 countries. EPRI's principal offices and laboratories are located in Palo Alto, Calif.; Charlotte, N.C.; Knoxville, Tenn.; Dallas, Texas; Lenox, Mass.; and Washington, D.C.

Together...Shaping the Future of Electricity

Programs:

Nuclear Power

Boiling Water Reactor Vessels and Internals

Pressurized Water Reactor Materials Reliability

3002018265

Electric Power Research Institute
3420 Hillview Avenue, Palo Alto, California 94304-1338 • PO Box 10412, Palo Alto, California 94303-0813 USA
800.313.3774 • 650.855.2121 • askepri@epri.com • www.epri.com